



**KTH Industrial Engineering  
and Management**

# Implementation And Validation Of Loss Prediction Methods To An Existing One Dimensional Axial Turbine Design Program

Rafael GUÉDEZ

**Master of Science Thesis**

KTH School of Industrial Engineering and Management  
Energy Technology EGI-2011-037MSC EKV840  
Division of Heat and Power Technology  
SE-100 44 STOCKHOLM



KTH Industrial Engineering  
and Management

**Master of Science Thesis**

**EGI 2011-037MSC EKV840**

**Implementation and Validation of Loss  
Prediction Methods To An Existing One-  
Dimensional Axial Turbine Design Program**

Rafael Guédez

Approved 12 - 04 - 2011	Examiner Björn Laumert	Supervisor Hina Noor
	Commissioner	Contact person

## **Acknowledgements**

First of all I wish to express my gratitude to Hina Noor, PhD candidate at KTH, for her guidance, advices and support during the development of the work at KTH. Similarly, I wish to thank Dr. Björn Laumert and my colleagues at the Turbine Group in KTH for the opportunity of letting me be part of them, and cooperate in my work and knowledge, been always enthusiastic and supportive.

I will also like to thank Mats Annerfeldt and all the project members from Siemens Industry Turbomachinery for their support and invitation to seminars, reference group meetings and fruitful discussions.

I wish to give special thanks to Sara Aniyar and Karl Göran Mäler, for all the good times and their support during my stay in Sweden. Similarly to all my friends and roommates who were always there to support me and for the good times shared.

Finally, I would like to express my infinite gratitude to my parents, Rafael Guédez and Oneida Mata, and also my family for their unconditional support and guidance even facing the adversity of being thousands of kilometers away. Thanks

## **Abstract**

One of the early steps in axial turbine design is the use of one-dimensional (1D) mean line calculations to predict the turbine performance and estimate the principal geometric parameters, such as radius and blade heights, that will be needed in further computational fluid dynamic (CFD) studies. This 1D analysis is based on the estimation of the aerodynamic losses expressed as a function of simple blade parameters and the velocity triangles. In this regard, there exist different loss correlations widely used in literature to estimate these losses but at the same time there is a lack of information regarding differentiation between them. Thereafter, the objective in this work was to judge and compare the behaviors of the Kacker-Okapuu, Craig-Cox and Denton loss correlations, all of them widely-used in turbine performance prediction.

Present work shows the implementation of these different loss correlations on an existing 1D mean line numerical tool, LUAX-T. Subsequently, once implemented, the correlations were compared and analyzed by the use of a validation process and performing a parametric study.

The results show that similar key parameters such as the flow turning, solidity and aspect ratio rule the different loss mechanisms in each correlation. On the other hand, the parametric study shows that the correlations are in agreement with the theory and give similar trends for performance prediction even though they all predict different values of efficiency for the same turbine stage. Moreover, the validation process show the correlations were found to be accurate enough when comparing against two different sets of experimental data. However, it was also proved that the models are only accurate if used within the range of applicability they were developed for, hence a complete knowledge of the limitations of each correlation should be known prior to using them.

Finally, the extension of the one-dimensional mean line numerical tool LUAX-T will serve to perform further studies related to turbine design, as there are very few non-confidential turbomachinery design tools available for teaching or researching. Furthermore, a parametric study tool was also developed as part of the program. This last extension and the loss implementation codes are described in this work.

Keywords: turbine design, turbomachinery, loss correlations, Kacker-Okapuu, Craig-Cox, Denton, aerodynamic loss, numerical tool, validation process and parametric study.

# Table of Contents

Acknowledgements.....	3
Abstract.....	4
Table of Contents .....	5
Nomenclature .....	7
Blade Terminology and Angle Definition.....	10
1. Introduction.....	11
1.1. Objective .....	11
1.2. Methodology.....	11
1.3. Limitations .....	12
1.4. Disposition and Reading Instruction.....	12
2. Theoretical Framework.....	13
2.1. Axial Gas Turbine's Fundamental Theory.....	13
2.1.1. <i>Fundamentals of Axial Turbine Expansion</i> .....	13
2.1.2. <i>Non-Dimensional Design Parameters</i> .....	16
2.1.3. <i>Stage Losses and Efficiency</i> .....	18
2.1.4. <i>Smith Chart</i> .....	19
2.2. Flow Field in Axial Gas Turbines .....	21
2.3. Aerodynamic Losses in Axial Gas Turbines.....	22
2.3.1. <i>Loss Sources</i> .....	22
2.3.2. <i>Classification of the Losses</i> .....	22
2.4. Loss Correlation Models.....	28
2.4.1. <i>AMDCKO</i> .....	28
2.4.2. <i>Craig &amp; Cox</i> .....	34
2.4.3. <i>Denton</i> .....	51
3. One-dimensional Design Tool – LUAX-T.....	55
4. Implementation and Verification of Loss Models.....	60
4.1. Craig and Cox.....	60
4.1.1. <i>Implementation of Craig and Cox Loss Model in LUAX-T</i> .....	60
4.1.2. <i>Verification of Craig and Cox Loss Model</i> .....	63
4.2. Denton.....	70
4.2.1. <i>Implementation of Denton Loss Model in LUAX-T</i> .....	70
5. Validation of Loss Models.....	74
6. Parametric Design Study.....	83

6.1.	Methodology.....	83
6.2.	LUAX-T Input Settings.....	84
6.3.	Results.....	87
7.	Discussion .....	94
7.1.	Individual Loss Mechanisms Analysis .....	94
7.1.1.	<i>Profile Loss</i> .....	94
7.1.2.	<i>Secondary Loss</i> .....	97
7.1.3.	<i>Trailing Edge Loss</i> .....	100
7.1.4.	<i>Clearance Loss</i> .....	102
7.2.	Loss Correlations Analysis .....	104
8.	Final Conclusions.....	107
9.	Future Work and Recommendations.....	109
	Bibliography.....	110
	Table Of Figures .....	112
	APPENDIX I.....	115
	APPENDIX II .....	130
	APPENDIX III .....	133

## Nomenclature

A	Fluid relative inlet angle by Craig-Cox
Aa	Annulus Area
A <sub>k</sub>	Clearance area
A <sub>T</sub>	Area of Throat
b	Blade backbone length
B	Fluid relative outlet angle by Craig-Cox
C	Flow absolute velocity
c	Blade Chord
C <sub>d</sub>	Blade surface dissipation coefficient by Denton
c <sub>f</sub>	Friction factor
C <sub>p</sub>	Specific heat capacity at constant pressure
CR	Contraction Ratio
C <sub>s</sub>	Blade surface length
C <sub>v</sub>	Specific Heat capacity at constant volume
C <sub>x</sub>	Axial component of the flow absolute velocity
D	Diameter
F <sub>k</sub>	Clearance Loss coefficient by Craig-Cox
F <sub>L</sub>	Lift Factor
g	Gravitational Constant
H	Blade span
h	Specific enthalpy
i	Incidence angle
J	Mechanical equivalent of Heat
k <sub>s</sub>	Surface sand roughness
l	Blade Chord
M	Mach number
n	Rotational speed
o	Blade throat width
p	Static pressure
p <sub>s</sub>	Stagnation pressure
R	Reaction Degree
r	Radius

$Re$	Reynolds number
$s$	Blade pitch
$s$	Specific entropy
$T$	Static temperature
$t_{\max}$	Maximum blade thickness
$te$	Trailing Edge Thickness
$U$	Rotational Velocity
$W$	Flow relative velocity
$x$	Distance in axial direction
$X$	Enthalpy Loss Coefficient by Craig-Cox
$y$	Distance in tangential direction
$Y$	Pressure loss coefficient
$\alpha$	Absolute Flow angle
$\alpha'$	Flow angle
$\alpha'$	Metal Angle
$\beta$	Relative flow angle
$\gamma$	Isentropic exponent
$\gamma$	Stagger angle
$\delta^*$	Boundary layer momentum thickness
$\Delta h$	Real enthalpy drop over the stage
$\Delta h_{is}$	Isentropic enthalpy drop over the stage
$\Delta p$	Static pressure drop
$\Delta S$	Entropy rate
$\Delta W$	Work
$\varepsilon$	Blade deflection
$\eta$	Efficiency
$\theta$	Boundary layer displacement thickness
$\mu$	Dynamic viscosity
$\nu$	Velocity ratio
$\xi$	Enthalpy Loss Coefficient by Moustapha.
$\xi$	Entropy Loss Coefficient by Denton
$\pi$	Pressure ratio
$\rho$	Density
$\tau$	Tip clearance distance
$\nu$	Kinematic viscosity

$\varphi$	Flow Coefficient
$\phi$	Kinetic energy loss coefficient
$\psi$	Stage-Loading Coefficient
$\psi$	Zweifel Blade Loading Coefficient

## Blade Terminology and Angle Definition

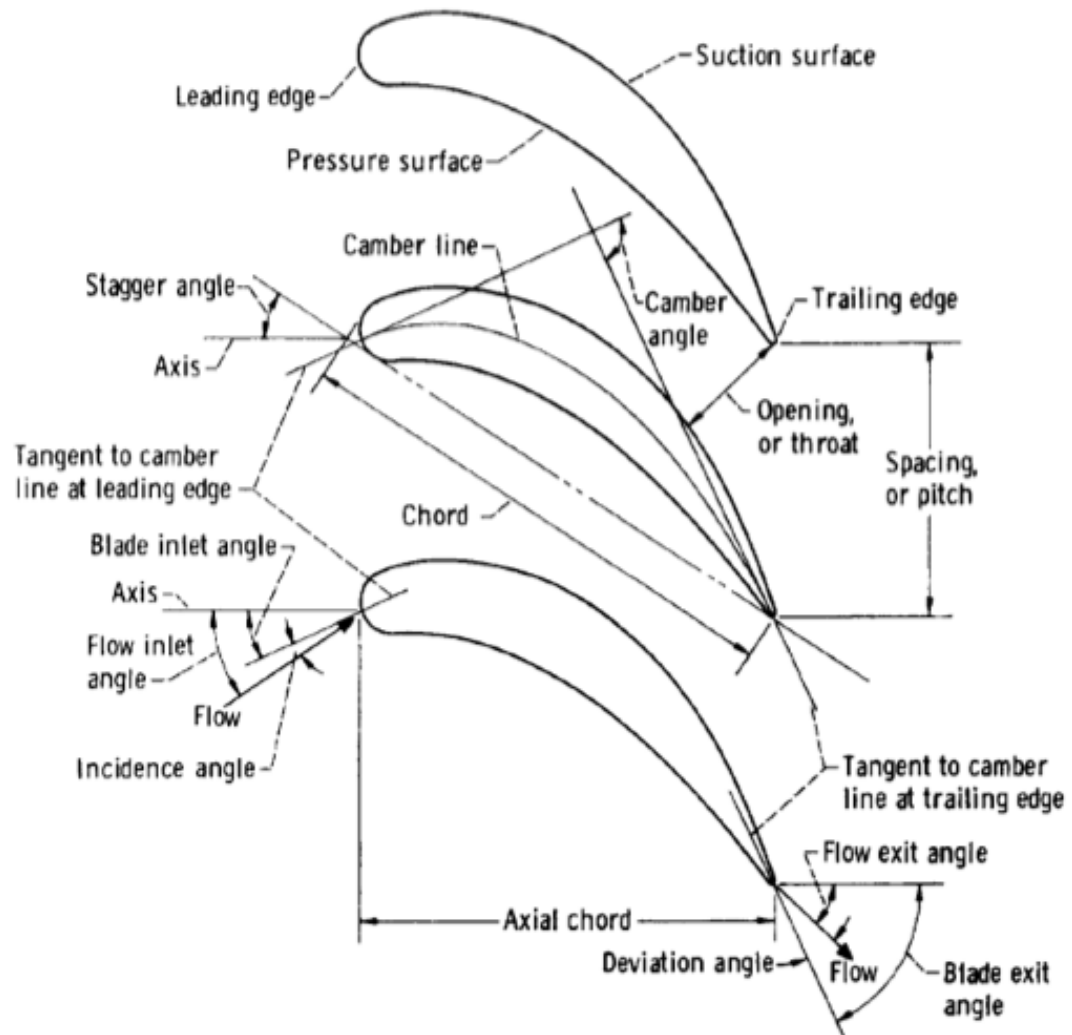
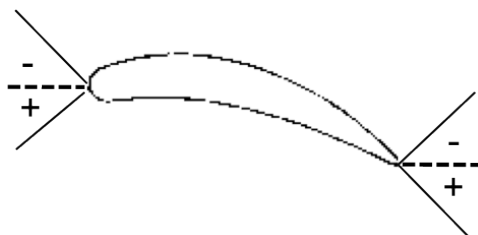
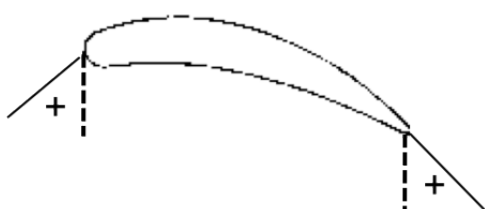


Figure - Blade Terminology as extracted from NASA-SP-290 J. Glassman fig. 2-17

Kacker & Okapuu (AMDCKO), Denton



Craig & Cox (CC)



## **1. Introduction**

Turbomachinery represents one of the most reliable and efficient sources of power generation and its application in future is considered to increase (Franus, 1994). In this regard, no matter which fuel is to be used in the future as main energy supply, it is likely to happen that thermal turbomachines will still be used in energy transformation processes. Turbines are thermal turbomachines able to convert energy from a flow, usually fuels, into mechanical work. Turbines must be designed with high efficiencies and low losses. In practice a turbine design involves detailed aerodynamic studies and relies on many experimental data for performance estimation.

For the design of turbines many computational tools are widely known and used. Those tools based on a three-dimensional analysis of the flow path are the main focus of study for incoming designs. Nevertheless, three-dimensional fluid dynamic studies require the main turbine blade and cascade geometric parameters to be already fixed in order to represent them on computational tools, otherwise the use of this technology for all possible geometries will be not only expensive but extensive in time. This brings in the importance of one-dimensional mean line velocity triangle analysis and calculations. Mean line design tools are based on loss correlations that predict the main losses held through the flow path and in the turbine stage by using basic blade parameters.

The existing one-dimensional loss models differ from one to another and, even though several studies have been made to improve them, only limited amount of work exists in open literature regarding differentiation between them, like the work performed by Lozza (Lozza, 1982). This leads to the main objective of the present work, which is explained next. In order to perform the task a methodology has been proposed which takes into account the scope and limitations, as well.

### **1.1. Objective**

The main objective of the present work is to judge the behavior of different one-dimensional loss correlation models as well as to identify the key design features and parameters that rule the loss mechanisms in an axial gas turbine. In order to establish the loss model implementation and validation some specific objectives are to be accomplished:

- Implement different loss correlation models on an existing one-dimensional tool design program developed in MATLAB (Mathworks Inc., 2010).
- Verify, through comparisons and based on existing state-of-the-art theory, the results obtained from such different correlations implementations.
- Validate the implemented loss models against experimental data measured at the KTH Test Turbine Facility (KTH, 2011).
- Perform a comparison task to determine which loss correlation model is more suitable under certain conditions based on the physics or assumptions behind them. This could lead to turbine aerodynamics design optimization and serve as a basis for further two or three-dimensional studies.

### **1.2. Methodology**

A literature review and research study is aimed as a first step involving books, articles, reports and papers associated with the physics and basic theory of flow behavior through axial turbomachines. This takes into account the importance of the fundamentals regarding loss prediction models and analyzing the most widely used methods proposed by different authors.

After a proper literature study and under complete knowledge of selected loss prediction methods, a review is provided on an existing one-dimensional tool under the name LUAX-T, previously developed by Lund University (Genrup, 2008) based on a MATLAB code (Mathworks Inc., 2010). This will be held in order to obtain a further extension of the code now considering the implementation of different loss correlations and subsequently their validation.

Finally a parametric study will be performed in order to characterize and compare the implemented loss models, which will further lead to the final conclusions. These conclusions consist on determining the range of applicability, trends and key parameters of each loss correlation. Lastly, there are given recommendations for future works and analysis of one-dimensional turbine design.

### **1.3. Limitations**

The study performed in this thesis has been held under certain limitations. These are described as follows:

- Loss correlations are based on one-dimensional mean line calculations.
- Film cooling losses are computed using Hartsel loss model (Hartsel, 1972), and will not be modified as the implementation only considers aerodynamic loss correlation methods.
- The range of application of the present study is only for axial gas turbines in industrial environment not including steam turbines even though some correlations can be applied in both cases.
- The only one-dimensional turbine design tool used for calculations in present work is the Lund University's Axial Turbine Tool, LUAX-T (Genrup, 2008) for estimation of turbine performance.

### **1.4. Disposition and Reading Instruction**

This thesis report is structured such that shown in the first chapter are the objectives, limitation and methodology of the work, followed by fundamental and relevant theory in next chapter, where the fundamental expansion process and non-dimensional design parameters on axial turbines, the loss mechanisms, the loss sources, loss classification and, the empirical methods developed for loss estimation are explained. The next chapter explains the 1D tool used for mean-line calculations, LUAX-T, its structure, inputs and outputs before the implementation. Chapter 4 explains how the implementation of the loss correlation models was done on the 1D tool. Chapter 5 shows the results of two validation studies against tests performed on Test Turbine Facility at the KTH Heat and Power Technology lab (KTH, 2011). Chapter 6 explains the methodology used for the parametric study and the results obtained from it. Lastly, chapter 7 contains all the discussion regarding the results shown on previous chapters, this considers the physics and detailed analysis of the phenomena occurring, based as well on the empirical correlations described in chapter 2. Finally, chapters 8 and 9, enclose the overall conclusions and recommendations for the future work, respectively.

## 2. Theoretical Framework

### 2.1. Axial Gas Turbine's Fundamental Theory

The present study is based on the fact that the reader has a background on turbomachinery basics and also in turbines design. However, this section will explain briefly the fundamentals in the axial gas turbine expansion and the most common non-dimensional parameters used in turbine design. This chapter provides understanding on the loss correlation models and how these loss coefficients are used to estimate the turbine's performance.

#### 2.1.1. Fundamentals of Axial Turbine Expansion

Among all the equations and diagrams developed in turbomachinery, two of the most important ones are the Euler turbomachine equation and the Enthalpy-Entropy Diagram. These will be explained in this section and also the relation between them. Euler's equation links the changes in flow velocity with the work output, thus being the foundation in the analysis of work extraction in a turbine stage for the turbine design. This is shown in Eq. 2-1. This equation is based on Newton's Second Law of Motion, in the angular frame of reference, where the torque developed is equal to the rate of change of angular momentum across any blade row (Moustapha, 2003). In Eq. 2-1 the suffix  $\theta$  denotes the tangential component of the velocity in each state and  $U$  is the product of the angular speed of the rotor and its radius, the blade velocity, generally assumed equal during the whole stage.

$$W = U_2 C_{\theta 2} - U_1 C_{\theta 1}$$

Eq. 2-1

In another terms the equation shown above bases on the fact that, in general, the axial and radial velocity components of a fluid particle moving through a turbine blade passage, do not contribute to the energy transfer in the turbine. Instead these velocity components represent the mass flow rate or the axial force caused on the shaft that must be absorbed by a trust bearing (Moustapha, 2003). The work done in the turbine can also be expressed as an enthalpy change of the fluid as expressed in Eq. 2-2. In this equation the work done on the stage by unit mass of fluid is equal to the stagnation enthalpy drop incurred by the fluid passing through the stage, this is true under the adiabatic flow assumption (Dixon & Hall, 2010).

$$\Delta W = h_{01} - h_{03}$$

Eq. 2-2

Euler's turbomachine equation as shown in Eq. 2-2 is related to another important tool in turbomachinery design, the enthalpy-entropy diagram, which is an enthalpy-entropy plot that shows the change of state through a complete turbine stage, including the effects of irreversibility (Dixon & Hall, 2010). The diagram is exhibited in Figure 2-1 and, as it is possible to follow with the red line, it shows how the flow enters the stage at state 1, expands through the stator to state 2, and finally through the rotor to reach last state, state 3. The figure also contains the stagnation points and the suffix  $s$  is used to denote those isentropic points whereas the blue lines are the isobars in the whole process. From the Figure 2-1 it is possible to determine its relation with Eq. 2-2 since the total stagnation enthalpy drop is shown on the left side, which means the total work output.

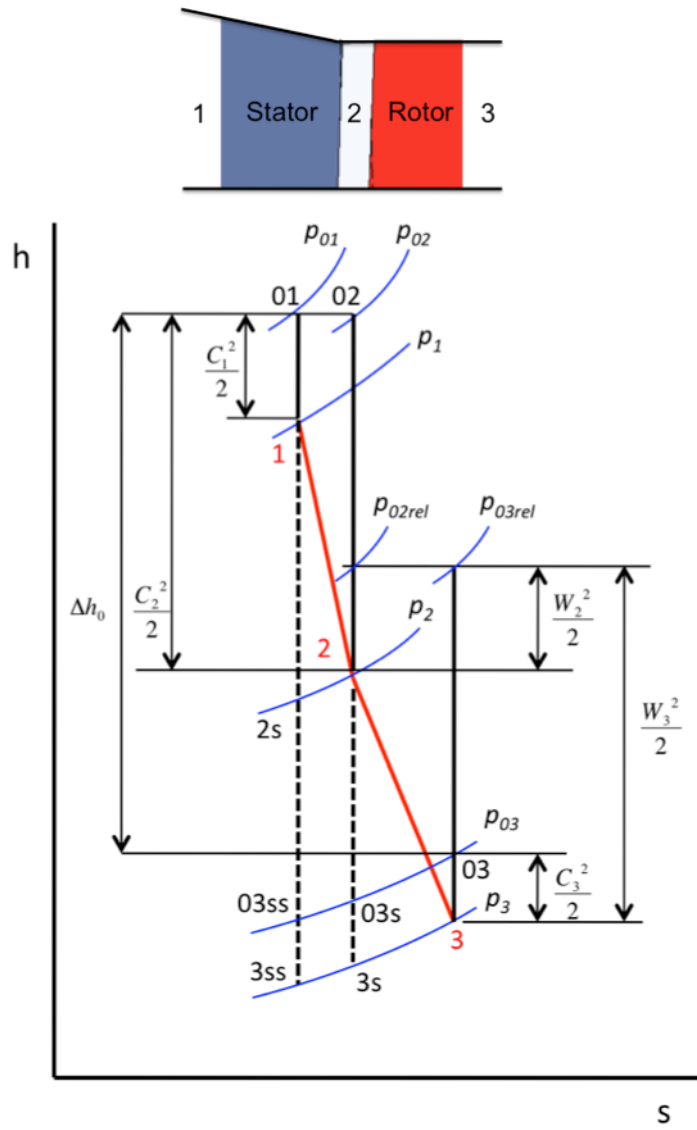


Figure 2-1 Enthalpy-Entropy Diagram (Moustapha, 2003)

Moreover the Figure 2-1 shows how the total stagnation enthalpy drop through the stator is zero, since points 01 and 02 are on the same horizontal line, this is represented in Eq. 2-3. Now if taking this into account Eq. 2-2 can be rewritten as shown in Eq. 2-4, which means that the total work done on the stage is equal to that done on the rotor. Furthermore the Enthalpy-Entropy Diagram shows how on each state the stagnation enthalpy can be obtain by adding the kinetic energy and the static enthalpy, this is described in expression Eq. 2-5, where the x is used to denote that Eq. 2-5 works for any of the 3 states. Finally, on the right side, the Enthalpy-Entropy Diagram also demonstrates that in the rotor (from state 2 to 3) the static enthalpy drop is a function of the relative velocity components, as written in Eq. 2-6. Considering these relations, a final expression for the output work as a function of velocity components is shown in Eq. 2-7 on the next page.

$$h_{01} = h_{02}$$

Eq. 2-3

$$\Delta W = h_{02} - h_{03}$$

Eq. 2-4

$$h_{0x} = h_x + \frac{C_x^2}{2}$$

Eq. 2-5

$$h_2 - h_3 = \frac{W_3^2}{2} - \frac{W_2^2}{2}$$

Eq. 2-6

$$\Delta W = \frac{1}{2} [(C_2^2 - C_3^2) + (W_3^2 - W_2^2)]$$

Eq. 2-7

All the information described in last paragraph can be summarized in the Eq. 2-8. Representing the work as a function of the velocity components is of great importance for the turbine design. This representation makes it is possible to analyze the axial turbine stage by sketching the velocity diagrams of the flow through the whole stage. An example of a velocity triangle diagram is shown next in Figure 2-2, where it is possible to differentiate the inlet and outlet both, absolute ( $\alpha$ ) and relative ( $\beta$ ), angles. This diagram provides a visual comparison of the magnitudes of the relative and absolute velocities. In Figure 2-2 the letter  $U$  is used to denote the blade velocity.

$$\Delta W = h_{01} - h_{03} = h_{02} - h_{03} = h_2 - h_3 + \frac{1}{2}(C_2^2 - C_3^2) = \frac{1}{2}[(C_2^2 - C_3^2) + (W_3^2 - W_2^2)]$$

Eq. 2-8

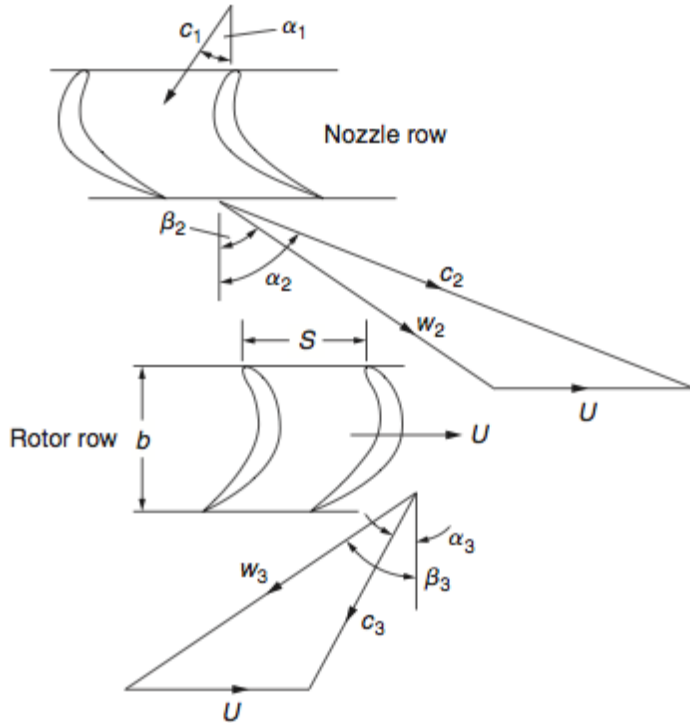


Figure 2-2 Velocity Triangles (Dixon & Hall, 2010)

Before concluding this section, as an example of the importance of the relationship between the velocity triangle diagrams and the work output, it is possible to state that from simple analysis of Eq. 2-8 and Figure 2-2 a high level of specific work output can be achieved if  $C_2$  is large and  $C_3$  is small. The rotor

inlet velocity triangle shows that this is possible by turning the flow in the stator, so that the exit flow angle,  $\alpha_2$ , is large.

### 2.1.2. Non-Dimensional Design Parameters

The design of each stage in a turbine is conveniently described by several non-dimensional parameters that allow the estimation of the turbine's performance (Moustapha, 2003). There exist three key non-dimensional parameters related to the shape of the turbine velocity triangles and that are used in fixing the preliminary design of a turbine stage, these are the reaction degree, the design flow coefficient and the stage loading coefficient (Dixon & Hall, 2010). In this section of the work all these parameters and the Zweifel coefficient will be concisely explained, as they will be of importance for the turbine performance estimation in the 1D tool.

#### Reaction Degree

The reaction degree is an important non-dimensional design parameter that defines how the complete turbine stage expansion process is split between the rotor and the stator (Moustapha, 2003). Regarding enthalpy definitions, the degree of reaction can be defined as the ratio of the static enthalpy drop in the rotor to the static enthalpy drop across the stage, which is shown in Eq. 2-9 (Dixon & Hall, 2010). Nevertheless, it can be also found in the open literature based on the ratio of the static pressures as shown in Eq. 2-10 (Moustapha, 2003). Furthermore, these two equations are related and it is possible to obtain Eq. 2-10 from Eq. 2-9 if it is assumed the flow through the turbine is nearly isentropic and ignoring compressibility effects (Dixon & Hall, 2010).

$$R = \frac{h_2 - h_3}{h_1 - h_3}$$

Eq. 2-9

$$R = \frac{p_2 - p_3}{p_1 - p_3}$$

Eq. 2-10

It is important to understand which definition is being used in any particular case regarding equations Eq. 2-9 and Eq. 2-10 since in a typical turbine stage they can differ up to 10% in value (Moustapha, 2003). However, the importance of the reaction degree as a design parameter relies on the fact that it describes the asymmetry of the velocity triangles and is therefore related to the blade angles and thus blade geometry (Dixon & Hall, 2010). Figure 2-3 shows the velocity triangles for three different reaction degrees.

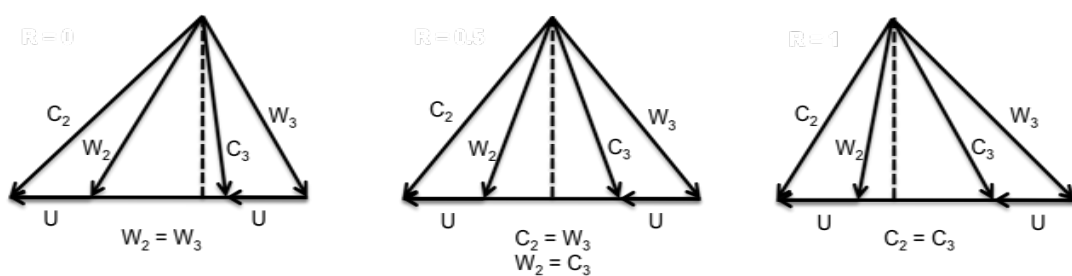


Figure 2-3 Reaction Degree and Velocity Triangles (Moustapha, 2003)

If the reaction degree is zero, as shown on the left side of Figure 2-3, it means there is no acceleration in the rotor at all and the rotor static enthalpy is therefore constant. This is the case for classic impulse turbine found in high head hydropower plants (Moustapha, 2003). Moreover, a zero reaction turbine

stage implies little pressure change through the rotor and this requires the rotor blades to be highly cambered so that the relative flow is not accelerated greatly. In contrary the zero reaction implies low cambered stator blades that produce highly accelerating flow (Dixon & Hall, 2010). On the other hand if the reaction degree is 0.5 then it is possible to see in Figure 2-3 that the triangles are symmetric. Therefore, as showed in Figure 2-3, the inlet absolute velocity ( $C_2$ ) is equal in magnitude to the relative outlet velocity ( $W_3$ ) and similarly the inlet relative velocity ( $W_2$ ) and the outlet absolute velocity ( $C_3$ ), which means that the acceleration and the gas deflection angles are equal in the stator and rotor (Moustapha, 2003). Finally, the triangle on the right in Figure 2-3 shows an example of a high reaction degree turbine stage ( $R = 1$ ), where all the work expansion is performed by the rotor (Moustapha, 2003).

#### Stage loading coefficient

The stage-loading coefficient is defined as the ratio of the stagnation enthalpy change through a stage to the square of the blade speed (Dixon & Hall, 2010), as shown in Eq. 2-11. This means that this parameter is a measure of the work output of a turbine stage as can be found in different literature (Moustapha, 2003).

$$\psi = \frac{\Delta h_0}{U^2}$$

Eq. 2-11

As described in section 2.1.1, in presence of an adiabatic flow, the stagnation enthalpy change is equal to the specific work and so the Eq. 2-11 can be rewritten as shown in Eq. 2-12, where the suffix  $\theta$  denotes the tangential component of the velocity. From Eq. 2-12 it is possible to state that a high stage loading implies large flow turning and thus highly twisted velocity triangles to achieve this turning (Dixon & Hall, 2010). A high stage loading is desirable since it means more work as an output, but it is limited by increased aerodynamic losses.

$$\psi = \frac{\Delta C_\theta}{U}$$

Eq. 2-12

#### Stage flow coefficient

The stage flow coefficient is strictly defined as the ratio of the meridional flow velocity to the blade speed, as shown in Eq. 2-13 (Dixon & Hall, 2010). Its value determines the relative flow angles in a stage velocity triangle. A stage with a low flow coefficient implies relative flow angles close to tangential whereas a high value for the flow coefficient implies low stagger and flow angles closer to axial line instead (Dixon & Hall, 2010). Eq. 2-14 shows the relation between the previously mentioned stage loading and the stage flow coefficient. This relation is deeper discussed in section 2.1.4, where the Smith Chart (Smith, 1965) is explained.

$$\phi = \frac{C_x}{U}$$

Eq. 2-13

$$\psi = \frac{\Delta h_0}{U^2} = \frac{U \Delta C_\theta}{U^2} = \phi(\tan \beta_2 - \tan \beta_3)$$

Eq. 2-14

#### Blade loading coefficient, Zweifel Coefficient

The Zweifel blade-loading coefficient can be defined as the ratio of the actual to the ideal tangential forces acting on the blade (Moustapha, 2003). It is used to provide an estimate of the optimum solidity (pitch to

chord ratio) and hence determine the blade number. The coefficient can be estimated from Eq. 2-15, which is valid assuming constant density, constant meridional velocity and constant blade speed (Moustapha, 2003).

$$\Psi = s \left( \frac{s}{c} \right) (\tan \alpha_1 + \tan \alpha_2) \cos^2 \alpha_2$$

Eq. 2-15

### 2.1.3. Stage Losses and Efficiency

The turbine efficiency and the loss coefficients are non-dimensional parameters used to describe the operation of a turbine (Moustapha, 2003). These parameters and the relation in between each other will be elaborated next in this section.

#### Loss Coefficients

The losses in the turbine are generated by non-isentropic flow features such as boundary layers or shear flows. These factors reduce the turbine efficiency and therefore its performance. Losses can be quantified by means of entropy increases as suggested by Denton in his work (Denton, 1993). Nevertheless, there exist other practical ways to quantify the losses. These are pressure loss coefficients, enthalpy loss coefficients or velocity loss coefficients. The pressure loss coefficients are the most frequently used way to quantify the total loss since it can be measured directly from turbine cascade experiments (Moustapha, 2003). There exist different ways of quantifying the aerodynamic losses. The equations used to quantify the loss coefficients and the relation between them will be shown next. Equations Eq. 2-16, Eq. 2-17 and Eq. 2-18 show the algebraic to quantify the loss coefficients in the nozzle, they are for pressure, enthalpy and velocity loss coefficients respectively.

$$K_N = \frac{p_{01} - p_{02}}{p_{02} - p_2}$$

Eq. 2-16

$$\xi_N = \frac{h_2 - h_{2s}}{\frac{1}{2} C_2^2}$$

Eq. 2-17

$$\Phi_N = \frac{C_2}{C_{2s}}$$

Eq. 2-18

To convert from one loss coefficient to another there exist different relations. The equations Eq. 2-19 and Eq. 2-20, are used to relate these parameters and have been suggested by Moustapha in his book (Moustapha, 2003).

$$K_N = \xi_N (1 + 0.5kM_2^2)$$

Eq. 2-19

$$\xi_N = \Phi_N^{-2} - 1$$

Eq. 2-20

There exist similarly a set of loss coefficient definitions for the rotor but with the difference that they are expressed in the rotors relative flow conditions. The equations to quantify the loss coefficients on the rotor and the relation between them are shown below where the subscript R denotes the rotor state (Moustapha, 2003).

$$K_R = \frac{p_{02rel} - p_{03rel}}{p_{03rel} - p_3}$$

Eq. 2-21

$$\xi_R = \frac{h_3 - h_{3s}}{\frac{1}{2} W_3^2}$$

Eq. 2-22

$$\Phi_R = \frac{W_3}{W_{3s}}$$

Eq. 2-23

$$K_R = \xi_R (1 + 0.5kM_{3rel}^2)$$

Eq. 2-24

$$\xi_R = \Phi_R^{-2} - 1$$

Eq. 2-25

The equations Eq. 2-19 and Eq. 2-24 are of main importance in the present work since the loss correlation models to be implemented quantify the losses in different ways. The Ainley and Mathieson

loss model estimates pressure loss coefficients (Ainley & Mathieson, 1951), whereas Craig and Cox give the correlations to predict enthalpy loss coefficients (Craig & Cox, 1971) and Denton computes the losses as entropy loss coefficients (Denton, 1993).

### Turbine Efficiencies

Turbines are designed to convert the available energy in a flowing fluid into useful mechanical work delivered at the coupling of the output shaft. The efficiency of this process is a performance factor of special interest for both designer and the user of the turbine (Dixon & Hall, 2010). The isentropic efficiency of the turbine has been defined as the ratio between the mechanical energy supplied by the rotor in unit time and the maximum energy difference possible for the fluid in unit time (Dixon & Hall, 2010). There are two ways of expressing the isentropic efficiency and the choice of the definition depends upon whether the exit kinetic energy is usefully employed or wasted. One example of the usefulness of the exit kinetic energy occurs in the case of the aircraft gas turbines where the energy contributes to the jet propulsive thrust. However, if the energy is useful then the ideal work occurs between points 01 and 02s on the Enthalpy-Entropy Diagram and hence the adiabatic efficiency is called '*total-to-total*' efficiency, shown in Eq. 2-26 with the '*tt*' subscript. On the contrary if the energy is wasted, the ideal work occurs between points 01 and 2s in the Enthalpy-Entropy Diagram and the adiabatic efficiency receives the name of '*total-to-static*' efficiency, shown in Eq. 2-27 with the '*ts*' subscript (Dixon & Hall, 2010).

$$\eta_{tt} = \frac{h_{01} - h_{02}}{h_{01} - h_{02s}}$$

Eq. 2-26

$$\eta_{ts} = \frac{h_{01} - h_{02}}{h_{01} - h_{2s}}$$

Eq. 2-27

### **2.1.4. Smith Chart**

The Smith Chart is a useful representation of the stage performance based on the stage loading and flow coefficients first published in 1965 by Smith (Smith, 1965). In the diagram, efficiency iso-lines are plotted as a function of the stage-loading coefficient and the flow coefficient. It is the result of the analysis of data obtained from 70 Rolls-Royce aircraft gas turbines (Dixon & Hall, 2010). The chart provides efficiency plots as determined with assumptions of constant axial velocity, reactions from 0.2 to 0.6, relatively large blade aspect ratios and not taking into account the tip leakage losses and cooling (Dixon & Hall, 2010). Confirmatory tests made by Kacker and Okapuu (Kacker & Okapuu, 1981) and Craig and Cox (Craig & Cox, 1971) have shown the usefulness of the Smith Chart in preliminary turbine design. The chart is shown in Figure 2-4. Here it is possible to see that for any fixed value of flow coefficient the trend for the stage efficiency falls as the stage-loading coefficient increases. Moreover when considering a constant stage loading factor there is possible to find an optimum flow coefficient where the efficiency of the stage is the highest according to the chart (Moustapha, 2003).

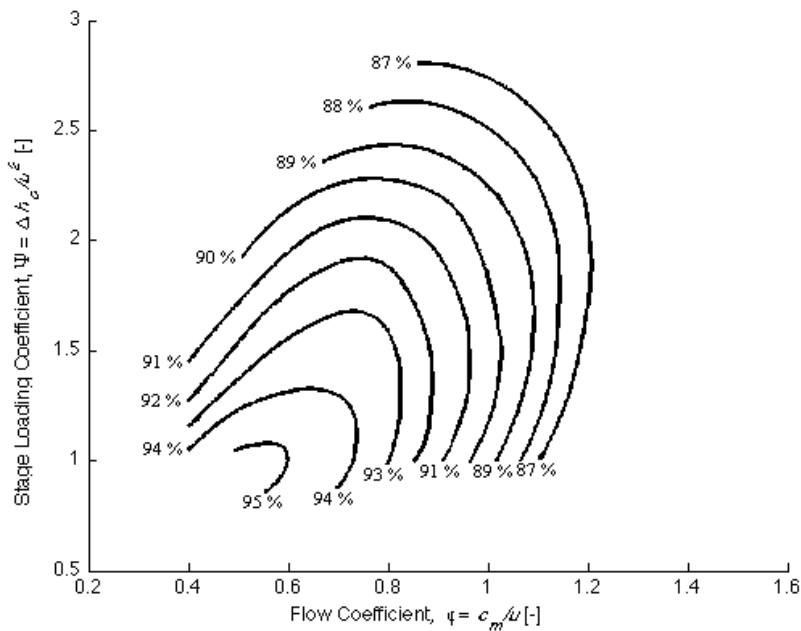


**Figure 2-4 Smith Chart (Olsson, 2008)**

The Smith Chart proves that best efficiency values occur at small values for both stage loading and flow coefficients. However, to minimize the stress in the root of the blade and maximize blade life both coefficients must be large, so the best compromise relation between blade life or higher efficiencies must be found by the designers, this means a proper selection of both, stage-loading and stage flow coefficients for design conditions (Moustapha, 2003).

## **2.2. Flow Field in Axial Gas Turbines**

Prior to understanding the aerodynamic losses in the blade passage it is relevant to know the behavior of the flow and the different flow conditions existing in the blade passage of axial gas turbines. This section will explain briefly all the different flows occurring in the passage, as they will be considered while explaining the loss classifications and the main loss sources.

Regarding the existing flows on the blade row, there is a primary flow field through it, which describes the mean flow path and which is responsible for the work extraction (Dahlquist, 2008). Nevertheless due to viscosity, the endwalls divert this primary flow produced by blade and vanes, to give rise to secondary flows, also known as endwall flows (Langston, 2001). The basic secondary flow picture for a turbine cascade is described in the next section, as can be found in Figure 2-6. Besides the vortices of the secondary flow there exist other flows disturbing the primary flow. Some of these are the leakage jet of flow across the tip clearance and the wakes created downstream the trailing edge. Both are also of utmost importance for the turbine performance prediction due to the generation of losses caused by mixing processes (Denton, 1993).

Moreover, the flow field phenomenon is not clearly understood yet, especially due to the complexity of the secondary flows (Dahlquist, 2008). Regarding this, Wei states in his work that the flows passing through an axial turbine blade passage are always three-dimensional, viscous and unsteady with the possibility of being compressible or not, hence considering subsonic, transonic or supersonic regimes that can be presented at the same time in different regions through the field (Wei, 2000). The complexity of the flow behavior is also mentioned by Denton. He explains the physical origins of loss in terms of entropy creation due to viscous effects on the boundary layer or mixing processes, shock waves and heat transfer. However he also clarifies that in some cases, as for the endwall loss estimation, there exists a great dependence on the empirical loss correlations rather than on the understanding of the physical process behind them (Denton, 1993). The mentioned flow conditions are responsible for aerodynamic losses in the turbine and will be described more in detail when explaining the losses in section 2.3.2.

Finally it is of significance to state another important fact concerning the flow field. This is that as it will be seen on the loss correlations, its description goes through many independent parameters. Some parameters are associated with the blade profile and other with the flow path. Those associated with the blade profile are the blade camber, chord, pitch, maximum thickness, thickness distribution, leading and trailing edge radius, surface roughness, cooling holes distribution and the stagger angle, in terms of the flow path the most common parameters encountered are radial distribution of stagger angle, camber and thickness, lean, twist, sweep, skew, flare, aspect ratio, hub to tip ratio, tip clearance, endwall curvature, change of flow path area, axial space in the blade rows and radial distribution of cooling holes (Wei, 2000).

## **2.3. Aerodynamic Losses in Axial Gas Turbines**

Even though turbines are designed with the aim of achieving high values for efficiencies, there are still some remaining losses occurring. This means that in any flow study or optimization research, loss accounting is very important in order to predict the performance of the turbine appropriately. Nowadays with the presence of three-dimensional studies it is possible to visualize or predict the behavior of the flow inside the turbine knowing its geometry and the flow characteristics. In any case, this three-dimensional study could be improved if one-dimensional approximations are very accurate in its prediction, therefore the need of knowing and understanding the types of losses occurring and their sources. In this section of the work are mentioned the principal loss sources and how are the losses classified. Chapter 7 gives a deeper analysis about the losses, after analyzed the loss correlations.

### **2.3.1. Loss Sources**

Roughly it is possible to state that most common sources for losses inside axial turbines are the mixing of different flows, friction on surfaces, shocks and specific geometry of the blading or casing in the turbine. In this regard, different authors have proposed loss correlation models and might differ on their methodology but agree in the fact that these causes mentioned above are the most common sources for the losses occurring.

The friction is present mainly on the blade surface, which is dragged during the expansion process, and it is related to the profile losses by most of the loss correlation authors. The surface drag is also occurring due to a pressure difference over the blade span. The fact that the flow is not necessarily uniform on its conditions, neither its velocity, will lead to understand that, besides the blade's geometry and material, these operating flow conditions could also lead to aerodynamic losses. Explanation could be understood better as Denton (Denton, 1993) states in his work, where the losses are analyzed from an entropy generation point of view.

Regarding the flow mixing as a source of loss, it is considered so because it consists of the mixing of two uniform flow conditions. Typically, the flows are one at very high velocity and pressure conditions and another one so-called secondary flow at lower velocity. The mixing can occur at the trailing edge giving the thickness of it, at the tip clearance or just endwall mixing.

On the other hand, there are shocks occurring across the flow path, sometimes originated and controlled as a way to decrease the flow velocity. However it happens that frequently a sudden deceleration instead of a series of small deceleration leads to several losses, especially those originated by the separation of the boundary layer, which causes major losses.

### **2.3.2. Classification of the Losses**

In order to study and implement loss models for turbine design, the overall loss is divided into different loss mechanisms. Each one of these mechanisms will have a different correlation for their study and then they will all be summed up to have the total stage loss. With this into account it is important to know that this division is not constant but rather depends on the loss models and, of course, their authors. In the present section of the work the loss mechanisms proposed by Ainley and Mathieson and its refinements (Kacker & Okapuu, 1981), Craig and Cox (Craig & Cox, 1971), and Denton (Denton, 1993) will be analyzed.

Kacker and Okapuu stand that the total loss coefficient should be the sum of the profile loss, secondary loss, trailing edge loss, and tip clearance loss; this loss division is a refinement of the correlation suggested by Ainley and Mathieson (Ainley & Mathieson, 1951). On the other hand, Craig and Cox loss correlation introduce the annulus loss coefficient but agree with Kacker and Okapuu on the division of total loss coefficient into profile, secondary and clearance loss (Craig & Cox, 1971). Last loss correlation analyzed in present work is that proposed by Denton. This loss correlation, unlike studies mentioned before, measures the losses as entropy production and classifies them in form of boundary layer losses, endwall

mixing losses, trailing edge loss, tip leakage loss and shock losses (Denton, 1993). In a rough approximation, endwall losses can be attributed to secondary flows and then considered as secondary losses while the mentioned boundary layer loss can be considered as the profile loss since it is mainly due to the blade profile. This approximation is done so the method can be somehow afterwards compared with other two correlations mentioned above. Next figure, extracted from Moustapha's book, shows where does each of the losses occur on the blade according to the loss classification referenced in the book (Moustapha, 2003).

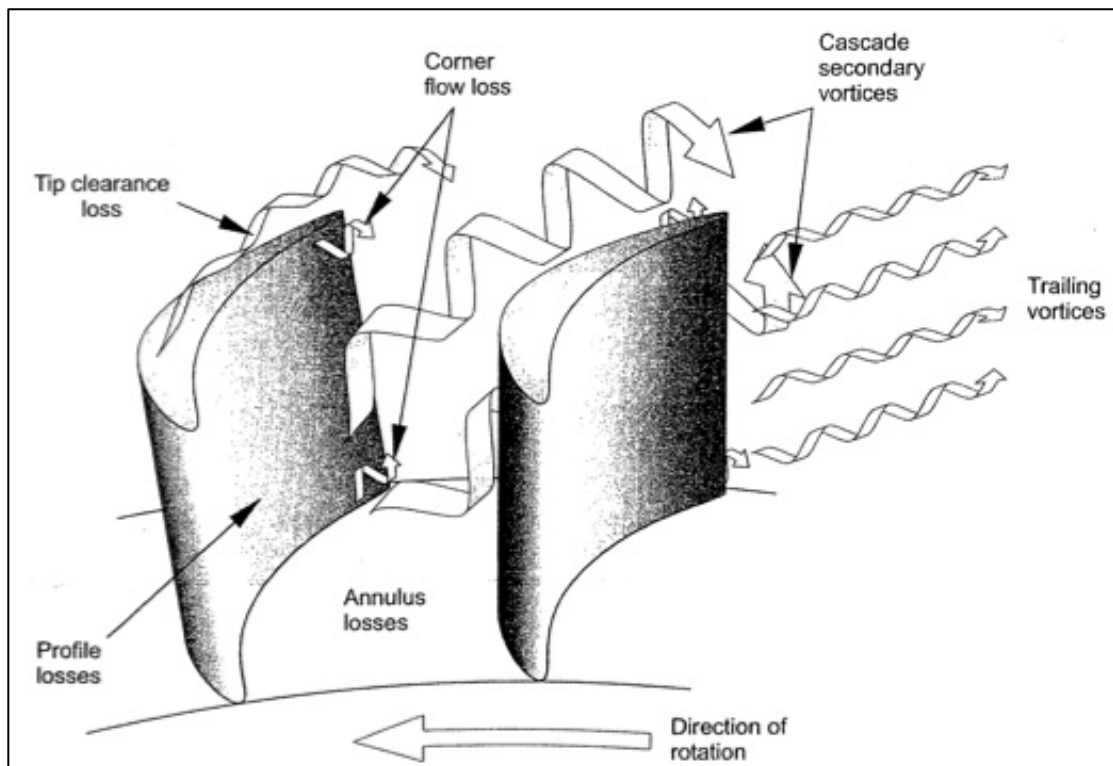


Figure 2-5 Classification of losses as extracted from the book "Axial and Radial Turbines" (Moustapha, 2003)

#### Profile Loss

The profile losses are considered to be the losses that occur as the result of the friction on the blade surface. These losses are mainly a function of the blade area in contact with the fluid, the surface finish and the Reynolds and Mach numbers of the flow through the passage. Therefore in Figure 2-5 the profile losses are pointed over the blade surface (Moustapha, 2003). Since the profile losses are related to the friction on the blade surface, it is possible to state that these losses are the result of the blade boundary layer leading to an entropy generation as Denton suggests (Denton, 1993). This entropy increase results into stagnation pressure loss and is considered to be one of the major components in the overall loss. However, it is difficult to predict the transition of the boundary layers. This means that the accuracy of the existing loss correlations in the prediction of the profile loss has been limited (Wei, 2000).

The loss correlation model initially developed by Ainley and Mathieson in 1951 includes the profile loss coefficient in the estimation of the total overall loss. The loss prediction is based on experimental data while the correlation is a function of different geometrical parameters as the pitch to chord ratio and the cascade exit gas angle (Kacker & Okapuu, 1981). The latter correlation developed by Kacker and Okapuu introduces new terms besides the basic profile loss parameter. These new factors are to consider the effect of shock losses, channel flow acceleration and supersonic drag rise. Finally, Kacker and Okapuu also introduced a correction factor to consider different Reynolds numbers (Kacker & Okapuu, 1981).

Craig and Cox define the profile loss as the energy in form of heat dissipated as a consequence of the friction on the blade profiles taking into account losses in blade wakes (Craig & Cox, 1971). In their work, Craig and Cox, base the estimation of the profile loss coefficient as a function of the pitch to backbone length and introduce two new terms, the lift parameter and the contraction ratio, both very related to the inlet and outlet relative flow angles. Similarly to Kacker and Okapuu's correlation, Craig and Cox's work is as well based on experimental data obtained from subsonic flow conditions. However, in order to measure the effect of high Mach number values, Craig and Cox introduced some corrections to the basic profile loss. These corrections rely on whether the profile has been designed with a straight suction surface or a pronounced convex suction surface curvature downstream of the throat. A final correction suggested is for Reynolds numbers beyond the reference used in turbines tested (Craig & Cox, 1971).

Finally, Denton considers the estimation of the profile losses exactly as the prediction of the entropy generated by the boundary layers. He states that the total entropy generation in the blade boundary layers can be evaluated by integrating a velocity distribution dependant function. This occurrence on relating the cube of the blade surface velocity with the loss mechanism shows that regions of high surface velocity contribute proportionally more. Finally, Denton introduces the use of a dissipation coefficient to measure the effect of the Reynolds number (Denton, 1993).

### Secondary Loss

The secondary loss is directly related to the secondary flows and is the loss originated as a consequence of the turbulent mixing and dissipation of energy when these flows and vortices are mixed together with the main flow and wall boundary layer (Dahlquist, 2008). It is also stated in literature that secondary loss is produced not only when secondary vortices and counter vortices are formed but also when they interact between each other (Wei, 2000). The secondary loss is usually given the name of endwall loss to describe all the loss arising on the annulus walls both within and outside the blade passage (Denton, 1993).

The secondary flows are defined by Langston as the flows originated due to viscous effects on the endwall that divert the primary flow produced by blades and vanes (Langston, 2001). In Figure 2-6 it is possible to see how at the endwall of the cascade, the inlet boundary layer separates at a saddle point and then the passage and counter vortices are formed. The passage vortex is formed on the cascade passage thanks to the pressure-to-suction endwall flow, while the counter vortices are smaller and have an opposite sense of rotation to the larger passage vortices, these last ones occur on an adjacent passage (Langston, 2001). The mixing in between both vortices, as stated by Wei, is also shown in Figure 2-6 (Wei, 2000).

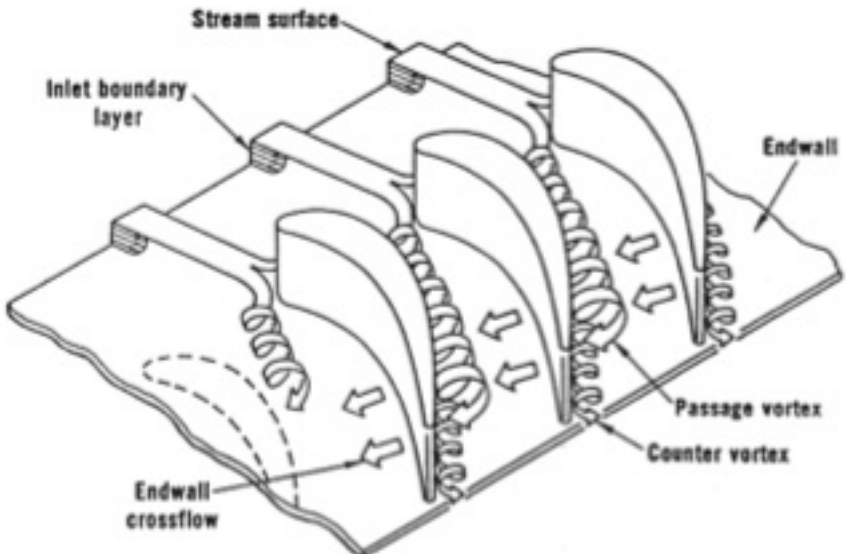


**Figure 2-6 3D Separation of a boundary layer entering a turbine cascade (Langston, 2001)**

It is also possible to see the secondary vortices formed on the blade in Figure 2-5 from a different perspective. The formation of these vortices and their mixing is responsible for a loss of lift and hence for an increment of the total aerodynamic loss or an efficiency decrease, from the turbine's designer point of view (Langston, 2001). It is important to quote that the mechanisms under which the secondary flow losses are produced are not completely understood yet, which makes it difficult to develop a 100% accurate correlation for its estimation (Langston, 2001).

Nonetheless, from several performed tests and experimental data many secondary loss correlations have been proposed in the past half-century (Benner, Sjolander, & Moustapha, 2006). Dunham (Dunham, 1970) and Sieverding (Sieverding, 1985) reviewed most of these existing correlations for secondary loss prediction and determined that the most common factors to influence this loss are the total airfoil loading, the flow acceleration, the size of endwall surface area and the velocity in the inlet endwall boundary layer. It was lately found by other researchers that the loading distribution is another important factor, but that the precise influence of each of the mentioned factors is not completely understood because of the complexity of the secondary flows (Benner, Sjolander, & Moustapha, 2006). Denton also stands that the endwall loss is the most difficult loss component to understand and predict. He mentions that existing correlations are mainly based on empirical data rather and lack in physics background. Furthermore it is important to understand that the fact they are called secondary loss doesn't mean they are secondary in magnitude or in importance. In this sense Denton states that for turbines, the enwall loss component is the major source of lost efficiency, frequently contributing with a third part of the total loss (Denton, 1993).

### Trailing Edge Loss

The trailing edge loss is the loss component originated as a consequence of the finite thickness of the trailing edge at a blade (Ainley & Mathieson, 1951). This finite thickness leads the flow to separate at surfaces close to the trailing edge, creating wakes within a recirculation zone (Dahlquist, 2008). Moreover, Denton states in his work that the trailing edge loss is the entropy generated as a consequence of the mixing out of a wake behind a blunt trailing edge. In this sense, he considers that the trailing loss analysis should take into account the effect of the boundary layers on the blade surface upstream the trailing edge and also the base pressure (Denton, 1993).

The finite thickness of the blade trailing edge causes flow separation and shock-expansion-wave interactions due to sharp corners (Wei, 2000), this flow separation is known to lead to mixing and entropy

generation. The trailing edge loss is more appreciable in transonic and supersonic conditions. This since the occurrence of shocks is related to high Mach number conditions. Figure 2-5 shows the trailing vortices formed at the trailing edge of the blade and give an idea of how these can lead to a mixing process with the main flow as Denton suggests (Denton, 1993).

### Tip Clearance Loss

The tip clearance loss is the loss produced as a consequence of the mixing between the main flow and the leakage flow. Being this last one understood as the flow coming from the clearance between the stator and the turbine shaft or the clearance between the rotor and the turbine casing (Dahlquist, 2008). In Figure 2-5 it can be distinguished the leakage flow over the blades creating vortices. One of the obvious effects of flow leakage over the tip is a change in the mass flow through the blade passage, which would be likely seen as a reduction in work, but this is not necessarily associated with a loss of efficiency (Denton, 1993).

This clearance loss is analyzed according to the blade category, shrouded or unshrouded. The distinction is made because the mixing process differs in each case and so the entropy generation. For unshrouded blades the leakage flow is driven as a consequence of the pressure difference between the blades pressure side and suction side. During this process the flow creates a recirculation bubble at the edge of the pressure side and reduces the effective area for the leakage flow. Hence, depending on the size of the bubble, this leakage flow might diffuse and get turbulent originating an entropy increase (Denton, 1993). Figure 2-7 shows the behavior of the flow over the tip gap for an unshrouded blade. In this figure it is possible to see how the thickness of the blade leads also to the mixing of the flows

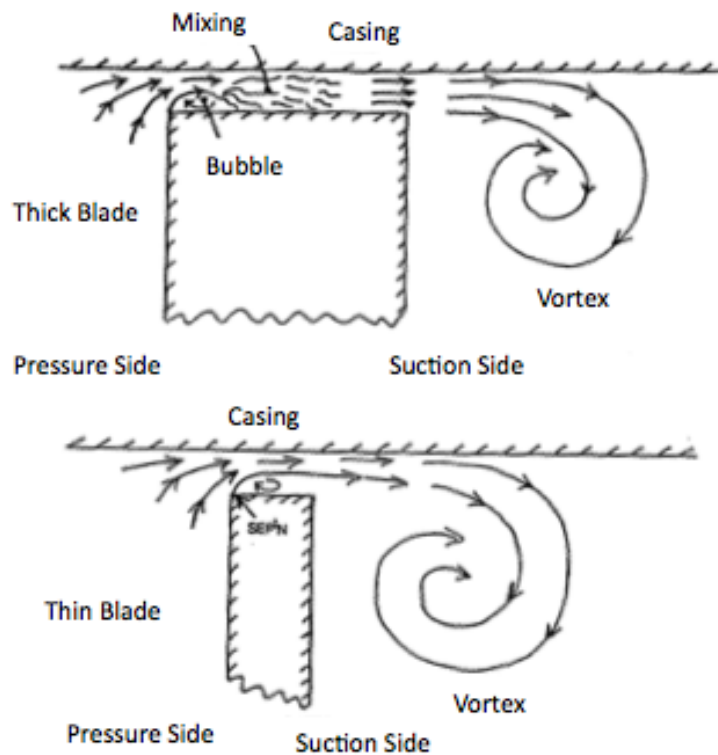


Figure 2-7 Flow over the tip gap for an unshrouded blade (Denton, 1993)

Regarding the shrouded blades, it is often common to have seals and these play an important role in the behavior of the leakage flow. In this case the leakage flow is considered to contract to a jet as a consequence of the top seal. This jet flow mixes out in the clearance space generating an entropy increase (Denton, 1993). When there is no such seal on the upstream of the blade, the shroud still gets the leakage flow to be skewed due to a great shear in the clearance gap affecting the main flow once they meet

downstream the blade (Dahlquist, 2008). In Figure 2-8 it is possible to visualize the behavior of the flow over a shrouded turbine blade with a single tip seal. Here is possible to distinguish how the leakage flow contracts to a jet and then a mixing process occurs in the clearance.

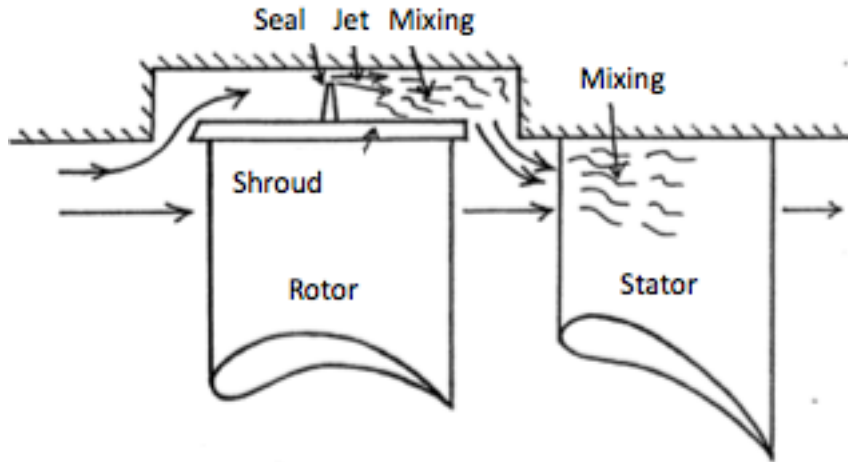


Figure 2-8 Flow over a shrouded tip seal (Denton, 1993)

The correlations exposed in both Kacker-Okapuu and Craig-Cox works agree in the fact that they were obtained from experimental data as the result of turbine cascade test. Kacker and Okapuu's correlation shows a methodology to estimate a direct pressure loss coefficient for shrouded blades, whereas for unshrouded they describe another method to estimate an efficiency debit instead (Kacker & Okapuu, 1981). Craig and Cox's correlation also describes an equation to obtain a total efficiency debit due to the tip leakage loss. This equation is applicable to shrouded blades but extendable to unshrouded by multiplying it by a constant factor (Craig & Cox, 1971). Finally Denton gives two complete different methods to estimate the tip clearance loss. For shrouded blades Denton provides a methodology mainly dependent on the mass flow going through the clearance and the relative flow angles. On the contrary, the cube of the velocity among the blade surface is the key parameter for the case of unshrouded blades (Denton, 1993).

## 2.4. Loss Correlation Models

Prior to performing the task of the implementation of loss correlation methods in the one-dimensional mean line calculation tool it is necessary to describe the more common loss models used in turbines performance estimation. The present section of the work will focus on describe the correlations suggested by different researchers, showing the equations and figures as extracted from their original work. No deep analysis of the correlations is performed in this section of the work, instead discussions are held in chapter 7. The first correlation explained is that provided by Kacker and Okapuu (Kacker & Okapuu, 1981), which was originally developed by Ainley and Mathieson (Ainley & Mathieson, 1951). This is the existing correlation in the 1D tool, LUAX-T (Genrup, 2008). For sake of simplicity the model will be called AMDCKO during the rest of the present work. This name is an acronym formed with the first letter of each one of the researchers that have either developed or refined the original model. There will be also explained two other loss correlations. The Craig-Cox (Craig & Cox, 1971) and Denton (Denton, 1993) loss correlations will be described in order to understand both methodologies properly before putting them into effect in LUAX-T (Genrup, 2008) and hence obtain a good implementation as a result.

### 2.4.1. AMDCKO

The AMDCKO loss correlation was originally developed by Ainley and Mathieson and some refinements have been made to the first model afterwards by Dunham and Came and by Kacker and Okapuu (Kacker & Okapuu, 1981). The description of the correlation in this section will focus on the methodology proposed by Kacker and Okapuu.

Kacker and Okapuu's refinement to Ainley and Mathieson's loss correlation has been found able to predict the efficiencies of a wide range of axial turbines of conventional stage loading coefficient within 1.5% of accuracy (Kacker & Okapuu, 1981). This method introduced new considerations regarding compressibility and shock losses into the calculation of profile and secondary losses. In the AMDCKO correlation the losses are measured as pressure loss coefficients. The total pressure loss coefficient is the result of the addition of different loss coefficients, one per each of the main loss mechanisms. These are the profile, secondary, tip clearance and trailing edge losses.

$$Y_{TOT} = Y_P + Y_S + Y_{TET} + Y_{clr}$$

Eq. 2-28

The correlations described by Kacker and Okapuu in their work to estimate each of the coefficients involved in Eq. 2-28 are next explained (Kacker & Okapuu, 1981).

#### Profile Loss Parameter

The basis for the profile loss coefficient in the AMDCKO correlation is a set of cascade test results. These results are expressed in terms of pitch to chord ratio and cascade exit gas angle (outlet relative flow angle) for two especial cases: nozzle and impulse blades (Kacker & Okapuu, 1981). Figures in next page show the loss coefficients for inlet blade angle equal to zero (nozzle) and for impulse blading respectively.

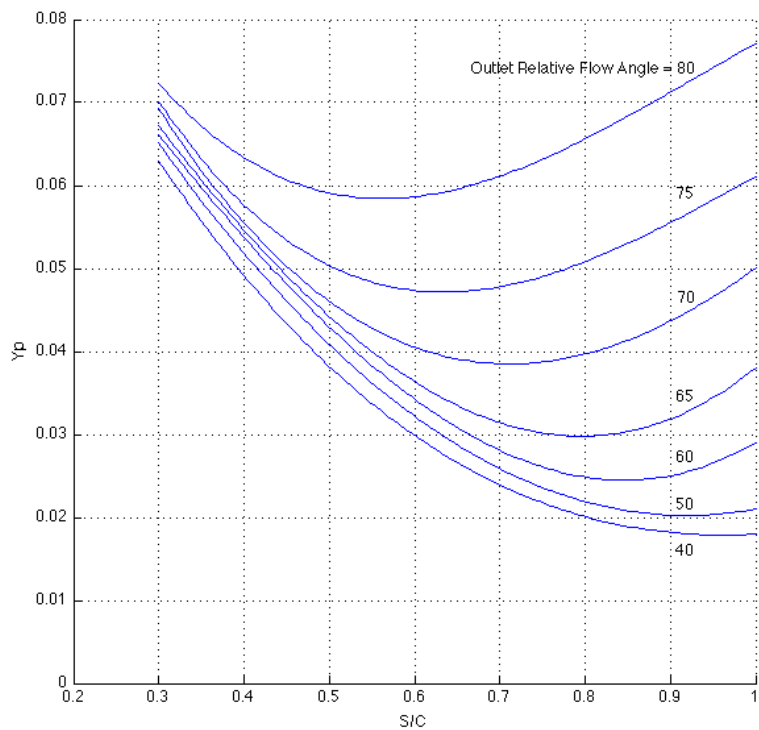


Figure 2-9 AMDCKO Profile Loss Coefficient – Nozzle blades (Kacker & Okapuu, 1981)

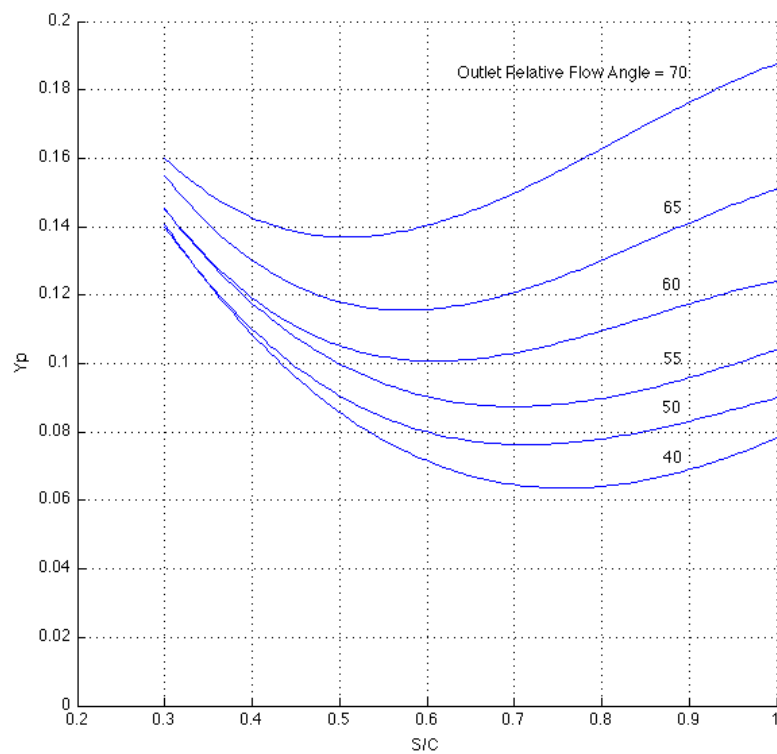


Figure 2-10 AMDCKO Profile loss Coefficient - Impulse blades (Kacker & Okapuu, 1981)

For any other combination of angles Ainley and Mathieson propose the use of the correlation exposed in Eq. 2-29.

$$Y_{P(i=0)} = \left\{ Y_{P(\alpha'_{in}=0)} + \left( \frac{\alpha'_{in}}{\alpha'_{out}} \right)^2 [Y_{P(\alpha'_{in}=\alpha'_{out})} - Y_{P(\alpha'_{in}=0)}] \right\} \left( \frac{t'_{max}/l}{0.2} \right)^{\frac{\alpha'_{in}}{\alpha'_{out}}}$$

Eq. 2-29

The figures showed in the previous page are delimited to turbine tests considering a fixed trailing edge thickness of 0.02 and for a Reynolds number of  $2.10^5$  (Ainley & Mathieson, 1951). Therefore it was needed to extend the correlation to consider a wider range of possibilities. Kacker and Okapuu's loss prediction method introduced a new Reynolds factor, which affects only the profile loss. For the use of this factor they assume a Reynolds number based on true chord and cascade exit flow conditions. The introduced factor can be estimated from Eq. 2-30 according to the flow conditions, whether laminar or turbulent.

$$\chi_{Re} = \begin{cases} \left( \frac{Re}{2 \times 10^5} \right)^{-0.4} & \text{if } Re \leq 2 \times 10^5 \\ 1.0 & \text{if } 2 \times 10^5 < Re \leq 10^6 \\ \left( \frac{Re}{10^6} \right)^{-0.2} & \text{if } Re > 10^6 \end{cases}$$

Eq. 2-30

The original methodology developed by Ainley and Mathieson was derived from cascade tests carried out at subsonic conditions. Thus, the method was not accurate enough for turbines operating at higher Mach number levels. Being aware of this, Kacker and Okapuu introduced a factor "K<sub>p</sub>", shown next in Eq. 2-31, as a correction to consider supersonic conditions. This factor is calculated for outlet Mach numbers greater than 0.2.

$$K_p = 1 - 1.25(M_{out} - 0.2) \left( \frac{M_{in}}{M_{out}} \right)^2$$

Eq. 2-31

However, higher Mach number conditions can lead to shocks and these to a loss generation. In this regard, Kacker and Okapuu give a correction parameter for shock loss estimation. This parameter is a function of the inlet Mach number at the hub and the inlet and outlet mean line Mach numbers (Kacker & Okapuu, 1981). Equations below show how to estimate this shock loss factor by calculating first the inlet Mach at the hub.

$$M_{in,H} = M_{in} \left( 1 + K \left| \frac{r_H}{r_T} - 1 \right|^{2.2} \right)$$

Eq. 2-32

$$Y_{shock} = 0.75(M_{in,H} - 0.4) 1.75 \left( \frac{r_H}{r_T} \right) \left( \frac{p_{in}}{p_{out}} \right) \frac{1 - \left[ 1 + \left( \frac{\gamma-1}{2} \right) M_{in}^2 \right]^{\frac{\gamma}{\gamma-1}}}{1 - \left[ 1 + \left( \frac{\gamma-1}{2} \right) M_{out}^2 \right]^{\frac{\gamma}{\gamma-1}}}$$

Eq. 2-33

Where K, in Eq. 2-32, is a constant which value depends on where is the correlation used, the stator or the rotor. In this regard the values for K are set to 1.8 and 5.2 for stator and rotor respectively. The last correction made to Eq. 2-29 by Kacker and Okapuu was to consider negative inlet angles. The Eq. 2-34 shows the final correlation proposed by Kacker and Okapuu to estimate the profile loss coefficient at zero incidence (Kacker & Okapuu, 1981).

$$Y_{P(i=0)} = \left\{ Y_{P(\alpha'_{in}=0)} + \left| \frac{\alpha'_{in}}{\alpha_{out}} \right| \left( \frac{\alpha'_{in}}{\alpha_{out}} \right) \left[ Y_{P(\alpha'_{in}=\alpha_{out})} - Y_{P(\alpha'_{in}=0)} \right] \right\} \left( \frac{t'_{max}/l}{0.2} \right)^{\frac{\alpha'_{in}}{\alpha_{out}}}$$

Eq. 2-34

Finally, the profile loss correlation given by Kacker and Okapuu is shown in Eq. 2-35. These authors claimed that due to the constant development of new technologies in turbomachinery, two multiplying factors were to be considered in the final correlation given. These factors were encountered to be 0.914 and 2/3 given that these values gave a closer approach to empirical data results (Kacker & Okapuu, 1981).

$$Y_p = 0.914 \left( \frac{2}{3} K_p \chi_i Y_{P(i=0)} + Y_{shock} \right)$$

Eq. 2-35 AMDCKO – Profile Loss parameter

#### Secondary Loss coefficient

Dunham and Came were the first to relate the secondary losses directly with the aspect ratio (Dunham & Came, 1979). The correlation proposed for the secondary loss estimation by these last authors in 1970 is shown in Eq. 2-36. The introduction of this ratio into the correlation was of main importance but not sufficiently accurate according to Kacker and Okapuu, who reviewed the correlation and proposed a new one.

$$Y_s = 0.0334 \left( \frac{l}{H} \right) [4(\tan \alpha_{in} - \tan \alpha_{out})^2] \left( \frac{\cos^2 \alpha_{out}}{\cos \alpha_m} \right) \left( \frac{\cos \alpha_{out}}{\cos \alpha'_{in}} \right)$$

Eq. 2-36

Kacker and Okapuu realized that for lower aspect ratio values the secondary loss was not linearly proportional to the inverse of this parameter. Hence they introduced a correction concerning the aspect ratio influence. This correction factor is calculated as shown below in Eq. 2-37. Finally, they considered that compressibility effects should be also considered in the estimation of the secondary loss mechanism. Thus the same factor ‘Kp’ introduced for profile loss is used for this loss mechanism. The final secondary loss correlation given by Kacker and Okapuu is shown in Eq. 2-38.

$$\chi_{AR} = \begin{cases} 1 - 0.25 \sqrt{2 - \frac{H}{l}} & \text{for } H/l \leq 2 \\ 1 & \text{for } H/l > 2 \end{cases}$$

Eq. 2-37

$$Y_s = 0.04 \left( \frac{l}{H} \right) \chi_{AR} [4(\tan \alpha_{in} - \tan \alpha_{out})^2] \left( \frac{\cos^2 \alpha_{out}}{\cos \alpha_m} \right) \left( \frac{\cos \alpha_{out}}{\cos \alpha'_{in}} \right) \left[ 1 - \left( \frac{lx}{H} \right)^2 (1 - K_p) \right]$$

Eq. 2-38 AMDCKO - Secondary loss parameter

### Tip Leakage Loss Coefficient

Kacker and Okapuu proposed two different loss correlations to estimate the tip clearance loss mechanism according to the blade category, whether shrouded or not.

#### - Shrouded Blades:

The correlation for shrouded blades is similar to the one described by Dunham and Came in their work (Dunham & Came, 1979). In change, Kacker and Okapuu introduced a new parameter defined by them as the effective tip clearance. This parameter was to be used instead of the tip clearance factor proposed by Dunham and Came. This effective tip clearance is obtained as a function of the number of seals on the shrouding as Eq. 2-39 shows.

$$\tau' = \frac{\tau}{(\# \text{ of } \text{seals})^{-0.42}}$$

Eq. 2-39

Finally, Eq. 2-40 shows the correlation for tip leakage loss estimation when considering shrouded blades given by Kacker and Okapuu (Kacker & Okapuu, 1981).

$$Y_S = 0.37 \frac{l}{h} \left( \frac{\tau'}{l} \right)^{0.78} 4(\tan \alpha_{in} - \tan \alpha_{out})^2 \left( \frac{\cos^2 \alpha_{out}}{\cos \alpha_m} \right)$$

Eq. 2-40 AMDCKO – Tip Leakage Loss Coefficient for shrouded blades

#### - Unshrouded blades:

For unshrouded blades, Kacker and Okapuu's correlation is based on estimating an efficiency debit due to tip leakage. The variation in the efficiency is a function of the total-to-total efficiency when the tip clearance is assumed to be zero, the tip to mean radius ratio, the outlet angle and the variation of tip clearance. This efficiency debit can be estimated from equation below (Kacker & Okapuu, 1981).

$$\Delta \eta_{tt} = 0.93 \left( \frac{r_T}{r_m} \right) \left( \frac{1}{H \cos \alpha_{out}} \right) \eta_{tt,0} \Delta \tau$$

Eq. 2-41 AMDCKO – Tip Leakage Efficiency debit for unshrouded blades

### Trailing Edge Loss Coefficient

Kacker and Okapuu were the first to introduce the effect of the thickness of the trailing edge as an individual pressure loss coefficient. This loss coefficient is mainly a function of the trailing edge thickness and the throat. It is predicted as an energy loss parameter, this means that it is necessary to convert it into a pressure loss coefficient. The Figure 2-11 shows how the energy loss coefficient due to trailing edge is a function of tests made for both axial entry nozzle and impulse blading. Afterwards in Eq. 2-42 it is shown the correlation for any combination of angles (Kacker & Okapuu, 1981). Finally Eq. 2-43 is used to convert this energy loss into a pressure loss coefficient.

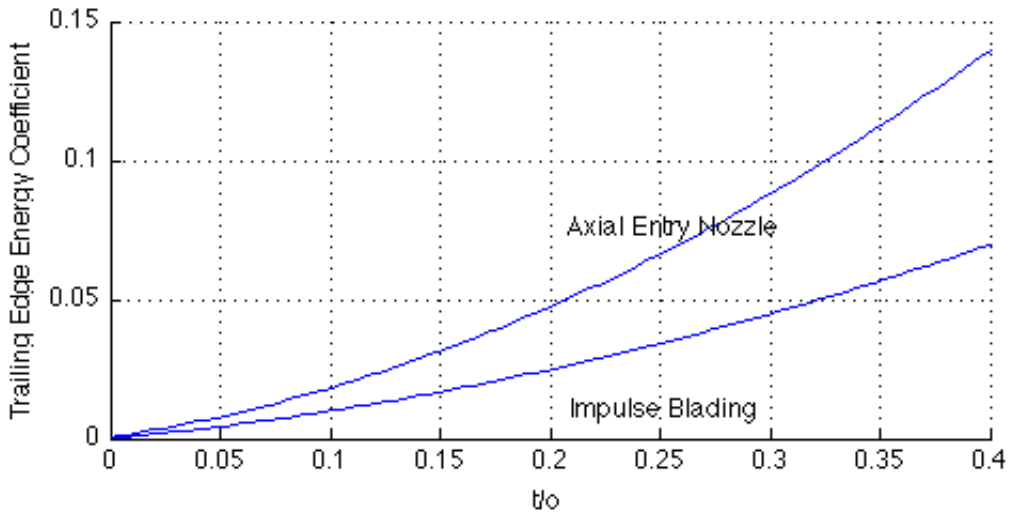


Figure 2-11 Trailing Edge loss energy coefficient

$$\Delta E_{Te} = \Delta E_{Te(\alpha'_{in}=0)} + \left| \frac{\alpha'_{in}}{\alpha'_{out}} \right| \left( \frac{\alpha'_{in}}{\alpha'_{out}} \right) \left[ \Delta E_{Te(\alpha'_{in}=\alpha_{out})} - \Delta E_{Te(\alpha'_{in}=0)} \right]$$

Eq. 2-42

$$Y_{Te} = \frac{\left[ 1 + \frac{\gamma-1}{2} M^2_{out} \left( \frac{1}{1-\Delta E_{Te}} - 1 \right) \right]^{\frac{-\gamma}{\gamma-1}} - 1}{1 - \left( 1 + \frac{\gamma-1}{2} M^2_{out} \right)^{\frac{-\gamma}{\gamma-1}}}$$

Eq. 2-43 AMDCKO – Trailing Edge Loss Coefficient

## 2.4.2.Craig & Cox

In 1971 Craig and Cox introduced a comprehensive method for estimating the performance of axial turbines based on the analysis of linear cascade tests on blading and on several turbine tests results. In their methodology, Craig and Cox's suggest that the total breakdown of losses should be subdivided in 2 groups of different loss mechanisms in which it is assumed that none of them interacts with another.

**Table 2-1 Craig and Cox - Group Losses Distribution (Craig & Cox, 1971)**

Group 1 Losses	Group 2 Losses
Guide profile loss	Guide gland leakage loss
Runner profile loss	Balance hole loss
Guide secondary loss	Rotor tip leakage loss
Runner secondary loss	Lacing wire loss
Guide annulus loss	Wetness loss
Runner annulus loss	Disc windage loss
	Losses due to partial admission

Craig and Cox have suggested to evaluate Group 1 losses as enthalpy loss factors based on measurable parameters. Some of these parameters are the relative outlet and inlet velocities, regarding profile and secondary losses. On the contrary, Group 2 losses are evaluated as a net deficit in stage efficiency. Under these assumptions, the authors define the overall stage total head efficiency as shown in Eq. 2-26.

$$\eta = \frac{\Delta W_{blading}}{\Delta W_{blading} + G1_{losses}} - \sum G2_{\eta_{debits}}$$

**Eq. 2-44 Turbine Efficiency**

The Group 1 losses term, shown in Eq. 2-44 can be calculated by approximating the term to Eq. 2-45. In this equation the first term (left side) refers to the guide blade losses and the second one to the runner blade.

$$G1_{losses} = (X_p + X_s + X_a)_S \frac{C_1^2}{200gJ} + (X_p + X_s + X_a) \frac{C_2^2}{W_2^2} R \frac{W_2^2}{200gJ}$$

**Eq. 2-45 Group 1 Losses**

Craig and Cox's loss correlation is an analysis of linear cascade data and relies on the choice of independent variables. Therefore it is necessary to check the final correlation against the range of variables encountered in practice to know if the right choice of independent variables has been made. Based on the analysis of over 100 specific cascade tests, Craig and Cox finally determined that the losses are related to velocity coefficients and also dependent on some parameters as Reynolds number, aspect ratio, blade angles, pitch to backbone length ratio and Mach number. Next is described the methodology proposed by these authors to estimate the loss mechanisms in each one of the two groups.

### Group 1 Losses

In this section are described the correlations proposed for estimating the loss mechanisms: profile loss, secondary loss and annulus loss. Craig and Cox's methodology involves one single equation for each loss mechanism. These equations are shown in next page. Nonetheless, it is possible to see that each equation

is the result of the interaction of different factors, which adds more complexity to the whole correlation. Below the equations are shown each of the methods needed to compute them.

$$X_P = x_{pb} N_{pr} N_{pi} N_{pt} + (X_P)_t + (X_P)_{s/e} + (X_P)_m$$

Eq. 2-46 C&C - Profile Loss Parameter

$$X_S = N_{sr} (N_s)_{h/b} X_{Sb}$$

Eq. 2-47 C&C - Secondary Loss Parameter

$$X_a = X_{a1} + X_{a2} + X_{a3}$$

Eq. 2-48 C&C - Annulus Loss Parameter

### Profile Loss

Craig and Cox proposed the use of Eq. 2-46 for estimation of the total profile loss parameter, in which each one of the parameters involved is obtained through different correlations and figures. Next paragraphs will describe how to obtain each one of them.

First parameter involved is the Reynolds effect factor. To measure this effect the authors suggest the use of a loss ratio  $N_{pr}$ , for profile losses. This ratio depends on the Reynolds number based on blade opening and the ratio between the equivalent sand grain size and the backbone length. It is important to mention that such correlation does not consider any Mach number effects. Figure 2-12 is used to obtain the loss ratio due to Reynolds effect.

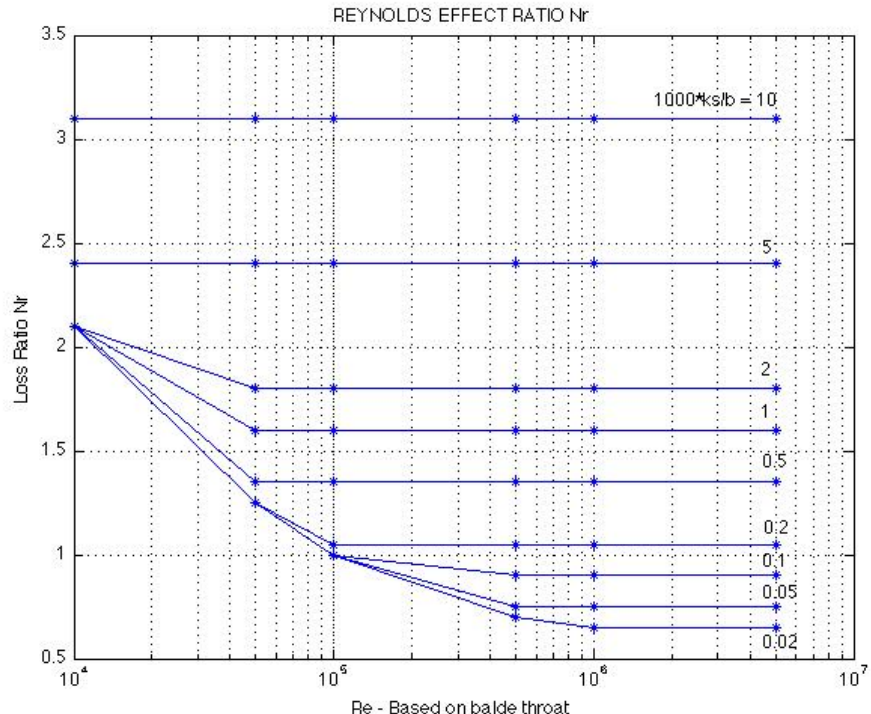


Figure 2-12 Reynolds Effect on Profile Loss Parameter (Craig & Cox, 1971)

In order to estimate the value of the basic profile loss parameter, Craig and Cox introduced two important terms: the lift parameter  $F_L$  and the Contraction Ratio. The lift parameter,  $F_L$ , must be obtained from a relation of the inlet and outlet flow angles. In Figure 2-13 are shown the values of  $F_L$  for different cases.

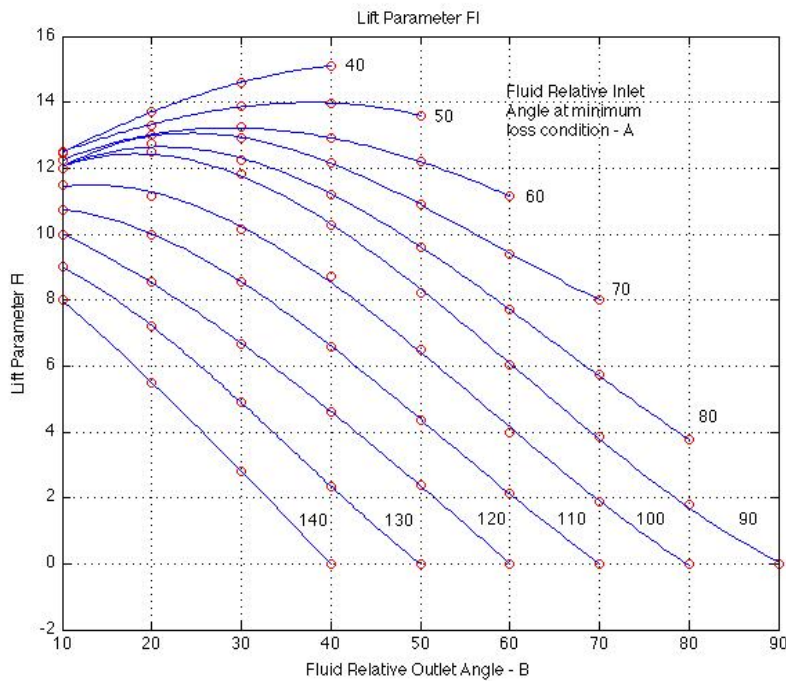


Figure 2-13 Lift Parameter (Craig & Cox, 1971)

The contraction ratio, CR, is a function of the pitch to backbone length and the inlet and outlet relative flow angles. The correlation proposed by Craig and Cox to estimate the value of this parameter is described as follows in Figure 2-14. Once estimated the values for the lift parameter and the contraction ratio, the basic profile loss parameter can be estimated from the diagram shown in next page.

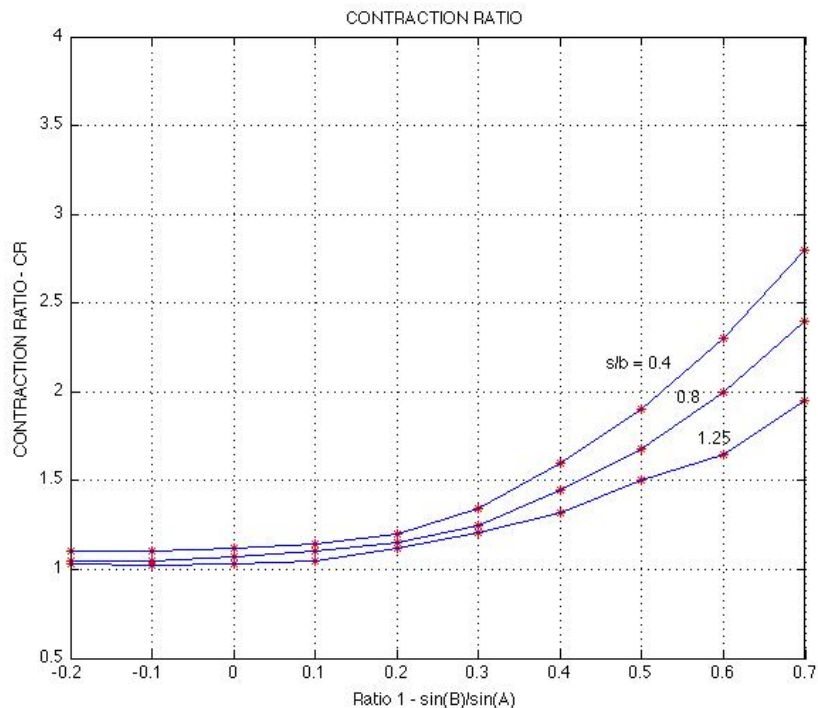


Figure 2-14 Contraction Ratio (Craig & Cox, 1971)

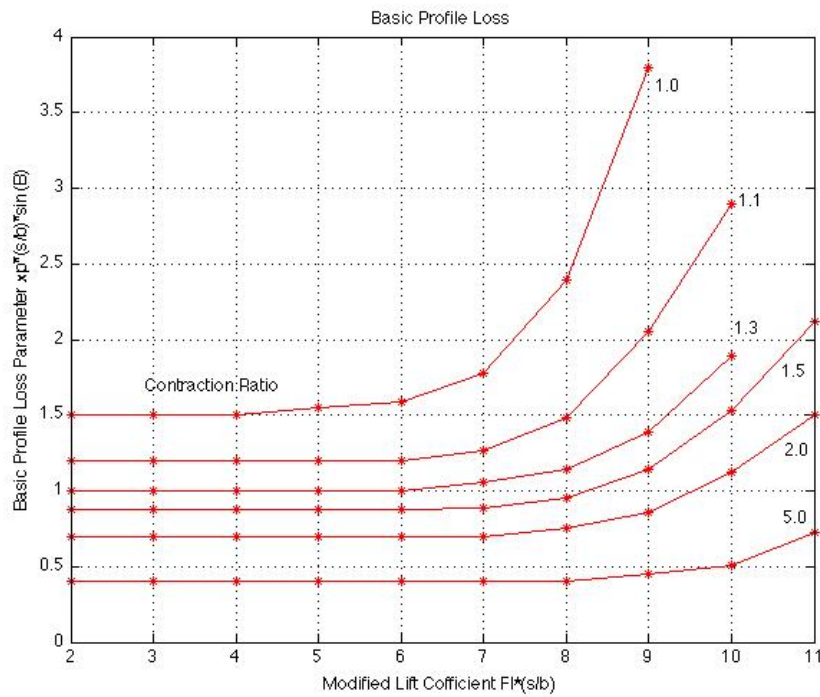


Figure 2-15 Basic Profile Loss Parameter (Craig & Cox, 1971)

However, Eq. 2-46 shows that the profile loss parameter is influenced by different ratios. First of these ratios was already discussed, the Reynolds effect ratio. Regarding the other two, one is to consider the trailing edge loss effect and the other for off design conditions and high incidence values. The trailing edge loss ratio parameter,  $N_{pt}$ , is obtained as a function of the trailing edge thickness to pitch ratio and the fluid outlet relative angle as shown in Figure 2-16. On the other hand, the incidence ratio will be explained at the end of this section since the main focus is for on design conditions.

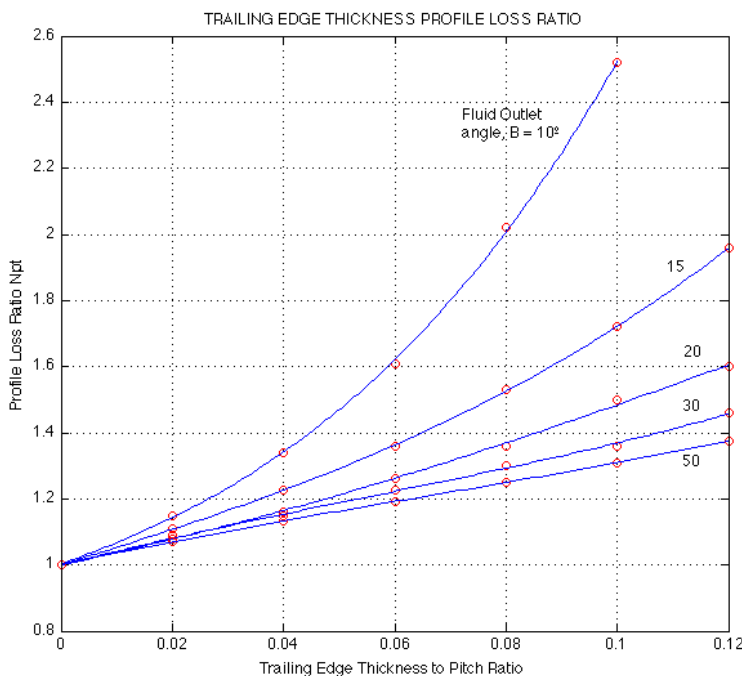
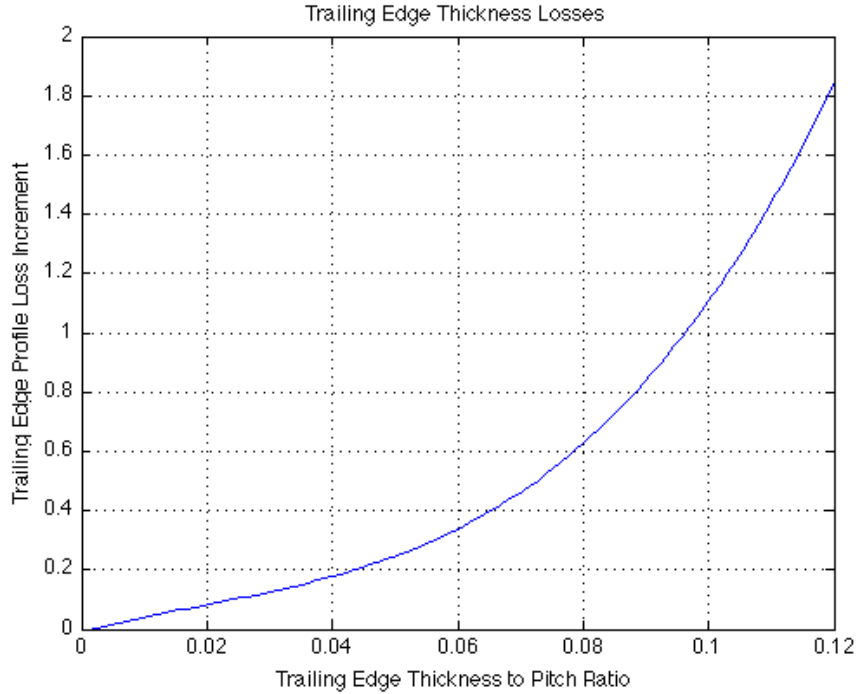


Figure 2-16 Trailing Edge Effect Profile Loss Ratio (Craig & Cox, 1971)

Besides the basic profile loss parameter and the different ratios, Eq. 2-46 contains three different profile loss increments. Two of these increments are to consider the influence of higher Mach number depending on the geometry of the blade profile. The last additive loss is an extra increment due to trailing edge thickness. It is next shown how to obtain these 3 different loss additives. First, similarly to the trailing edge loss ratio, the trailing edge loss increment is a function of the trailing edge thickness to pitch ratio (Figure 2-17).



**Figure 2-17 Trailing Edge Profile Loss Increment (Craig & Cox, 1971)**

The other two loss additives are corrections regarding high Mach number values at the blade outlet. These additions are since the whole correlation was originally developed under subsonic conditions. First of these loss increments is shown in Figure 2-18 as a function of the isentropic outlet Mach number, the throat length and the trailing edge thickness. This fundamental additive is referred specifically to convergent profiles designed with a straight suction surface downstream of the throat. The second additive, on the other hand, is only required for profiles designed with a pronounced convex suction surface curvature downstream of the throat. Hence this last coefficient is a function, not only of the outlet isentropic Mach number but, of the pitch to back radius ratio, as can be seen in Figure 2-19, in next page.

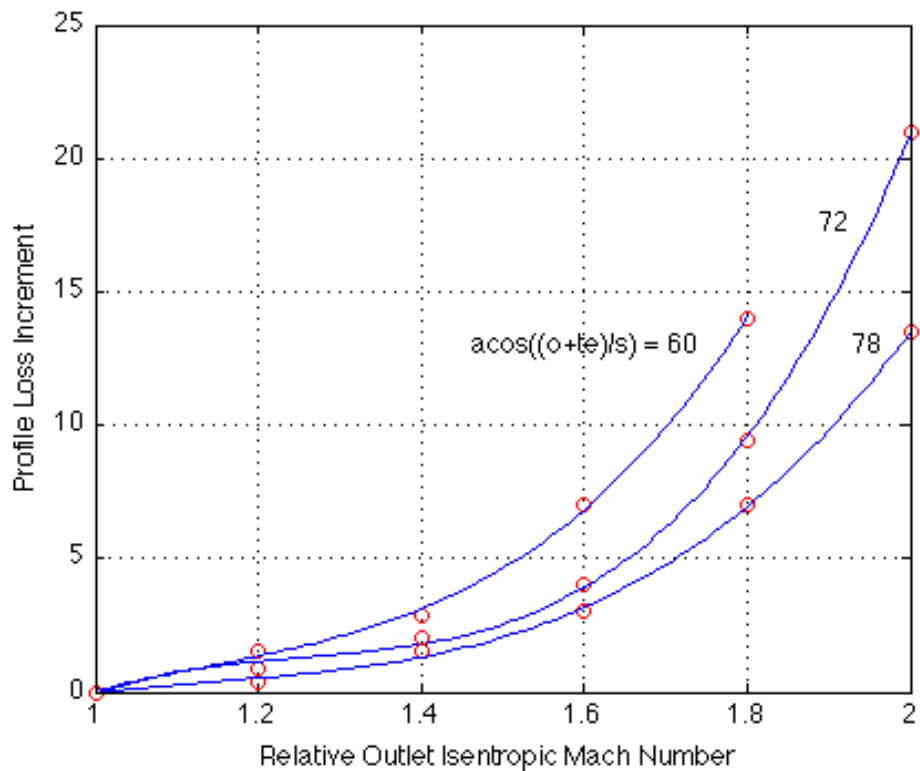


Figure 2-18 Mach Effect on Profile Loss Increment (Craig & Cox, 1971)

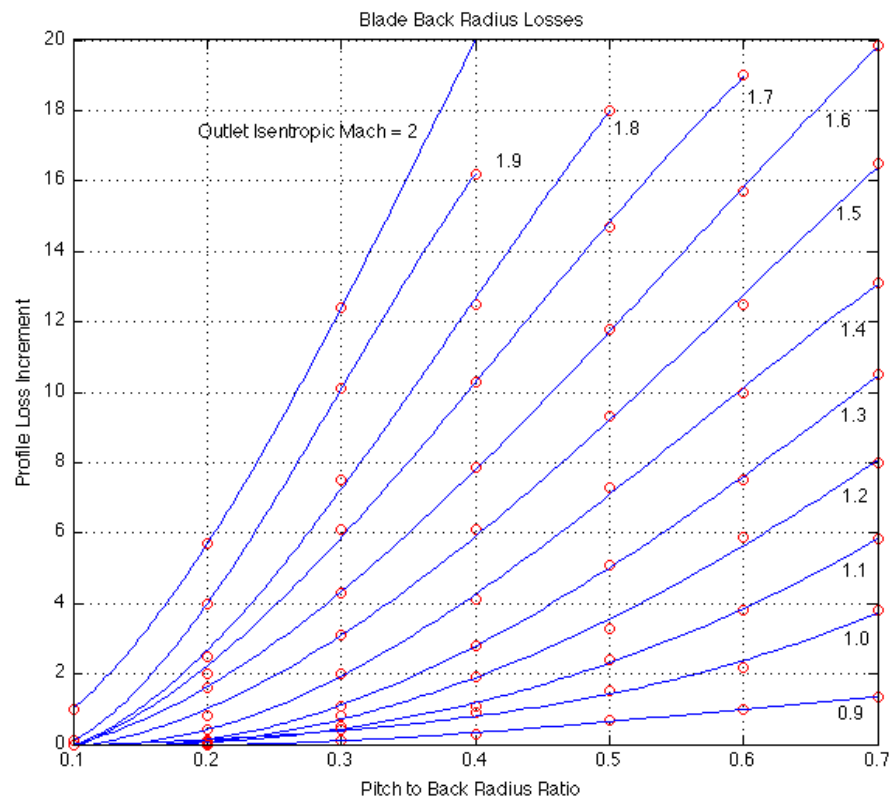


Figure 2-19 Profile Loss Increment due Pitch to Blade Back Ratio (Craig & Cox, 1971)

Finally, regarding profile loss estimation, Craig and Cox describe a methodology and correlations considering off-design application in which cases incidence losses might become appreciable. The incidence effect ratio,  $N_{pi}$ , is shown in Figure 2-20. It is a function of the incidence ratio, which in instance relies on the minimum incidence and the stalling incidence. This means that in order to obtain the incidence loss ratio it is necessary to evaluate first each one of the individual incidence parameters. Equations and correlations for calculating such parameters are shown below next figure and depend on if the inlet angle is over 90° or not.

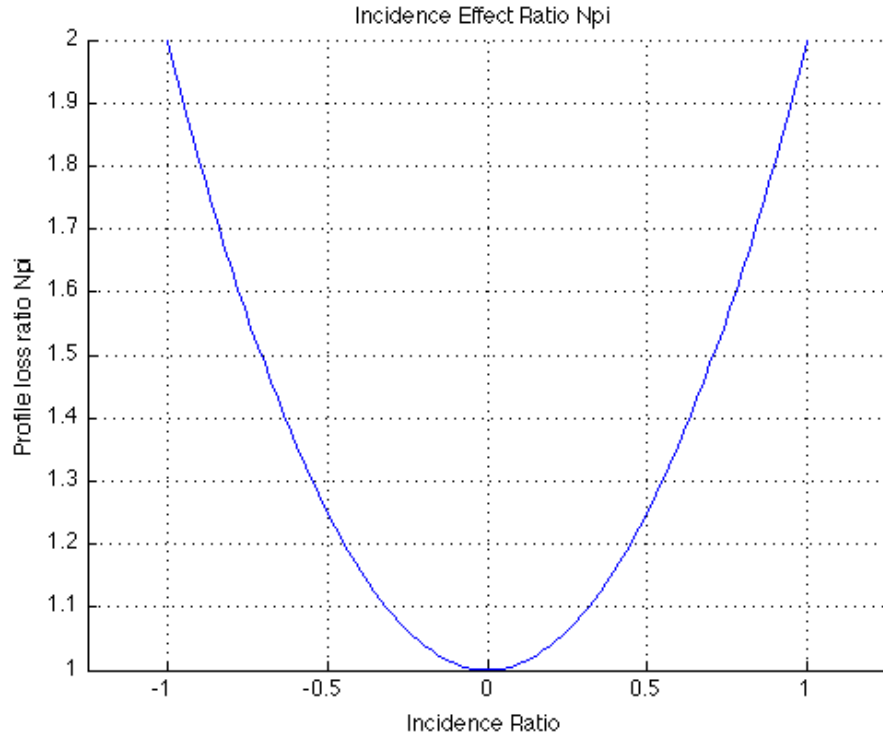


Figure 2-20 Incidence effect on Profile Loss (Craig & Cox, 1971)

When  $\alpha \leq 90^\circ$

$$i + stall = (i + stall)_{basic} + (\Delta i + stall)_{s/b} + (\Delta i + stall)_{CR}$$

Eq. 2-49

In Eq. 2-49 all terms come from different figures and correlations. The parameter  $(i+stall)_{basic}$  is obtained from Figure 2-21. Similarly, the pitch to backbone increment and the contraction ratio increment are extracted from Figure 2-22 and Figure 2-23, respectively.

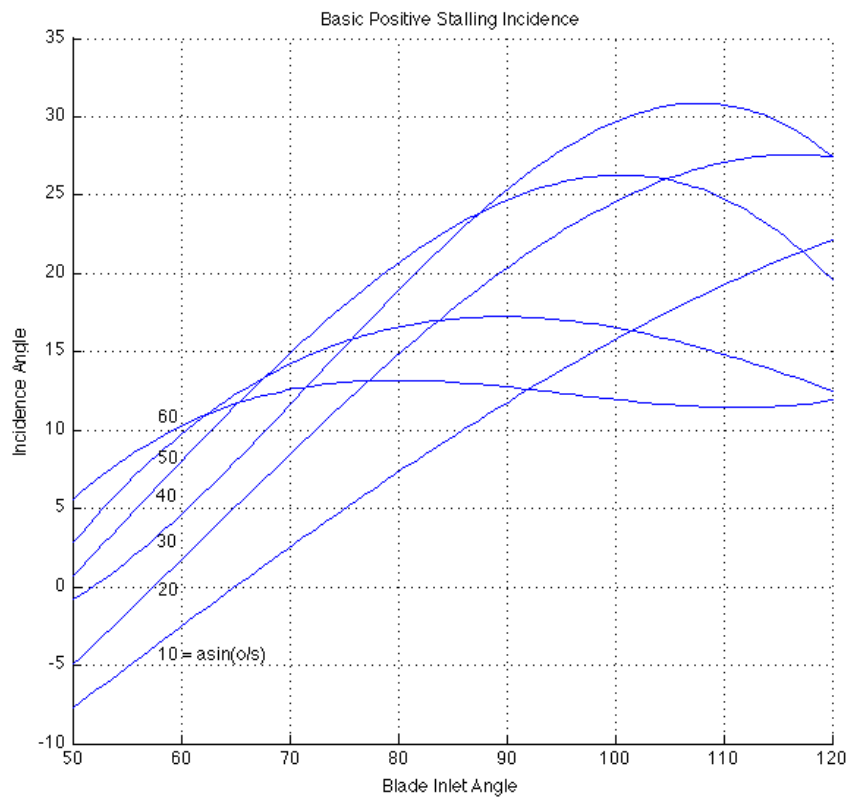


Figure 2-21 Basic Positive Stalling Incidence Parameter (Craig & Cox, 1971)

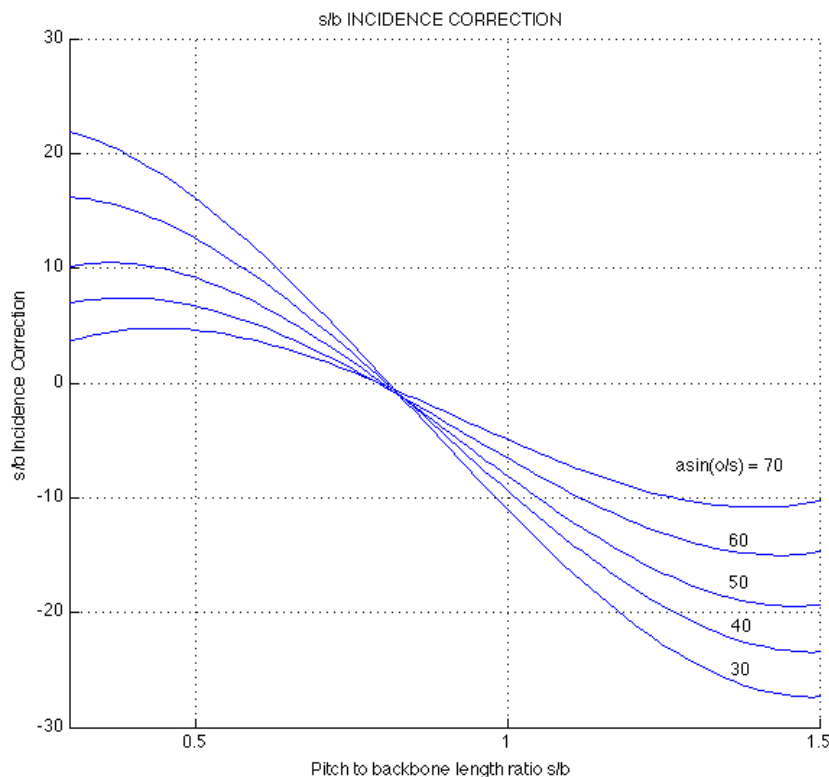
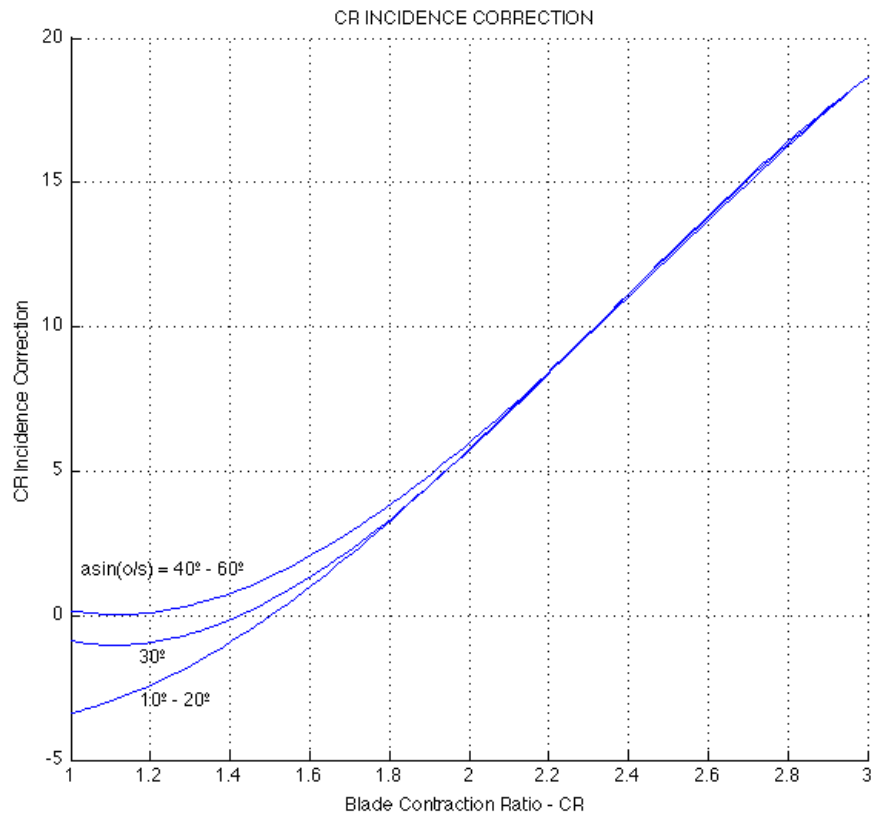


Figure 2-22 s/b Incidence Correction For Positive Stalling Incidence (Craig & Cox, 1971)



**Figure 2-23 CR Incidence Correlations for Positive Stalling Incidence (Craig & Cox, 1971)**

Next, it is needed to determine the value for the negative stalling incidence. The term (*i*-stall) is calculated from Eq. 2-50 in which the values for the parameters (*i*-stall)<sub>basic</sub> and ( $\Delta i$ -stall)<sub>s/b</sub> are extracted from Figure 2-24 and Figure 2-25 respectively, both shown in next page.

$$i - \text{stall} = (i - \text{stall})_{\text{basic}} + (\Delta i - \text{stall})_{s/b}$$

Eq. 2-50

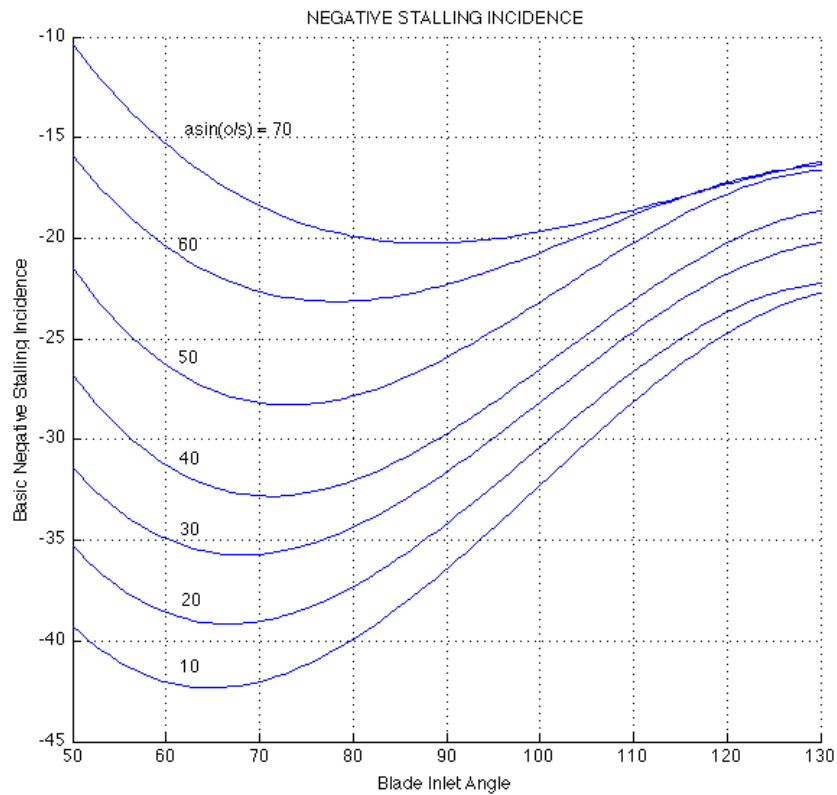


Figure 2-24 Incidence corrections for negative stalling incidence (Craig & Cox, 1971)

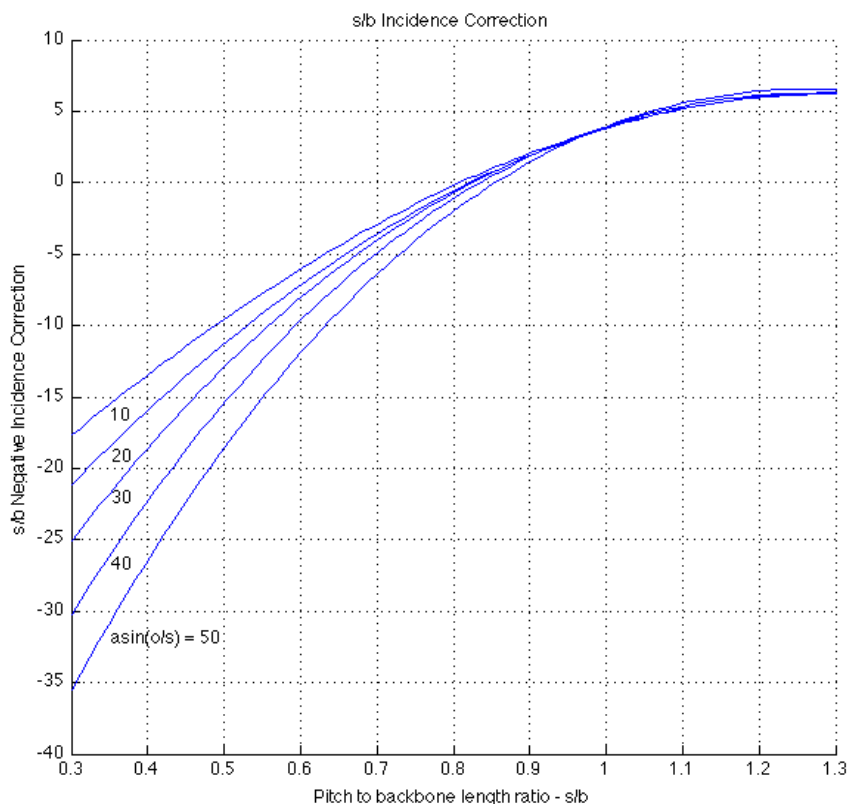


Figure 2-25 s/b Incidence Correction for Negative Stalling Incidence (Craig & Cox, 1971)

When  $\alpha > 90^\circ$ :

For this case, Craig and Cox gave different correlations to estimate the positive and negative stalling incidence values. The methodologies suggested are shown next. First, as similar to other case, it is calculate the positive stalling incidence as show in Eq. 2-51.

$$i + stall = (i + stall)_{basic} + \left(1 - \frac{\alpha - 90}{90 - \sin^{-1}(o/s)}\right)[(\Delta i + stall)_{s/b} + (\Delta i + stall)_{CR}]$$

Eq. 2-51

Where the  $(i+stall)_{basic}$  term is obtained from the upper part of Figure 2-26 and both last terms on the right side of Eq. 2-51 are similar to the corrections shown in figures Figure 2-22 and Figure 2-23. Next it is necessary to calculate the total negative stalling incidence term,  $i-stall$ . This term is calculated from Eq. 2-52. The factor  $(i-stall)_{basic}$  is extracted form the lower side of Figure 2-26 and the correction for pitch to backbone ratio from Figure 2-25.

$$i - stall = (i - stall)_{basic} + \left(1 - \frac{\alpha - 90}{90 - \sin^{-1}(o/s)}\right)(\Delta i - stall)_{s/b}$$

Eq. 2-52

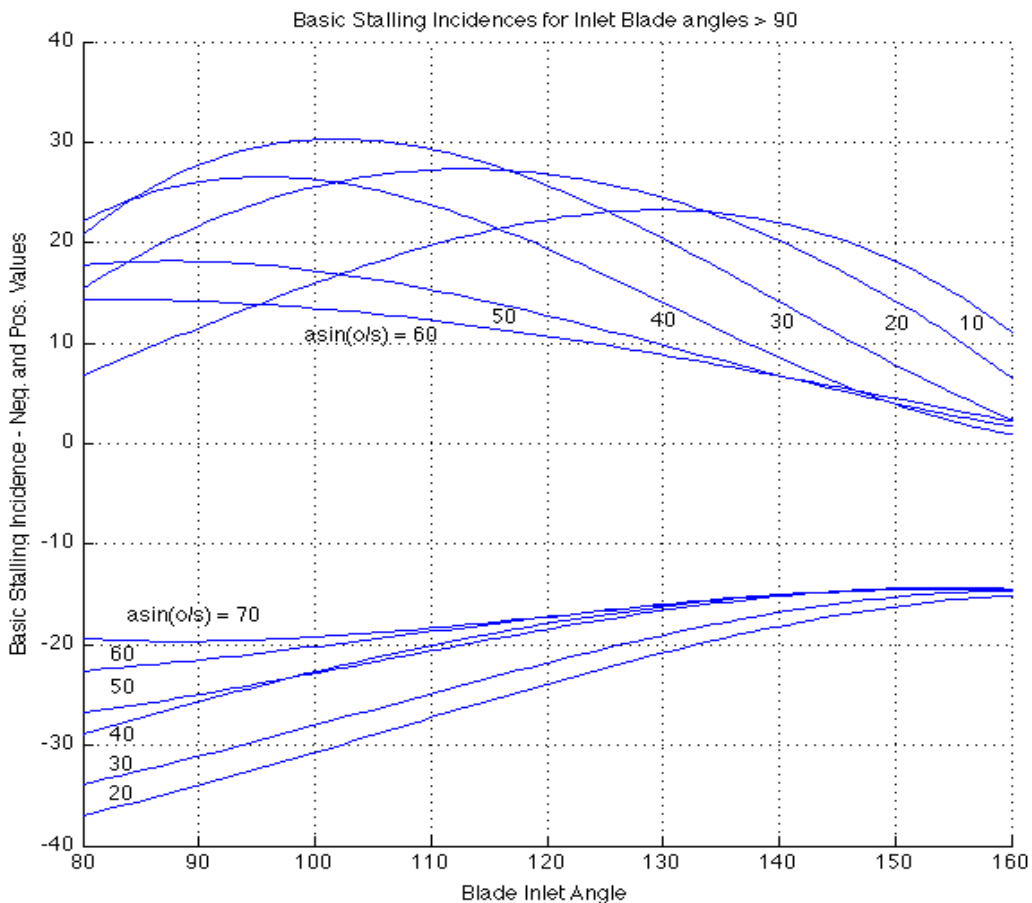


Figure 2-26 Basic Stalling Incidences for Inlet Blade angle over  $90^\circ$  (Craig & Cox, 1971)

Finally, same procedure follows for both of the inlet angle cases. The minimum loss incidence is evaluated from the Eq. 2-53, where  $F_i$  is the minimum loss incidence range ratio and is given in Figure 2-27.

$$i_{\min} = \frac{(i + \text{stall}) + F_i(i - \text{stall})}{1 + F_i}$$

Eq. 2-53

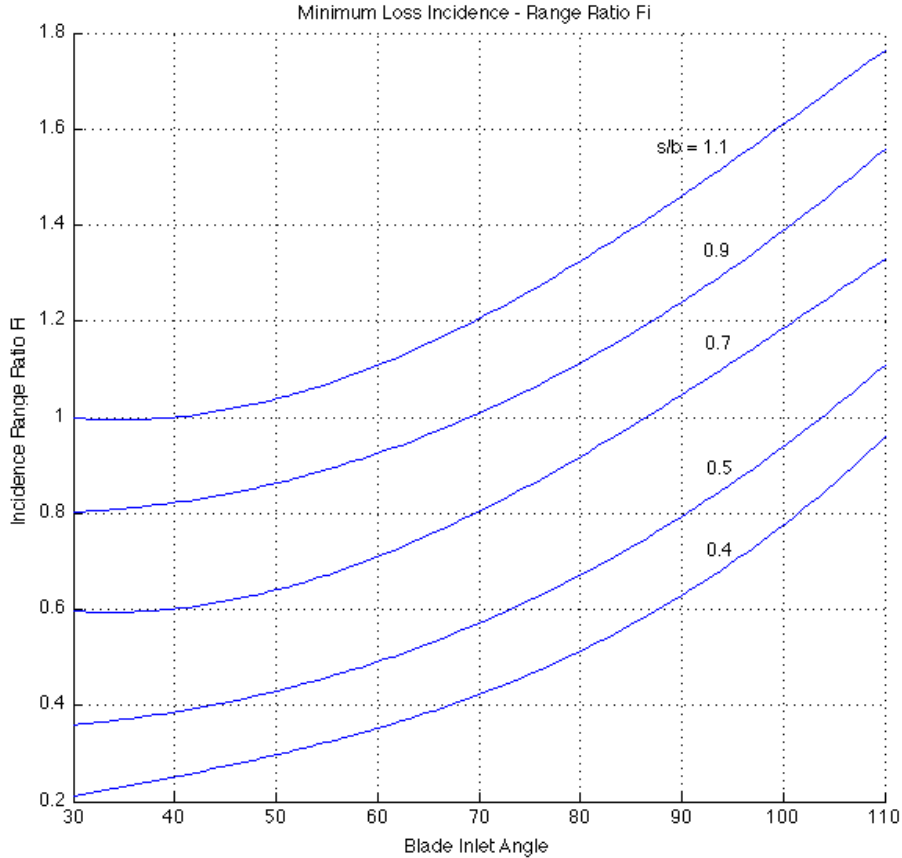


Figure 2-27 Minimum loss incidence range Ratio – Fi (Craig & Cox, 1971)

Once calculated the minimum incidence now it is possible to estimate the profile loss ratio  $N_{pi}$  from Figure 2-20, for this is needed the incidence ratio parameter. This factor is calculating by the use of Eq. 2-54 as shown below.

$$i_{RATIO} = \frac{i - i_{\min}}{|i_{stall} - i_{\min}|}$$

Eq. 2-54

It is important to notice that in this last equation it is mentioned a stalling incidence term without differentiating if the user should consider the use of the negative stalling incidence or the positive one. Craig and Cox suggest the use of the negative stalling incidence,  $(i-stall)$ , in cases where the design incidence,  $i$ , is less than the minimum incidence, otherwise the use of the positive stalling incidence,  $(i+stall)$ , is suggested.

### Secondary Loss

As shown before in Eq. 2-47, to estimate the secondary loss parameter, Craig and Cox's correlation implies the use of other factors and ratios besides the basic secondary loss parameter. The first ratio needed is the secondary loss ratio to measure the effect of Reynolds number. This parameter is similar to the one needed to compute the profile loss and shown in Figure 2-12. Second ratio needed for Eq. 2-47, is a function of the aspect ratio of the blade (Figure 2-28).

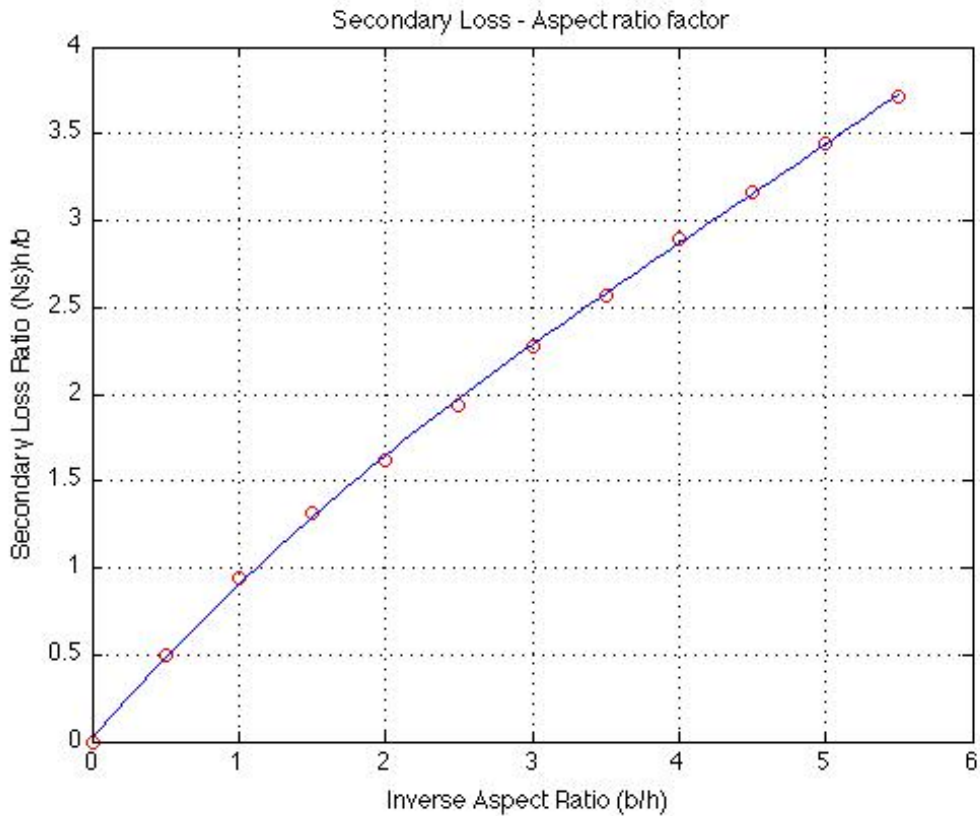


Figure 2-28 Secondary Loss Aspect Ratio Factor (Craig & Cox, 1971)

Finally, the last term of Eq. 2-47 refers to the basic secondary loss coefficient. Craig and Cox describe the basic secondary loss coefficient as a function of the lift factor,  $F_L$  (Figure 2-13) and the square of the relative mean velocity ratio across blading. For the stator this ratio should consider absolute velocities, whereas for the rotor relative velocities instead. The basic loss coefficient for this loss mechanism is shown in the next page.

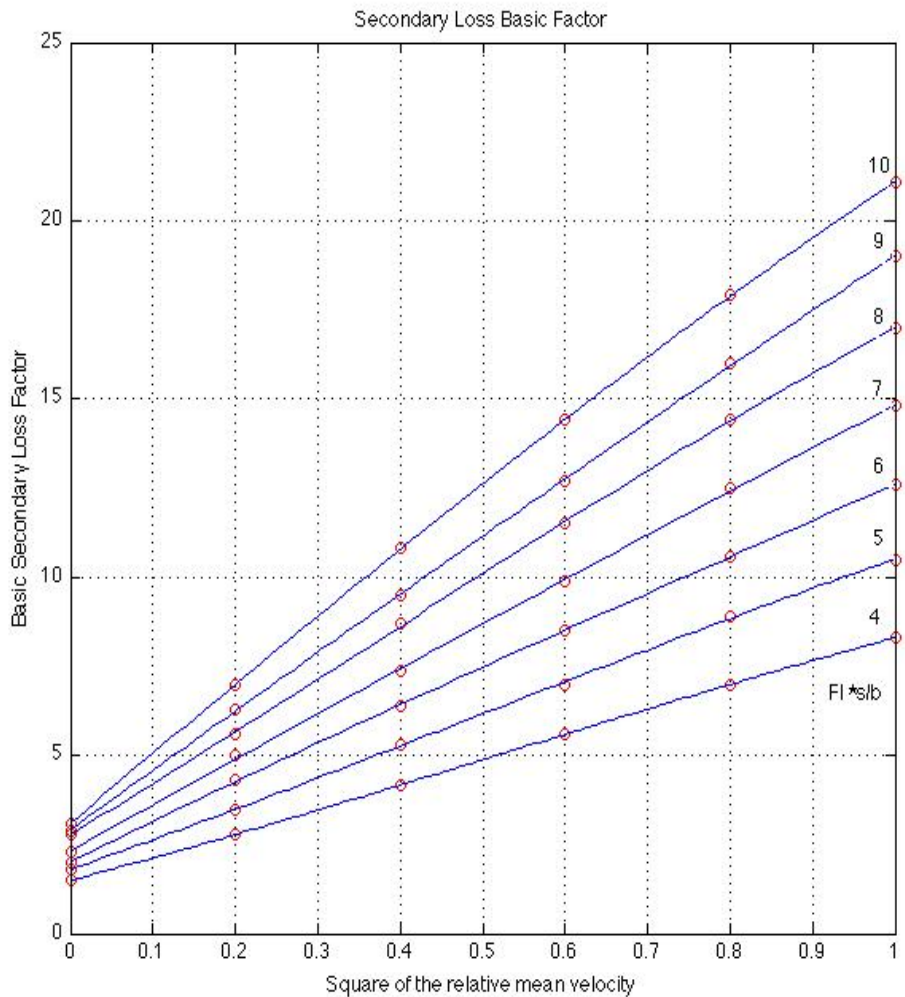


Figure 2-29 Secondary Loss - Basic loss factor (Craig & Cox, 1971)

### Annulus Loss

The annulus loss coefficient, as shown in Eq. 2-48, is the addition of three different factors; these are the annulus wall loss parameter, and two cavity loss factors. The annulus wall loss is obtained from Figure 2-30 and differs for controlled (red lines) or uncontrolled expansion (blue lines). In case of controlled expansion the factor is a function of the equivalent half cone angle and, on the other hand, if in presence of an uncontrolled expansion it is a function of the blade height to back radius ratio. Regarding the cavity loss factor,  $X_{a2}$ , Craig and Cox's correlation for its estimation is shown in Figure 2-32. This correlation is based on the geometry of the cavity. In Figure 2-32, the cavity factor  $F_a$  is a function of different cavity geometrical parameters that can be obtained from Figure 2-31 and Eq. 2-55. However, previous studies prove that this loss mechanism becomes important in the case of steam turbines with bleed of steam to feed water heaters for example (Dahlquist, 2008); hence is not present in the implementation of the model in LUAX-T. In addition, the detailed geometry of cavity and annulus wall remains unknown for first steps designs.

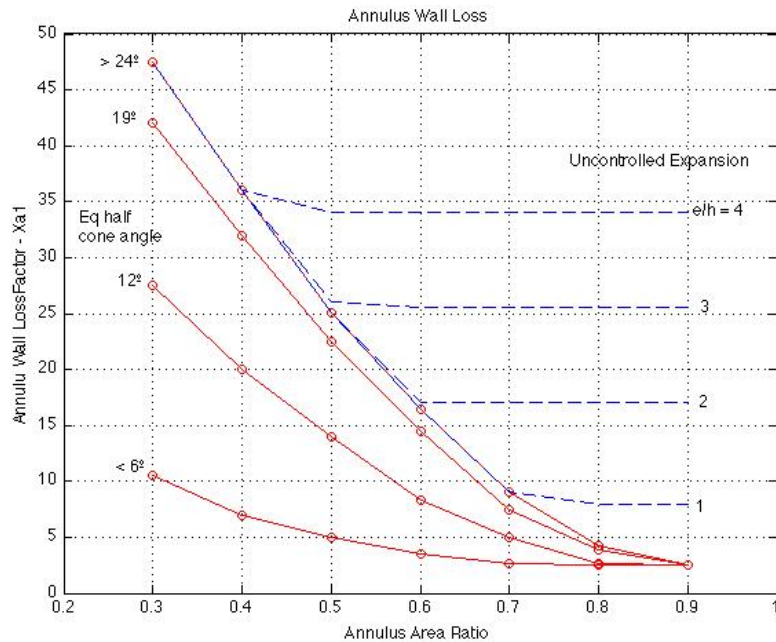


Figure 2-30 Annulus Wall Loss (Craig & Cox, 1971)

$$F_a = \frac{C_f |2(u + V) - q|}{q \cos(B)_{tip}}$$

Eq. 2-55 Cavity Factor

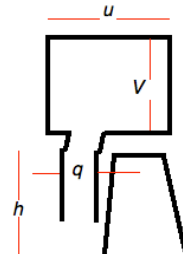


Figure 2-31 Cavity Geometry

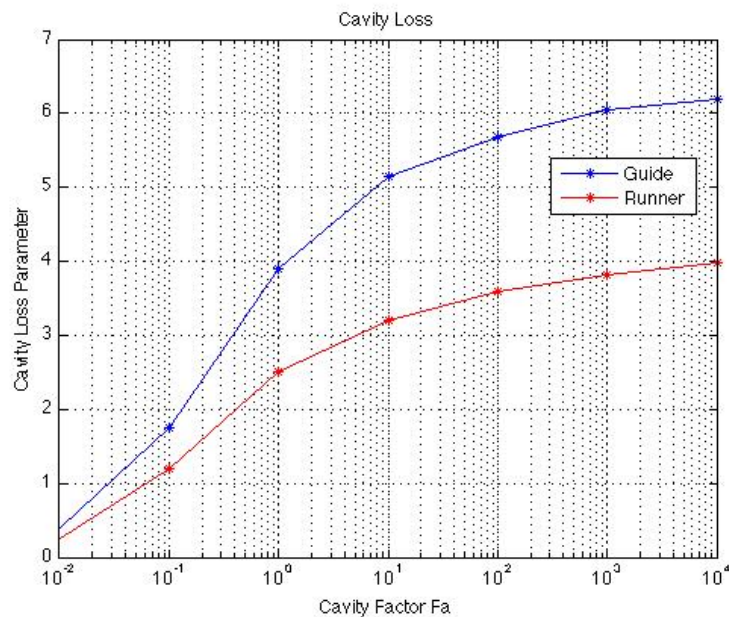


Figure 2-32 Cavity Loss (Craig & Cox, 1971)

## Group 2 losses - Efficiency debits

The efficiency debits taken in account by Craig and Cox in their work are those regarding clearance leakage and other miscellaneous losses. In this section equations and correlations proposed from Craig and Cox's work for estimation of clearance and leakage through glands will be briefly explained. Other miscellaneous losses might be explained as they are introduced on Craig and Cox's work too but, as they have stood, all of these miscellaneous are smaller in comparison with rest of the losses mentioned in their work.

### Tip Clearance Loss

For a shrouded blading the authors developed a typical clearance loss correlation in which from Figure 2-33 is obtained the efficiency debit factor  $F_k$  and then, as shown in Eq. 2-56, it is possible to calculate the efficiency debit by assuming a value for the efficiency without clearance loss. In case of unshrouded blading the authors suggest that it should be obtained the same value for shrouded blades and then multiply it by a factor of 1.5.

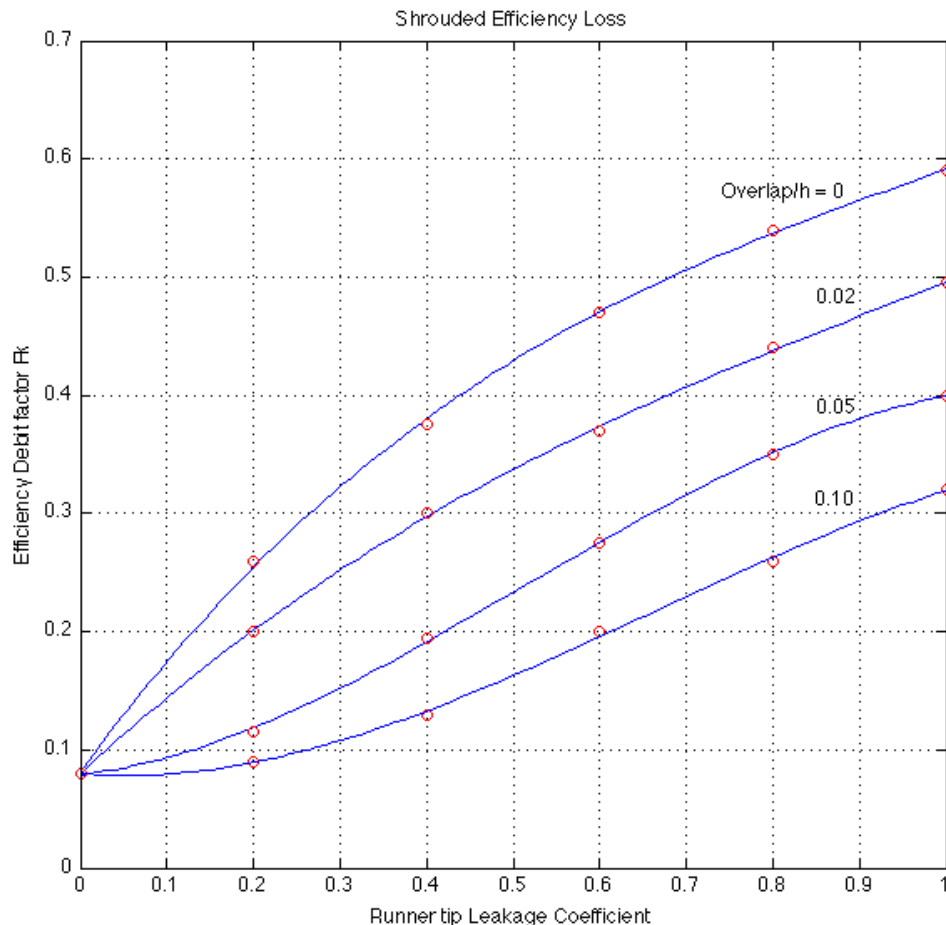


Figure 2-33  $F_k$  Efficiency debit factor for Shrouded Blades (Craig & Cox, 1971)

$$\Delta\eta_k = F_k \frac{A_k}{A_t} \eta_{Cl=0}$$

Eq. 2-56

### Leakage Flow through Glands

The leakage flow through glands can be calculated by standard formulae shown in Eq. 2-57. In this equation is calculated an efficiency debit as a function of the leakage fraction, which in instance is a function of the gravitational constant and the leakage flow bypassing blades.

$$\Delta\eta_{leakage} = \left( \frac{\Delta g}{G + \Delta g} \right) \eta_{blading}$$

Eq. 2-57

#### Miscellaneous Losses

Regarding other miscellaneous losses Craig and Cox suggest to consider efficiency debits due to lacing wire, wetness losses, disc windage and partial admission. The lacing wire loss correlation proposed is based on wires of circular section with a drag coefficient correction  $C_d$  for non-circular wires. The correlation for lacing wire losses is shown below in Eq. 2-58.

$$\Delta\eta_l = \frac{\left\{ \frac{(A_{Wire})(C_d)(W^2_{local})}{(A_{Passage})2gJ} \right\}}{\Delta W \times D_{blading}} \eta_{blading}$$

Eq. 2-58

The wetness loss are to be taken into account for steam turbines which is beyond the scope of present work, nonetheless Craig and Cox do not propose any new correlation but instead suggest the use of that mentioned by Baumann (Baumann, 1921). Finally, regarding the disc windage loss and the partial admission loss, Craig and Cox recommend the use of correlations suggested by Daily and Nece (Daily & Nece, 1960) and by Suter and Traupel (Suter & Traupel, 1959) respectively.

### 2.4.3. Denton

Denton proposed a loss correlation for loss prediction based on the statement that the only rational measure of loss in an adiabatic machine is entropy creation even though it cannot be measured directly (Denton, 1993). Denton based his model making no distinction between energy and entropy loss coefficients due to its similarity according to Eq. 2-59 that is of order  $10^{-3}$ .

$$\xi_s - \xi = 0.25(\gamma - 1)M^2 \xi \xi_s$$

Eq. 2-59

Considering this, Denton's method stands that the total losses concerning a turbine cascade is a sum of individual losses generated through all the expansion process. These individual losses are the blade boundary layer, trailing edge; tip leakage, endwall mixing, endwall boundary layer and shock losses among other miscellaneous losses. A general equation for his statement is shown below. This equation is applicable to both stator and rotor losses. Next are described the equations to obtain each of these individual coefficients to the stator and rotor loss parameter calculation, following Denton's methodology.

$$\xi = \xi_{Bb} + \xi_{Te} + \xi_{Tl} + \xi_{Eb} + \xi_{shock}$$

Eq. 2-60

#### Blade Surface Boundary Layer Loss

The blade surface boundary layer loss mechanism is the definition Denton gives to the profile loss mechanism. Denton's methodology to measure this loss is based on the relationship between the boundary layer on the blade surfaces and the entropy generation. The coefficients for losses, stator and rotor respectively, are obtained as follows, where the subscript N represents the Stator and R the rotor.

$$\xi_{Bb,N} = \frac{T_1 \Delta S_{Bb,N}}{m(c_1^2/2)}$$

Eq. 2-61

$$\xi_{Bb,R} = \frac{T_2 \Delta S_{Bb,R}}{m(w_2^2/2)}$$

Eq. 2-62

In which cases the entropy change is obtained in a similar way but differing on the velocity parameters:

$$\Delta S_{Bb,N} = \sum_s^p H C_s \int_0^1 \frac{C_d \rho c^3}{T} d\left(\frac{s}{C_s}\right)$$

Eq. 2-63

$$\Delta S_{Bb,R} = \sum_s^p H C_s \int_0^1 \frac{C_d \rho w^3}{T} d\left(\frac{s}{C_s}\right)$$

Eq. 2-64

In both cases it is possible to see that the author suggests a different correlation from those developed by Kacker-Okapuu and Craig-Cox. Denton states that the entropy generation is proportional to the cube of the blade surface velocity (Denton, 1993). He also stands that the values of the loss coefficients obtained from equations above are dominated by the location of the transition point where  $C_d$  undergoes a rapid change. This will depend on the Reynolds number, turbulence level and the velocity distribution. In general, Denton considers the use of the Eq. 2-65 to obtain the dissipation coefficient under laminar

conditions for boundary layers, otherwise under turbulent conditions the author suggests to assume a value of 0.002.

$$C_d = 0.2 \text{Re}_{\Theta}^{-1}$$

Eq. 2-65

### Trailing Edge Loss

As mentioned in the Classification of the Losses section, these losses occur due to the finite thickness of the blade trailing edge. Denton's correlation considers that the calculation of this loss coefficient is similar for both, stator and rotor. In both cases the loss coefficient is described as a function of the base pressure, flow angle at the cascade outlet, blade pitch, thickness of the trailing edge, and boundary layer displacement and momentum thickness at the trailing edge. The model is based on the equations for mass conservation, energy and momentum in control volumes between the blade throat and a certain point in which the mixing process is assumed to have restored the flow back to a uniform condition. Equations shown below describe the methodology to obtain the loss coefficients. These equations contain three different terms. First of these terms is commonly obtained from empirical data and represents the losses due to low base pressure. Second term is related to the mixed out losses generated by the boundary layers on the blade surface just before the trailing edge. Lastly, the third term is related to the blockage generated by the trailing edge and the formation of boundary layers.

For the stator the loss coefficient associated with the trailing edge losses provided by Denton is:

$$\xi_{Te,N} = -\frac{C_{pb} t'_N}{t_N \cos \alpha_1} + \frac{2\Theta_N}{t_N \cos \alpha_1} + \left( \frac{\delta^*_N + t'_N}{t_N \cos \alpha_1} \right)^2$$

Eq. 2-66

Where the pressure base coefficient is calculated as follows:

$$C_{pb} = \frac{P_{b,N} - P_1}{P_{c1} - P_1}$$

Eq. 2-67

Similarly, equations Eq. 2-68 and Eq. 2-69 show how to calculate the trailing edge loss coefficient for the rotor.

$$\xi_{Te,R} = -\frac{C_{pb} t'_R}{t_R \cos \beta_2} + \frac{2\Theta_R}{t_R \cos \beta_2} + \left( \frac{\delta^*_R + t'_R}{t_R \cos \beta_2} \right)^2$$

Eq. 2-68

$$C_{pb} = \frac{P_{b,R} - P_2}{P_{c2} - P_2}$$

Eq. 2-69

### Endwall Boundary Layer Loss

Denton stated that the endwall loss is the most difficult loss mechanism to measure and understand. However, he provides the equations needed to estimate these loss components based on the fact that this mechanism is related to the boundary layer on the endwall. The methodology is similar to the one described for the profile loss. The equations are shown in the next page, and once again the cube of the flow velocity is proportional to the loss. This means the higher the velocity is, then the larger the entropy generated because of the endwall boundary layer and thus the loss component.

For the stator:

$$\Delta S_{Ebl,N} = 0.25 \int_0^{l_x} \frac{C_d(c_s^4 - c_p^4)}{T(c_s - c_p)} \rho y_N dx$$

Eq. 2-70

$$\xi_{Ebl,N} = \frac{T_1 \Delta S_{Ebl,N}}{(0.5)mc_1^2}$$

Eq. 2-71

For the rotor:

$$\Delta S_{Ebl,R} = 0.25 \int_0^{l_x} \frac{C_d(w_s^4 - w_p^4)}{T(w_s - w_p)} \rho y_R dx$$

Eq. 2-72

$$\xi_{Ebl,R} = \frac{T_2 \Delta S_{Ebl,R}}{(0.5)mw_2^2}$$

Eq. 2-73

Besides the boundary layer on the enwall, Denton considers the boundary layer between blade rows as part of the total endwall loss mechanism. The equation provided to estimate the loss generated due to this boundary layer is shown next. This equation is proportional to the cube of the absolute velocity in this area and to the area of the endwall.

$$\xi_{Eb,Bt} = \frac{T_1 \Delta S_{Eb,Bt}}{(0.5)mc_1^2}$$

Eq. 2-74

$$\Delta S_{Eb,Bt} = \int_0^{A_w} \frac{C_d \rho c_1^3}{T} dA$$

Eq. 2-75

### Tip Leakage Loss

In concordance with the methods described by Kacker-Okapuu and Craig-Cox, Denton in his work (Denton, 1993) suggests different correlations for each, shrouded and unshrouded blading. For shrouded blades the correlation shows that the loss is a function of the ratio between the leakage flow and the main flow, and the respective flow conditions regarding angles and velocities. Eq. 2-76 allows a direct calculation of the loss parameter for this case.

$$\xi_{tl,R} = 2 \frac{m_L}{m_m} \left(1 - \frac{\tan \beta_1}{\tan \beta_2}\right) \sin^2 \beta_2$$

Eq. 2-76

In case of unshrouded blades the model proposed involves more calculation, given more complexity for the mixing occurring in the clearance area. The correlation is a function of the velocity distribution and geometry aspects. In order to simplify it Denton suggests assuming the same distribution used for calculation of the blade boundary layer loss coefficient (Denton, 1993). The correlation is shown below in

Eq. 2-77. Once again the velocity parameters in the suction and pressure side play an important role in the compute of the loss mechanisms.

$$\xi_{Tl,R} = 1.5 \frac{\tau l}{Ht \cos \beta_2} \int_0^1 \left( \frac{w_s}{w_2} \right)^3 \left( 1 - \frac{w_p}{w_s} \right) \sqrt{\left( 1 - \left( \frac{w_p}{w_s} \right) 2 \right)} d(\frac{s}{l})$$

Eq. 2-77

### Shock Loss

Denton associates the shock losses with the entropy generation due to heat conduction and high viscous normal stresses within the shock wave (Wei, 2000). The shock loss coefficient and its entropy associated can be calculated with the equations shown below. These equations are mainly a function of the inlet Mach number.

$$\xi_{shock} = \frac{T_{out} \Delta S_{shock}}{(0.5)mV_{out}^2}$$

Eq. 2-78

$$\Delta S_{shock} = C_v \frac{2\gamma(\gamma-1)}{3(\gamma+1)^2} (M_{in}^2 - 1)^3$$

Eq. 2-79

The methodology described by Denton implies large physics understanding and knowledge of the flow conditions through the whole path. A priori, the velocity distribution among the blade surface is not known and even if assumed it might be erroneous. Thereafter, Denton's model implemented in this work is that proposed by him based on simplified assumptions (Denton, 2008). This is shown in chapter 4 of the work, where the implementation steps are mentioned.

### 3. One-dimensional Design Tool – LUAX-T

One of the specific objectives of this study is to implement the loss models discussed in chapter 2 on a one-dimensional (1D) calculation tool for turbine design. It was stated already on the limitations section that among the existent programs or tools the only to be used in present work is the Lund's University Axial Flow Turbine tool (LUAX-T) (Genrup, 2008). Present section of the work will focus on explain the fundamentals of the program, its structure and outputs prior to its extension.

LUAX-T is an advanced mean-line flow calculation tool for highly loaded cooled or un-cooled turbines, developed for aero-thermal turbine design. The tool is based on Matlab (Mathworks Inc., 2010) and has graphical user interfaces for swift usage. LUAX-T is available for free academic usage and was originally developed in 2008 by Olsson and Genrup in Lund University as a part of the LUAX suite tool, which include mid-line calculations for both, axial turbines and compressors. In the tool the user has an array of options when specifying the flow path, where it is possible to set net power from a compressor turbine, stage loading, reaction degree, flow coefficient, cylindrical rotors, turbine diffuser, among other parameters (Olsson, 2008). In a similar way the user is able to set as input different turbine geometrical specifications and some of the blade geometry, otherwise these are estimated by optimum correlations employed in the 1D tool. In Figure 3-1 it is possible to see the graphical user interface input window for turbine specifications regarding the flow path and in Figure 3-2 the blade geometry input window.

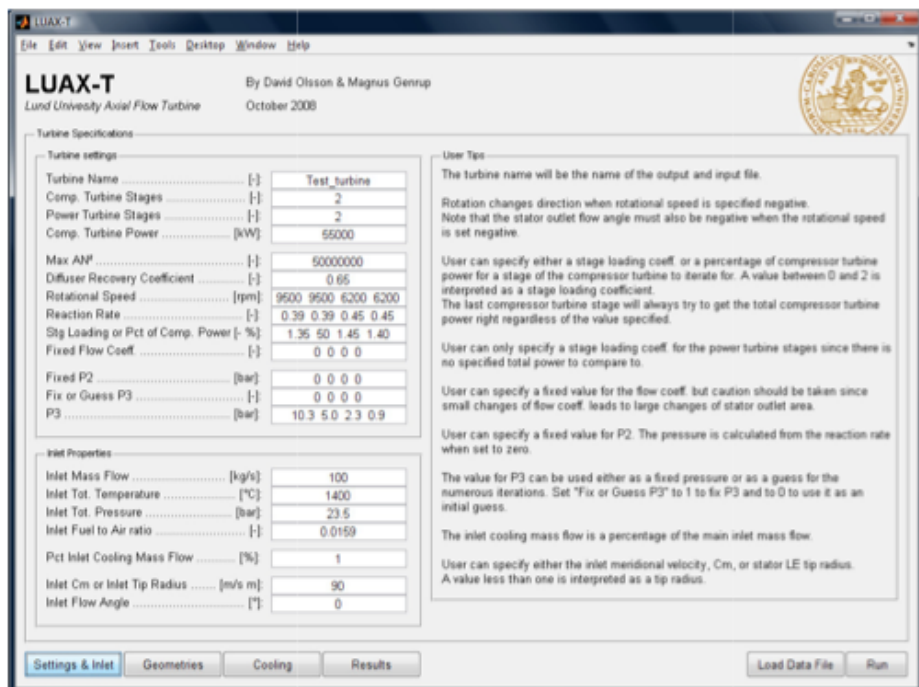


Figure 3-1 Turbine Specifications GUI - LUAX-T (Olsson, 2008)

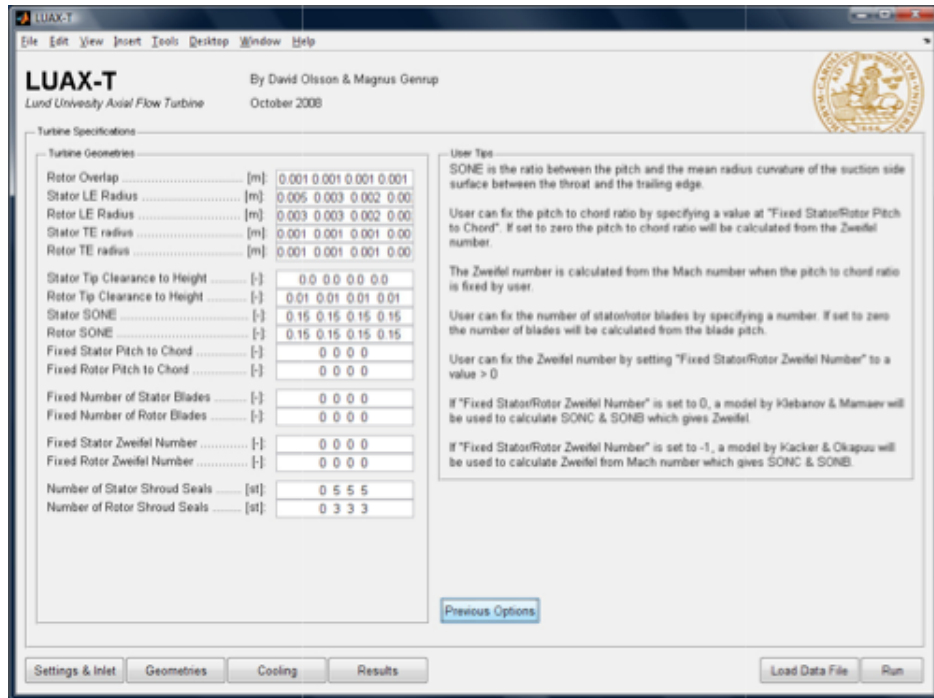


Figure 3-2 Blade Geometry Specifications GUI - LUAX-T (Olsson, 2008)

The 1D tool uses different models and equations in order to perform its task of predicting the turbine's performance given basic parameters as inputs. The equations and models used to compute the expansion process in the turbine are mentioned at the beginning of the second chapter of the present work. These equations are those regarding the Enthalpy-Entropy Diagram, as shown in Figure 2-1, and the ones needed for the calculation of the non-dimensional design parameters like the Zweifel number, the stage loading coefficient and the flow coefficient (Genrup, 2008).

Moreover, what is of main importance for present work is the understanding of the loss model utilized in LUAX-T. This is important since is within the scope of the work to compare its results against other loss models after implementation and proper validation of the latter ones have been performed. The loss model used in LUAX-T is based on the model developed by Ainley and Mathieson (Ainley & Mathieson, 1951) and then refined by Dunham and Came (Dunham & Came, 1979) and Kacker and Okapuu (Kacker & Okapuu, 1981). The AMDCKO correlation considers that the most important losses in a blade passage are the profile loss, the secondary loss, the clearance loss and the trailing edge loss (Olsson, 2008). As suggested by the AMDCKO model all these losses are estimated individually by the use of different correlations and then added together to determine the total pressure loss through the blade passage.

Nonetheless it has been previously mentioned that is beyond the scope of present work the estimation of losses due to blade cooling, it will be briefly explained the cooling model implemented by Olsson and Genrup in LUAX-T (Genrup, 2008). The cooling model used in the tool is a standard "m-star" to compute the required air mass flow. This model expresses the mass flow and can be derived from the first law of thermodynamics (Incropera, De Witt, Bergman, & Lavine, 2006). Once the needed mass flow for cooling has been calculated, then the program uses two different mixing loss models. The first one is a simplified model originally developed by Hartsel to compute the losses due to mixing of inlet cooling air. This model is based on the assumption that the mixing losses can be superimposed on the basic boundary losses (Hartsel, 1972). The second one is a more advanced two-dimensional model use to estimate the trailing edge injection-mixing model. The implementations carried through in present work do not modify those already existing in LUAX-T for estimation of loss due to mixing of cooling flows and the main flow.

As it is possible to guess, the program is structured with many calculations so also many iteration loops are needed. The calculation procedure is complex and might be difficult to understand even for Matlab

(Mathworks Inc., 2010) frequent users. Hence, in complete knowledge of the programs complexity its authors try to explain all these calculations and iterations in form of flow charts as well as describing the program code at the end of the LUAX-T report (Olsson, 2008).

The LUAX-T guide user interface windows were briefly discussed at the beginning of this section, and figures Figure 3-1 and Figure 3-2 showed two of the first three input windows. These input windows created to ease the use of the program for those not related to Matlab (Mathworks Inc., 2010) generate an input text file and, of course, an input code needed for the main calculation and supervising routines by the program. After running the main calculations and supervised them, the program its ready to give its different outputs. These outputs consist of a detailed text file with the turbine performance and different output windows in LUAX-T's user interface containing plots and figures. The different figures shown are the turbines profile view, the total breakdown of losses in percentage and the efficiency plotted over the Smith Chart (Figure 2-4). All of these outputs will be concisely discussed and shown below.

The output text file given by LUAX-T (Genrup, 2008) can be considered as the most important output of the program. This consideration since it allows the user to know all the geometry calculated and the performance of the turbine in each stage. It also gives a complete description of the turbines performance after simulation. An example of how does the output text file looks like is shown next in Figure 3-3, nonetheless the figure does not displays a whole output file since its size is large and depending on the turbine object of study with LUAX-T (Genrup, 2008) can contain several pages.

```

Test_turbine_Outputdata - Anzeichnungen
Arkv. Bediener Format Viga Help
=====
# LUAX-T
# Version 3.0
# David Olsson & Magnus Genrup
# 2008
=====

Test_turbine
23-Sep-2008 17:21:14

Compressor turbine stages: 2
Revolutions per minute: 2
Total turbine stages: 4
Specific compressor turbine power: 55.00 kW
Total turbine power: 132.00 kW
Diffuser Recovery coefficient: 0.85

Turbine performance
Power [kW]: 55000
Compressor Turbine Power [kW]: 52780
Total Turbine Power [kW]: 507780
Average loading coefficient: 1.248
Pressure ratio (TR): 1.248
Pressure ratio (TR): 4.25
Isentropic efficiency (TR): 85.43
Isentropic iso efficiency (TR): 85.75
Polytropic iso efficiency (TR): 83.23
Polytropic efficiency (TR): 83.23
Thermodynamic efficiency (Pax): 85.94
Thermodynamic efficiency (xurake): 82.94
Thermodynamic efficiency (xurake): 82.94

Total cooling massflow [kg/s]: 22.29
Pct of inlet massflow: 22.29
Power transferred to cooling air [kW]: 6.29
Power transferred to cooling air [kW]: 6.29

INLET CONDITIONS

Inlet Properties
Inlet massflow [kg/s]: 100.00
Inlet temperature [°C]: 1400.00
Inlet pressure [bar]: 23.59
Inlet enthalpy [kJ/kg]: 1641.1
Inlet entropy [kJ/kg K]: 11.12
Inlet entropy change [kJ/kg K]: -0.03
Inlet fuel to air ratio [-]: 0.0159
Inlet gas constant [J/kg K]: 290.82
Inlet specific heat [J/kg K]: 1290.3
Inlet density [kg/m³]: 4.798
Inlet flow angle [-]: 0.00
Inlet absolute velocity [m/s]: 90.00
Inlet meridional velocity [m/s]: 90.00
Inlet tangential velocity [m/s]: 0.00
Inlet speed of sound [m/s]: 791.9
Inlet mach number [-]: 0.11

```

Figure 3-3 LUAX-T Output text file example (Olsson, 2008)

Another output file after simulation is the turbines profile plot. An example for a 4 stages turbine is shown in next page in Figure 3-5. This figure shows all the turbine stages and is obtained according to how LUAX-T divides the turbine stage for its calculation points. This division consists of seven calculation points that can be distinguished in Figure 3-4. In order of calculation, these points are: the stator inlet, stator outlet prior to mixing of stator blade cooling air, stator outlet state after mixing of stator blade cooling air, rotor inlet state after mixing of stator disc cooling air, rotor outlet state prior to mixing of rotor blade cooling air, rotor outlet state after mixing of rotor blade cooling air and next stator inlet state after mixing of rotor disc cooling air.

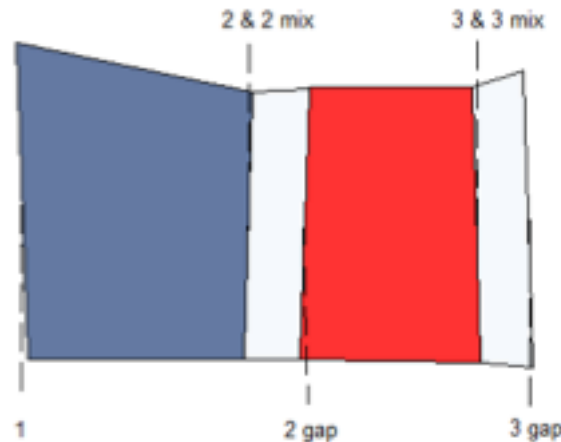


Figure 3-4 Turbine calculation points (Olsson, 2008)

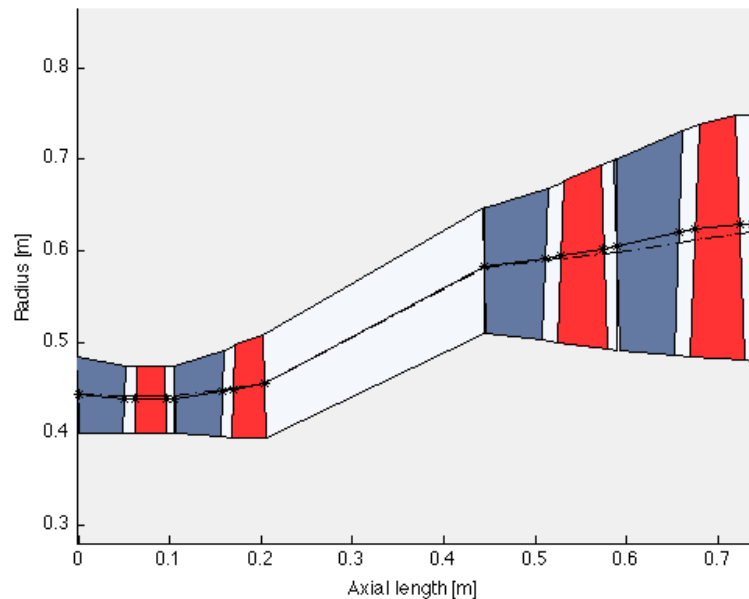


Figure 3-5 Profile plot for a 4 Stages Turbine (Olsson, 2008)

Finally, in Figure 3-6 is shown how does LUAX-T reflect the breakdown of losses occurring through each stage in the turbine. In this figure losses are measured in percentage rates, and each kind of loss receives a different color so that the user could perform a proper comparison regarding the main losses occurring.

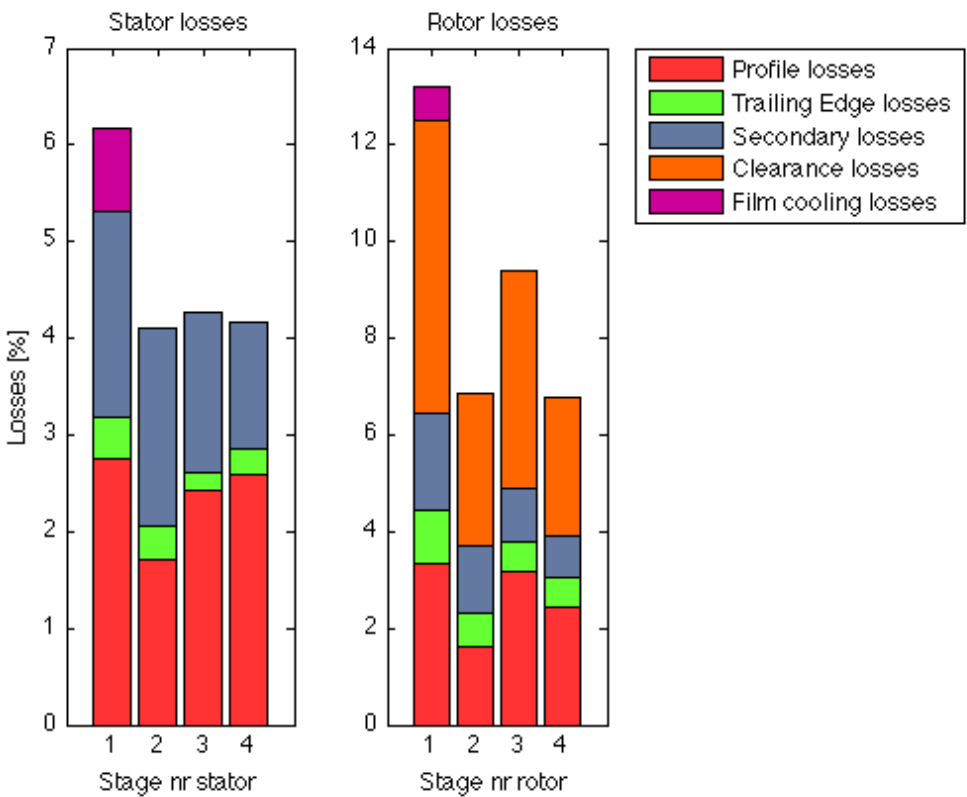


Figure 3-6 Example of a breakdown of losses for a 4 Stages Turbine (Olsson, 2008)

## **4. Implementation and Verification of Loss Models**

The implementation of the loss correlations in LUAX-T is one of the major objectives of the present work. This implementation is performed in order to judge the most accurate loss model and be able to compare and understand the loss representation provided by different models. In this regard, only by having the loss models implemented, subsequent validation and parametric design studies can be performed in order to compare them and give conclusions concerning their accuracy or differences. Present chapter will explain how did the Craig & Cox and Denton loss models were implemented in the one-dimensional tool, LUAX-T, described in chapter 3.

### **4.1. Craig and Cox**

#### **4.1.1. Implementation of Craig and Cox Loss Model in LUAX-T**

For the implementation of the Craig and Cox loss correlation, it were followed the steps mention on section 2.4.2. The implementation of the loss correlation is based on a Matlab (Mathworks Inc., 2010) code in order to be part of the LUAX-T routine.

The code implemented is a sub-routine of the main turbine calculation code so that LUAX-T is calculating the same parameters for the turbines performance as it was with the AMDCKO loss model but now basing its results on the loss coefficients calculated by Craig and Cox loss correlation (Craig & Cox, 1971). In a more detailed and technical explanation, the implemented routine computes all the parameters needed to obtain the loss coefficients. Once the loss coefficients are calculated they are converted into pressure loss coefficients. This is because AMDCKO computes pressure loss coefficients. The equations used to convert from enthalpy loss coefficients to pressure loss coefficients are the equations Eq. 2-19 and Eq. 2-24 of present work (Moustapha, 2003).

In order to implement the loss correlation completely, the code includes the optimum solidity correlation proposed by Crag and Cox. This is a function of the inlet and outlet relative flow angles and is shown in Figure 4-1. However, within the program, the user has the option to specify which correlation for optimum solidity is to be used. In this regard, LUAX-T has already implemented the Zweifel correlation and one developed by Mamaev and Klebanov (Mamaev & Klebanov, 1969).

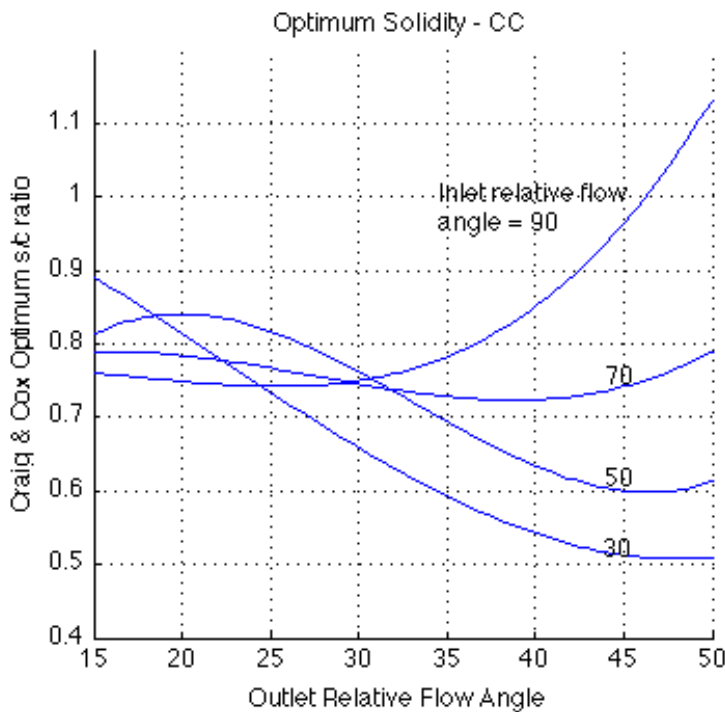
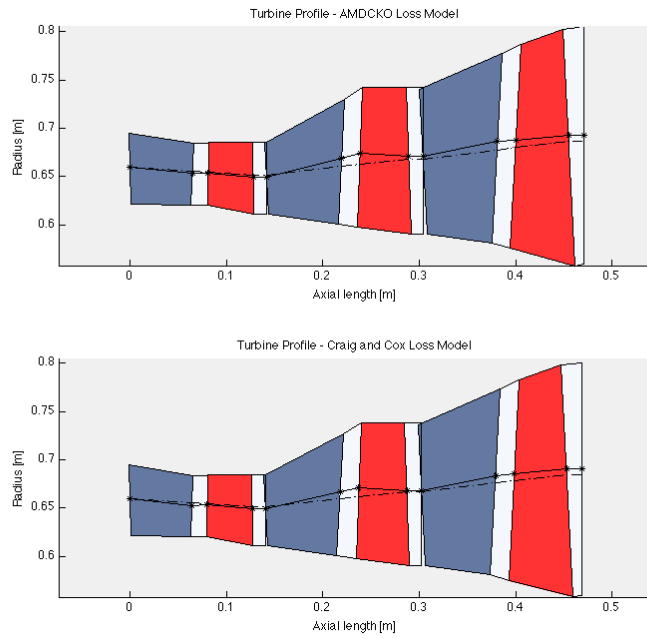


Figure 4-1 Optimum Solidity as extracted from "A comparison between the Craig-Cox and the Kacker-Okapuu methods of Turbine Performance Prediction" (Lozza, 1982)

As described in chapter 2 the Craig and Cox loss model bases most of the correlations on the camber line or backbone length of the blade. This parameter is not calculated by LUAX-T so present works calculates the backbone length as suggested by Lozza in his work (Lozza, 1982). He assumes that the blade mean-line is constituted by the addition of a circular arc from the inlet to the throat and a straight line up to the outlet. This is based on known blade geometry factors such as the pitch, the throat and the relative angles. To compute the backbone length from these parameters a sub-routine in the Craig and Cox loss correlation is implemented in LUAX-T. The code implemented is shown in the APPENDIX I of present work and explained are the sub-routines with a respective description of each one of the parameters needed by each routine. Furthermore, the code contains an explanation of the outputs as well. However, these outputs are similar to those obtained before with the AMDCKO loss model.

After performing the implementation of the Craig and Cox loss model in LUAX-T, the program has been now extended and can perform a complete prediction of the turbine's performance with one of the loss models or with both at the same time, based upon the decision of the user. It is important to clarify once again that the rest of the structure of the program remains the same except for the outputs. This is because the addition of the Craig and Cox loss model allows the program to give figures for both models and different output text files, one per each model. The new figures obtained as outputs of the 1D tool are shown on the next page. The first one, Figure 4-2, contains both turbine profiles calculated, one per each method so that it is possible to compare visually the results obtained. The second, Figure 4-3, is of importance for the present work since will allow the user to directly compare the estimation of the breakdown of the losses calculated with both loss models concerning stator and rotor in each of the stages. In the y-axis of this figure the losses are represented as percentage and margins have been set up so that they remain the same for both models. On the x-axis there are represented each of the stages of the turbine object of study, in this particular case, a 3-stage turbine is shown as example.



**Figure 4-2** Turbine's profile view as extracted from LUAX-T after Craig & Cox loss model implementation

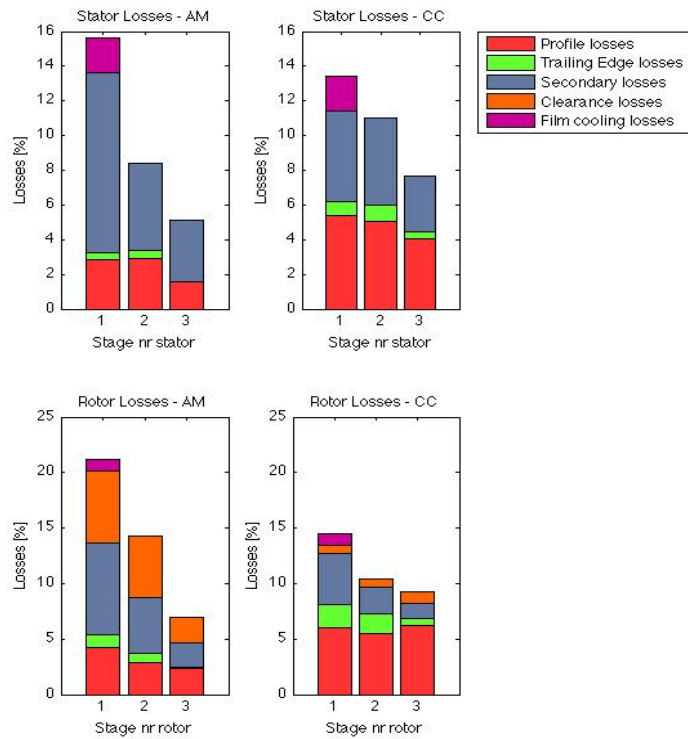


**Figure 4-3** Breakdown of losses as extracted from LUAX-T after Craig & Cox loss model implementation

#### 4.1.2.Verification of Craig and Cox Loss Model

Once implemented in LUAX-T (Genrup, 2008), next step was to check and verify the Craig and Cox's loss correlation implemented (Craig & Cox, 1971). In order to do so, there were compared the results between the model implemented in LUAX-T and a previous study performed by Lozza in 1982. In this study there were examined two loss correlations for estimating the performance of axial-flow turbines, the Craig and Cox and the Ainley-Mathieson loss correlation. In his work, Lozza evaluates the losses in a number of representative cascades, having various solidities, aspect ratios, Reynolds and Mach numbers using both loss correlation methods (Lozza, 1982). The results show that both methods are in agreement for subsonic cascades having high flow coefficients, while some significant differences were found when considering high deflection blades, specially for the secondary losses.

Only the steps followed by Lozza to perform the implementation of Craig and Cox loss model and obtained results from such study are of interest. Following the same steps and assuming same conditions as Lozza's study the results obtained with the implemented code in LUAX-T were similar. First, as discussed on previous section 4.1.1, the optimum solidity was chosen according to the model proposed by Craig and Cox and it is shown in Figure 4-1 (Lozza, 1982). Lozza analyzed three typical cascades, with aspect ratios varying from 0.5 to 3 and operating at three isentropic outlet Mach numbers. The first Mach number considered was 0.4 to consider an almost incompressible flow, then 1 for highly compressible flow and finally 1.3 to see the behavior of the model when important supersonic effects like shocks take effect (Lozza, 1982). Another important assumption is that all the analyses have been done for a perfect gas having a specific heat ratio of 1.1 (Lozza, 1982). The optimum solidity values found for each one of the cases analyzed by Lozza are showed in Table 4-1, where it is also possible to distinguish the parameters considered by him when analyzing '*three typical cascades*'. These parameters are the inlet and outlet relative flow angle, the trailing edge to throat ratio, and a Reynolds number on throat of  $5 \times 10^5$  in conjunction with an equivalent sand grain ( $k_s$ ) size below  $2 \times 10^{-3}$  (Lozza, 1982). These last two parameters (Re and ' $k_s$ ') have been chosen to such values with the intention of fixing the Reynolds effect ratio as closest as possible to 1 as can be obtained from Figure 2-12.

**Table 4-1 Cascade parameters assumed by Lozza (Lozza, 1982)**

Cascade #	1	2	3
Inlet Relative Flow Angle, $\alpha_1$	90	90	30
Outlet Relative Flow Angle, $\alpha_2$	30	15	30
Trailing edge radius to opening ratio, t/o	0.10	0.10	0.10
Optimum Solidity, s/c	0.77	0.76	0.64

As mentioned on section 4.1.1, Lozza suggests the estimation of the backbone length, needed for several correlations assuming that the blade mean-line is constituted by a circular arc from the inlet to the throat and then by a straight line up to the outlet and based on known blade geometry factors as the pitch, the throat and the relatives angles, all of them can be estimated from values in Table 4-1 (Lozza, 1982). Finally, it is of importance to realize that the author is fixing the pitch to chord and trailing edge to opening ratios instead of mentioning the specific values for each parameter used in his model to calculate the losses. On the contrary in some correlations in the implemented model in LUAX-T (Genrup, 2008) are needed not the ratio but the value of each parameters instead. Furthermore, it is of relevance then to say that for the simulation of the implemented code, there were set different values of the chord from 0.03 to 0.05 [m] to see how would fixing this value change the results obtained. It was found that the differences between all the results were minimum; hence the ratios assumed by Lozza were ruling the behavior of the model as expected and not the specific parameter values assumed.

The results obtained by Lozza in his work for each of the cases are shown in figures below respectively (blue lines) where there are also shown the results obtained by the use of the implemented model in LUAX-T (red lines). There are shown a total of nine figures, one per each operation conditions (three different outlet isentropic Mach numbers) for each one of the 3 cascades described in Table 4-1. From comparing the outcomes of the implemented model against the results of the study realized by Lozza it is possible to conclude that the loss model implemented is behaving as expected and hence well implemented. It is possible to see on the figures in present section not only that the values are very accurate, but also that the trends displayed for each case are the same.

Figures 4-4, 4-5 and 4-6 are related to the first cascade tested by Lozza (Table 4-1) concerning incompressible, compressible and supersonic flow respectively. For all of the cases the predictions from LUAX-T remained close to those calculated by Lozza. In this regard it is possible to see how there is no dependence on the aspect ratio by the profile losses or trailing edge losses, as they remain the same for all the aspect ratio range tested. Nevertheless, if considering the secondary losses then figures show a decrement of the total loss as the aspect ratio increases. The reason for this is further explained in chapter 7 of present work, however it is mainly because at shorter blades the endwall boundary layer affects a greater portion of the blade surface area. Moreover, if analyzing the 3 figures it is possible to see that for supersonic flow conditions (Figure 4-6) the profile and trailing edge losses are relatively higher than those calculated for the first two cases. This last phenomenon was expected since the Craig-Cox loss correlation considers supersonic Mach corrections for Mach number values over 1. Moreover, at low flow acceleration (Figure 4-4) the secondary losses were found to be higher than for compressible or supersonic flow conditions. Fast accelerating flow will imply less turning in the vortices formed in the passage and also give less time for the boundary layer on the endwall to pass from the pressure side to the suction side of another blade, therefore at higher outlet Mach values the secondary losses are lower.

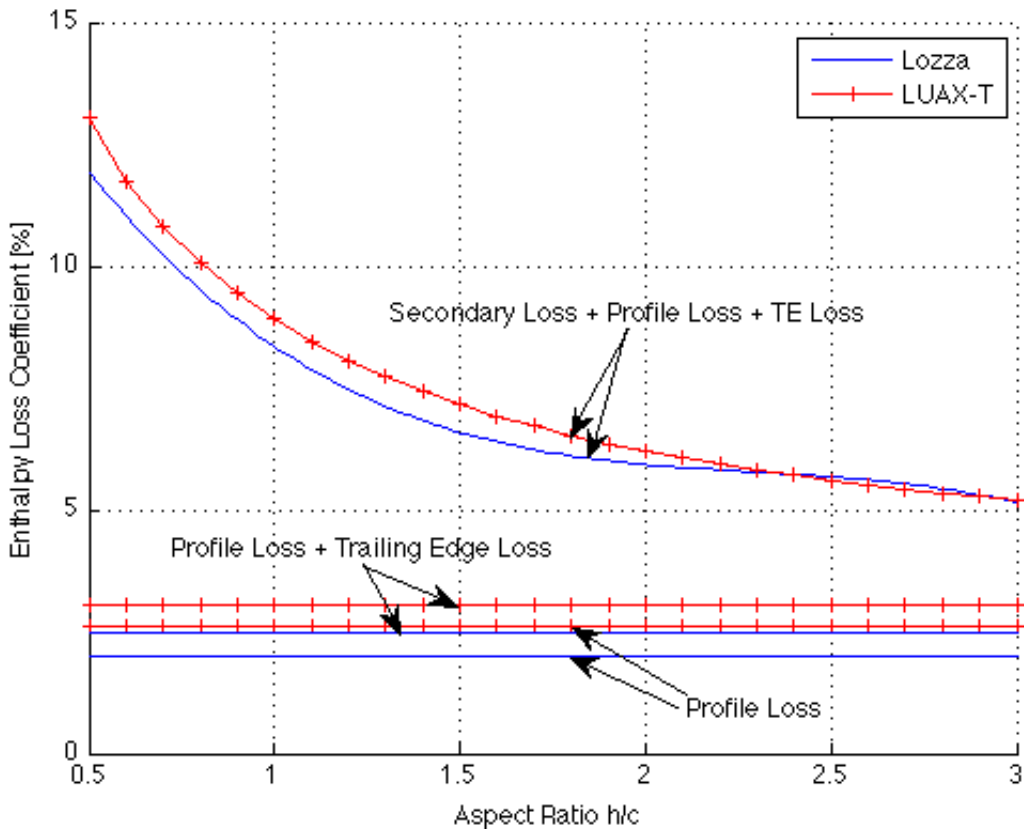


Figure 4-4 – Verification of Cascade 1 for  $\text{Ma} = 0.4$

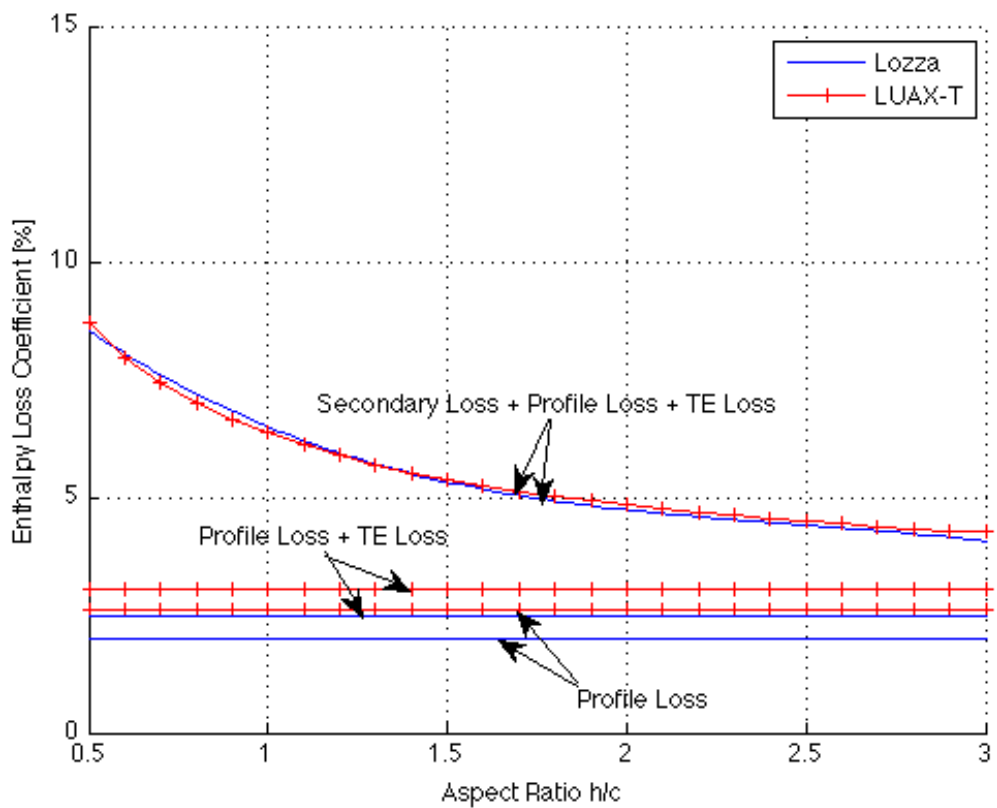


Figure 4-5 - Verification of Cascade 1 for  $Ma = 1.0$

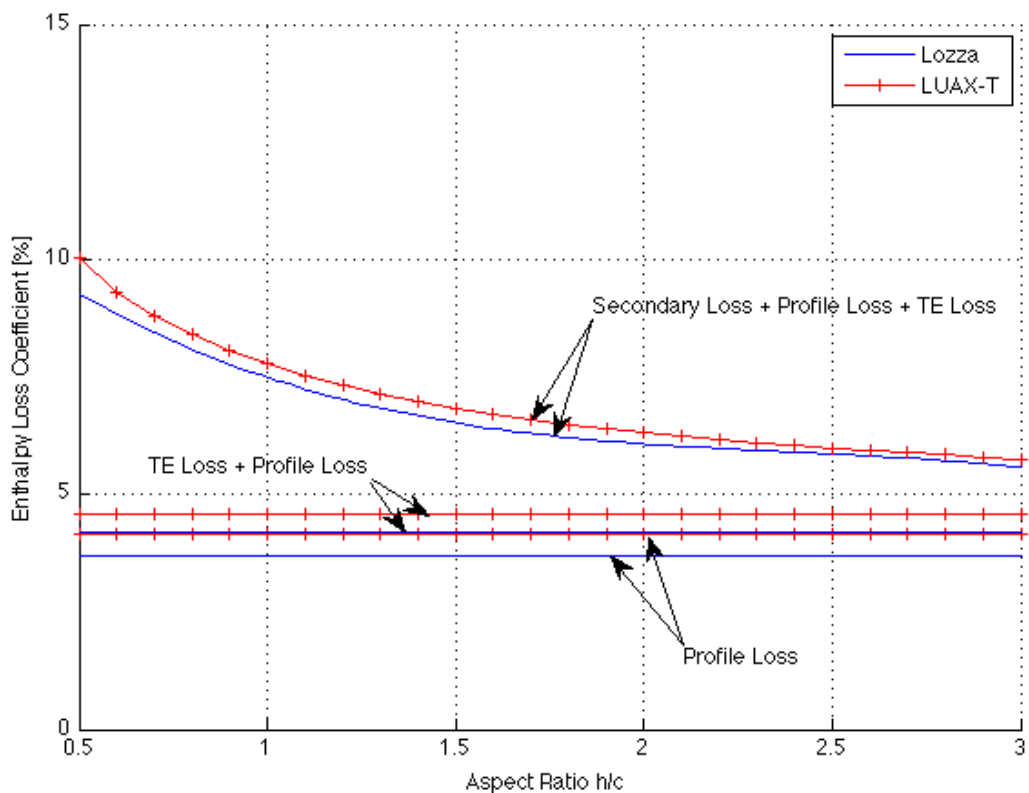


Figure 4-6 - Verification of Cascade 1 for  $Ma = 1.3$

Similarly, Figures 4-7, 4-8 and 4-9 show results concerning reaction runners for turbines having loss flow coefficients which represents the Cascade #2 in Table 4-1. Once again, results show that LUAX-T predictions remain close to those calculated by Lozza. Moreover, the trends discussed for the Cascade #1 shown in previous figures remain the same. In this regard, profile losses do not vary with a variation of aspect ratio and are higher for the case of supersonic flow conditions. Likewise, the secondary losses do not affect the variation of aspect ratio, remaining higher for shorter blades.

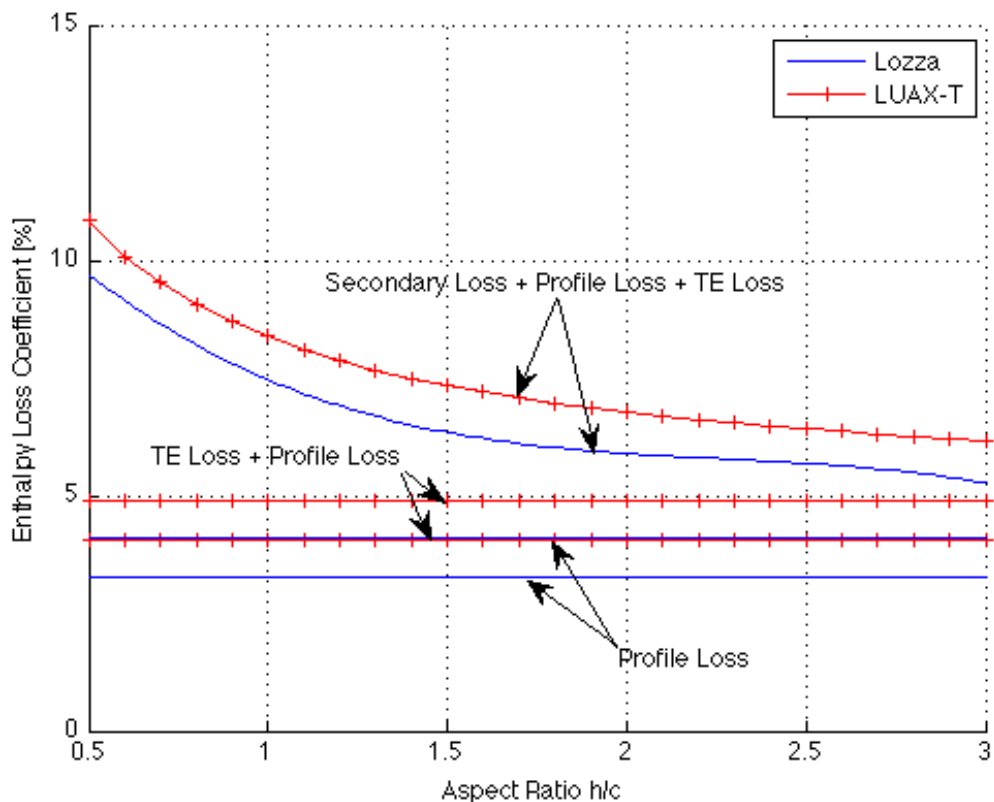


Figure 4-7 Verification of Cascade 2 for  $Ma = 0.4$

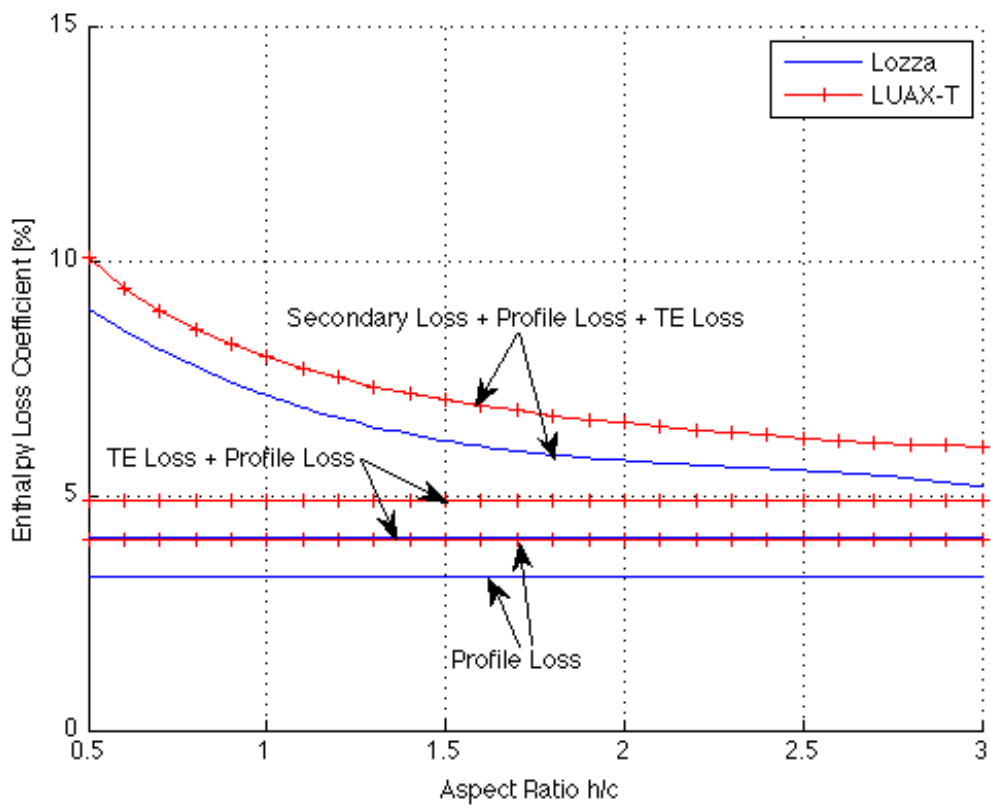


Figure 4-8 Verification of Cascade 2 for  $Ma = 1.0$

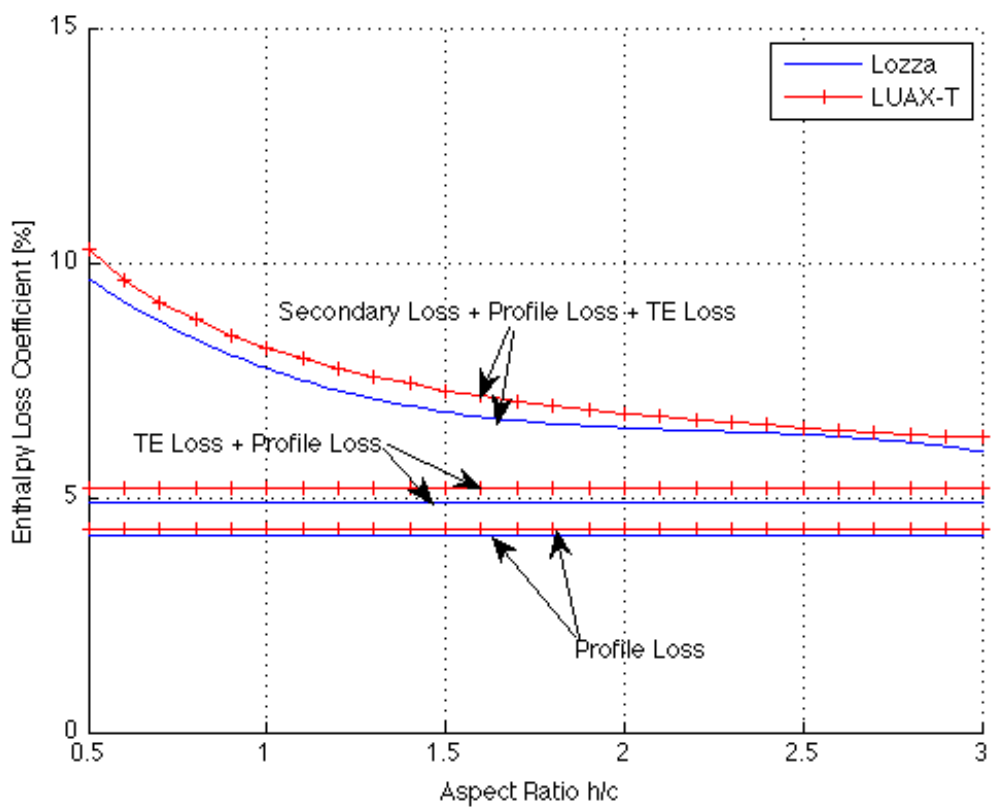


Figure 4-9 - Verification of Cascade 2 for  $Ma = 1.3$

Lastly, next are shown the results for an impulse runner with high deflection, the third cascade case tested by Lozza. Results are in agreement with trends described for previous cascades and show that LUAX-T predictions are close to the values calculated by Lozza. Furthermore if comparing the 3 different cascades analyzed it is of interest to see that the total losses calculated are considerably higher for this last case. The total loss curve shown in Figure 4-10 gives considerably higher values than those curves from figures 4-7 and 4-4. The reason for this to occur is associated with the blade loading as it is correlated with the flow turning and deflection in the Craig and Cox model. Regarding the secondary losses, the greater the blade loading, the sooner the boundary layer moves from pressure to suction side in the passage. Moreover high blade loading increases the profile losses as this is related to flow separation on the suction side.

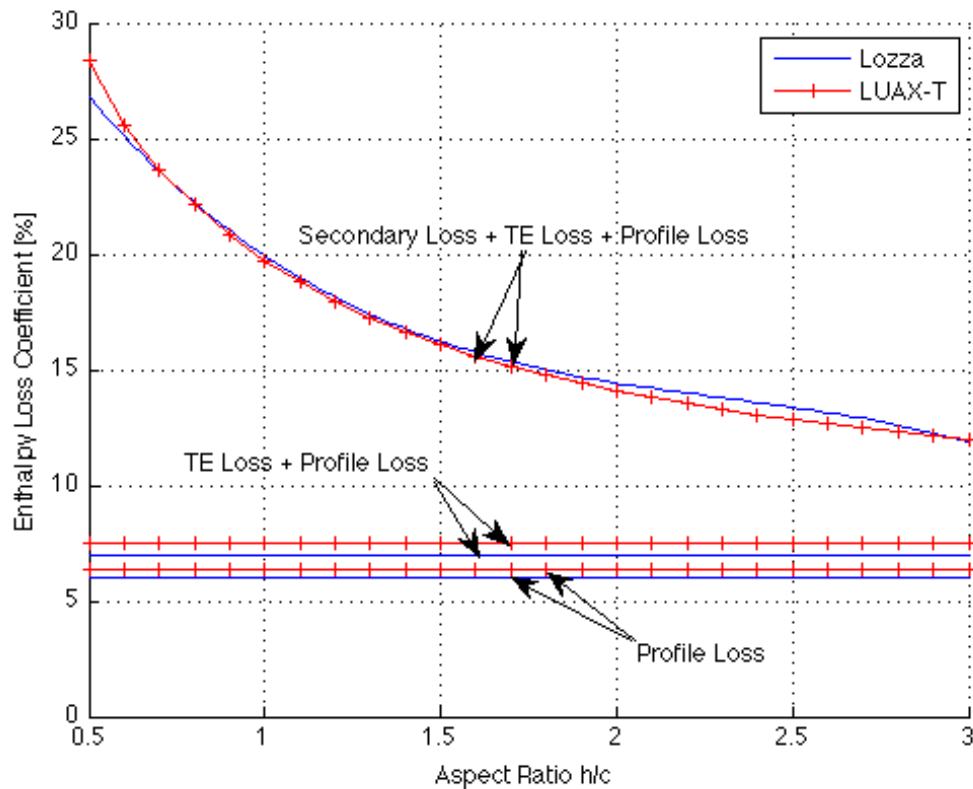


Figure 4-10 - Verification of Cascade 3 for  $Ma = 0.4$

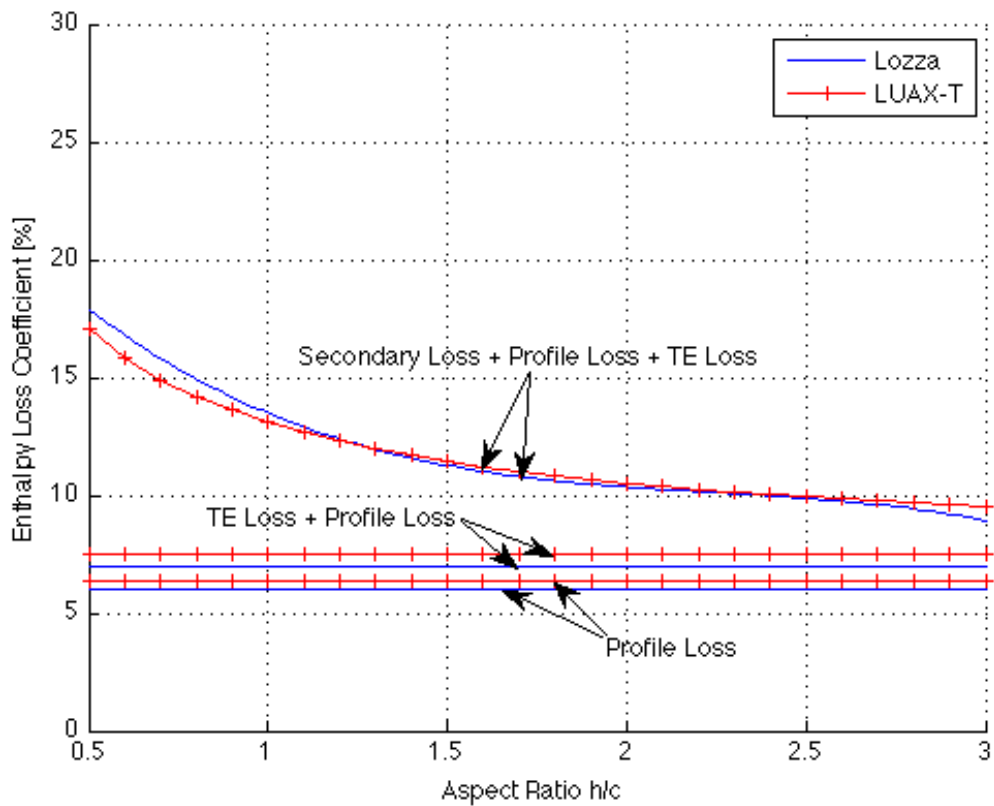


Figure 4-11 - Verification of Cascade 3 for  $Ma = 1.0$

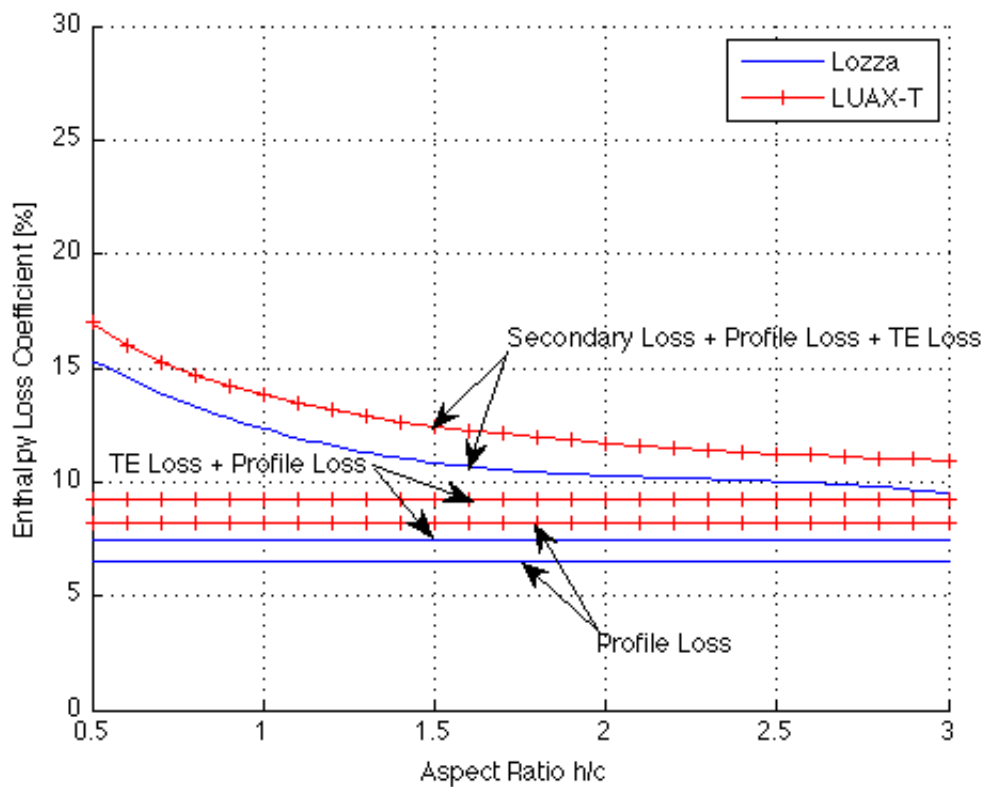


Figure 4-12 - Verification of Cascade 3 for  $Ma = 1.3$

In conclusion from previous figures and this verification process it is possible to confirm that the implemented Craig and Cox model behaves as expected. As said before, the results obtained from the model implemented are similar to those encountered by Lozza in his work for all the three different cascades tested (Lozza, 1982). However, as for figures 4-7, 4-8 and 4-12, some discrepancies regarding the magnitude estimation were found remaining this magnitude difference less than 10% of the value calculated by Lozza. Interpolation issues regarding the use of the correlations to predict the profile losses could be leading to this magnitude difference.

## 4.2. Denton

### 4.2.1. Implementation of Denton Loss Model in LUAX-T

Rather than giving a specific methodology for the estimation of the loss coefficients and the turbine performance, Denton focuses on explaining the physics associated with the loss generation in his work. In this regard, as stated before, Denton considers that the best mechanism to describe the loss generation is in terms of entropy production giving its irreversibility. The equations in section 2.4.3 were provided by Denton as the theoretical equations to explain the loss process on going in the blade path. However, the use of these equations implies the complete knowledge of the velocity distribution among the blade surface on both, suction and pressure side. Therefore, Denton proposed a simplified methodology for the estimation of the turbine performance (Denton, 2008). According to this correlation, the total losses are the addition of the profile, trailing edge, secondary and clearance losses. In LUAX-T there was implemented this simplified version suggested by Denton, which is considered by him to give accurate results.

In this implementation, the profile losses are estimated from a correlation provided by Denton after assumed the velocity distribution. In his work, Denton states that by systematically varying the guessed velocity distribution it is possible to estimate the optimum pitch to chord ratio and the minimum profile loss associated with it (Denton, 1993). The results for optimum pitch to chord ratios and minimum profile losses associated with them under assumptions of realistic velocity distributions like the one in Figure 4-13 (Greitzer, 2004).

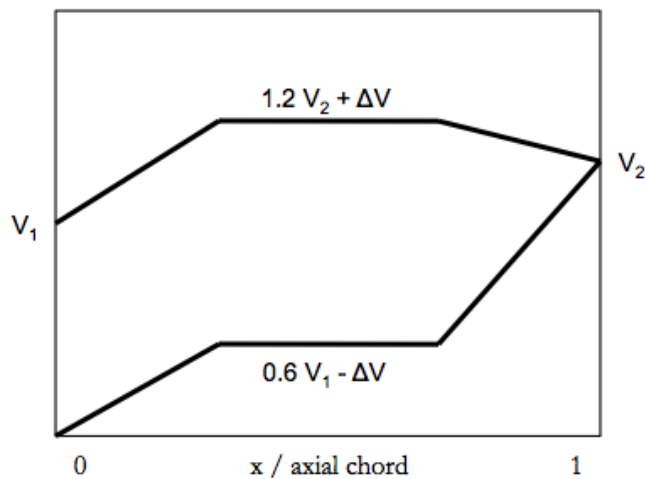


Figure 4-13 Generic Velocity Distribution as used by Denton in his work (Greitzer, 2004)

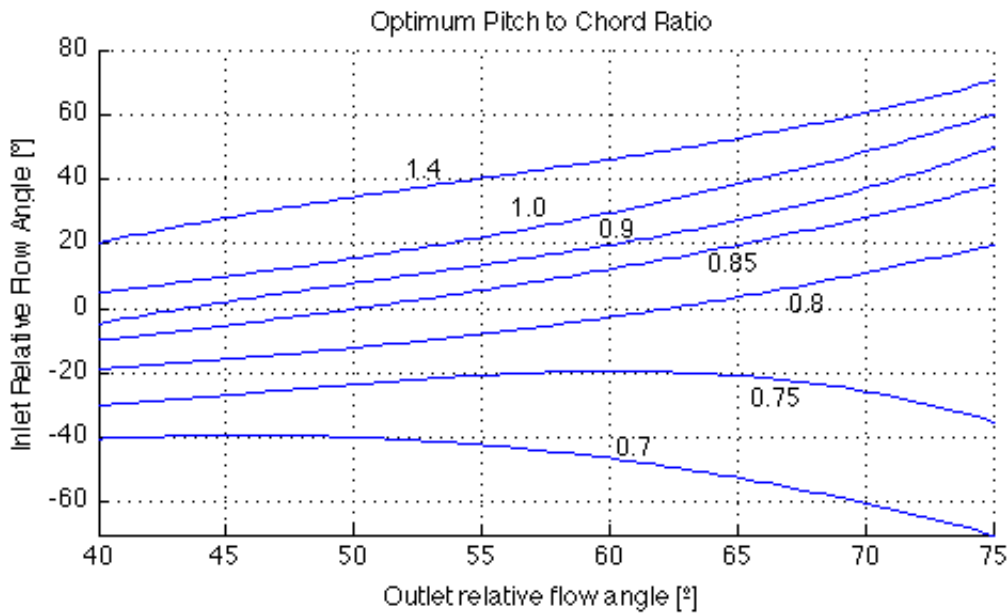


Figure 4-14 Optimum Pitch to Chord Ratio proposed by Denton (Denton, 1993)

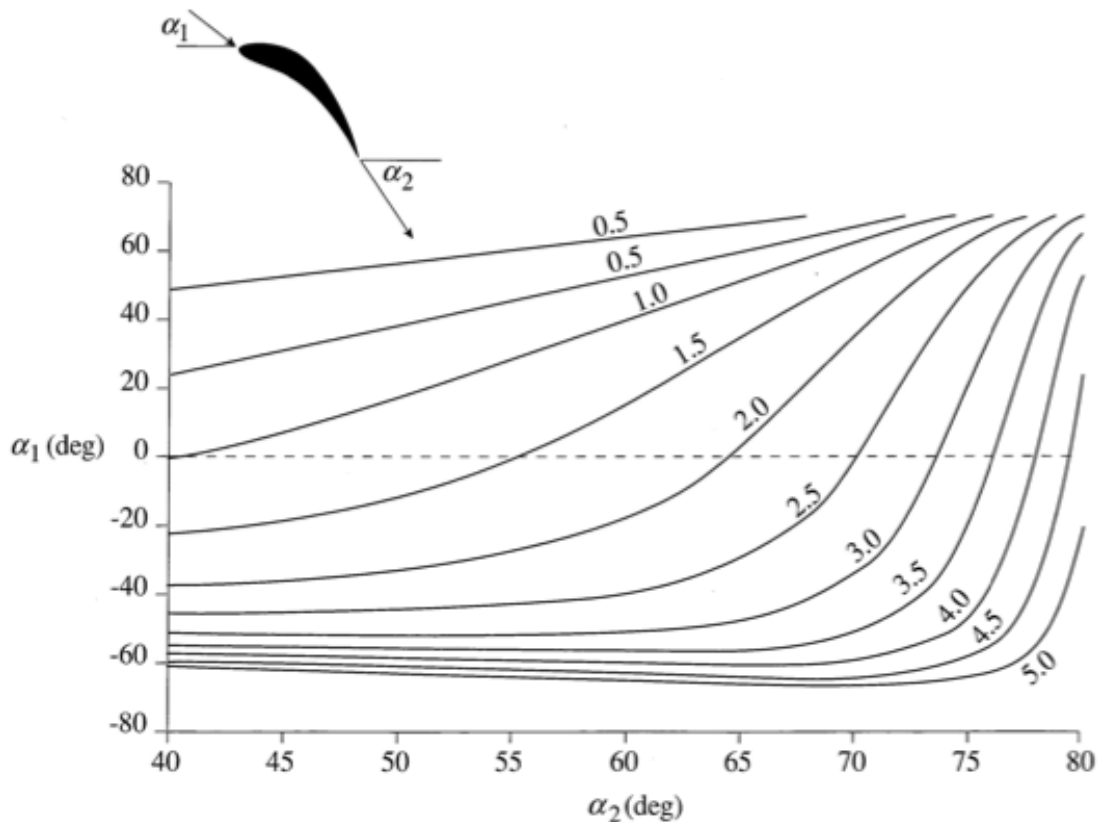


Figure 4-15 Minimum Profile Loss predicted for Optimum Pitch to Chord Ratios  
as extracted from the book Internal Flows (Greitzer, 2004)

The entropy-based profile loss coefficient provided by this correlation was found by Denton to be in agreement with cascade measurements of loss coefficients. Similarly the optimum pitch to chord correlation is considered by Denton to agree well with the predictions of Zweifel rule shown in section

2.1.2. One limitation to the simplified methodology proposed by Denton is that is based on the assumption of a constant dissipation coefficient, which is used to measure the Reynolds effect.

Regarding the secondary loss, the model implemented in LUAX-T is similar to that proposed by Dunham and Came (Dunham & Came, 1979). The use of this correlation is based on the suggestion made by Denton where he stands that this correlation is one of the best methods for the endwall loss predictions. The correlation suggested by Denton is a modification of the model proposed by Dunham and Came, introducing a reduction factor of 0.375 based on a large number of comparisons with test data (Denton, 2008). Eq. 4-1 shows the correlation implemented in LUAX-T for secondary loss estimation as modified by Denton.

$$Y_s = 0.375 * 0.1336 \frac{c}{h} \frac{\cos^3 \alpha_2}{\sqrt{\cos \alpha_1}} \frac{(\tan \alpha_1 - \tan \alpha_2)^2}{\cos \alpha_m}$$

Eq. 4-1

The trailing edge loss is estimated in LUAX-T by the use of the Eq. 2-66 where the base pressure coefficient has been fixed to -0.15 based on Denton suggestion. In this correlation the main important feature is the trailing edge to throat ratio, which is calculated by LUAX-T. However, the boundary layer displacement and momentum thickness values are not calculated in LUAX-T and so the contributions of these coefficients to the loss have been neglected based on the fact that Denton states that the first term of Eq. 2-66, related to the influence of the base pressure, is likely to contribute a 75% to the total trailing edge loss (Denton, 1993).

There are two different correlations implemented in LUAX-T regarding clearance loss for Denton model. These are considering shrouded or unshrouded blades. For unshrouded blades Denton gives a correlation that works for 1% of clearance on height ratio and is mainly a function of the inlet and outlet relative flow angles in the rotor. This correlation is shown in Figure 4-16 as it is implemented in LUAX-T.

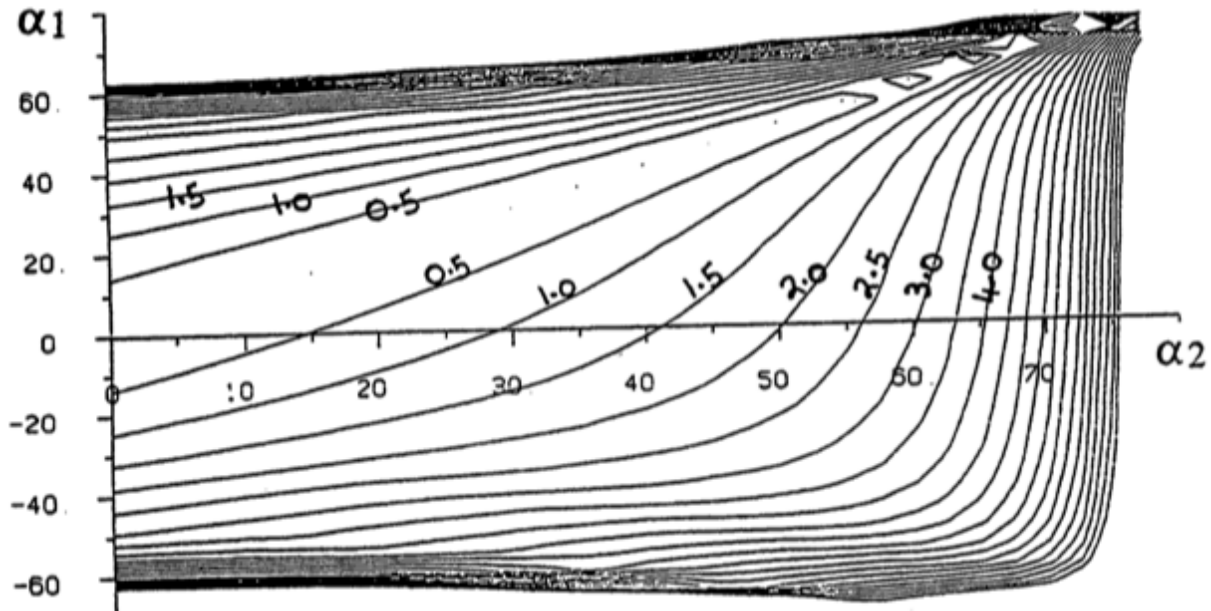


Figure 4-16 Clearance Loss for Unshrouded Blades with 1% of Clearance on Height (Denton, 1993)

On the other hand, the correlation implemented to estimate the clearance loss of shrouded blades is similar to that exposed in section 2.4.3 of the present work. Here the mass fraction ratio is estimated from Eq. 4-2 as it is suggested by Denton, where the contraction coefficient has been set to 0.6 (Denton, 2008).

$$\frac{m_{leak}}{m_{inlet}} = 0.6 \frac{\text{clearance}}{\text{span}} \frac{\text{pitch}}{\text{throat}} \frac{1}{\sqrt{N_{seals}}}$$

Eq. 4-2

While the Craig-Cox loss correlation was based on different tabulated data, Denton's correlation is more direct and uses less equations or in fact only one correlation for each loss mechanism. Therefore the correlation was manually verified instead of comparing it against previous studies given its simplicity. However, the secondary, trailing edge and clearance loss of shrouded blades correlations were assumed to be correct as they were just implemented exactly as shown in the literature (Denton, 2008).

Finally after implementing the Denton loss correlation in LUAX-T now the program has been extended to perform a complete simulation with one of the three-implemented models or else with all of them at the same time to compare results, upon user's decision. The outputs of the program still remain similar but now adding one more text file including the results from this last implemented correlation. This text file is similar to that given by the other correlations, now under the name Output\_Data\_D.txt. Regarding the output figures, here is shown below an example of the breakdown of losses results figure for a complete simulation in LUAX-T using all the correlations for a 3 stage high pressured turbine.

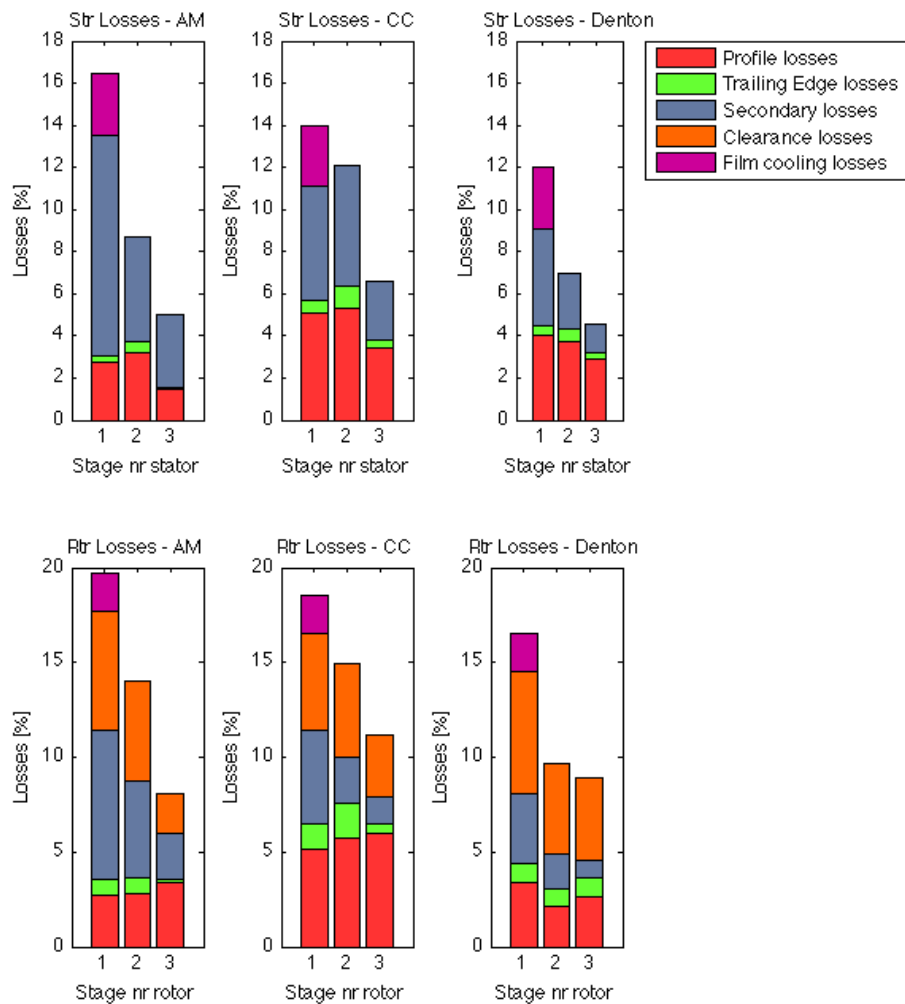


Figure 4-17 Breakdown of Losses as shown in LUAX-T for a complete simulation using the 3 loss correlations

## 5. Validation of Loss Models

The loss correlations implemented in LUAX-T have been validated by each one of their authors respectively. They have tested the accuracy of their model against different experimental data obtained from a large number of turbines for which adequate test information was available. However, in order to improve the understanding of the flow and loss mechanisms of axial turbines, the present section of the work will investigate the accuracy of the correlations against measurements performed at the turbine test facility in KTH (KTH, 2011). The aim of this chapter is not only to validate the implemented correlations but also to differentiate the models and give conclusions about their accuracy. The methodology used to perform the validation process consists of the development of an iterative program in Matlab (Mathworks Inc., 2010). This program adapts the experimental data so that it can be used by each of the loss correlations implemented. Finally the program gives the results by showing the efficiency curves obtained by each correlation and comparing them against the measured torque efficiency. This last means that the experimental efficiency is calculated by measuring the stagnation enthalpy drop mechanically by torque rather than thermodynamically. The equation to calculate the total-to-static efficiency from experiment is shown in Eq. 5-1, where the isentropic enthalpy drop is calculated as shown in Eq. 5-2. Similarly, the stagnation enthalpy drop equation is shown below, where the torque M is the sum of the shaft torque, the friction torque on bearing and the friction torque between air and rotor disc (Svensdotter & Wei, 1995).

$$\eta_{ts} = \frac{\Delta h_c + C_1^2 - C_3^2}{\Delta h_{is} + \frac{C_1^2}{2}}$$

Eq. 5-1

$$\Delta h_{is} = CpT_1 \left[ 1 - \left( \frac{P_3}{P_1} \right)^\gamma \right]$$

Eq. 5-2

$$h_c = n \frac{\pi}{30} \frac{M}{\dot{m}}$$

Eq. 5-3

Validation studies were performed for two different axial gas turbines characterized for having low reaction but differing in geometric parameters and flow conditions. The validation study will prove that both, geometry and flow conditions, are of great importance for the loss correlations in the turbines performance prediction. Due to a confidentiality agreement signed for one of the validation cases, the measured efficiency values and the flow field measurements for the two cases considered will not be shown to keep the same structure in the work. In this regard, the efficiency values have been normalized with the maximum measured efficiencies. Similarly, the individual geometric parameters will not be shown but instead some of the ratios needed by the correlations. However, the information and measurements regarding the second validation were extracted from a published work (Svensdotter & Wei, 1995) and so it can be found in APPENDIX II.

The chapter is divided in two different sections. The first section applies for both validation studies. Explained in that section is the turbine test facility and also the method for how the experimental data was used to predict the turbine efficiency with the models. Finally, the last section will go through characterize each turbine and show the results and conclusions for the validation studies. These results and conclusions will be further mentioned in the discussion chapter of this thesis.

### Test Turbine Facility and Numerical Calculations with Experimental Data

In order to achieve the proposed objective, for both cases the turbine test facility was equipped with a single stage. The validation experiment is based on different operation conditions. In each operation condition measurements taken were all the parameters needed as inputs for the loss correlations in three different sections. These sections are per inlet and outlet of stator and rotor. The most important parameters measured in these sections were the inlet and outlet flow angles, the absolute and relative velocities and the air properties such as temperature, pressure and density. The Reynolds number was

estimated from Eq. 5-4, where the dynamic viscosity was approximated by the use of Eq. 5-5 (Fridh et al, 2004).

$$Re = \frac{\rho V c}{\mu}$$

Eq. 5-4

$$\mu = 0.00001748 + 0.0000000431(T)$$

Eq. 5-5

In Eq. 5-4 the characteristic length used is the chord. This is used since the codes implemented need this value and from here they calculate the Reynolds effect in each correlation. On the other hand, the Mach numbers at stator and rotor's outlet were calculated from Eq. 5-6. All the values needed in this equation were measured at the test turbine. Results show that both turbines operated under turbulent and subsonic conditions, thus no major portion of the losses is due to Reynolds or Mach number effects.

$$Ma = \frac{V}{\sqrt{kRT}}$$

Eq. 5-6

Figure 5-1 shows a cross-section of the test turbine used for the present study where it is possible to distinguish the axial measurement sections. The first two of these sections are referred to as the stator inlet and outlet conditions (Sections 4 and 5). As the stator outlet is used for rotor inlet conditions then the last measurement point considered was downstream of the rotor (Section 7).

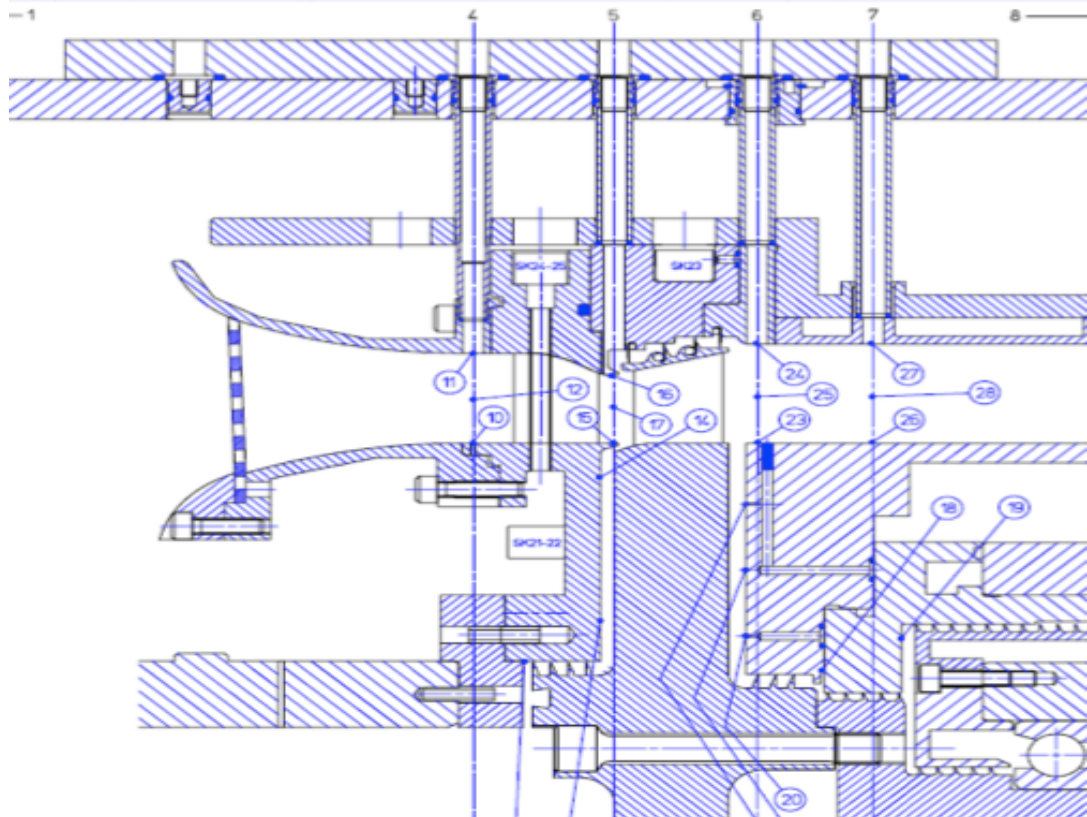


Figure 5-1 Cross Section of the Test Turbine in KTH used for the measurements in present work (KTH, 2011)

The rest of the numerical calculations are referring the prediction of the turbine performance while using measured data. The loss correlations will give the loss coefficients, whether enthalpy, entropy or pressure

based according to the correlation. The calculated loss coefficients (enthalpy based) were used to estimate the total-to-static efficiency from Eq. 5-7 (Asuaje, 2009).

$$\eta_{ts} = \left[ 1 + \frac{\xi_R W_3^2 + \xi_N C_2^2 + C_1^2}{2(h_1 - h_3)} \right]^{-1}$$

Eq. 5-7

As stated before, the velocities and the enthalpy changes are all measured by the experiment. Moreover, the formula used to convert from pressure to enthalpy based loss coefficients is the same described at the beginning of the present work, provided by Moustapha (Moustapha, 2003).

#### Validation Results and Conclusions

Described in next pages are the results of the validation processes for both turbines. It was chosen to plot the normalized efficiency against the reaction degree for each validation case. However, in APPENDIX II similar plots can be found for the efficiency but using the velocity ratio, as defined in Eq. 5-8, instead of the degree of reaction. Both parameters, reaction and velocity ratio, are related to the velocity triangles.

$$v = \frac{U}{\sqrt{2\Delta h_{is}}}$$

Eq. 5-8

#### - Validation Study for Turbine 1

The first turbine analyzed is characterized by having a low reaction, tangential inlet rotor flow angles and axial rotor outlet flow angles, which means a more accelerating cascade. The geometrical ratios and some of the parameters needed for the estimation of losses are shown in Table 5-1.

Table 5-1 Validation 1. Geometry Ratios

Geometrical Ratio	Stator	Rotor
Pitch to Chord Ratio	0.83	0.81
Aspect Ratio	0.77	1.32
Trailing Edge to Throat Ratio	0.04	0.04

The results confirm the accuracy of one of the models and conclusions from previous works. In this regard, Figure 5-2 shows the normalized calculated total to static efficiency curves against the pressure based reaction degree. If comparing the experimental data curve against the Craig and Cox results, it is possible to see that the correlation was found to be able to accurately predict the turbine's performance for all the complete range of reaction degrees. On the contrary, the other two loss correlations were found to diverge from the experimental data as the reaction degree decreased. Figure 5-2 shows that for reaction degrees closer to 0.2 all the loss models predicted the efficiency within a range of less than 5% when comparing it against the experimental data, while for reaction degrees closer to zero only Craig and Cox's correlation stayed within this error range. Furthermore, the design reaction degree for the present turbine is 0.16 and it is possible to see that Denton and Craig-Cox models give an error of less than 3% for that operation point.

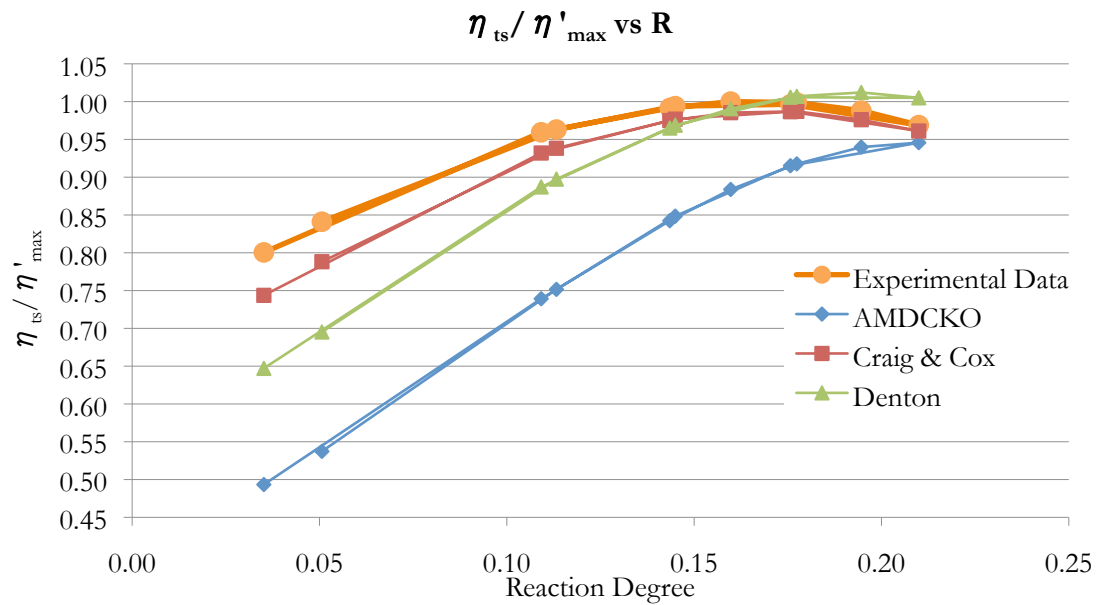


**Figure 5-2 Validation 1. Efficiency Curves predicted for a one-stage Impulse Turbine with tangential inlet rotor angle**

In order to analyze the results, it was of special interest to see how do the enthalpy-based loss coefficients calculated by each correlation were behaving for both stator and rotor. In this regard, Figure 5-3 shows that no major change was found for the enthalpy based stator loss coefficient, being Denton's correlation the most optimistic, given lower coefficients. The Craig and Cox correlation and the Denton's coefficient remain constant since they are mainly a function of the flow angles and the pitch to chord ratio and these values do not change in any of the 11 operation points. On the other hand, the AMDCKO model does not give a constant value since the secondary losses increase, as they are a function of the loading factor introduced by Ainley and Mathieson (Ainley & Mathieson, 1951). This factor is calculated in the program as a function of the average velocity ratio, which is a function of the inlet and outlet stator meridional velocities, which slightly varied from point to point.

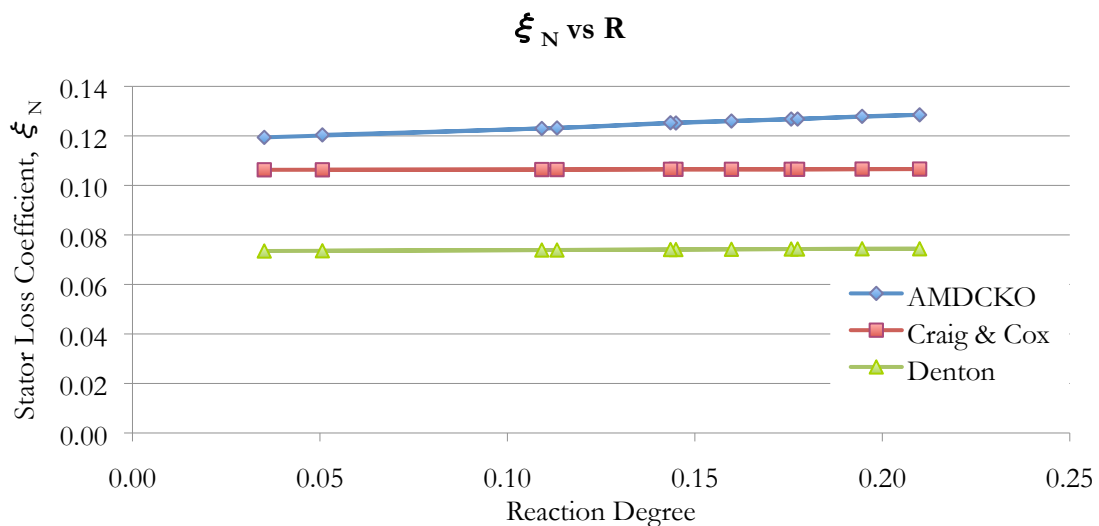


**Figure 5-3 Validation 1. Stator Loss Coefficients Vs. Reaction Degree**

Regarding the enthalpy-based loss coefficients calculated for the rotor, it is possible to see a greater difference. Figure 5-4 shows how these values behave for the same range of reaction degrees. As was expected, in concordance with Figure 5-2, for lower reaction degrees the AMDCKO and Denton correlations give much higher coefficients when comparing them against the ones calculated with Craig

and Cox correlation. Regarding these results, many observations are clear and they might explain the occurrence of these discrepancies.

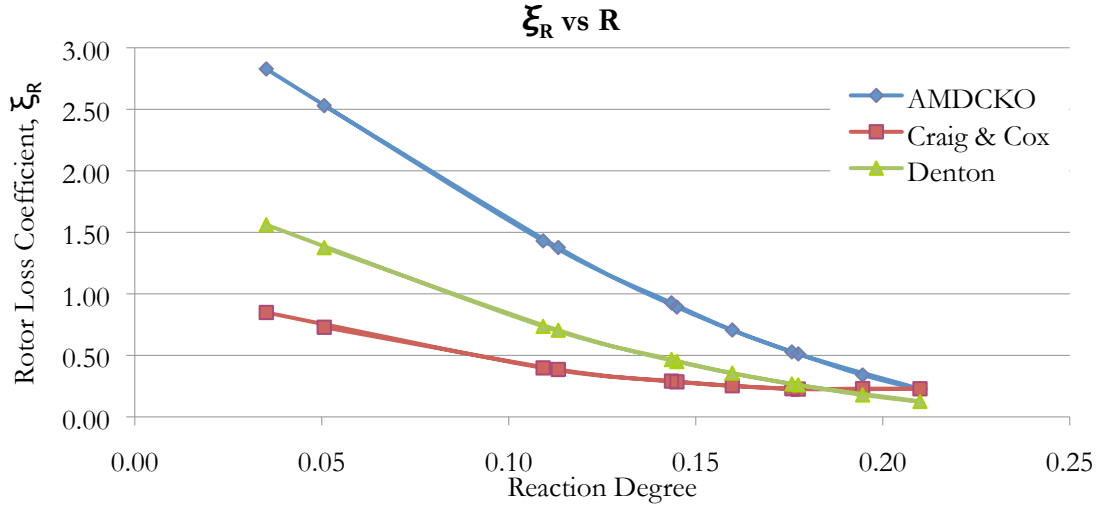


Figure 5-4 Validation 1. Rotor Loss Coefficients Vs. Reaction Degree

First, in a gross-way of analyzing the results, when comparing the breakdown of losses between each model it was found that the main reason for this phenomenon to occur were the higher secondary losses calculated by the AMDCKO model. Now, the implemented Denton and AMDCKO correlations for estimation of secondary loss differ only on the aspect ratio function and a factor of 0.375 introduced by Denton, this explains their similitude in trends. Moreover, the aspect ratio function, whether different in each correlation, does not change its value since the geometry of the turbine is fixed. This implies that the main source of the problem regarding the secondary loss correlation, are the inlet and outlet flow angles. These angles, besides the aspect ratio, were found in this work to be the key parameters governing this loss mechanism since they are used in the models to correlate the blade loading. High blade loading is related to the boundary layer movement from pressure to suction side of the blade, which generates a mixing process in the passage and hence more secondary losses.

In this regard, if analyzing the input data, the rotor outlet flow angles measured in each of the 11 operation conditions were very small (measured from axial line) and out of the range of applicability for the AMDCKO model (Figure 5-5). Furthermore, for lower reaction degrees it was found that the Ainley's loading factor used to calculate the secondary losses was higher, leading to overestimate the secondary loss for these cases. This exists since the loading factor is proportional to the secondary loss coefficient. As shown in Eq. 5-9, the loading factor is proportional to the square of the outlet flow angle's cosine and inversely proportional to the cube of the vector mean air angle's cosine, parameter introduced by Dunham (Dunham, 1970). In this particular validation case, not only the values for the outlet angles were low, but also the vector mean air angle values were high, especially for the large inlet flow angles (angles measured from axial direction as shown in Figure 5-5).

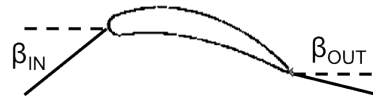


Figure 5-5 Rotor Blade Sketch in Validated Turbine 1 - Small Outlet Flow Angles

$$Z = \left( \frac{Cl}{s/c} \right)^2 \frac{\cos^2(\alpha_2)}{\cos^3(\alpha_m)}$$

Eq. 5-9

In consequence it can be concluded that the tests performed to validate the secondary loss correlation by Dunham or Kacker and Okapuu did not consider the combination of inlet and outlet flow angles present in this validation process. Moreover, the relationship between the larger inlet flow angles in the rotor and the low reaction degree can be observed below (De Andrade, 2010).

$$R = \frac{Cx}{2U} |\tan\beta_3 - \tan\beta_2|$$

Eq. 5-10

In spite of the discrepancies encountered, the correlations implemented in LUAX-T behave as expected. In a work performed by Lozza, he concludes that the Kacker and Okapuu's loss correlation is not to be applied for turbine impulse stages with high deflection as the one in present study. He also states that the model accuracy is greatly dependent on the flow angles (Lozza, 1982). Present validation's results confirm Lozza's conclusion and proves that the main source for this to occur are the secondary loss correlations. Moreover the accuracy of the Craig and Cox loss correlation has been validated to work for low reaction degrees and therefore remains as a better model to choose in these cases. Regarding the simplified Denton's model, it is only possible to conclude that its behavior is due to its similarity with the AMDCKO correlation for the secondary loss estimation. Therefore Denton's correlation is not likely to approach reality for lower reaction degree turbine stages with the flow angles present in this validation case neither.

#### - Validation Study for Turbine 2

Similarly as the first turbine tested, this second turbine is characterized for a low reaction degree in on-design conditions ( $R=0.10$ ) but on the contrary the inlet and outlet rotor flow angles measured were more tangential, as can be seen in page 131 in APPENDIX II. The geometrical ratios of the main parameters used for the prediction of losses are shown in Table 5-2. In this case there are smaller aspect ratios and solidities when comparing against the first turbine validated.

**Table 5-2 Validation 2. Geometry Ratios**

Geometrical Ratio	Stator	Rotor
Pitch to Chord Ratio	0.69	0.72
Aspect Ratio	0.58	0.96
Trailing Edge to Throat Ratio	0.04	0.04

Results show that all the correlations were found able to predict accurately the performance of the turbine (Figure 5-6). Below is possible to see that the AMDCKO and Craig and Cox correlations showed similar efficiency curves having close values to the experimental data. On the contrary, Denton's correlation efficiency curve seems to underestimate the losses and hence provides higher efficiency values. However the trend showed for this last correlation is found to be similar to the experimental data.

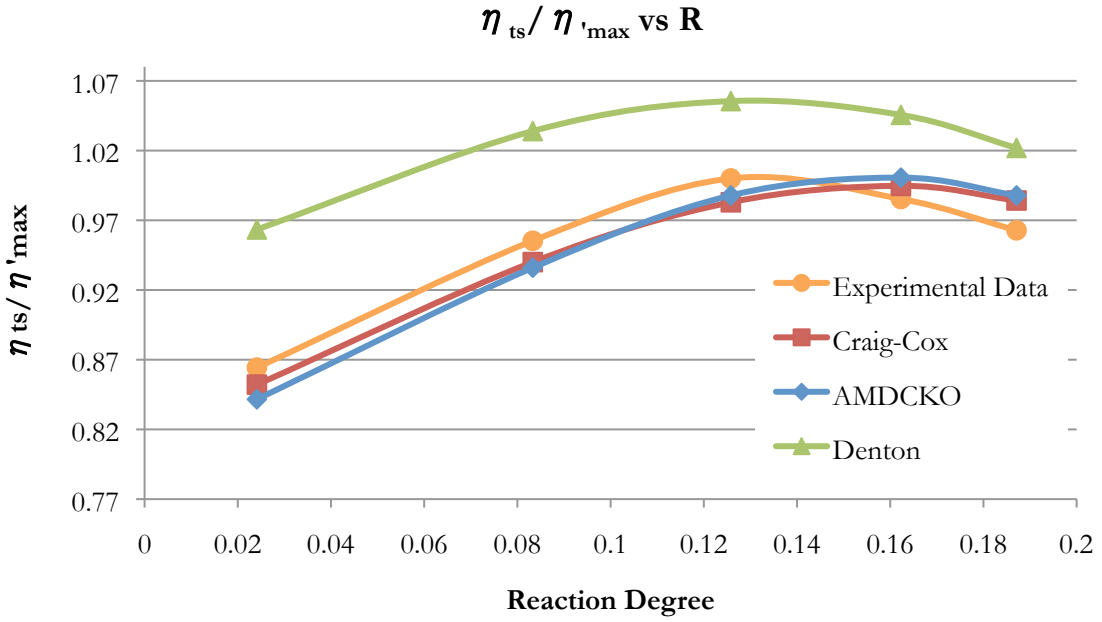


**Figure 5-6 Validation 2. Efficiency curves predicted for a one-stage Impulse Turbine with axial rotor inlet flow angle**

The next page shows the enthalpy loss coefficients calculated by each model for the stator and rotor blades respectively. In concordance with Figure 5-6 all the models show similar trends for the enthalpy loss coefficients measured. Moreover, as mentioned at the beginning of this section, the rotor inlet and outlet relative flow angles were both large if measured from axial (APPENDIX II). These angles were found to be part of the range of applicability given by the correlations. This last point means that, in difference with the previous validation study, no extrapolation was needed regarding the flow angles for the loss prediction, which gives more reliability for the correlation and would lead us to think that even though both cases are impulse turbines, the operation conditions present in this second validated turbine were considered when each of the authors validated their own correlations respectively.

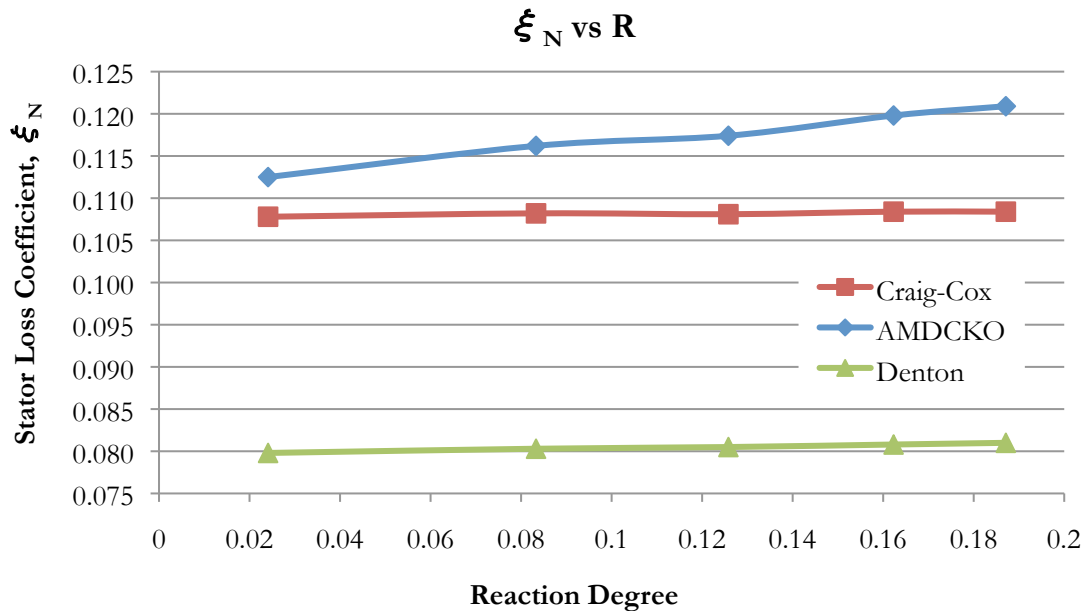


**Figure 5-7 Validation 2. Stator Losses Vs. Reaction Degree**

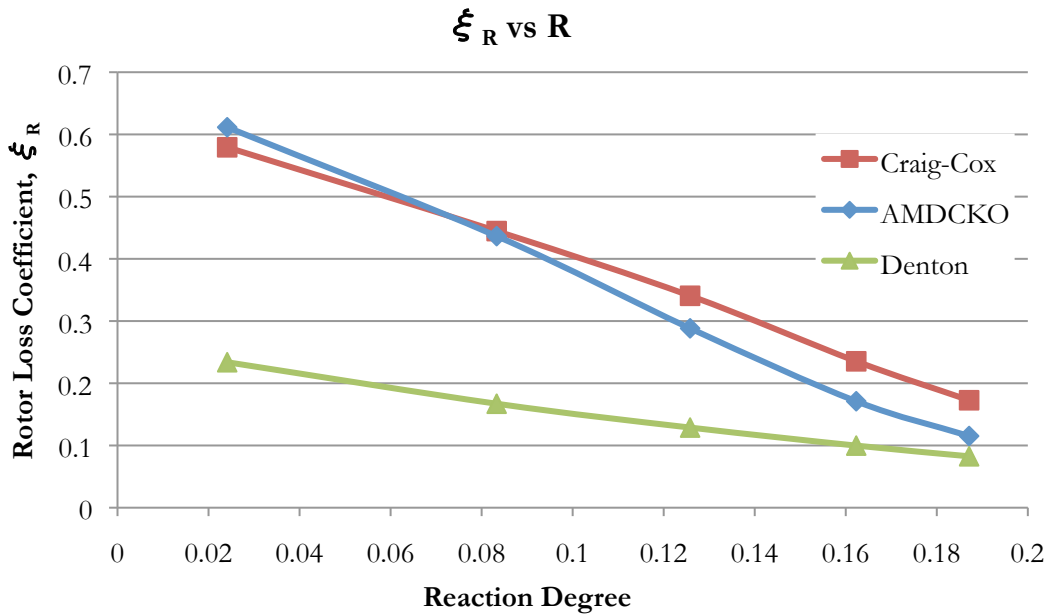


**Figure 5-8 Validation 2. Rotor Losses Vs. Reaction Degree**

Figure 5-8 shows that the trend exposed for the efficiency is mainly ruled by the rotor loss coefficient. However, even though the efficiency prediction by each correlation was similar it was interesting to see how each loss correlation predicted each of the loss mechanisms coefficients. If analyzing the breakdown of losses it could be noticed that the results are completely different. In this regard, Table 5-3 shows the profile and secondary loss coefficients predicted by each los mechanism for the rotor case. It is possible to see that for the lowest reactions AMDCKO predicts considerably higher secondary losses while Craig-Cox gives higher values for the profile loss coefficient. Nonetheless, this helps to prove that the authors verified the accuracy of their own correlations by testing the overall performance of the turbine and not the single contributions from the loss mechanisms, which is different for each model (Table 5-3).

**Table 5-3 Breakdown Of Losses - Validation 2**

Reaction	AMDCKO		Craig and Cox		Denton	
	$\xi$ Profile	$\xi$ Secondary	$\xi$ Profile	$\xi$ Secondary	$\xi$ Profile	$\xi$ Secondary
0.024	0.014	0.544	0.308	0.276	0.004	0.220
0.083	0.012	0.378	0.206	0.219	0.005	0.150
0.126	0.012	0.238	0.146	0.169	0.006	0.107
0.162	0.013	0.130	0.085	0.118	0.010	0.071
0.187	0.013	0.079	0.054	0.085	0.013	0.048

#### - Conclusion

From the validation study it is possible to confirm that the loss correlations do accurately predict the turbines performance if applied within the range of applicability they were developed for. This last point means that models behave properly if no extrapolation is needed, as for the case of the second validation. Moreover, the Craig and Cox loss correlation was found to better approach reality for both impulse turbines tested when comparing results against he experimental data.

Results confirm that the AMDCKO loss model is not to be applied in the case of turbine stages with characteristics different from conventional gas turbines such as low aspect ratios with axial outlet flow angles. In this regard, it was found that the main cause was the miss-prediction of the secondary loss. In consequence, Denton's correlation should not be considered neither for impulse stages with small exit flow angles neither given its similarity with the Kacker-Okapuu model.

Furthermore, as two different turbines were analyzed, the influence of the geometry in the loss prediction could be tested. In this regard, as the second turbine has shorter blades, more effect from the growth of the endwall boundary layer is appreciated. However, the total secondary losses are also a function of the blade loading, related to the angles, which were found to highly influence the estimation of the turbine 1 performance.

Finally, the validation proved that loss models should be used independently from one to another as each one has their own way of estimating the individual loss mechanisms. Even though estimating similar total loss components, the prediction for each of the loss mechanisms is completely different. Hence any mixing between the correlations could lead to overestimate or underestimate the total losses. Moreover, the similarities found for the total loss predictions prove that the correlations were validated testing the overall performance of the turbine rather than each loss mechanism.

## 6. Parametric Design Study

Loss models are implemented in LUAX-T and in order to check if they show similar trends for design it was performed a parametric design study. The study consists of predicting the performance of different turbines while varying design parameters such as the stage-loading coefficient and flow coefficient for a range of reaction degrees. This chapter will explain the methodology followed for this study and their respective results, which consider comparisons between the different loss models.

### 6.1. Methodology

First it should be acknowledged that the main parameters for turbine design are those exposed in section 2.1.2 of present study. The stage loading, the flow coefficient and the Reaction Degree are important in the prediction of the turbines performance. The main objective of the study is to analyze how would the different correlations behave by systematically varying each of these coefficients. In this regard, the study will not only show the efficiency curves but also determine which values of reaction degree give higher efficiencies given fixed design parameters. The study is performed for the first stage of a high-pressure cooled turbine, which specifications are showed in next section. Table 6-1 shows the range of values taken into account for each parameter. The selection of these values is to perform the study around the reference case. This is a three-stage turbine, which first stage has a stage-loading coefficient of 1.6 and a stator outlet angle of  $73.6^\circ$  (axial measure). As can be seen in the table, it was chosen to fix the stator outlet angle and not the flow coefficient. The flow coefficient and the flow angles are related as discussed in Chapter 2 of present work. If measured from axial line, the higher the outlet flow angle then the lower the flow coefficient and hence higher efficiency.

Table 6-1 Parametric Study: Range of Values

	$\Psi = 1.5$	$\Psi = 1.6$	$\Psi = 1.7$
$\alpha_2 = 73$	R = [0.05; 0.60]	R = [0.05; 0.60]	R = [0.05; 0.60]
$\alpha_2 = 74$	R = [0.05; 0.60]	R = [0.05; 0.60]	R = [0.05; 0.60]
$\alpha_2 = 75$	R = [0.05; 0.60]	R = [0.05; 0.60]	R = [0.05; 0.60]
$\alpha_2 = 76$	R = [0.05; 0.60]	R = [0.05; 0.60]	R = [0.05; 0.60]

The total-to-total and total-to-static isentropic efficiencies curves were obtained for each model to see if whether or not the models gave similar design trends for both cases. In this regard, in order to perform the study a new program was developed as a plug-in for LUAX-T (Genrup, 2008) under the name LUAX-T Parametric Study Tool. This tool allows the user to select the range of values for each parameter and gives different graphical and text outputs. Figure 6-1 shows an example of the initial graphical user interface of the tool while Figure 6-2 is an example of the text output file. The text output includes tables with the efficiency calculations for all of the different set of design parameters set by the user and also the optimum reaction degree for each particular set of stage-loading coefficient and stator outlet angle. Complete graphical and output text files of the program can be reviewed in the APPENDIX III section of the work, which contains the results from present parametric design study. Finally, the results from the outputs were analyzed and compared. It was of interest to compare the models between them but also review if the trends were as expected according to the literature.

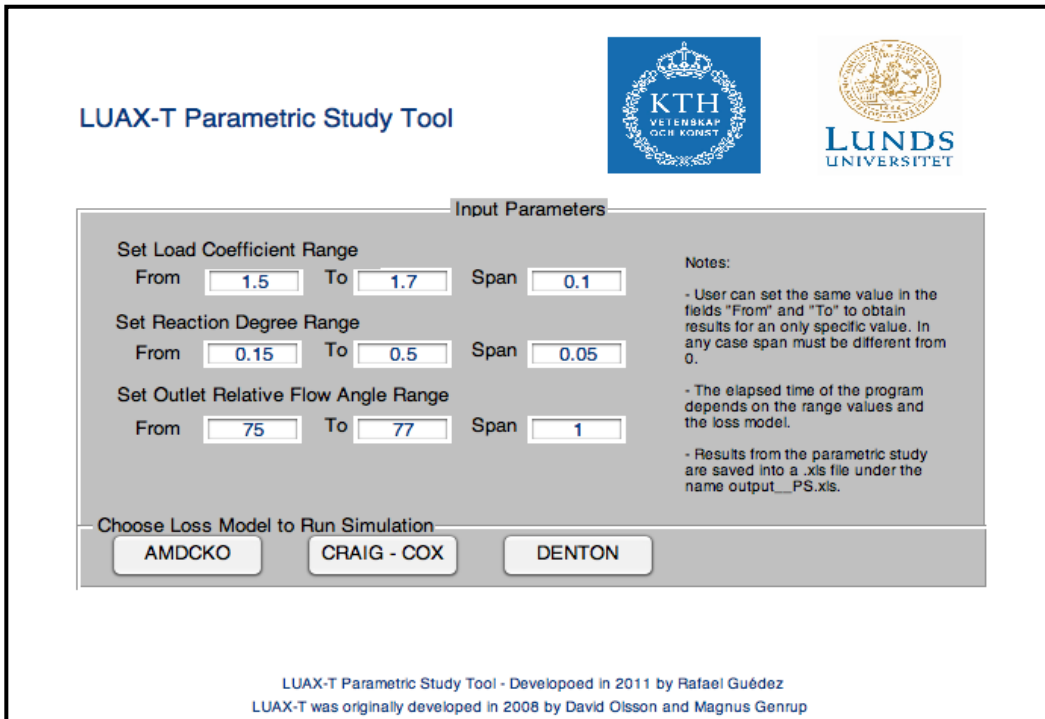


Figure 6-1 Graphical User Interface for LUAX-T Parametric Study Tool

```
Test_turbine_1_Outputparam_AM.txt
=====
#           LUAX-T      #
#           Version 2.0   #
#           David Olsson & Magnus Genrup   #
#           2008          #
#           #           #
#           Rafael Guedez    #
#           2011          #
=====

Test_turbine_1
14-Mar-2011 00:06:38
PARAMETRIC STUDY
Ainley & Mathieson et al. RESULTS
=====

Stage 1
Outlet Angle      73.00
Load Coefficient   1.50
Optimum Point:    R =  0.25      TS Isentropic Efficiency =  71.00
=====
Reaction Degree == Flow Coeff == PR t-t == TT Iso Effic. == TS Iso Effic. == TT Pol Effic. == TS Pol Effic == T. Effic P&W == T. Effic Kurzke ===
  0.15    0.51    2.38    77.79    71.53    77.47    80.51    80.88    69.57
  0.20    0.49    2.36    77.98    71.77    77.71    80.76    80.41    69.36
  0.25    0.46    2.35    78.09    71.80    77.85    80.97    79.90    69.11
  0.30    0.44    2.34    78.13    71.63    77.92    81.14    79.35    68.81
  0.35    0.42    2.34    78.08    71.26    77.89    81.26    78.74    68.46
  0.40    0.40    2.34    78.00    70.74    77.81    81.38    78.11    68.09
=====
Load Coefficient   1.60
Optimum Point:    R =  0.20      TS Isentropic Efficiency =  71.42
=====
Reaction Degree == Flow Coeff == PR t-t == TT Iso Effic. == TS Iso Effic. == TT Pol Effic. == TS Pol Effic == T. Effic P&W == T. Effic Kurzke ===
  0.15    0.53    2.54    77.69    71.34    77.11    80.30    80.77    70.27
  0.20    0.50    2.52    77.91    71.42    77.38    80.66    80.32    70.07
```

Figure 6-2 Parametric Study Output text file for AMDCKO loss correlation as extracted from LUAX-T

## 6.2. LUAX-T Input Settings

The inputs for the program are shown next in a tabular form. Each of the tables shows the different input parameters for LUAX-T prior to the simulation. First of them is regarding the general turbine settings. In this regard it is possible to see that for the first stage the fields “Reaction Rate” and the “Stage Loading Coefficient” are filled with a “-“, meaning that they are changing within a range as specified in Table 6-1

and set by the user in the GUI showed in Figure 6-1. The second table shows the inlet properties of the working fluid.

**Table 6-2 Parametric Study - Input general turbine settings.**

<b>General Turbine Settings</b>			
Stage Number	Stage 1	Stage 2	Stage 3
Compressor Turbine Stages [-]	0		
Power Turbine Stages [-]	3		
Compressor Turbine Power [kW]	0		
Max stress level in blade, AN <sup>2</sup> [-]	55000000		
Diffuser Recovery Coefficient [-]	0,84		
Rotational Speed [rpm]	6600	6600	6600
Reaction Rate [-]	-	0,36	0,45
Stage Loading Coefficient [-]	-	1,3	1,4
Fixed Flow Coefficient [-]	0	0	0
Fixed P2 [bar]	0	0	0
Fix or Guess P3 [bar]	0	0	0
P3 [bar]	7,000	3,003	0,985

**Table 6-3 Parametric Study - Input inlet properties**

<b>Inlet Properties</b>	
Inlet Mass Flow [kg/s]	100,00
Inlet Total Temperature [°C]	1423
Inlet Total Pressure [bar]	18,52
Inlet Fuel to Air Ratio [-]	0,02
Inlet Cooling Mass Flow [%]	0,00
Inlet Cm [m/s]	85,00
Inlet Flow Angle [°]	0,00

Next tables are regarding the specific geometry of the turbine. Table 6-4 shows the specific geometry of the Hub Line and Duct geometry. Here it is possible to see that, similarly, the value of the stator trailing edge angle at stage 1 is not mentioned as it is changing for the specified range shown in Table 6-1. Table 6-5 shows the specific blade geometry.

**Table 6-4 Parametric Study - Input Hub Line and Duct Geometry Settings**

<b>Hub Line and Duct Geometry Settings</b>			
Stage Number	Stage 1	Stage 2	Stage 3
Stator TE Flow Angle [°]	-	72,47	69,45
Fixed r2_mix_hub option [-]	1	1	0
r1_hub [m]	0,622		
r2_mix_hub [m]	0,620	0,600	0,577
r2_gap_hub [m]	0,617	0,598	0,574
r3_hub [m]	0,611	0,591	0,560
r3_gap_hub [m]	0,606	0,586	0,000
Rel. Stator Gap [%]	25	25	25
Rel. Rotor Gap [%]	30	30	30
Fixed Stator axial chord [m]	0,065	0,077	0,077

Fixed Rotor axial chord [m]	0,054	0,053	0,075
Stator Hub HADE [°]	0,00	-8,00	-8,00
Stator Gap Hub HADE [°]	0,00	-8,00	-7,00
Rotor Hub HADE [°]	-3,00	-8,00	-5,00
Rotor Gap Hub HADE [°]	-3,00	-8,00	0,00
Fix Stator Gap Tip HADE [°]	0,00	0,00	1,00
Stator Gap Tip HADE [°]	0,00	0,00	20,00
Rotor Tip HADE [°]	0,00	0,00	20,00
Fix Rotor Gap Tip HADE [°]	0,00	0,00	1,00
Rotor Gap Tip HADE [°]	0,00	0,00	0,00
Stator TAPER Angle [°]	-2,00	-3,00	-3,00
Rotor TAPER Angle [°]	1,00	2,00	3,00

Table 6-5 Parametric Study - Input Blade Specific Geometry Settings

Blade Specific Geometry Settings			
Stage Number	Stage 1	Stage 2	Stage 3
Rotor Overlap [m]	0,001	0,000	0,000
Stator LE Radius [m]	0,00560	0,00590	0,00411
Rotor LE Radius [m]	0,00410	0,00330	0,00295
Stator TE Radius [m]	0,00113	0,00137	0,00074
Rotor TE Radius [m]	0,00128	0,00134	0,00058
Stator Tip Clearance to Height [-]	0	0	0
Rotor Tip Clearance to Height [-]	0,01	0,01	0,01
Stator SONE [-]	0,15	0,15	0,15
Rotor SONE [-]	0,15	0,15	0,15
Fixed Stator Pitch to Chord [-]	0	0	0
Fixed Rotor Pitch to Chord [-]	0	0	0
Fixed N° of Stator Blades [-]	0	0	0
Fixed N° of Rotor Blades [-]	0	0	0
Fixed Stator Zweifel N° [-]	0	0	0
Fixed Rotor Zweifel N° [-]	0	0	0
N° of Stator Shroud Seals	0	5	5
N° of Rotor Shroud Seals	0	0	3

Finally, the last table concerns the cooling specifications for the simulation. Only the first stage considers cooling calculations, which is set in the program by fixing both inputs stage 1 stator and rotor cooling type to 2, as shown in the table below.

Table 6-6 Parametric Study - Input Cooling Settings

Cooling Settings			
Stage Number	Stage 1	Stage 2	Stage 3
Max Stator Metal Temperature [°C]	900	900	900
Max Rotor Metal Temperature [°C]	900	900	900
Stator Cooling Type [-]	2	1	1
Rotor Cooling Type [-]	2	1	1

Compressor Polytropic Efficiency [-]	0,918		
Compressor Extraction Pressures [bar]	20	16	10
Stator Cooling Position [-]	1	2	4
Rotor Cooling Position [-]	1	3	4
Option to fix Stator Cooling Mass Flow [-]	0,00	0,00	0,00
Fixed Stator Cooling Mass Flow [kg/s]	10,88	3,25	0,00
Option to fix Rotor Cooling Mass Flow [-]	0,00	0,00	0,00
Fixed Rotor Cooling Mass Flow [kg/s]	5,93	1,49	0,00
Stator Disc Cooling [%]	-2,47	-1,40	0,00
Rotor Disc Cooling [%]	-4,45	-2,58	1,50
Stator Film Cooling [%]	70,00	0,00	0,00
Rotor Film Cooling [%]	50,00	0,00	0,00
Overall Temp. Distribution Factor [-]	0,10		
Radial Temp. Distribution Factor [-]	0,05		
Abs. Cooling Air Velocity Ratio [-]	0,95		
Rel. Cooling Air Velocity Ratio [-]	0,95		

### 6.3. Results

In this section of the chapter are shown and discussed the results of the parametric study. The first result discussed is regarding the influence of varying the stator outlet angle in the performance prediction. Second about how were the trends for design by each model for a fixed stator outlet angle. This last point means to check what were the optimum reaction degrees calculated for each stage loading, and how was the stage loading coefficient affecting the efficiency curves.

For all the loss correlations the stator outlet angle was found to be influencing directly the efficiency value. The main reason for this relationship was due to the influence of the stator outlet angle on the flow coefficient calculation, which is related to the efficiency prediction. In this regard, a larger stator outlet angle (axial measured) implies lower flow coefficient and this means higher efficiency as could be seen in the Smith Chart shown in Figure 2-4.

Second objective was to see the difference in performance prediction for a same stator outlet angle. It was noticed that at lower stage loading coefficients the efficiency predicted was higher for all the correlations. This is in concordance with Smith predictions as shown in Chapter 2 (Smith, 1965). A simple analysis can explain one of the reasons for this phenomenon to occur. At higher stage loading coefficients, for similar flow coefficients, the velocity triangles are more skewed and hence there is more flow turning in the blade. More flow turning, related to blade loading, implies higher losses. This relation between the stage-loading coefficient and the velocity triangles can be observed from the dimensionless velocity triangles as shown in Figure 6-3. This figure is obtained after dividing all the velocities by the rotational speed “U” so that it is possible to see a relation between the stage-loading coefficient, the flow coefficient and the velocity triangles.

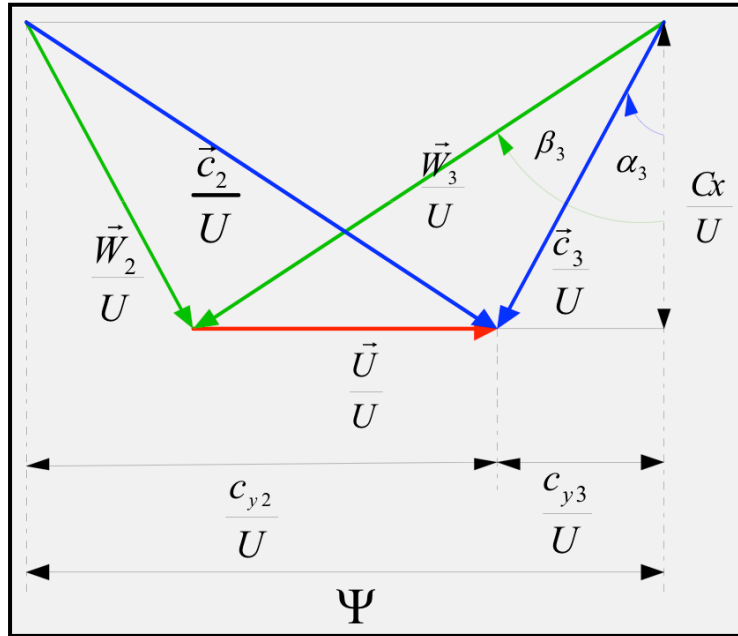
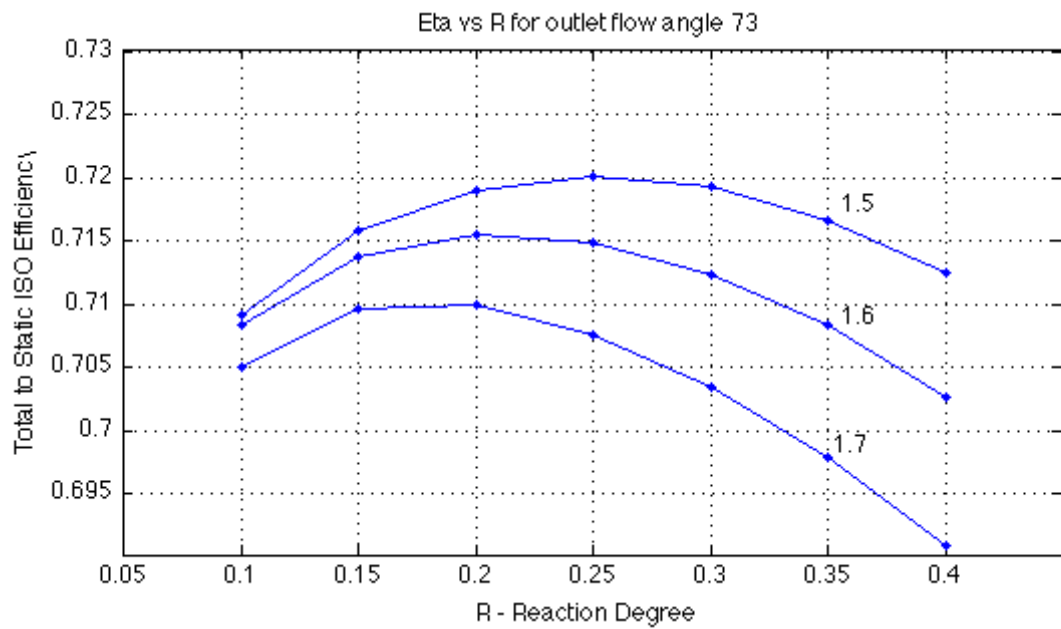


Figure 6-3 Dimensionless Velocity Triangles (Asuaje, 2009)

Last results were regarding the predictions of the optimum reaction degree. These depend on the different definitions of efficiency, therefore first are shown the results for the total- to-static efficiency and then the total-to-total efficiency. This is performed so for both definitions of efficiency it can be observed if the design trends are similar or not for the loss correlations. However, since the study was performed for the first stage of the turbine the selection of an optimum reaction should be considering that the energy from the first stage is used by the next stage and hence the total-to-total efficiency is more representative.

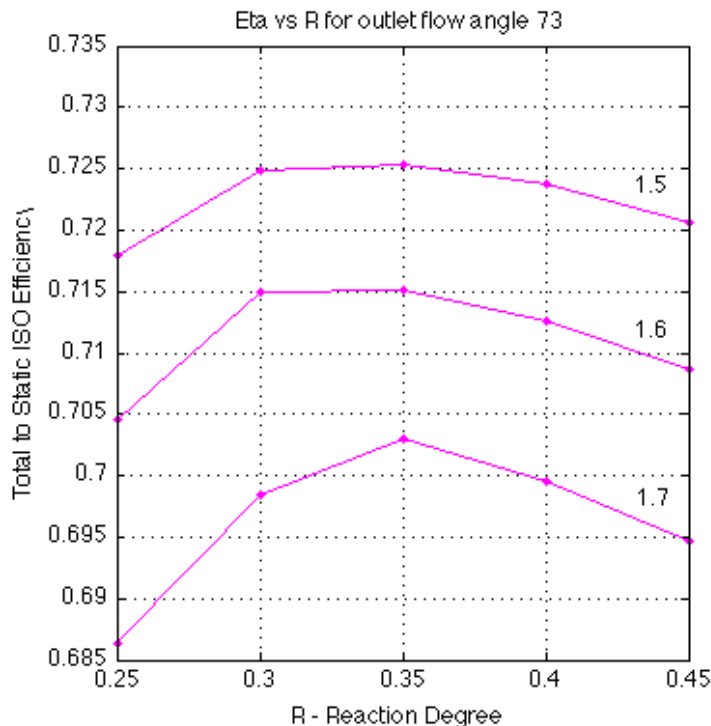
Regarding the total-to-static efficiency definition, all the loss correlations show that as the stage loading increased, the value for the optimum reaction degree was decreasing. These trends are in concordance with the theory described by Moustapha. He analyzed two different single stage turbines with different loadings and concluded that a turbine with lower stage loading is related to a lower pressure ratio and hence it requires a higher reaction to ensure that there is sufficient acceleration of the gas to provide high efficiency (Moustapha, 2003). On the contrary, he also states that the pressure ratio itself will give the needed acceleration of the gas in the case of turbines with high stage loading. Nonetheless, even though all models show similar trends, different values for efficiency and optimum reaction are predicted. This was expected as all the loss models, even when considering same parameters, are based on different correlations for predicting each loss mechanism.

Figure 6-4 shows the total to static efficiency curves for a 73° fixed outlet stator angle and stage-loading coefficients varying from 1.5 to 1.7 for the AMDCKO loss model. It is possible to see that the trends described in previous paragraph remain. Moreover, for this loss model and the selected design parameters, figure shows that the maximum efficiency values were in a range between 71% and 72%, while the optimum reaction varied from 0.17 to 0.25.



**Figure 6-4 AMDCKO Loss model predictions for total-to-static efficiency at 73° for stator outlet angle and different stage-loading coefficients**

Similarly, Figure 6-5 shows the parametric design study results for the Craig-Cox model for a 73° fixed stator outlet angle and stage-loading coefficients varying from 1.5 to 1.7. Results from Craig-Cox model corroborate that higher loading is related with lower efficiencies but show similar results for optimum reaction degree for all of the cases. The maximum efficiencies calculated varied within a range from 72.5% to 70.3% while the reaction degree remained around 0.35 for all the cases.



**Figure 6-5 Craig-Cox Loss model predictions for total-to-static efficiency at 73° for stator outlet angle and different stage-loading coefficients**

Lastly, the results calculated by Denton loss model agreed in both stage-loading coefficient and optimum reaction degree trends described by the AMDCKO model as shown in Figure 6-6. Nonetheless, this last model remained as the most optimistic one, showing higher maximum efficiencies within a range from 73.75% to 74.6% for the same stage-loading coefficients tested. Moreover, even though the optimum reaction trend was similar to that shown in Figure 6-4, values differed as the optimum reaction degrees calculated by Denton model varied from 0.14 to 0.22.

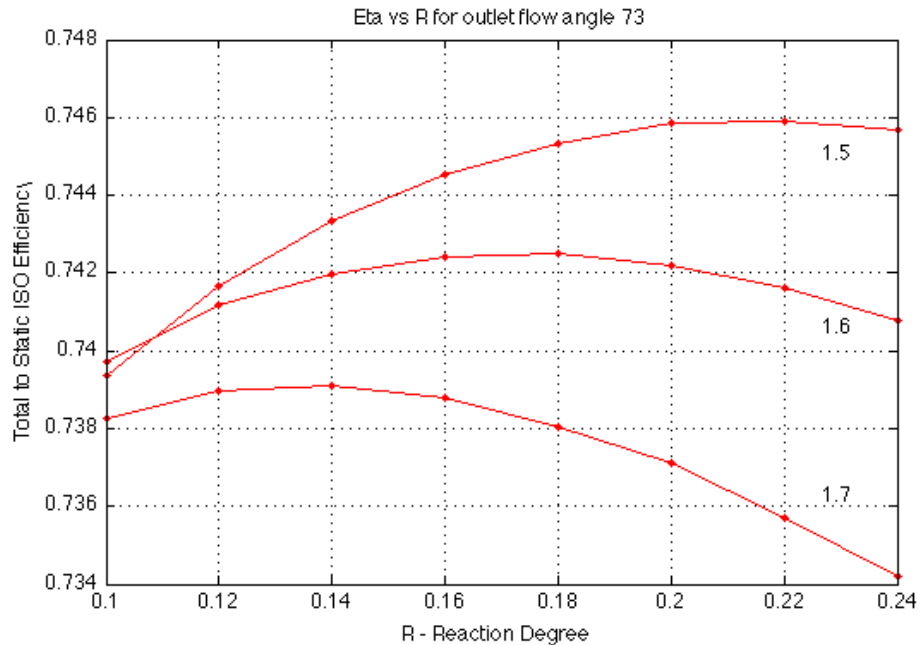


Figure 6-6 Denton Loss model predictions for total-to-static efficiency at 73° for stator outlet angle and different stage-loading coefficients

Table 6-7 summarizes the results from the parametric design study for all the models at the reference conditions. It is possible to see that Craig-Cox and AMDCKO loss models predicted similar maximum efficiency values at the reference point while on the other hand, the optimum reaction degree calculated by the Craig-Cox model differed from that one estimated by the other two loss models.

Table 6-7 Predictions of the loss correlations for optimum reaction degree regarding Total-To-Static Efficiency

Loss Correlation	$\alpha_2 [^{\circ}]$	$\Psi$	Optimum R	$\eta_{ISO-ts} [\%]$
Denton	73,0	1,60	0,22	74,59
AMDCKO	73,0	1,60	0,21	71,58
Craig-Cox	73,0	1,60	0,32	71,59

Regarding the total-to-total efficiency curves, similar parametric design study was performed for all the loss models. In this regard, Table 6-8 summarizes the results for the reference turbine. The AMDCKO and Craig-Cox models predicted reaction degrees around 0.5, whether Denton's loss correlation predicted a pressure-based reaction of 0.25. For the reference case it is possible to see that the models differ in efficiency prediction in a range of 2% and figures in APPENDIX III show detailed breakdown of losses.

Table 6-8 Predictions of the loss correlations for optimum reaction degree regarding Total-To-Total Efficiency

Loss Correlation	$\alpha_2 [^{\circ}]$	$\Psi$	Optimum R	$\eta_{ISO-tt} [\%]$
Denton	73,0	1,60	0,25	80,95
AMDCKO	73,0	1,60	0,55	78,58
Craig-Cox	73,0	1,60	0,55	79,75

The models predicted similar trends for design. The stage-loading coefficient was found to influence the total-to-total efficiency prediction in a similar way that for the total-to-static efficiency calculations while the trend for the optimum reaction degree for this case was not to vary as the stage-loading coefficient did. De Andrade in his lectures explains that while the reaction directly affects the total-to-static efficiency, no similar relation exists with the total-to-total efficiency, being this in agreement with the results (De Andrade, 2010). Figures 6-7 and 6-8 show the total-to-total efficiency curves calculated by the AMDCKO and Craig-Cox model respectively. It is possible to see that the maximum efficiencies calculated by both loss model varied in less than 1% for all the stage-loading coefficients tested. In this regard AMDCKO predicted values around 78.5% while Craig-Cox 79.5%. Efficiency curves for both models show optimum reaction degrees varying from 0.5 to 0.55.

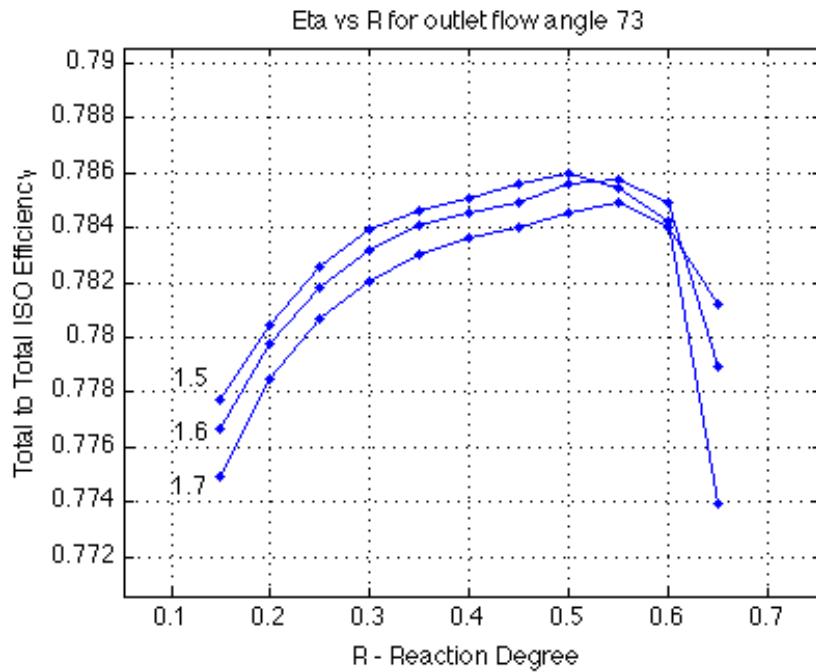


Figure 6-7 AMDCKO - Total to Total Efficiency

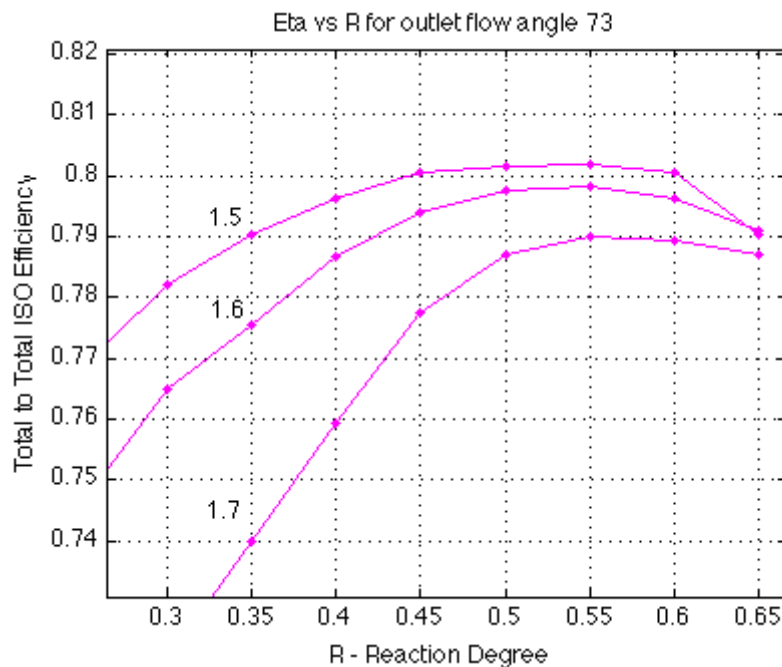


Figure 6-8 Craig-Cox - Total to Total Efficiency

Lastly, Figure 6-9 shows the results for Denton loss model. As stated in previous paragraphs, design trends shown by the model for different stage-loading coefficients and optimum reaction degree calculations remained similar to those trends showed by the other 2 loss models. Nonetheless, values for maximum efficiencies were calculated around 80.9% while the optimum reaction degree predicted was 0.25.

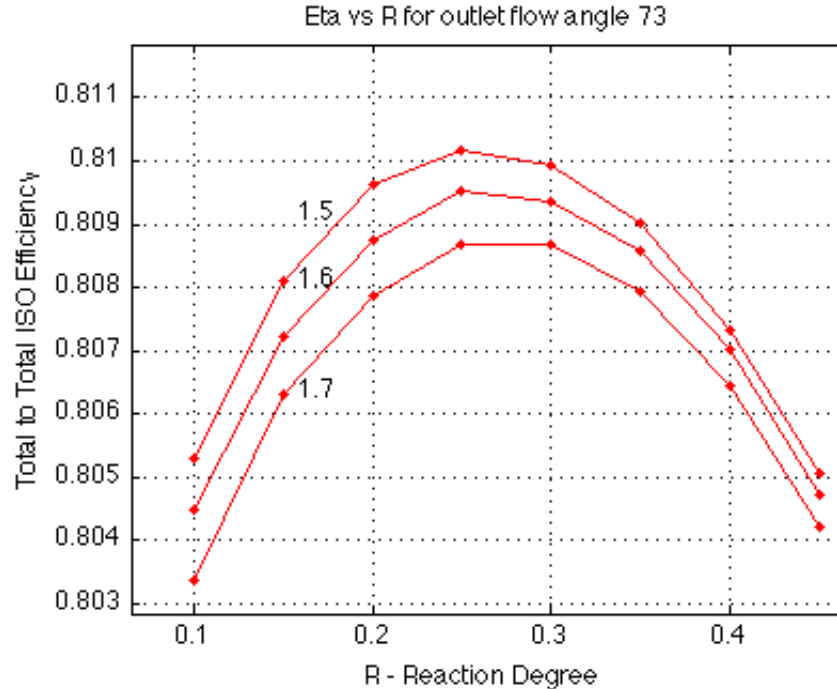


Figure 6-9 Denton - Total to Total Efficiency

Furthermore, the difference between the correlations when comparing the results predicted relies on how the reaction degree influences on the loss estimation in each model. Figures in APPENDIX III show the behavior of losses for the stator and rotor blades while varying the reaction degree. Here is shown that as the reaction increases the trends are for the clearance losses to increase and for the secondary losses to decrease. In this regard, it will be discussed in next chapter that at higher reaction degrees the greater is the difference between the leakage flow and the main flow velocities, which generates more mixing and losses. On the contrary, low accelerating flows allow the growing of the endwall boundary layer, which will mix with the vortices formed because of the inlet boundary layer and hence generate more secondary losses.

Even though this similitude in trends, when considering the whole breakdown of losses, the behavior of each model was different. Denton's model prediction for clearance loss is notably more influenced by the increase of reaction degree. A reason for this remarked influence could be the high sensitivity of the correlation for high outlet relative flow angles. The relative outlet flow angle increases as the reaction increases because of the relation shown in Eq. 5-5. This occurs given the fact that the rotor inlet relative angle is not varying considerably as the stator outlet flow angle is fixed. Moreover, the profile losses are considered by some authors to be the main source of loss in the flow path and only Craig-Cox results confirmed such statement (Sharma & Butler, 1987). Even if out of the scope of the present work, it was also noticed that the cooling losses do not vary greatly with a change of reaction degree (APPENDIX III).

### - Conclusion

The stage-loading coefficient was found to directly affect the efficiency estimations. All correlations agree in the fact that higher loading implies less efficiency no matter which definition is used for this last one. Regarding the optimum reaction degree, the study proves that the choice of this parameter depends on the efficiency definition used. For the first stage of a multiple-stage turbine, the total-to-total efficiency definition should be considered, as the energy is not wasted. For these cases, the study shows that the optimum reaction degree remains almost constant while varying the stage-loading coefficient. Craig and Cox and AMDCKO models were in agreement to estimate an optimum reaction degree close to 0.5 as the one deduced by Asuaje in his lectures (Asuaje, 2009). On the contrary, for a single-stage turbine the total-to-static efficiency is more adequate and results confirm studies from Soderberg and Moustapha where for higher stage loading coefficients it was proved that the optimum reaction degree decreases (Moustapha, 2003).

It was found that even if similar efficiency values were calculated, the breakdown of losses for each model was different and hence each model should be used independently. This last point because the predictions for each individual loss mechanism (profile, secondary, etc.) could be completely different from one model to another. Furthermore, the reaction degree was proved to affect the loss estimation. An increase of reaction degree was proved to have an influence on the individual loss mechanisms prediction.

## 7. Discussion

The implemented loss correlations use different parameters to predict the individual loss mechanisms. However, as it will be shown in the present chapter, the loss correlations agree in most of the key parameters for each individual loss mechanism. This chapter is split in two greater analysis discussions. First of them is related to the description of the individual loss mechanisms. Here are discussed the key parameters ruling the mechanisms, their range of applicability and the impact of extrapolations. The second part of this chapter will give an overall comparison between the models considering the results from previous chapters.

### 7.1. Individual Loss Mechanisms Analysis

#### 7.1.1. Profile Loss

The different authors agree in the fact that profile loss is related to drag and friction on the blade surface. In this regard, it was found that the three loss correlations show an important effect of two key parameters in the estimation of this loss mechanism. These are the flow turning and solidity. However, before discussing the impact of these two parameters in the profile loss, first it will be reviewed the rest of the parameters considered by each correlation in this loss mechanism and why.

##### AMDCKO

The loss correlation proposed by Kacker and Okapuu describes the profile loss as a function of the flow angles, the blade solidity and takes into account the Reynolds and the Mach numbers effects. Reynolds effect is measured based on true chord and cascade exit gas conditions. These authors consider that in turbulent regime this effect is lower as is shown in Eq. 2-30. However, Kacker and Okapuu state that a true estimation of the loss variation due to Reynolds number should also consider detail knowledge of blade shapes (Kacker & Okapuu, 1981).

Kacker and Okapuu show that the profile loss coefficient is, in general, not independent of Mach number, even in subsonic regimes. Therefore the authors introduced the shock loss component and the channel flow acceleration coefficients into the profile loss formulae. Dahlquist held a study to determine the influence of the Mach number on this loss mechanism (Dahlquist, 2008). He found that Kacker and Okapuu's correlation considers an increase of the loss for Mach numbers over 0.8. Moreover, Dahlquist shows that the influence of outlet Mach in AMDCKO was even more relevant for Mach numbers greater than 1. In this regard, an outlet Mach number of 1.14 was found able to duplicate the basic profile loss coefficient (Dahlquist, 2008).

The inlet and outlet flow angles were found to be relevant in the estimation of this loss coefficient. From figures shown in page 29 it can be seen that a higher outlet angle implies higher profile loss coefficients. These figures also show that there is only a range of optimum solidity values for which the profile loss coefficient is lower. This range is around 0.85 for cero inlet metal angles and 0.7 for impulse turbines (Ainley & Mathieson, 1951).

It is important to state too that, since the correlation is based on cascade measurements, the input parameters must be within a range of applicability for which the study was developed. Kacker and Okapuu's correlation is designed for outlet flow angles between 40° and 70°, measured from axial line. Any angle outside this range might lead to overestimate or underestimate the loss mechanism coefficient. In fact, extrapolating for outlet flow angles greater than 70° will lead to predict a greater value of the profile loss coefficient, hence a lower performance of the turbine and this is uncertain. Regarding the solidity, AMDCKO was developed for values within 0.3 to 1.0. Any extrapolation beyond these values leads to an uncertain increment in the profile loss coefficient. Finally, Kacker and Okapuu considered that there exists a continuous advance in aerodynamic analysis and hence the loss correlations should be

continuously reviewed (Kacker & Okapuu, 1981). In this regard, the basic profile loss coefficient suggested by Kacker and Okapuu decreased by a factor of 2/3 when comparing to the one developed by Dunham and Came. It is believed by the author of present work that given the lack of fundaments to introduce this factor, this value might be uncertain and is affecting the whole loss mechanism. Therefore a proper study to consider the improvements in turbomachinery and their effect in loss estimation should be done before introducing an empirical factor.

#### Craig and Cox

The flow turning and the pitch to backbone ratio play an important role in the profile loss coefficient estimation according to Craig and Cox (Craig & Cox, 1971). Rests of the parameters needed by the correlation are to consider Reynolds and Mach effects. According to this correlation, the Reynolds effect is more relevant when in presence of laminar conditions (Figure 2-12). Craig and Cox have based the Reynolds number on the blade opening considered by them to give better correction. Their Reynolds factor introduces the effect of the blade surface roughness. The surface roughness is considerer by the authors to control effectively the boundary layer thickness in presence of turbulent regime.

Craig and Cox's correlation was developed under subsonic conditions. Hence, they introduced corrections to consider the effect of higher outlet Mach numbers. These corrections become relevant when Mach exceeds unity. However, the corrections are based on the blade profile design. When the profiles are designed with a pronounced convex suction surface curvature downstream of the throat, even outlet Mach numbers of 0.7 are considered to add an increment to the basic profile loss coefficient. Dahlquist found that for Craig and Cox correlation, outlet Mach number values around 1.16 could lead to duplicate the basic loss coefficient (Dahlquist, 2008).

The flow turning is of main importance for the estimation of the basic profile loss in Craig and Cox correlation. The basic profile loss is estimated as a function of the lift parameter and the contraction ratio. The lift parameter is a function of the flow turning and was found to be proportional to the profile loss. On the other hand, the contraction ratio is a term used to denote the internal blade passage width ratio of the particular cascade considered based on inlet to throat (Craig & Cox, 1971). This last term can be estimated from the flow angles values and the pitch to backbone ratio. The higher the pitch to backbone ratio then the lower the contraction ratio and lower contraction is related to higher profile loss coefficient. From this it can be seen that flow turning and solidity are related in this correlation. In this sense, for determined flow angles there exist an optimum solidity in which the profile loss is lower. However, greater flow turning certainly leads the profile loss to increase, this meaning that the effect of the lift parameter and loading is important for Craig and Cox's correlation.

Being an empirical model, the values encountered in Craig and Cox's correlation are only valid within a range of applicability. The obtaining of any value by extrapolating outside the ranges provided by the correlation might lead to uncertain results. In this regard, the outlet flow angle should be in a range from  $10^\circ$  to  $90^\circ$  measured from tangential line. Similarly, the inlet flow angle should not be outside the range from  $10^\circ$  to  $140^\circ$ . Finally, all of this is valid for solidity values within 0.4 to 1.25.

#### Denton

Denton's profile loss correlation is mainly related to the entropy generated due to friction in boundary layer on blade surfaces. More than providing an exact empirical methodology to estimate the loss, instead he tries to go through the physics and origins of this loss mechanism. Denton states that the exact estimation of the profile loss cannot be achieved without knowing full details of the state of the boundary layer. He gives a correlation in which the key parameters ruling the mechanism are a dissipation coefficient, and the flow velocity distribution among the blade surface. This dissipation coefficient varies greatly when in presence of laminar or turbulent conditions, hence is related to the Reynolds number. For turbulent conditions, Denton estimates that constant values around 0.002 are good approximations based on studies realized by Cebeci and Moore & Moore (Denton, 1993).

However, the complexity of estimating the profile loss by the use of Eq. 2-63 punctuates in the possible lack of knowledge of the velocity distribution on blade surfaces. Therefore the distribution must be assumed if it is unknown. Regarding this, Denton suggests the use of a linear variation of the velocity along the mean camber line. Furthermore, Denton provides simplified correlations to obtain optimum solidity and minimum loss coefficients. He obtained these correlations, shown in chapter 4, after systematically varied the velocity distribution considering more realistic assumptions than a linear distribution. The main parameters ruling these correlations are the flow angles. For greater exit flow angles the profile loss coefficient increases. The range of applicability extends only for outlet flow angles from  $40^\circ$  to  $80^\circ$  and inlet flow angles between  $-60^\circ$  to  $60^\circ$  measured from axial line.

Finally, Denton considers that there exists a possible increment of the loss due to high sonic conditions. In this regard, he states that only few experimental evidence of this relation exists in open literature. On the other hand, he considers the shock losses as a function of the inlet Mach. However, he states that the predicted loss due to this last mentioned mechanism depends greatly on the value of the average pressure acting on the blade surface, which is unlikely to be accurate enough to give a useful prediction.

#### Conclusions on profile loss

All loss correlations agree in the fact that flow turning and optimum solidity are the key parameters governing the loss mechanism. In this regard, it was found in general that for optimum solidity values the flow turning is related to the profile loss, as could be seen in Figure 7-1. This figure was obtained after performing a simulation study with LUAX-T considering same input parameters but varying the exit outlet flow angle for a fixed inlet angle. Furthermore, it can be discussed from the figure that AMDCKO loss correlation is more conservative than the rest of the correlations regarding the profile loss estimation. However, in this regard the influence of the  $2/3$  factor introduced by Kacker and Okapuu plays an important role.

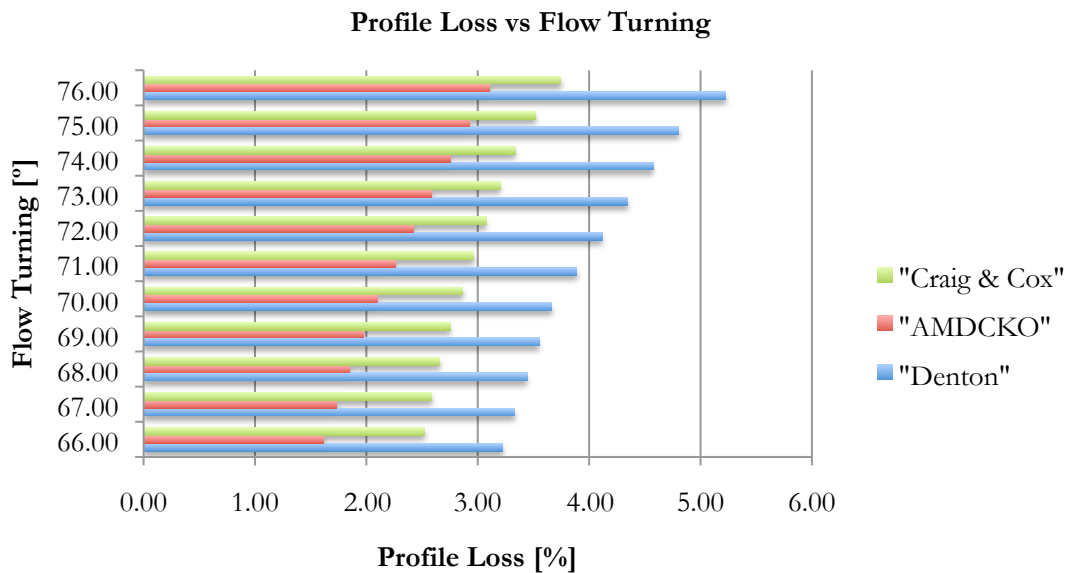


**Figure 7-1 Influence of the Flow Turning in the Profile Loss for all the loss correlations after assuming same conditions and geometry**

This influence of the flow turning was expected. The flow turning is used to correlate the blade loading. In presence of high blade loading the diffusion processes could stall, if taken too far, and lead the blade boundary layers to separate from the surface, causing a large increase in loss. This effect is more appreciable in the suction side of the blade. In this regard, if flow separates as a consequence of excessive suction side diffusion, it might not be able to re-attach before the trailing edge. As a consequence of the flow separation on suction side of the blade, the flow will not turn as intended and hence do less work.

Moreover, such separation is considered to affect the flow field entering a downstream stage. On the contrary, flow separation on the pressure side of blade occurs close to the leading edge instead. Therefore it has more time to re-attach and accelerate before the trailing edge of the blade (Moustapha, 2003).

Furthermore, high flow turning also implies larger blades and greater blade surface area. More contact between the blade surface and the flow are associated with more frictional losses. These are associated with the profile loss mechanism.

All the models were found to be associated with the choice of an optimum solidity. Even different for each correlation, the choice of an optimum solidity is done so there is reached an optimum point where none frictional or diffusion losses have major effect. Less number of blades means less blade surface and friction, whereas on the contrary it also means more loading and hence diffusion losses.

Finally, the three loss correlations consider that this loss mechanism is greatly influenced by viscosity effects and the Reynolds number. All the correlations agree that this influence is less evident for turbulent regimes. Regarding Mach influence, all the three different studies mention that higher Mach and supersonic conditions lead to a loss increment. However, Denton states clearly that predictions regarding this effect on loss estimation are not completely accurate.

### **7.1.2. Secondary Loss**

Secondary losses, similarly to secondary flows, are not yet completely understood and hence not fully described in the loss mechanisms. This statement is commonly mentioned in the different works from Kacker and Okapuu, Craig and Cox and Denton. Nonetheless, it is known that the secondary losses arise mainly as a consequence of vortices mixing and the endwall boundary layer. Therefore, there exist different models based on empirical data that aim to predict this loss mechanism. The parameters requested per each correlation vary and are not necessarily the same. However, it was found that two key parameters drive the loss mechanism in all the correlations; these are the aspect ratio and the flow angles. This section of the work explains the physics, if any, behind the computation of the secondary loss in each loss correlation. The parameters needed in each correlation, as well as their range of applicability, will be explained. At the end, overall conclusions regarding this loss mechanism are shown.

#### AMDCKO

Kacker and Okapuu gave a correlation similar to that found by Dunham and Came. This last correlation assumed that for a complete range of aspect ratios, the secondary loss coefficient was inversely proportional. Nevertheless, after comparing the results from other studies, Kacker and Okapuu changed the correlation considering that the change of the loss coefficient was affected differently by aspect ratios smaller than 2. To correct this, they introduced a function of the aspect ratio. Besides the influence of the aspect ratio, the flow turning was also considered relevant (Eq. 2-38). Both inlet and outlet flow angles are used in the correlation, mainly for the calculation of the loading factor.

Kacker and Okapuu do not consider any Reynolds number coefficient for the estimation of the secondary loss coefficient. However, a subsonic Mach correction is considered in their work. This correction is to take into account the compressibility effects of the acceleration of the flow next to endwalls. The subsonic correction proposed is a function of the inverse aspect ratio. This highlights even more the importance of the aspect ratio in secondary loss estimation.

The correlation is valid for a complete range of aspect ratios. However Kacker and Okapuu, verified the loss predicted for aspect ratios lower than 2. Regarding the flow angles, as there is not shown any range of values where the model is valid; it would be recommendable to apply the model only between the same ranges shown for the profile losses.

#### Craig and Cox

The correlation proposed by Craig and Cox for secondary loss prediction consists partly of a true aerodynamic secondary loss and partly because of wall friction. The authors assume that the secondary

losses are approximately inversely proportional to the aspect ratio of the blading. They consider that a decrease in the aspect ratio will lead the secondary loss concentrations at tip and root to merge together. Hence Craig and Cox consider that the rate of increase in loss would be lower. Similarly to the profile loss, in this correlation is used the backbone length instead of the true chord for the parameters. In this regard, the aspect ratio used is the blade height to backbone length ratio.

Besides the aspect ratio, Craig and Cox's secondary loss correlation is a function of the pitch to backbone length, the flow turning and the relative velocity ratio. The flow turning and pitch to backbone are used to estimate the modified lift parameter, which is related to the blade loading. From Figure 2-15 it is easy to conclude that the greater this parameter is, then the higher values for the basic secondary loss coefficient will be calculated. Regarding the relative velocity ratio, this parameter physically relates the flow acceleration with the secondary loss coefficient. A lower acceleration of the flow is related to higher losses in Craig-Cox's correlation.

Contrary to Kacker and Okapuu, Craig and Cox consider the Reynolds number effect in the estimation of the secondary loss. The effect of the Reynolds number is suggested by the authors to be similar to that shown in Figure 2-12 for the profile loss. Craig and Cox consider that at high values of Reynolds number measured from opening, the Reynolds effect will become negligible. Finally, the correlation is delimited to flow angles and solidity values similar to those ranges mentioned for the profile loss estimation, whereas the aspect ratio range is wide and extends until low 0.1 aspect ratios.

#### Denton

In his work, Denton describes the secondary loss as complex and the most difficult loss mechanism to understand. He considers that the existing correlations to predict this loss coefficient are lacking physics theory and only rely on empirical data. In this regard, Denton explains how is this loss mechanism related to the boundary layer formation in the endwall and vortices formation. He states that the losses due to endwall boundary layer might represent up to two thirds of the total secondary losses and that the rest should be associated with the mixing loss of the inlet boundary layer and the increase of the secondary kinetic energy related to the vortices formation. In this sense, he mentions that no known function exists to measure this mixing loss of the inlet boundary layer but it is known that this loss is a function of the blade load and turning. Moreover, while explaining the influence of the endwall boundary layer in the entropy generation, Denton considers both Reynolds effect and the aspect ratio. He explains the effect of the Reynolds number by the use of the same dissipation coefficient proposed for the profile losses, now arguing that the state of the boundary layer is a major unknown and will have a larger effect on this coefficient so that it shouldn't be assumed as a constant.

Regarding the aspect ratio, Denton considers that the ratio of the surface area of the endwall to the blade suction surface is inversely proportional to the aspect ratio based on true chord. In this regard, the formula he provides is to measure the entropy generation per unit surface area of the endwalls and hence the aspect ratio is inversely proportional to the total entropy generation, being in agreement with other loss correlations.

Nonetheless, the correlation implemented in LUAX-T for Denton's prediction is that provided by Dunham and Came with a factor added by Denton (Denton, 2008). He considered that this correlation based on empirical data gave good predictions and included the effect of the turning and the aspect ratio for secondary loss computation.

#### Conclusions on Secondary Loss

It can be concluded from the discussion that all the correlations consider the blade loading and aspect ratio as most relevant parameters in the prediction of the secondary loss mechanism. Figure 7-2 shows how all the loss correlations show the same trend for a range of aspect ratios. Here is possible to see that for lower aspect ratios the secondary losses increases. Now what is of importance is to understand why is the aspect ratio one of the key parameters ruling the loss mechanism. First of all, it should be mention that the correlations analyzed the aspect ratio influence by changing the blade height for a determined

chord. In this regard, if for a same chord there are considered two different heights, for the lower blade height a major portion of the blade is affected by the boundary layer growth on the endwalls, hence an increment of the secondary loss coefficient. However, same argument applies if the height is fixed and the chord changes. For larger chords then the effect of the boundary layer on the endwalls will be more appreciable than for shorter chords, as this allows the boundary layer to grow or separate.

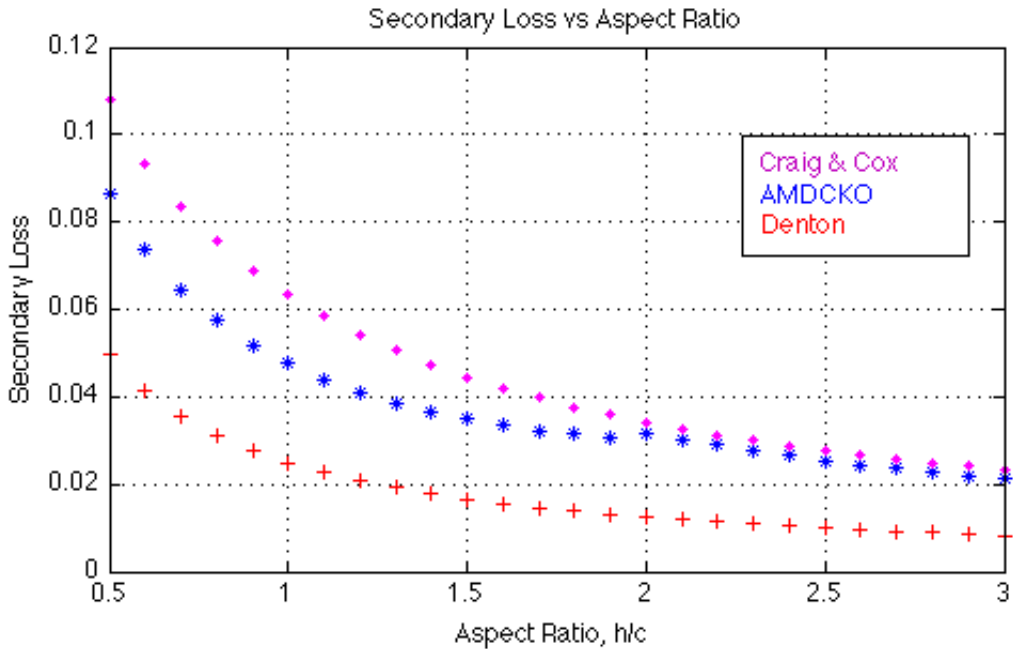
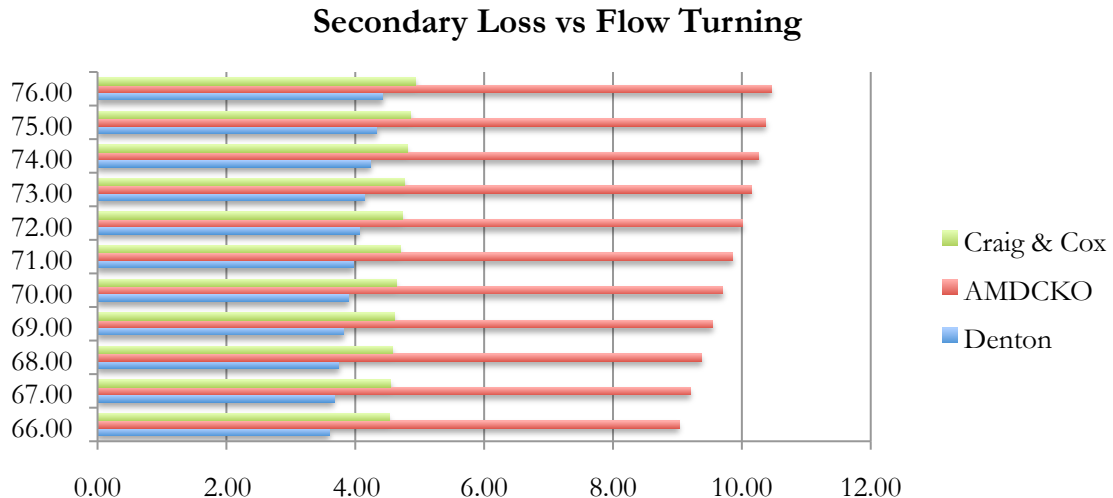


Figure 7-2 Influence of the Aspect Ratio in the Secondary loss

Therefore, the use of the aspect ratio as a parameter to predict the effect of the boundary layers on the endwalls is considered to be correct even if the boundary layer behavior is unknown. However, the impact of the aspect ratio might give only a certain approximation based on experimental data. It would be better for the loss prediction if the boundary layer transition were further studied. This would imply that by knowing the velocity distribution and the transition from laminar to turbulent, the use of Denton's integral could give better approaches. Nonetheless, as Denton states in his work, the influence of the endwall boundary layer represents approximately two thirds of the total secondary loss coefficient. In this regard, the existing correlations are lacking physics related to the effect of the inlet boundary layer in loss generation. The inlet boundary layer should be considered as it mixes at the blade row and also leads to the formation of vortices. This vortex formation is associated with an increment of kinetic energy, which is not initially a loss but the decay of this energy due to the dissipation within a vortex core is related to an entropy increase (Denton, 1993). The formation of the vortex and the mixing of the inlet boundary layer are related to the flow turning and blade loading, according to studies performed by Sharma and Butler (Sharma & Butler, 1987). On the other hand, experience and tests confirm that the vortices formation is far from being as shown in Figure 2-5, but instead only few turns could be visualized in reality (SIT, 2011).

Besides the aspect ratio, flow turning and loading were also considered in the different loss correlations. Figure 7-3 shows how, for all the loss correlations, more turning is related to higher losses. This is also associated to the boundary layer on endwalls. The greater the blade turning and loading, the sooner the endwall boundary layer moves onto the suction surface, hence higher losses are accounted (Denton, 1993). In this regard, validation studies proved that the angles could lead the model to predict erroneously the turbine efficiency by overestimating this loss mechanism.



**Figure 7-3 Influence of the Flow Turning in the Secondary Losses after assuming same conditions and geometry for all the correlations**

One last difference, regarding the Reynolds effect, should be pointed out between the loss correlations. If certainly the transition of the boundary layers on endwalls is unknown, it is true that some of the ongoing flows are not inviscid and hence there is some effect produced by the Reynolds number. In this regard, Craig and Cox correlation considers a parameter similar to the one used for the profile loss estimation, even though the behavior of the boundary layers is different. The accuracy in the use of this parameter is uncertain since it should depend on studies over the boundary layer on endwalls instead. However, its consideration is an approach to relate somehow the effect of viscosity that is not encountered in Kacker and Okapuu's correlation. Finally, it is important to mention that the figures were plotted with information extracted from LUAX-T and thus the similarity between the Denton and AMDCKO model, given the fact both are based on Dunham and Came's correlation (Dunham & Came, 1979).

### 7.1.3. Trailing Edge Loss

The prediction of the trailing edge loss in all the loss correlations relies on the trailing edge thickness and the flow acceleration. This part of the discussion is aimed to understand the physics of the loss generation at the trailing edge. In order to do this, there are explained each of the correlations to predict this loss mechanism. These correlations will be further analyzed and compared to see if they consider same arguments and if some recommendation could be done regarding the prediction of this loss.

#### AMDCKO

Kacker and Okapuu's correlation for trailing edge loss prediction is based on the fact that there exist a pressure loss due to trailing edge blockage. In this regard, they consider that the best way to approach this loss mechanism is by means of the trailing edge thickness to throat opening ratio and its effect on accelerating flows. Their study is based on tests performed on axial entry nozzles and impulse blades. The physics under this loss correlation are no further explained, instead this correlation bases on empirical data. The only explanation provided by Kacker and Okapuu is that thicker boundary layers, as found on impulse turbines, are related to lower base pressure coefficients in the wake behind the trailing edge; while for highly accelerating cascades (as for axial entry nozzle) the trailing edge thickness is likely to contribute significantly to the drag, and hence have higher losses. The correlation is given for subsonic conditions but considering that for supersonic exit velocities the correlation proposed for the profile loss includes the trailing edge loss effect.

Regarding the limitation of this correlation, the empirical data is based on trailing edge to throat ratios from 0 to 0.4 and was measured only in impulse blading and axial entry nozzles. For other blades the correlation suggests an interpolation between these two.

#### Craig and Cox

The prediction of the trailing edge loss in Craig and Cox's work is not explained carefully considering the physics under it. The correlation is a function of the trailing edge thickness to pitch ratio and the fluid outlet angle. At more flow deflection the loss ratio increases. In this regard, at high flow deflection, flow accelerates and the influence of the difference in pressure given the base pressure coefficient at the wake becomes more evident. Similarly, at smaller trailing edge to pitch ratios, then lower number of blades and hence less affection because of the trailing edge. This correlation considers outlet flow angles from 10° to 50° measured from tangential direction, and trailing edge thickness to pitch ratios from 0 to 0.12.

#### Denton

Denton considers in his work that the mixing out of a wake behind a trailing edge represents an important example of the mixing process. The correlation provided by Denton to predict this loss coefficient involves three different terms, regarding different physics each. The most significant term is related to the loss due to the low base pressure acting on the trailing edge. Second term considers the mixed out of the boundary layers on the blade surface just before the trailing edge. Lastly, the third term is related to the combined blockage of the trailing edge and the boundary layers. Denton states that it is physically difficult to decide if the low base pressure produces the dissipation in the wake or if the dissipation causes the low pressure. However, Denton states that a complete estimation of the entropy generation due to the trailing edge is only possible if full details of the state of the boundary layer are known. In this regard, he emphasizes on how the boundary layer thickness affects the mixing and also separated boundary layers might have an influence on the loss, but an accurate method to measure the effect of this last is still unknown.

#### Conclusions on Trailing Edge Loss

The trailing edge loss is similarly calculated in all the implemented correlations. In this regard, the flow acceleration and trailing edge thickness to pitch or throat ratios are the key parameters. The correlations agree that as this last ratio increases so does the loss. A thicker trailing edge increases the influence of the base pressure acting after the trailing edge. This negative base pressure could lead to greater drag in the case of highly accelerating cascades as Kacker-Okapuu described in their work (Kacker & Okapuu, 1981). Here the influence of the flow acceleration, which is correlated in the models through the flow angles. Moreover, the trailing edge thickness to pitch ratio is also a measure of the number of blades. As the pitch increases then the number of blades decreases and therefore the losses because of the trailing edge decrease too. Lastly, there exists a mixing process behind a wake after the trailing edge between the different boundary layers coming from both blade sides. This mixing process is known to originate a blockage of the flow as well. However, the estimation of the boundary layer parameters is complex, principally because the state of the boundary layer is not certainly known. An improvement to all the correlations could be to add the effect of the separated boundary layers if not considered already in the profile loss computation. This separation is known to give rise to high loss, based on measured data (Denton, 1993).

Another important point is the effect of supersonic operation conditions in the trailing edge loss. This effect is not considered by all the correlations but studies have proved that at higher Mach numbers the trailing losses increase. As a suggestion, the correlations should consider the effect of the Mach numbers on the base pressure coefficient. This is suggested since studies have proved that the base pressure coefficient for zero losses increases as the Mach number increases too (Sieverding, 1985).

#### **7.1.4. Clearance Loss**

In addition to the profile and secondary losses, the clearance loss mechanism was found to be one of the most important loss generation processes in the blade flow path. The different correlations show that the estimation of this loss is complex but they all agree in the fact that, whether the blade is shrouded or not, it is a function of the flow conditions and the area of clearance. This section will show that the flow acceleration and angles play an important role in the prediction of this loss. Next paragraphs will give a brief description of the physics behind the correlation for estimation of clearance loss in all the loss models. At the end overall conclusions regarding this loss mechanism are discussed.

##### AMDCKO

Kacker and Okapuu's correlation for predicting the tip clearance loss coefficient is based on a large set of experimental data. In their work, there are proposed two distinct correlations depending on the type of blading, shrouded or unshrouded. The correlations are shown in chapter 2 of the present work. It is possible to see that they are mainly a function of the ratio between the clearance divided by blade height and the relative flow angle from the rotor. Specifically for the case of shrouded rotor blades, the aspect ratio is also considered by these authors to be important, as shown in Eq. 2-40, where it is proportional to the loss. The clearance over height ratio represents a measure of the leakage mass flow through the area of clearance in this correlation. The greater this ratio is implies that more leakage flow exists and hence more mixing will occur after the trailing edge, therefore the loss coefficient increases. Similarly, more turning of the flow will lead to increase the mixing loss. This last phenomenon is because the angle of re-injection of the leakage flow would be different from that in the main flow at the blade exit.

##### Craig and Cox

The clearance loss mechanism is analyzed in the Craig and Cox correlation as an efficiency debit based on a set of experimental data. They stand that the clearance loss could represent up to one third of the total loss and that it increases as the reaction degree increases. The correlation provided by these authors is mainly a function of the clearance area and the flow acceleration (inlet and outlet relative velocities). In this correlation, as the area of clearance increases, so does the efficiency debit. Likewise, more flow acceleration is related to higher losses. This last is a consequence of the mixing once the leakage flow is re-injected to the mass flow, since more acceleration means a greater difference in velocity between both leakage and main, flows. Regarding differentiation between the types of blade, the authors state that their correlation is applicable for both unshrouded and shrouded blades.

##### Denton

The clearance loss as a loss mechanism is widely analyzed in Denton's work (Denton, 1993). In brief, Denton gives two different correlations, each one according to the type of blade, shrouded or unshrouded. In both cases the key parameters are the ratio between the leakage flow and the main flow, the inlet and outlet velocities and the outlet flow angle. Hence, both correlations are based on the fact that more leakage flow will produce more loss, especially at higher velocities and more tangential outlet angles. Similarly as what happened with the profile loss, Denton gives simplified correlations for the estimation of this loss mechanism that are mainly a function of the inlet and outlet flow angles (Denton, 2008). However, these simplifications are under the assumption of a clearance over height of 1%, being this term directly related to the ratio between the leakage flow and the main flow. Denton states in his work that the blade thickness also influences the loss generation. Nevertheless, he emphasizes that the leakage flow rate and the difference in the streamwise velocity of the mainstream flow and the leakage flow remain more important for this loss estimation.

##### Conclusions on Tip Clearance Loss

Even though the differences between the loss correlations provided by each of the researchers, all of them are governed by similar key parameters. It was found that all the correlations agree in the fact that a greater area of clearance implies more losses. This is believed by the author of this work to be correct

given the fact that more leakage flow over the blade would lead to a greater mixing process once this flow is re-injected to the main flow. Similarly, the difference in angles and velocities between the leakage and the main flow is well related to more mixing as this would lead to more entropy production. However, next figures show how even based on same physics, the correlations predict different losses for similar conditions. Figure 7-4 shows the trends for the AMDCKO and Denton models for a similar clearance over height rate of 1% in an unshrouded blade. Here is shown that even though both correlations have the same trend for increasing the loss prediction as the outlet angle increases, the AMDCKO increases considerably faster if compared against Denton's correlation. Similarly the Figure 7-5 shows how all the correlations predict higher losses for higher degrees of reaction, meaning that more acceleration of the main flow is estimated to increase the mixing process. However, once again here is also possible to see that even though the correlations predict a loss increment with higher reactions, each one of them does it differently. In this regard, Denton's correlation appears to be greatly influenced, as it increases rapidly if compared against the other loss models.

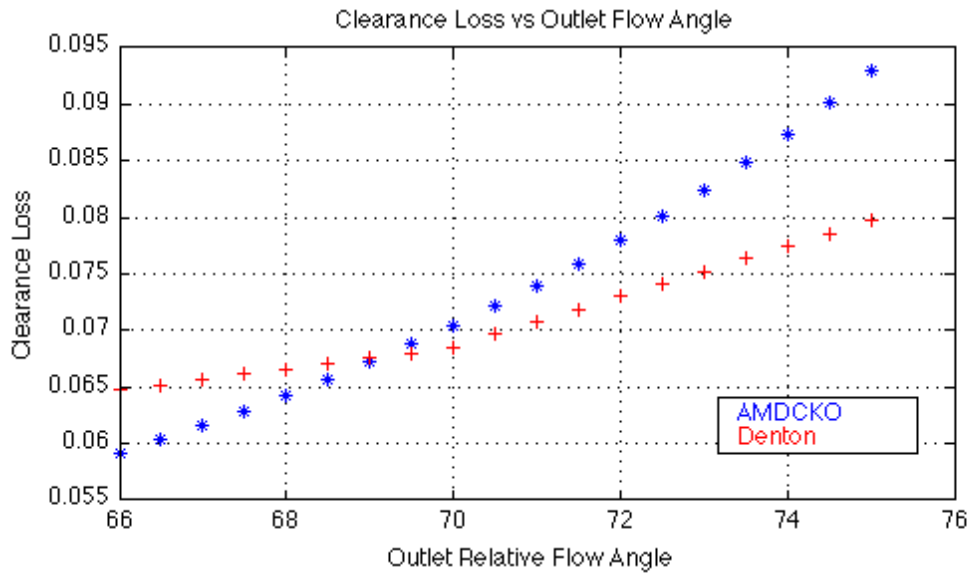


Figure 7-4 Influence of the Outlet Flow Angle in the prediction of Clearance Loss for Unshrouded blades and 1% Clearance over Height Ratio

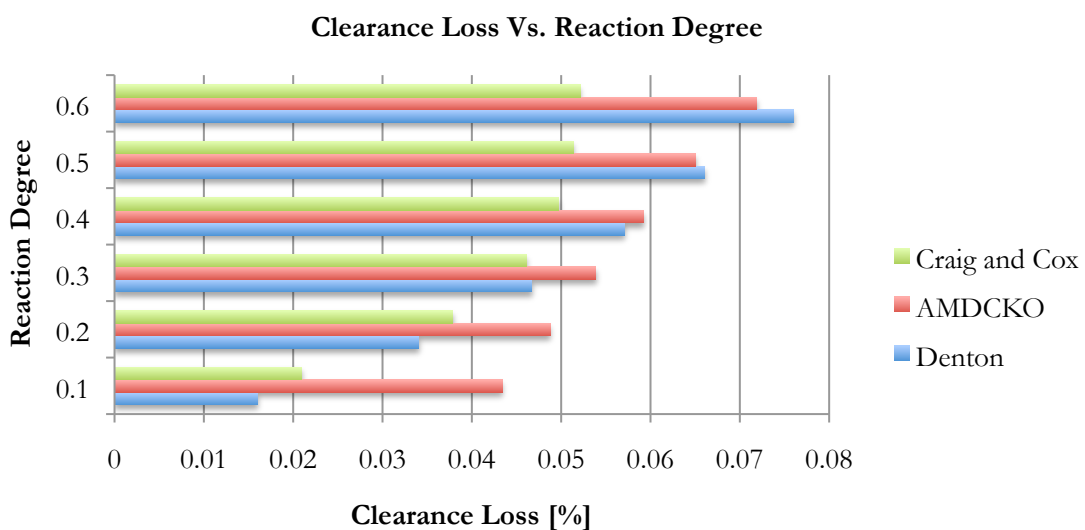


Figure 7-5 Influence of the Reaction Degree in the prediction of Clearance Loss for Unshrouded blades and 1% Clearance over Height ratio

Moreover, the effects of the area of clearance, the reaction degree and the outlet flow angle in the estimation of the clearance loss were also measured in a work performed by the National Aeronautics and Space Administration of America (NASA, 1994). In this work, there is stated that the clearance loss is a complicated flow problem influenced by many factors and not easy to predict with accuracy. Nonetheless, their work proved that an increment of the loss could be related to big clearance gap over blade height ratios, and influenced by the reaction degree, showing similar trends than those predicted by the implemented correlations in LUAX-T (Figure 7-5), giving more reliability to these last ones.

## 7.2. Loss Correlations Analysis

In the present section of the work will be discussed different comparisons and conclusions from the previous chapters. In brief, it was found that all the models were properly implemented in LUAX-T, as they are able to predict often with great accuracy the efficiency of the turbines as shown in chapter 5. Similarly, all models were proved to give analogous trends regarding the results from the parametric study in chapter 6.

Concerning the accuracy of each correlation, it was beyond the scope of this work to determine which correlation is better. However, Chapter 5 shows that all of them are in agreement and able to predict the turbine performance with accuracy. Hence the use of any of the three models is found to be appropriate for a first step in turbine design, prior to performing a three-dimensional analysis. Moreover, both studies 1D and 3D should be part of an optimization routine of the turbine design and hence the results from the 3D study should be used to perform again a 1D analysis but more accurate or acquainted to reality. Nonetheless, the validation performed in this present work shows that there exist some limitations for the use of the correlations under different circumstances. In this regard, AMDCKO model was found to miss-predict the turbine performance for small axial outlet flow angles in impulse turbines. Similarly, Denton's implemented correlation behaves wrong under same circumstances as both correlations are based on same secondary loss prediction, provided originally by Dunham (Dunham, 1970). It is possible to conclude that the use of the correlations should be under complete knowledge of their limitations and range of applicability. The range of applicability of each correlation depends on the turbines used for their development, from where the authors got the tabulated data. It would be of interest to validate the models against a larger number of turbines to determine when is a model suitable to use. However, the previous section of this chapter describes the range of values for the parameters involved in the correlations. In this regard any extrapolation in the use of the correlations might lead to erroneous results in the turbines performance.

Furthermore, it is shown in chapter 6 the three correlations agree that for the total-to-static efficiency case, as the stage-loading coefficient increases not only the efficiency decreases, but also the optimum reaction degree. Similarly, the trends regarding predictions for total-to-total efficiency for all the loss correlations show a decrease in efficiency as the stage-loading increases. However, the ranges predicted by each model are different. These differences in the prediction of efficiency and the optimum reaction degree are because of the different ways each model has for estimating each individual loss mechanism. Nevertheless, it was also observed with the breakdown of losses that the increase of reaction degree affected differently the loss correlations. This is since the reaction degree is a related to the flow angles and velocity components, parameters that rule some of the loss mechanisms. The clearance losses for example, do increase with higher reaction, in agreement with theory, but in each model the rate of increment is different as shown in previous section in Figure 7-5.

On the other hand, the 0.375 reduction factor in the secondary loss prediction in Denton's model was found to have a large influence in the performance prediction by this methodology. This was found since for some cases the total losses are underestimated, as shown in the validation chapter. Figure 7-6 shows the results for the validation of turbine 2 for Denton's model with and without the factor. Here the curve without the factor is more accurate and closer to the measured torque efficiency values. Moreover, it was found that without the reduction factor the optimum reaction degree its around 0.4 for the reference case

considered in Chapter 6, which is similar to the values proposed by the other correlations, which predicted an optimum reaction around 0.5 in the case of the total-to-total efficiency (Figure 7-7). Lastly, Figure 7-8 shows the direct influence on the rotor loss breakdown, where the impact of the factor is clearer. Therefore, the use of the factor should be reviewed in order to tune the loss model. However, the unique way of verifying this factor is by testing the model against a larger amount of turbine data, which is expensive and takes time.

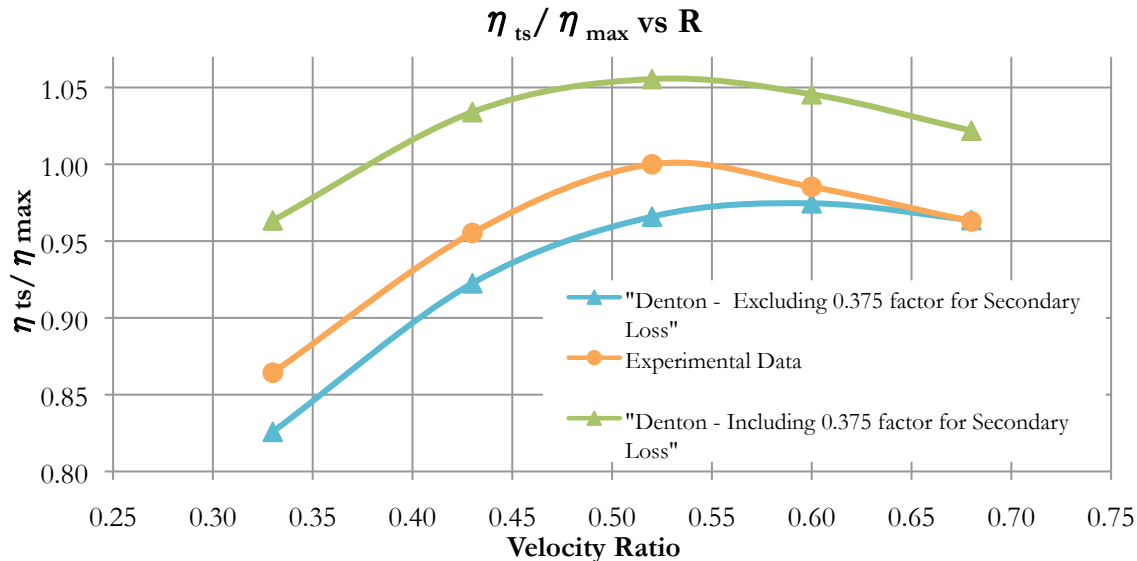


Figure 7-6 Validation 2 - Influence of the 0.375 factor on Dunham's Secondary Loss Correlation and Denton's model

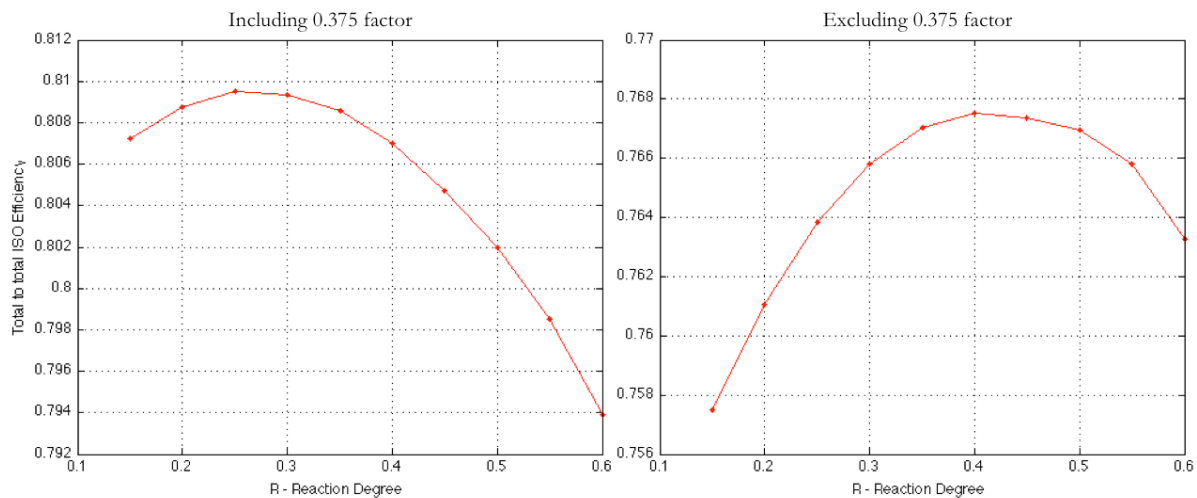
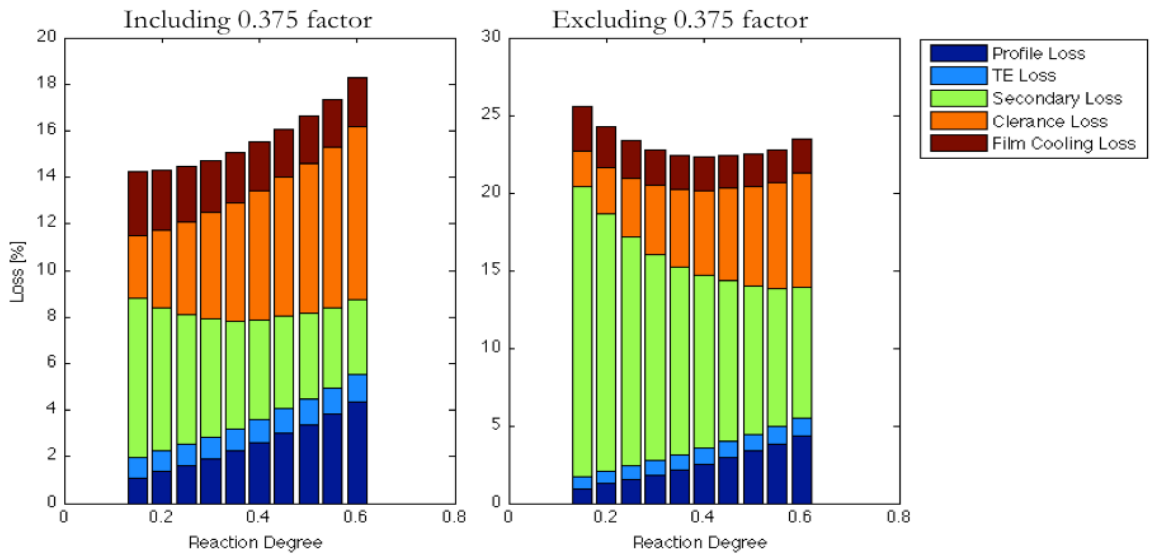


Figure 7-7 Influence of the 0.375 factor on Denton's correlation for the total-to-total efficiency prediction



**Figure 7-8 Influence of the 0.375 factor in the Rotor Breakdown of Losses**

Finally, even though the correlations have different formulae to estimate each of the loss mechanisms, they often predict similar total losses. It was found that for some cases the profile loss prediction from Craig and Cox's correlation was higher than Kacker and Okapuu's but this difference was then compensated with the secondary loss, which was greater for AMDCKO model. One reason for this could be that the AMDCKO model takes into account a major affection from blade loading into the secondary loss correlation. In this regard this could only mean that each correlations should be used independently in order to give accurate results. However, in general it was found that when considering the physics behind each loss correlation, there are many similarities between the models as the key parameters ruling the loss mechanisms are mostly the same even though the trends and dependence on these parameters by each model is not necessarily similar.

## 8. Final Conclusions

One of the principal aims of this work was to implement the different loss correlations in a numerical tool for prediction of turbine performance. In this regard, one of the major conclusions of the work is the extension of LUAX-T by having validated and verified the implemented methods, adding a new parametric study tool. However, this implementation was held prior to proceed with further analysis of the loss correlations. The overall conclusions of the performed studies and comparisons between the loss mechanisms and correlations can be summarize in the next points:

- The choice of a loss correlation could be determinant for turbine design. Even often similar, each model has different correlations and was validated differently. However, now having 3 models implemented in LUAX-T will allow giving more reliability to first steps in design. This is because if the models behave similar when predicting the performance for a specific turbine case then it is likely that the results are correct, while different performance predictions will imply further analysis of which loss model is appropriate to rely on for a determine case.
- Loss predictions with Denton, Kacker-Okapuu and Craig-Cox loss models were performed. All 3 correlations studied allow the user to predict with accuracy the turbine performance in the case of subsonic conditions, non-low reaction degrees and higher flow coefficients. Hence, the use of any of them for conventional gas turbines as a first step in turbine design is recommendable. However, Craig and Cox loss model was found to remain closer to the experiment than the other correlations for the validations performed. Kacker and Okapuu's correlation should not be used for impulse stages neither for blades with axial outlet flow angles (low flow coefficients). Especially one recommendation should be not to use one loss model if any of the parameters needed as inputs are out of their range of applicability or induces to perform extrapolations. In this regard, a large influence of the flow angles on the models was found.
- Every loss correlation has its own logic and was properly validated by each of their developers. Hence no mixing should occur when choosing one methodology. In this regard, if certainly all the correlations predict similar values for total loss, they were found to predict different coefficients for each loss mechanism.
- The profile losses are mainly consequence of the boundary layer effect on the blade surfaces. All the correlations consider that the flow turning and the solidity are the key parameters ruling this loss mechanism. More flow turning implies more friction with the blade surface and hence a loss increment. Moreover, more loading could lead to increase the diffusion losses as well. This is because of the effect that diffusion has on the boundary layer separation on the suction side of the blade. On the other side for every combination of angles there exists an optimum solidity for which the profile losses are lower and this is different for each model. The optimum solidity choice was found to be a balance in between the frictional and diffusion losses. However the choice of an optimum solidity should take into account not only the losses but also the less weight and cost as possible. In the case of the Kacker and Okapuu's correlation the 2/3-reduction factor could lead to underestimate this individual loss mechanism.
- The secondary losses are still not fully understood and hence not completely represented in the loss correlations. Nonetheless, all of them agree in the fact that the aspect ratio and the flow angles are the key parameters ruling this loss mechanism. The major source of this loss is the effect of the boundary layer in the endwall, which also generates vortices and hence mixing processes. The shorter the aspect ratio more portion of the blade will be affected. However, even if discussed in their works, like Denton, none of the correlations considers the effect of the inlet boundary layer or the energy associated with the vortices formation. Studies have proved that these last two could mean up to one third of the total loss coefficient. One final conclusion about the methods it's that often the Kacker-Okapuu's model might overestimate this loss predicting

higher values than for the profile loss, whereas some studies suggest that in the extreme case they could be similar but its more frequent to have higher profile losses (Sharma & Butler, 1987).

- The trailing edge losses, sometimes included in the profile losses, are mainly a function of the flow and a geometrical ratio involving the trailing edge thickness. The base pressure after the trailing edge was found to have larger influence for the case of high accelerating cascades. Moreover, the wake behind a trailing edge could lead to mixing processes between the boundary layers coming from each side of the blade. Denton's approach is considered to take more into account all of the effects of the trailing edge loss but bases on parameters that are hard to predict as the boundary layer displacement and momentum thickness.
- Clearance loss could represent up to one third of the total loss coefficient in the rotor blades. The correlations agree that a greater area of clearance leads to more losses. Also the difference between the flow conditions of the leakage and main flow are important for their mixing. However, even if similar, Denton and Kacker and Okapuu's models are more influenced by the flow angles whereas Craig-Cox's correlation considers more important the flow acceleration and mainstream velocity of the flow at the blade exit. This last point could lead to predict different coefficients regarding this loss.
- Turbine performance prediction was performed with all the correlations. It was confirmed that the choice of stage-loading coefficient, flow coefficient and degree of reaction could greatly affect the performance of a turbine. In this regard, lower stage loading and flow coefficients were proved to give higher efficiencies. At the same time a parametric study proved that there exist one optimum reaction degree for which the efficiency of the turbine is higher. The results for this optimum reaction varied between the loss correlations as they are differently affected by this design parameter. Concerning this, AMDCKO and Craig and Cox showed more congruency between their results. However, even if lower stage loading is desirable to have better performance, at the same time this compromises the blade life by increasing the stresses so an optimum point must be reached.

## **9. Future Work and Recommendations**

### Regarding the loss correlations:

Based on the fact that the boundary layer is one of the major sources for loss but still no direct relation between this and the correlations exist, the first recommendation should be to improve the understanding of some of the phenomena related to it. In this regard, the laminar to turbulent transition and the boundary layer separation in the trailing edge are still not well represented. Moreover, the relation between the boundary layer and the whole secondary loss mechanism is not yet fully understood. Hence, one consideration could be to further study and understand the separation process of the inlet boundary layer and the vorticity occurring in the flow path.

It would be of special interest to extend the validation process to a wider range of turbines and be able to tune or suggest some modifications to the loss correlations. However this is not only expensive but also extensive in time and insufficient information is free available in order to do so.

### Regarding LUAX-T:

LUAX-T could be further improved to a two-dimensional software analysis and provide the blade geometry needed to perform blade-to blade studies. In this regard it could be of special interest if some connection between the LUAX-T and one of the two-dimensional analysis software could be performed to continue the turbine design optimization process.

## Bibliography

- Ainley, D., & Mathieson, G. (1951). A Method Of Performance Estimation for Axial Flow Turbines. *British ARC R. and M.*, 2974.
- Asuaje, M. (2009 йил September). Lecture on Axial Turbines. *Máquinas Térmicas - Turbinas Axiales*. Caracas, Venezuela: Universidad Simon Bolivar.
- Baumann, K. (1921). Some recent developments in large steam turbine practice. *J. Instn elect. Engrs*, 59, 565.
- Benner, M., Sjolander, S., & Moustapha, S. (2006). An Empirical Prediction Method For Secondary Losses In Turbines: A New secondary Loss Correlation. *ASME Journal Of Turbomachinery*, 128, 281-291.
- Craig, H., & Cox, H. (1971). Performance Estimation Of Axial Flow Turbines. *Ordinary Meeting*, Rugby, UK.
- Dahlquist, A. (2008). *Investigation of Losses Prediction Methods in 1D for Axial Gas Turbines*. MSc Thesis, Lund University, Department of Energy Sciences, Lund, Sweden.
- Daily, J. W., & Nece, R. E. (1960). Chamber dimension effects on induced flow and frictional resistance of enclosed rotating discs. *J. bas. Engng. Trans. ASME*, 174, 217.
- De Andrade, J. (2010 йил March). Lectures on Axial Turbines. *Turbinas Axiales*. Caracas, Venezuela: Universidad Simon Bolívar.
- Denton, J. (2008). Cambridge Turbomachinery Course. *Lecture on Axial Turbines Design*. Cambridge, United Kingdom: University Of Cambridge.
- Denton, J. (1993). Loss Mechanisms in Turbomachines. *International Gas Turbine and Aeroengine Congress and Exposition*. Cincinnati, USA.
- Dixon, S., & Hall, C. (2010). *Fluid Mechanics and Thermodynamics of Turbomachinery*. United States Of America: Butterworth - Heinermann .
- Dunham, J. (1970). A Review Of Cascade Data On Secondary Losses in Turbines. *Journal Of Mechanical Engineering Science*, 12.
- Dunham, J., & Came, P. (1979). Improvements to the Ainley/Mathieson Method of Turbine Performance Prediction. *ASME Journal Of Engineering for Power*, 252-256.
- Fowler, T. W. (1989). *Jet Engines and Propulsion Systems For Engineers*. GE Aircraft Engines, Cincinnati.
- Franus, D. (1994). The World Gas Turbine Industry Production Trends and Key Factors. *ASME Turbo Expo-Land, Sea & Air*. The Hague: ASME.
- Fridh, J., Bunkute, B., Fakhrai, R., & Fransson, T. (2004). Experimental Study On Partial Admission In A Two-Stage Axial Air Test Turbine With Numerical Comparisons. *ASME Turbo Expo 2004: Power for Land, Sea and Air*. Vienna, Austria: ASME.
- Genrup, M. (2008). LUAX-T. *Lund's University Axial Flow Turbines Tool*. Lund, Sweden.
- Greitzer, M. (2004). *Internal Flow: Concept and Applications*. Cambridge, UK: Cambridge University Press.
- Hartsel, J. (1972). *Prediction of Effects of Mass-Transfer Cooling on the Blade-Row Efficiency of Turbine Airfoils*. Evendale, Ohio: American Institute of Aeronautics and Astronautics.

- Incropera, F., De Witt, D., Bergman, T., & Lavine, A. (2006). *Fundamentals of Heat and Mass Transfer* (6th Edition ed.). Danvers, MA, USA: Wiley.
- Kacker, S., & Okapuu, U. (1981). A Mean Line Prediction Method for Axial Flow Turbine Efficiency. *International Gas Turbine Conference and Product Show*. Houston, USA: American Society of Mechanical Engineers (ASME).
- KTH. (2011). Turbine Test Facility - KTH. Stockholm, Sweden.
- Kurzke, J. (2007). *GasTurb Details 5 - An utility for GasTurb 11*. Germany.
- Langston, L. (2001). *Secondary Flows in Axial Turbines - A Review*. Connecticut, USA: University Of Connecticut.
- Lozza, G. (1982). A Comparison Between the Craig-Cox and the Kacker-Okapuu Methods of Turbine Performance Prediction. *La Meccanica*, 17, 211-221.
- Mamaev, B., & Klebanov, G. (1969). *Optimal pitch for a turbine blade cascade*. Kuibyshev Motor Works.
- Mathworks Inc. (2010 йил 5-March). MATLAB 7.10 R2010a. Natick, Masachussets, USA.
- Moustapha, H. (2003). *Axial and Radial Turbines*. United States Of America: Concepts ETI, Inc.
- Moustapha, S., Kacker, S., & Tremblay, B. (1990). An Improved Incidence Losses Prediction Method for Turbine Airfoils. *ASME Journal Of Turbomachinery*, 112.
- NASA. (1994). *Turbine Design and Applications*. Lewis Research Center. Linthicum Heights, USA: National Aeronautics and Space Administration.
- Olsson, D. (2008). *Axial Flow Turbine Mean Line Design*. Lund University, Department of Energy Sciences, Division of Thermal Power Engineering. Lund, Sweden: Lund University.
- Sharma, O., & Butler, T. (1987). Predictions of Endwall Losses and Secondary Flows in Axial Flow Turbine Cascades. *ASME Journal Of Turbomachinery*, 109, 229-236.
- Sieverding, C. (1985). Recent Progress in the Understanding of Basic Aspects of Secondary Flows in Turbine Blade Passages. *ASME Journal Of Turbomachinery*, 107, 248-257.
- SIT. (2011). Discussion Lecture on Secondary Flows. Finspång, Sweden: Siemens Industry Turbomachinery.
- Smith, S. (1965). A Simple Correlation Of Turbine Efficiency. *Journal of the Royal Aeronautical Society*, 69, 467-470.
- Soderberg, C. R. (1949). Unpubllished Note. *Gas Turbine Laboratory*. Boston, MA, USA: Massachusetts Institute of Technology.
- Suter, P., & Traupel, W. (1959). *Investigations into the windage loss of turbine wheels*. Inst. Fur Therm Turbomasch. Zurich: ETH.
- Svensdotter, S., & Wei, N. (1995). *Investigation of the Flow Through an Axial Turbine Stage*. Kungliga Tekniska Högskolan (KTH), Energy Department - Division of Heat and Power Technology. Stockholm: KTH.
- Wei, N. (2000). *Significance of Loss Models in Aerothermodynamics Simulation for Axial Turbines*. Doctoral Thesis, Royal Institute of Technology - KTH, Department Of Energy Technology , Stockholm, Sweden.

## Table Of Figures

FIGURE 2-1 ENTHALPY-ENTROPY DIAGRAM (MOUSTAPHA, 2003).....	14
FIGURE 2-2 VELOCITY TRIANGLES (DIXON & HALL, 2010).....	15
FIGURE 2-3 REACTION DEGREE AND VELOCITY TRIANGLES (MOUSTAPHA, 2003) .....	16
FIGURE 2-4 SMITH CHART (OLSSON, 2008) .....	20
FIGURE 2-5 CLASSIFICATION OF LOSSES AS EXTRACTED FROM THE BOOK “AXIAL AND RADIAL TURBINES” (MOUSTAPHA, 2003) .....	23
FIGURE 2-6 3D SEPARATION OF A BOUNDARY LAYER ENTERING A TURBINE CASCADE (LANGSTON, 2001) .....	25
FIGURE 2-7 FLOW OVER THE TIP GAP FOR AN UNSHROUDED BLADE (DENTON, 1993) .....	26
FIGURE 2-8 FLOW OVER A SHROUDED TIP SEAL (DENTON, 1993) .....	27
FIGURE 2-9 AMDCKO PROFILE LOSS COEFFICIENT – NOZZLE BLADES (KACKER & OKAPUU, 1981).....	29
FIGURE 2-10 AMDCKO PROFILE LOSS COEFFICIENT - IMPULSE BLADES (KACKER & OKAPUU, 1981).....	29
FIGURE 2-11 TRAILING EDGE LOSS ENERGY COEFFICIENT .....	33
FIGURE 2-12 REYNOLDS EFFECT ON PROFILE LOSS PARAMETER (CRAIG & COX, 1971).....	35
FIGURE 2-13 LIFT PARAMETER (CRAIG & COX, 1971) .....	36
FIGURE 2-14 CONTRACTION RATIO (CRAIG & COX, 1971).....	36
FIGURE 2-15 BASIC PROFILE LOSS PARAMETER (CRAIG & COX, 1971) .....	37
FIGURE 2-16 TRAILING EDGE EFFECT PROFILE LOSS RATIO (CRAIG & COX, 1971) .....	37
FIGURE 2-17 TRAILING EDGE PROFILE LOSS INCREMENT (CRAIG & COX, 1971) .....	38
FIGURE 2-18 MACH EFFECT ON PROFILE LOSS INCREMENT (CRAIG & COX, 1971).....	39
FIGURE 2-19 PROFILE LOSS INCREMENT DUE PITCH TO BLADE BACK RATIO (CRAIG & COX, 1971) .....	39
FIGURE 2-20 INCIDENCE EFFECT ON PROFILE LOSS (CRAIG & COX, 1971).....	40
FIGURE 2-21 BASIC POSITIVE STALLING INCIDENCE PARAMETER (CRAIG & COX, 1971).....	41
FIGURE 2-22 s/b INCIDENCE CORRECTION FOR POSITIVE STALLING INCIDENCE (CRAIG & COX, 1971).....	41
FIGURE 2-23 CR INCIDENCE CORRELATIONS FOR POSITIVE STALLING INCIDENCE (CRAIG & COX, 1971).....	42
FIGURE 2-24 INCIDENCE CORRECTIONS FOR NEGATIVE STALLING INCIDENCE (CRAIG & COX, 1971) .....	43
FIGURE 2-25 s/b INCIDENCE CORRECTION FOR NEGATIVE STALLING INCIDENCE (CRAIG & COX, 1971) .....	43
FIGURE 2-26 BASIC STALLING INCIDENCES FOR INLET BLADE ANGLE OVER 90° (CRAIG & COX, 1971) .....	44
FIGURE 2-27 MINIMUM LOSS INCIDENCE RANGE RATIO – Fi (CRAIG & COX, 1971) .....	45
FIGURE 2-28 SECONDARY LOSS ASPECT RATIO FACTOR (CRAIG & COX, 1971) .....	46
FIGURE 2-29 SECONDARY LOSS - BASIC LOSS FACTOR (CRAIG & COX, 1971).....	47
FIGURE 2-30 ANNULUS WALL LOSS (CRAIG & COX, 1971).....	48
FIGURE 2-31 CAVITY GEOMETRY .....	48
FIGURE 2-32 CAVITY LOSS (CRAIG & COX, 1971) .....	48
FIGURE 2-33 FK EFFICIENCY DEBIT FACTOR FOR SHROUDED BLADES (CRAIG & COX, 1971) .....	49
FIGURE 3-1 TURBINE SPECIFICATIONS GUI - LUAX-T (OLSSON, 2008).....	55

FIGURE 3-2 BLADE GEOMETRY SPECIFICATIONS GUI - LUAX-T (OLSSON, 2008).....	56
FIGURE 3-3 LUAX-T OUTPUT TEXT FILE EXAMPLE (OLSSON, 2008).....	57
FIGURE 3-4 TURBINE CALCULATION POINTS (OLSSON, 2008).....	58
FIGURE 3-5 PROFILE PLOT FOR A 4 STAGES TURBINE (OLSSON, 2008).....	58
FIGURE 3-6 EXAMPLE OF A BREAKDOWN OF LOSSES FOR A 4 STAGES TURBINE (OLSSON, 2008).....	59
FIGURE 4-1 OPTIMUM SOLIDITY AS EXTRACTED FROM "A COMPARISON BETWEEN THE CRAIG-COX AND THE KACKER-OKAPUU METHODS OF TURBINE PERFORMANCE PREDICTION" (LOZZA, 1982) .....	61
FIGURE 4-2 TURBINE'S PROFILE VIEW AS EXTRACTED FROM LUAX-T AFTER CRAIG & COX LOSS MODEL IMPLEMENTATION.....	62
FIGURE 4-3 BREAKDOWN OF LOSSES AS EXTRACTED FROM LUAX-T AFTER CRAIG & COX LOSS MODEL IMPLEMENTATION.....	62
FIGURE 4-4 – VERIFICATION OF CASCADE 1 FOR $MA = 0.4$ .....	64
FIGURE 4-5 - VERIFICATION OF CASCADE 1 FOR $MA = 1.0$ .....	65
FIGURE 4-6 - VERIFICATION OF CASCADE 1 FOR $MA = 1.3$ .....	65
FIGURE 4-7 VERIFICATION OF CASCADE 2 FOR $MA = 0.4$ .....	66
FIGURE 4-8 VERIFICATION OF CASCADE 2 FOR $MA = 1.0$ .....	67
FIGURE 4-9 - VERIFICATION OF CASCADE 2 FOR $MA = 1.3$ .....	67
FIGURE 4-10 - VERIFICATION OF CASCADE 3 FOR $MA = 0.4$ .....	68
FIGURE 4-11 - VERIFICATION OF CASCADE 3 FOR $MA = 1.0$ .....	69
FIGURE 4-12 - VERIFICATION OF CASCADE 3 FOR $MA = 1.3$ .....	69
FIGURE 4-13 GENERIC VELOCITY DISTRIBUTION AS USED BY DENTON IN HIS WORK (GREITZER, 2004).....	70
FIGURE 4-14 OPTIMUM PITCH TO CHORD RATIO PROPOSED BY DENTON (DENTON, 1993) .....	71
FIGURE 4-15 MINIMUM PROFILE LOSS PREDICTED FOR OPTIMUM PITCH TO CHORD RATIOS AS EXTRACTED FROM THE BOOK INTERNAL FLOWS (GREITZER, 2004) .....	71
FIGURE 4-16 CLEARANCE LOSS FOR UNSHROUDED BLADES WITH 1% OF CLEARANCE ON HEIGHT (DENTON, 1993) .....	72
FIGURE 4-17 BREAKDOWN OF LOSSES AS SHOWN IN LUAX-T FOR A COMPLETE SIMULATION USING THE 3 LOSS CORRELATIONS .....	73
FIGURE 5-1 CROSS SECTION OF THE TEST TURBINE IN KTH USED FOR THE MEASUREMENTS IN PRESENT WORK (KTH, 2011) .....	75
FIGURE 5-2 VALIDATION 1. EFFICIENCY CURVES PREDICTED FOR A ONE-STAGE IMPULSE TURBINE WITH TANGENTIAL INLET ROTOR ANGLE.....	77
FIGURE 5-3 VALIDATION 1. STATOR LOSS COEFFICIENTS Vs. REACTION DEGREE.....	77
FIGURE 5-4 VALIDATION 1. ROTOR LOSS COEFFICIENTS Vs. REACTION DEGREE .....	78
FIGURE 5-5 ROTOR BLADE SKETCH IN VALIDATED TURBINE 1 - SMALL OUTLET FLOW ANGLES .....	78
FIGURE 5-6 VALIDATION 2. EFFICIENCY CURVES PREDICTED FOR A ONE-STAGE IMPULSE TURBINE WITH AXIAL ROTOR INLET FLOW ANGLE .....	80
FIGURE 5-7 VALIDATION 2. STATOR LOSSES Vs. REACTION DEGREE .....	80
FIGURE 5-8 VALIDATION 2. ROTOR LOSSES Vs. REACTION DEGREE .....	81
FIGURE 6-1 GRAPHICAL USER INTERFACE FOR LUAX-T PARAMETRIC STUDY TOOL.....	84

FIGURE 6-2 PARAMETRIC STUDY OUTPUT TEXT FILE FOR AMDCKO LOSS CORRELATION AS EXTRACTED FROM LUAX-T.....	84
FIGURE 6-3 DIMENSIONLESS VELOCITY TRIANGLES (ASUAJE, 2009).....	88
FIGURE 6-4 AMDCKO LOSS MODEL PREDICTIONS FOR TOTAL-TO-STATIC EFFICIENCY AT 73° FOR STATOR OUTLET ANGLE AND DIFFERENT STAGE-LOADING COEFFICIENTS .....	89
FIGURE 6-5 CRAIG-COX LOSS MODEL PREDICTIONS FOR TOTAL-TO-STATIC EFFICIENCY AT 73° FOR STATOR OUTLET ANGLE AND DIFFERENT STAGE-LOADING COEFFICIENTS .....	89
FIGURE 6-6 DENTON LOSS MODEL PREDICTIONS FOR TOTAL-TO-STATIC EFFICIENCY AT 73° FOR STATOR OUTLET ANGLE AND DIFFERENT STAGE-LOADING COEFFICIENTS .....	90
FIGURE 6-7 AMDCKO - TOTAL TO TOTAL EFFICIENCY.....	91
FIGURE 6-8 CRAIG-COX - TOTAL TO TOTAL EFFICIENCY.....	91
FIGURE 6-9 DENTON - TOTAL TO TOTAL EFFICIENCY.....	92
FIGURE 7-1 INFLUENCE OF THE FLOW TURNING IN THE PROFILE LOSS FOR ALL THE LOSS CORRELATIONS AFTER ASSUMING SAME CONDITIONS AND GEOMETRY .....	96
FIGURE 7-2 INFLUENCE OF THE ASPECT RATIO IN THE SECONDARY LOSS.....	99
FIGURE 7-3 INFLUENCE OF THE FLOW TURNING IN THE SECONDARY LOSSES AFTER ASSUMING SAME CONDITIONS AND GEOMETRY FOR ALL THE CORRELATIONS.....	100
FIGURE 7-4 INFLUENCE OF THE OUTLET FLOW ANGLE IN THE PREDICTION OF CLEARANCE LOSS FOR UNSHROUDED BLADES AND 1% CLEARANCE OVER HEIGHT RATIO .....	103
FIGURE 7-5 INFLUENCE OF THE REACTION DEGREE IN THE PREDICTION OF CLEARANCE LOSS FOR UNSHROUDED BLADES AND 1% CLEARANCE OVER HEIGHT RATIO .....	103
FIGURE 7-6 VALIDATION 2 - INFLUENCE OF THE 0.375 FACTOR ON DUNHAM'S SECONDARY LOSS CORRELATION AND DENTON'S MODEL.....	105
FIGURE 7-7 INFLUENCE OF THE 0.375 FACTOR ON DENTON'S CORRELATION FOR THE TOTAL-TO-TOTAL EFFICIENCY PREDICTION .....	105
FIGURE 7-8 INFLUENCE OF THE 0.375 FACTOR IN THE ROTOR BREAKDOWN OF LOSSES.....	106

## **APPENDIX I**

**MATLAB™ CODES FOR THE LOSS CORRELATIONS AS IMPLEMENTED IN LUAX-T**

## Craig and Cox Loss Model Implementation

```
%#####
%## Craig and Cox Loss Model ##
%## Rafael Guedez, 2011 ##
%## ##
%## ##
%## ##
%## #####
function [Ytot,Yp,Yte,Ys,Yann,Yclr,SONC] = CC
(Re,ks,ang_in_b,desinc,rel_ang_in,rel_ang_out,pitch,OONS,r_te,SONE,Ma,W_in,W_out,area1,area2,height,o,cho
rd,axchord,gamma,CEorUE,q,u,V,NorR,CLONH,VCOEFF,AKONAT,Nseal,kappa)

% Inputs
% Re = Reynolds Number
% ks = equivalent sand grain size fix at 2e-6
% ang_in_b = inlet blade angle
% desinc = design incidence
% rel_ang_in = inlet relative angle measured from axial guide
% rel_ang_out = outlet relative angle measured from axial guide
% pitch = pitch
% OONS = opening to pitch ratio
% r_te = trailing edge thickness
% SONE = pitch on back surface radius ratio
% Ma = relative outlet isentropic Mach number
% W_in = inlet relative velocity for the rotor or inlet absolute velocity for the stator
% W_out = outlet relative velocity for the rotor or outlet absolute velocity for the stator
% area1 = annulus area at inlet
% area2 = annulus area at outlet
% height = blade height at exit
% o = opening or throat
% chord = chord
% axchord = axial chord
% gamma = Equivalent half cone angle used for annulus loss estimation
% NorR = define if calculate nozzle (NorR == 1) or rotor
% q = cavity geometry parameter
% u = cavity geometry parameter
% V = cavity geometry parameter
% CEorUE = define if controlled expansion (CEorUE == 1) or uncontrolled expansion
% VCOEFF = velocity coefficient used at clearance loss estimation set to 1
% CLONH = clearance on height ratio
% AKONAT = total effective area of clearance on total blade throat area ratio
% kappa = Cp/Cv ratio
%
% Outputs
% Ytot = total loss coefficient
% Yp = Profile loss coefficient
% Yte = trailing edge loss coefficient
% Ys = Secondary loss coefficient
% Yclr = Clearance loss coefficient
% Yann = Annulus loss coefficient

% Angles measured from tangential line
A = 90 - rel_ang_in;
B = 90 - rel_ang_out;
Aratio = area1/area2;

% Subroutine 1: backbone length approximation
bb = CC_bb(A,B,o,axchord,OONS);

% Subroutine 2: Incidence effect for off design conditions
Npi = CC_Npi(ang_in_b,desinc,o,pitch,A,B,bb,chord);

% Subroutine 3: Reynolds effect
Npr = CC_Npr(Re,o,chord,ks);
```

```

% Subroutine 4: Profile loss calculation
[Xp,Npt,dXpt,dXpm,dXp_se,Xp_basic] = CC_Xp(Npr,A,B,r_te,SONE,Ma,bb,pitch,o,chord);

% Subroutine 5: Secondary loss calculation
Xs = CC_Xs(Npr,pitch,height,A,B,W_in,W_out,bb);

% Subroutine 6: Annulus loss calculation
Xa = CC_Xa(Aratio,height,gamma,NorR,B,q,u,V,CEorUE);

% Subroutine 7: Clearance loss calculation
if NorR == 1
    Yclr = 0;% Stator
else
    % Calculation for rotor
    Xclr = CC_Xclr(CLONH,W_in,W_out,VCOEFF,AKONAT);% Clearance loss for shrouded blades.
    if Nseal == 0
        Yclr = 1.5*Xclr;% Aproximation suggested by Craig and Cox for Unshrouded blades.
    else
        Yclr = Xclr;
    end
end

% Pressure Loss coefficients estimation:
% Profile loss
Yp = 0.01*(Xp_basic*Npr*Npi + dXp_se + dXpm)*(1+0.5*kappa*Ma^2);
% Secondary loss
Ys = 0.01*(Xs)*(1+0.5*kappa*Ma^2);
% Trailing Edge loss as obtained from tloss.f
Yte = 0.01*(Xp_basic*(Npt-1)*Npr*Npi + dXpt)*(1+0.5*kappa*Ma^2);
% Annulus loss
Yann = 0.01*(Xa)*(1+0.5*kappa*Ma^2);

% Total Loss not in percentage
Ytot = Yp + Ys + Yte + Yclr;

```

```

#####
function bb = CC_bb(A,B,o,axchord,OONS)
% Function to approximate the backbone length by assuming it a circular arc
% from inlet to throat and then a straight line up to the outlet

t = o/cos(B*pi/180);
r = (axchord - t)/sqrt(2*(1-cos(2*A*pi/180)));
bb = 2*pi*r*(A/360) + o*sqrt((1/OONS^2)-1);
end

#####
function CR = CC_cr(pitch,chord,A,B)

% Calculates the contraction ratio from figure 7 for C&C model
%inputs
% SONC = s/b = s/c aprox
% A = inlet relative angle
% B = outlet relative angle

%output
% CR = contraction ratio

% Two ratios must be defined
R = 1 - sin(B*pi/180)/sin(A*pi/180);

x = -0.2:0.1:0.7;
y_1 = [1.1 1.105 1.12 1.14 1.2 1.34 1.6 1.9 2.3 2.8];
y_2 = [1.05 1.05 1.07 1.1 1.15 1.25 1.5 1.68 2 2.4];
y_3 = [1.03 1.02 1.035 1.05 1.12 1.21 1.32 1.53 1.65 1.95];

f(1) = interp1(x,y_1,R,'spline','extrap');
f(2) = interp1(x,y_2,R,'spline','extrap');
f(3) = interp1(x,y_3,R,'spline','extrap');

xx = [0.4 0.8 1.25];

SONC = pitch/chord;
CR = interp1(xx,f,SONC,'linear','extrap');
end

#####
function FL = CC_FL(A,B)
B_140 = [10 20 30 40];
FL_140 = [8 5.5 2.8 0];
f(1) = interp1(B_140,FL_140,B,'spline','extrap');

B_130 = [10 20 30 40 50];
FL_130 = [9 7.2 4.9 2.35 0];
f(2) = interp1(B_130,FL_130,B,'spline','extrap');

B_120 = [10 20 30 40 50 60];
FL_120 = [10 8.55 6.66 4.6 2.4 0];
f(3) = interp1(B_120,FL_120,B,'spline','extrap');

B_110 = [10 20 30 40 50 60 70];
FL_110 = [10.75 10 8.55 6.6 4.35 2.15 0];
f(4) = interp1(B_110,FL_110,B,'spline','extrap');

B_100 = [10 20 30 40 50 60 70 80];
FL_100 = [11.5 11.15 10.15 8.7 6.5 4 1.9 0];
f(5) = interp1(B_100,FL_100,B,'spline','extrap');

B_90 = [10 20 30 40 50 60 70 80 90];
FL_90 = [12 12.5 11.83 10.275 8.2 6.05 3.85 1.8 0];
f(6) = interp1(B_90,FL_90,B,'spline','extrap');

B_80 = [10 20 30 40 50 60 70 80];
FL_80 = [12 12.75 12.25 11.2 9.6 7.7 5.75 3.75];
f(7) = interp1(B_80,FL_80,B,'spline','extrap');

B_70 = [10 20 30 40 50 60 70];
FL_70 = [12 13 12.9 12.15 10.9 9.4 8];
f(8) = interp1(B_70,FL_70,B,'spline','extrap');

```

```

B_60 = [10 20 30 40 50 60];
FL_60 = [12.25 13 13.25 12.9 12.2 11.15];
f(9) = interp1(B_60,FL_60,B,'spline','extrap');

B_50 = [10 20 30 40 50];
FL_50 = [12.5 13.3 13.9 13.95 13.6];
f(10) = interp1(B_50,FL_50,B,'spline','extrap');

B_40 = [10 20 30 40];
FL_40 = [12.45 13.7 14.6 15.1];
f(11) = interp1(B_40,FL_40,B,'spline','extrap');

xx = 140:-10:40;
FL = interp1(xx,f,A,'linear','extrap');
end

#####
function dxp_m = CC_MACH(Ma,r_te,pitch,throat)
X_1 = 1:0.2:1.8;
X = 1:0.2:2;

Y_1 = [0    1.5    2.9    7     14];
Y_2 = [0    0.9    2       4     9.4    21];
Y_3 = [0    0.4    1.5    3       7     13.5];

if Ma < 1
    dxp_m = 0;
else
    f(1) = interp1(X_1,Y_1,Ma,'spline','extrap');
    f(2) = interp1(X,Y_2,Ma,'spline','extrap');
    f(3) = interp1(X,Y_3,Ma,'spline','extrap');

    T = asin(throat/pitch + r_te/pitch)*180/pi;
    xx = [30 18 12];

    dxp_m = interp1(xx,f,T,'linear','extrap');
if dxp_m < 0
    dxp_m = 0;
end
end

#####

function Npi = CC_Npi(ang_in_b,desinc,o,pitch,A,B,bb,chord)
% Function to estimate the Npi ratio due to incidence effect
%if desinc < -5 || desinc > 10

t = asin(o/pitch)*180/pi;
SONBB = pitch/bb;
ang_in_b = 90 - ang_in_b;
desinc = - desinc;

% Figure 12a
CR = CC_cr(pitch,chord,A,B);
X3 = 1:0.5:3;
Y3(1,:) = [0      2      5      13     18.5];
Y3(2,:) = [0      2      5      13     18.5];
Y3(3,:) = [0      2      5      13     18.5];
Y3(4,:) = [-1     1      5      13     18.5];
Y3(5,:) = [-3.5   0.5    5      13     18.5];
Y3(6,:) = [-3.5   0.5    5      13     18.5];

for i=1:6
    f3(i) = interp1(X3,Y3(i,:),CR,'linear','extrap');
end

xx3 = 60:-10:10;
di_plus_stall_cr = interp1(xx3,f3,t,'linear','extrap');

% Figure 12b
X4 = 0.3:0.2:1.7;
Y4(1,:) = [20.5    18.5    7.5    -8     -18    -23    -25.5    -24];
Y4(2,:) = [15.5    14       5       -5.5   -14.5  -20.5  -22.5    -20];
Y4(3,:) = [10       9.5     4       -5     -11.5  -17.5  -19.5   -14.5];

```

```

Y4(4,:) = [7      6.5     3      -4      -9      -14      -15      -10];
Y4(5,:) = [4      4      2      -2.5    -6.5    -10.5   -11      -5];
for i=1:5
    f4(i) = interp1(X4,Y4(i,:),SONBB,'linear','extrap');
end

xx4 = 30:10:70;
di_plus_stall_sb = interp1(xx4,f4,t,'linear','extrap');

% Figure 13b
X5 = 0.3:0.2:1.5;
Y5(1,:) = [-17.5   -10     -3      2.5     5.5     5.5     5.5];
Y5(2,:) = [-21     -11.5   -4      2.5     5.5     5.5     5.5];
Y5(3,:) = [-25     -13     -4.5   2.5     5.5     5.5     5.5];
Y5(4,:) = [-30     -16     -5      2.5     5.5     5.5     5.5];
Y5(5,:) = [-35     -20     -6      2.5     5.5     5.5     5.5];

for i=1:5
    f5(i) = interp1(X5,Y5(i,:),SONBB,'linear','extrap');
end

xx5 = 10:10:50;
di_minus_stall_sb = interp1(xx5,f5,t,'linear','extrap');

% Figure 15
X6 = 30:10:110;
Y6(1,:) = [1      1      1.04    1.1     1.2     1.35    1.45    1.6     1.77];
Y6(2,:) = [0.8    0.82   0.88    0.92    1       1.1     1.25    1.4     1.55];
Y6(3,:) = [0.59   0.61   0.65    0.7     0.8     0.91    1.05    1.2     1.32];
Y6(4,:) = [0.35   0.4     0.44    0.48    0.56    0.67    0.8     0.95   1.1];
Y6(5,:) = [0.21   0.25   0.3     0.35    0.43    0.51    0.61    0.8     0.95];

for i=1:5
    f6(i) = interp1(X6,Y6(i,:),ang_in_b,'linear','extrap');
end

xx6 = [1.1     0.9     0.7     0.5     0.4];
Fi = interp1(xx6,f6,SONBB,'linear','extrap');

if ang_in_b <= 90

    % Figure 11
    X1 = 50:10:120;
    Y1(1,:) = [5      11.5    12.5    12.4    12.4    12.3    12.1    11.5];
    Y1(2,:) = [3      9       15      16.5    17      16.5    15       12.5];
    Y1(3,:) = [1      7.5     14.5    21      25.5   26      24      20];
    Y1(4,:) = [-1     5       11.5    18.5    25.5   30      30.5    27.5];
    Y1(5,:) = [-5     2       8       15      20.5   24.5    27      27.5];
    Y1(6,:) = [-8     -2      2.5     7       11.5   16      19.5    22];

    for i=1:6
        f1(i) = interp1(X1,Y1(i,:),ang_in_b,'linear','extrap');
    end

    xx1 = 60:-10:10;
    i_plus_stall = interp1(xx1,f1,t,'linear','extrap');

    % Figure 13a
    X2 = 50:10:130;
    Y2(1,:) = [-10    -16     -18.5   -19.5   -20     -19.5    -19     -17.5   -16];
    Y2(2,:) = [-15    -22     -23     -22     -21.5   -21     -19.5    -17.5   -16];
    Y2(3,:) = [-20.5   -28     -28.5   -27     -25     -23     -21     -18.5   -16];
    Y2(4,:) = [-26    -32.5   -33     -32     -28.5   -26     -24     -21     -18];
    Y2(5,:) = [-31    -35.5   -36     -34     -31.5   -27.5   -25     -22.5   -19.8];
    Y2(6,:) = [-35    -39     -39.3   -37     -34     -30     -27     -24     -22];
    Y2(7,:) = [-39    -42.5   -42     -40     -36     -32     -28.5   -25     -22.5];

    for i=1:7
        f2(i) = interp1(X2,Y2(i,:),ang_in_b,'linear','extrap');
    end

    xx2 = 70:-10:10;
    i_minus_stall = interp1(xx2,f2,t,'linear','extrap');

```

```

i_p_stall = i_plus_stall + di_plus_stall_cr + di_plus_stall_sb;
i_m_stall = i_minus_stall + di_minus_stall_sb;

else

% Figure 14
X7 = 70:10:170;
Y7(1,:) = [2      7      13     15.5    19     22     23     22.5   18     12     0];
Y7(2,:) = [7.5   15     21     25     27     27.1   26.5   21     14     2.5    0];
Y7(3,:) = [10.5  19     26     30     30.1   27.5   22.5   14     4      2.5    0];
Y7(4,:) = [14    21.5   26     26.5   24     20     14     7      4      2.5    0];
Y7(5,:) = [16    17.5   17.8   17.5   16     13     8.5    7      4      2.5    0];
Y7(6,:) = [14    14     14     13.5   12.5   11     8.5    7      4      2.5    0];

Y8(1,:) = [-18   -19.5  -20    -19.7  -18    -16.5  -16    -15    -15    -15];
Y8(2,:) = [-23   -22.5  -22    -21    -18    -16.5  -16    -15    -15    -15];
Y8(3,:) = [-28   -27    -25    -23    -21    -18    -16    -15    -15    -15];
Y8(4,:) = [-32.5 -28.5  -26    -23.5  -20    -17    -16    -15    -15    -15];
Y8(5,:) = [-36   -34    -31.5  -27    -25    -22.5  -19    -16.5  -15    -15];
Y8(6,:) = [-39   -37.5 -34.5  -30    -27    -24    -21    -18    -16.5  -15];

for i=1:6
    f7(i) = interp1(X7,Y7(i,:),ang_in_b,'linear','extrap');
    f8(i) = interp1(X7,Y8(i,:),ang_in_b,'linear','extrap');
end

xx7 = 10:10:60;
xx8 = 70:-10:20;
i_plus_stall = interp1(xx7,f7,t,'linear','extrap');
i_minus_stall = interp1(xx8,f8,t,'linear','extrap');

i_p_stall = i_plus_stall + (1-(ang_in_b - 90)/(90 - t))*(di_plus_stall_cr + di_plus_stall_sb);
i_m_stall = i_minus_stall + (1-(ang_in_b - 90)/(90 - t))*di_minus_stall_sb;

end

i_min = (i_p_stall + Fi*i_m_stall)/(1+Fi);

if abs(desinc) < abs(i_min)
    IR = (desinc - i_min)/abs(i_m_stall - i_min);
else
    IR = (desinc - i_min)/abs(i_p_stall - i_min);
end

XX = -1:0.5:1;
YY = [2      1.25      1      1.25      2];

Npi = interp1(XX,YY,IR,'linear','extrap');

% else
%     Npi = 1;
% end
end

#####
function Npr = CC_Npr(Re,o,chord,ks)

x = [1e4   5e4   1e5   5e5   1e6   5e6];
for i = 1:length(x)
    X(i) = log(x(i));
end

Y(1,:) = [3.1    3.1    3.1    3.1    3.1    3.1];
Y(2,:) = [2.4    2.4    2.4    2.4    2.4    2.4];
Y(3,:) = [2.1    1.8    1.8    1.8    1.8    1.8];
Y(4,:) = [2.1    1.6    1.6    1.6    1.6    1.6];
Y(5,:) = [2.1    1.35   1.35   1.35   1.35   1.35];
Y(6,:) = [2.1    1.25   1.05   1.05   1.05   1.05];
Y(7,:) = [2.1    1.25   1      0.9     0.9    0.9];
Y(8,:) = [2.1    1.25   1      0.75   0.75   0.75];
Y(9,:) = [2.1    1.25   1      0.7     0.65   0.65];

REONO = Re*o/chord;
for i = 1:9

```

```

f(i) = interp1(X,Y(:,i),REONO,'linear','extrap');
end

T = ks*1e3/chord;
xx = [10      5      2      1      0.5     0.2     0.1     0.05      0.02];
Npr = interp1(xx,f,T,'linear','extrap');
end

#####
function Npt = CC_Npt(B,pitch,r_te)
X = 0:0.02:0.12;
X_1 = 0:0.02:0.10;
Y_1 = [1    1.15    1.34    1.61    2.02    2.52];
Y_2 = [1    1.11    1.225   1.36    1.53    1.72    1.96];
Y_3 = [1    1.09    1.16    1.26    1.36    1.5     1.6];
Y_4 = [1    1.08    1.15    1.225   1.3     1.36    1.46];
Y_5 = [1    1.07    1.135   1.19    1.25    1.31    1.375];

TEONS = r_te/pitch;
f(1) = interp1(X,Y_1,TEONS,'spline','extrap');
f(2) = interp1(X,Y_2,TEONS,'spline','extrap');
f(3) = interp1(X,Y_3,TEONS,'spline','extrap');
f(4) = interp1(X,Y_4,TEONS,'spline','extrap');
f(5) = interp1(X,Y_5,TEONS,'spline','extrap');

xx = [10 15 20 30 50];
Npt = interp1(xx,f,B,'linear','extrap');
end

#####
function NsHONC = CC_NsHONC(bb,height)
% Function used to obtain the Secondary loss ratio as described on figure
% 17 from C&C work

% inlet
% b = backbone length
% h = Height

% outlet
% Ns_tb = Secondary loss ratio

% fitting curve:
X = 0:0.5:5.5;
Y = [0 0.5 0.94 1.31 1.62 1.94 2.28 2.57 2.9 3.16 3.45 3.71];

NsHONC = interp1(X,Y,(bb/height),'spline','extrap');
end

#####
function dXp_se = CC_SONE(SONE,Ma)
% Function used to obtain the profile loss increment due to blade back radius losses parameter as described on
figure
% 9 from C&C work

% input
% Ma = Otlet isentropic mach number
% sone = pitch to blade back radius ratio (s/e)

% output
% dXp_se = Profile loss increment due to blade back radius losses parameter

% fitting curve:
if Ma < 0.8
    dXp_se = 0;
else
    X = 0:0.1:0.7;
    X_1 = 0:0.1:0.4;
    X_2 = X_1;
    X_3 = 0:0.1:0.5;
    X_4 = 0:0.1:0.6;

    Y_1 = [0    1      5.7    12.4    20];
    Y_2 = [0    0.1    4      10.1    16.2];
    Y_3 = [0    0      2.5    7.5     12.5    18];

```

```

Y_4 = [0    0     2     6.1   10.3   14.7   19];
Y_5 = [0    0     1.6   4.3   7.85   11.8   15.7   19.85];
Y_6 = [0    0     0.8   3.1   6.1    9.3    12.5   16.5];
Y_7 = [0    0     0.4   2     4.1    7.3    10     13.1];
Y_8 = [0    0     0.1   1.1   2.8    5.1    7.5    10.5];
Y_9 = [0    0     0.05  0.8   1.9    3.3    5.9    8];
Y_10= [0    0     0.02  0.5   1.1    2.4    3.8    5.85];
Y_11= [0    0     0.01  0.4   0.9    1.5    2.2    3.8];
Y_12= [0    0     0     0.1   0.3    0.67   1     1.35];

f(1) = interp1(X_1,Y_1,SONE,'spline','extrap');
f(2) = interp1(X_2,Y_2,SONE,'spline','extrap');
f(3) = interp1(X_3,Y_3,SONE,'spline','extrap');
f(4) = interp1(X_4,Y_4,SONE,'spline','extrap');
f(5) = interp1(X,Y_5,SONE,'spline','extrap');
f(6) = interp1(X,Y_6,SONE,'spline','extrap');
f(7) = interp1(X,Y_7,SONE,'spline','extrap');
f(8) = interp1(X,Y_8,SONE,'spline','extrap');
f(9) = interp1(X,Y_9,SONE,'spline','extrap');
f(10)= interp1(X,Y_10,SONE,'spline','extrap');
f(11)= interp1(X,Y_11,SONE,'spline','extrap');
f(12)= interp1(X,Y_12,SONE,'spline','extrap');

xx = 2:-0.1:0.9;
dXp_se = interp1(xx,f,Ma,'linear','extrap');

if dXp_se < 0
    dXp_se = 0;
end
end
end
#####
function Xa = CC_Xa(AAR,height,gamma,c1,B,q,u,V,c2)
% Function to estimate the annulus loss parameter as described on Craig
% and Cox model, extracted from "Performance Estimation of Axial Flow
% Turbines"

% inputs
% AAR = Annulus area ratio
% distance ratio e/h
% h = height
% e = distance - back surface radius?
% gamma = half equivalent cone angle.
% c1 = 1 or 0 for controlled or uncontrolled expansion respectively
% B = Outlet relative angle
% q = distance in hub between blades?
% [u,V] = cavity dimensions
% c2 = value to control if runner or guide calculations

% output
% Xa = Annulus loss parameter for Craig and Cox model

% Annulus loss parameter Xa1 calculus
Xa1 = CC_Xa1(AAR,gamma,c1);
% Cavity loss parameter Xa2 calculus
Xa2 = CC_Xa2(B,height,q,u,V,c2);

% Finally annulus loss parameter Xa is obtained:
Xa = Xa1 + Xa2;
%End

#####
function Xa1 = CC_Xa1(AAR,gamma,c)
% Function used to obtain the annulus wall loss parameter as described on figure
% 19 from C&C work

% input
% Ar = Annulus area ratio
% distance ratio e/h
% h = height
% e = distance - back surface radius?
% gamma = half equivalent cone angle.
% c = 1 or 0 for controlled or uncontrolled expansion

```

```

% output
% Xa1 = Annulus wall loss factor

% fitting curve:

if c == 1
    X = 0.3:0.1:0.9;
    Y(1,:) = [47.5      36      25      16.5       9      4.3      2.5];
    Y(2,:) = [42         32     22.5     14.5      7.5      3.9      2.5];
    Y(3,:) = [27.5      20      14      8.3       5      2.7      2.5];
    Y(4,:) = [10.5       7       5      3.5       2.6      2.5      2.5];
    for i=1:4
        f(i) = interp1(X,Y(i,:),AAR,'spline','extrap');
    end
    xx = [24      19      12      6];
    Xa1 = interp1(xx,f,gamma,'linear','extrap');
else
    X = 0.3:0.1:0.8;
    Y(1,:) = [47.5      36      34      34      34      34];
    Y(2,:) = [47.5      36      26      26      26      26];
    Y(3,:) = [47.5      36      25      16.5     16.5     16.5];
    Y(4,:) = [47.5      36      25      16      9       7.5];
    for i=1:4
        f(i) = interp1(X,Y(i,:),AAR,'linear','extrap');
    end
    EONH = 1.2;
    xx = [4      3      2      1];
    Xa1 = interp1(xx,f,EONH,'linear','extrap');
end

#####
function Xa2 = CC_Xa2(B,height,q,u,V,c)
% Function used to obtain the cavity loss parameter as described on figure
% 20 from C&C work

% input
% B = Outlet relative angle
% HONC = height over chord relationship
% b = chord or backbone length
% q = distance in hub between blades?
% [u,V] = cavity dimensions
% c = value to control if runner or guide calculations

% output
% Xa2 = cavity loss parameter

% fitting curve:

X_1 = [10^-2      10^-1      10^0      10^1      10^2      10^3      10^4];
for i = 1:length(X_1)
    X(i) = log(X_1(i));
end
Y1= [0.4      1.75      3.9      5.15      5.67      6.05      6.2];
Y2= [0.25      1.2      2.5      3.2      3.6      3.82      3.99];

P = 2*(u+V)-q;
Fa = log(0.02*P/(q*cos(B*pi/180)));
if c == 1
    f = interp1(X,Y1,Fa,'spline','extrap');
    Xa2 = f*(height*sin(B))/q;
else
    f = interp1(X,Y2,Fa,'spline','extrap');
    Xa2 = f*(height*sin(B))/q;
end

#####

```

```

function Xclr = CC_Xclr(CLONH,W_in,W_out,VCOEFF,AKONAT)
% Function used to obtain the efficiency debit factor from clearance as described on figure
% 21 from C&C work

% input
% dl = overlap on clearance
% HONC = height on chord relation
% W_in = relative velocity at inlet to runner
% W_out = relative velocity at outlet to runner
% Load = Load coefficient
% AKONAT = Clearance area on total blade throat area ratio

% output
% Fk = Efficiency debt factor due to tip clearance loss

% fitting curves:

x = 0:0.2:1;
Y(1,:) = [0.08    0.26      0.375     0.47       0.54       0.59];
Y(2,:) = [0.08    0.2       0.3        0.37       0.44       0.495];
Y(3,:) = [0.08    0.115     0.195     0.275     0.35       0.4];
Y(4,:) = [0.08    0.090     0.130     0.200     0.26       0.32];

Coeff = (1-VCOEFF^2)/VCOEFF^2+(W_out^2-W_in^2)/W_out^2;

for i = 1:4
    f(i) = interp1(x,Y(i,:),Coeff,'spline','extrap');
end

t = CLONH;
xx = [0 0.02 0.05 0.1];
Fk = interp1(xx,f,t,'linear','extrap');

end
#####
function [Xp,Npt,dXpte,dXpm,dXp_se,Xp_basic] = CC_Xp(Npr,A,B,r_te,SONE,Ma,bb,pitch,throat,chord)

Xp_basic = CC_Xpb(pitch,A,B,bb,chord);

% Npt is the trailing edge effect on profile loss ratio parameter
Npt = CC_Npt(B,pitch,r_te);

% dXpte is the loss increment due to trailing edge effect
dXpte = CC_Xpte(r_te,pitch);

% dXpm is the loss increment due to Mach number - supersonic/ subsonic conditions
dXpm = CC_MACH(Ma,r_te,pitch,throat);

% dXp_se is the loss increment due to sone relation
dXp_se = CC_SONE(SONE,Ma);

% Finally profile loss parameter estimation
Xp = Xp_basic*Npr*Npt + dXpte + dXpm + dXp_se;
end

% End

#####
function Xp_basic = CC_Xpb(pitch,A,B,bb,chord)

X_1 = [2      3      4      5      6      7      8      9];
Y_1 = [1.5    1.5    1.5    1.55   1.59   1.78   2.39   3.8];

X_2 = [2      3      4      5      6      7      8      9      10];
Y_2 = [1.2    1.2    1.2    1.2    1.2    1.27   1.48   2.05   2.9];

X_3 = [2      3      4      5      6      7      8      9      10];
Y_3 = [1      1      1      1      1      1.06   1.14   1.39   1.89];

X_4 = [2      3      4      5      6      7      8      9      10      11];
Y_4 = [0.88  0.88  0.88  0.88  0.88  0.89  0.95  1.14  1.53  2.12];

X_5 = [2      3      4      5      6      7      8      9      10      11];
Y_5 = [0.7    0.7    0.7    0.7    0.7    0.75   0.86   1.12   1.5];

```

```

X_6 = [2     3     4     5     6     7     8     9     10    11];
Y_6 = [0.4   0.4   0.4   0.4   0.4   0.4   0.4   0.45  0.507  0.725];

FL = CC_FL(A,B);

%FL_1 is the modified lift coefficient
FLSONC = FL*pitch/bb;

f(1) = interp1(X_1,Y_1,FLSONC,'spline','extrap');
f(2) = interp1(X_2,Y_2,FLSONC,'spline','extrap');
f(3) = interp1(X_3,Y_3,FLSONC,'spline','extrap');
f(4) = interp1(X_4,Y_4,FLSONC,'spline','extrap');
f(5) = interp1(X_5,Y_5,FLSONC,'spline','extrap');
f(6) = interp1(X_6,Y_6,FLSONC,'spline','extrap');

CR = CC_cr(pitch,chord,A,B);

xx = [1 1.1 1.3 1.5 2.0 5.0];
yy = interp1(xx,f,CR,'linear','extrap');

Xp_basic = yy/((pitch/bb)*sin(B*pi/180));
end

#####
function dxpte = CC_Xpte(r_te,pitch)

% Function to obtain the trailing edge loss increment as described on
% figure 6 from C&C

% Inputs
% te = trailing edge thickness
% s = pitch

% Outputs
% dxpt = loss increment

X = 0:0.02:0.12;
Y = [0      0.06    0.17    0.385   0.6     1.1     1.85];

TEONS = r_te/pitch;

dxpte = interp1(X,Y,TEONS,'spline','extrap');
end

#####
function Xs = CC_Xs(Nsr,pitch,height,A,B,W_in,W_out,bb)
% Function to estimate the secondary loss paremeter as described on Craig
% and Cox model, extracted from "Performance Estimation of Axial Flow
% Turbines"

% inputs
% Nsr = Reynolds number effect as obtained from function Npr = Re_effect
% bb = backbone length
% s = pitch
% h = height
% A = inlet relative angle
% B = outlet relative angle
% s = pitch
% W_i = inlet relative velocity
% W_o = outlet relative velocity

% output
% Xs = Secondary loss parameter for Craig and Cox model

% Calculus of the basic secondary loss parameter from function
% sec_basicloss
Xsb = CC_Xsb(A,B,pitch,W_in,W_out,bb);

% Calculus of the Secondary loss aspect ratio factor from function
% Sec_lossratio(b,h)
NsHONC = CC_NsHONC(bb,height);

% Calculus of the secondary loss parameter

```

```

Xs = Xsb*Nsr*NsHONC;
% End

#####
function Xsb = CC_Xsb(A,B,pitch,W_in,W_out,bb)
% Function used to obtain the Secondary basic loss parameter as described on figure
% 17 from C&C work

% inlet
% b = backbone length
% s = pitch
% A = inlet relative angle
% B = outlet relative angle
% W_i = inlet relative mean velocity
% W_o = outlet relative mean velocity

% outlet
% Xsb = Seondary basic loss parameter

% fitting curve:
X = 0:0.2:1;
Y_1 = [3.1      7      10.8    14.4    17.9    21.1];
for i =1:6
    Y(1,i) = Y_1(i);
end
Y_2 = [2.9      6.3     9.5     12.7    16      19];
for i =1:6
    Y(2,i) = Y_2(i);
end
Y_3 = [2.8      5.6     8.7     11.5    14.4    17];
for i =1:6
    Y(3,i) = Y_3(i);
end
Y_4 = [2.3      5       7.35   9.9     12.5    14.8];
for i =1:6
    Y(4,i) = Y_4(i);
end
Y_5 = [2        4.3     6.4     8.5     10.6    12.6];
for i =1:6
    Y(5,i) = Y_5(i);
end
Y_6 = [1.8      3.5     5.3     7       8.9     10.5];
for i =1:6
    Y(6,i) = Y_6(i);
end
Y_7 = [1.5      2.8     4.15   5.6     7       8.3];
for i =1:6
    Y(7,i) = Y_7(i);
end

Vr = W_in^2/W_out^2;
FL = CC_FL(A,B);
FLSONC = FL*(pitch/bb);

for i = 1:7
f(i) = interp1(X,Y(i,:),Vr,'spline','extrap');
end

xx = [10      9      8      7      6      5      4];
Xsb = interp1(xx,f,FLSONC,'linear','extrap');

end

```

## Denton Loss Model Implementation

```

#####
##### Denton Loss Model #####
#####
##### Rafael Guedez, 2011 #####
#####
#####

function [SONC,Ytot,Yp,Yte,Ys,Ycl] = Denton(rel_ang_in,rel_ang_out,ang_in_b,te,throat,c,pitch,h,cax,CLONH,NorR,SorU,kappa,Ma_in,Ma)

% Inputs
% rel_ang_in = Relative inlet angle
% rel_ang_out = Relative outlet angle
% ang_in_b = blade inlet angle
% te = trailing edge thickness
% throat = blade opening or throat
% chord = blade chord
% h = blade height
% cax = axial chord
% CLONH = clearance on height, usually 0.01. Input from LUAX-T
% NorR = if NorR = 1 then loss calculations are for stator, else for rotor.
% SorR = Shrouded or Unshrouded. Here is input the number of seals, if it is 0 then calculation for unshrouded blades will be used.
% kappa = Cp/Cv
% Ma_in = Inlet Mach number
% Ma = Mach number at outlet
%
% Outputs
% SONC = Optimum pitch to chord ratio provided by Denton
% Ytot = Total pressure loss coefficient
% Yp = Profile Loss
% Yte = Trailing Edge Loss
% Ys = Secondary Loss
% Ycl = Clearance Loss

#####
##### Profile Loss #####
if rel_ang_out < 40 || rel_ang_out > 80
    Xp = 0.02;
    disp('Profile Loss Value has been fixed to 0.02 since the relative outlet flow angle is out of the range of applicability')
else
    X1 = 40:5:80;
    Y1 = 80:-10:-40;
    % Optimum SONC as extracted from figure 19 in Denton's work (1993)
    Z1 = [[1.55 1.525 1.5 1.475 1.45 1.425 1.415 1.405 1.4];
    [1.525 1.5 1.475 1.45 1.425 1.415 1.405 1.4 11];
    [1.5 1.475 1.45 1.425 1.415 1.405 1.4 1.2 0.9];
    [1.475 1.45 1.425 1.415 1.4 1.3 1.2 0.9 0.85];
    [1.45 1.425 1.415 1.4 1.3 1.2 0.9 0.85 0.825];
    [1.425 1.35 1.25 1.15 1.0 0.9 0.865 0.83 0.79];
    [1.4 1.2 1.05 0.95 0.9 0.85 0.83 0.8 0.782];
    [1.1 1.0 0.94 0.88 0.84 0.82 0.8 0.795 0.79];
    [0.95 0.89 0.85 0.825 0.81 0.795 0.790 0.785 0.775];
    [0.85 0.83 0.81 0.795 0.785 0.7825 0.78 0.7775 0.774];
    [0.8 0.78 0.785 0.78 0.78 0.7775 0.775 0.775 0.775];
    [0.75 0.745 0.74 0.735 0.7325 0.73 0.74 0.76 0.765];
    [0.7 0.7 0.7 0.705 0.71 0.72 0.73 0.74 0.76]];
    SONC = interp2(X1,Y1,Z1,rel_ang_out,rel_ang_in,'linear');

    % Profile Loss in [%] for optimum SONC, extracted from figure 20 in
    % Denton's work (1993)
    Z2 = [[0.08 0.12 0.14 0.16 0.25 0.34 0.45 0.5 2.3];
    [0.125 0.16 0.18 0.2 0.3 0.4 0.48 0.45 3.0];
    [0.2 0.25 0.3 0.42 0.47 0.5 1.0 2.0 3.5];
    [0.4 0.45 0.47 0.49 0.7 1.2 1.7 2.5 4.2];
    [0.47 0.485 0.5 0.75 1.0 1.4 1.95 2.75 4.4];
    [0.485 0.55 0.7 0.95 1.25 1.6 2.2 2.95 4.6];
    [0.65 0.75 0.9 1.2 1.425 1.75 2.3 3.1 4.7];
    [0.8 0.9 1.2 1.35 1.6 1.9 2.4 3.25 4.74];
    [1.0 1.2 1.3 1.5 1.75 2.1 2.5 3.3 4.75];
    [1.2 1.35 1.45 1.7 1.85 2.2 2.65 3.4 4.8];
    [1.45 1.5 1.65 1.75 2.0 2.3 2.7 3.45 4.9];
    [1.7 1.8 1.9 2.0 2.2 2.45 2.85 3.6 5.15];
    [2.05 2.1 2.15 2.35 2.45 2.6 2.95 3.7 5.4];];

    Xp = interp2(X1,Y1,Z2,rel_ang_out,rel_ang_in,'linear')/100;
end

#####
##### Trailing Edge Loss #####
% - Cpb = -0.13 as suggested by Denton. Denton states that values must be in a range between -0.1 to -0.2
% - The boundary layer displacement thickness (aka delastartOnh) and the momentum thickness have been both
% fixed from values encountered in LUAX-T.
% delastartOnh = 0.015 fixed from LUAX-T
%
% The equation to estimate the trailing edge loss is used as shown in
% Denton's work (1993)
Cpb = -0.15;
Xte = (-Cpb*te/throat) + ((0.015 + te)/throat)^2/100;

```

```

#####
    † Secondary Loss      #####
####

% As suggested by Denton in CTC 2008 page 25, the best approx method is
% that proposed by Dunham and Come (1970) with a new factor of 0.375 to
% which approaches the method better to reality. The agreement with the
% correlation proposed by Dunham is basically because it is proportional
% to the inverse aspect ratio as Denton suggests it should in his work
% (1993).

ang_m = atand(0.5*(tand(rel_ang_in) - tand(rel_ang_out)));
CLONSONC = 2*(tand(rel_ang_in) + tand(rel_ang_out))*cosd(ang_m);
if h/c <= 2
    f_AR = (1 - 0.25*sqrt(2-(h/c)))/(h/c);% Aspect Ratio Factor
else
    f_AR = 1/(h/c);% Aspect Ratio Factor
end
if Ma > 0.2
    K1 = 1 - 1.25*(Ma - 0.2);% Factor to consider high Mach operation conditions
else
    K1 = 1;
end
K2 = (Ma_in/Ma)^2;
K3 = (1/h*cax)^2;
Kp = 1 - K2*(1 - K1);
Ks = 1 - K3*(1 - Kp);
%Ys = 0.375*1.2*0.0334*f_AR*(cosd(rel_ang_out)/cosd(ang_in_b))*CLONSONC^2*((cosd(rel_ang_out)^2)/(cosd(ang_m)^3))*Ks; %Secondary pressure loss
%coefficient by Kacker.
Ys = 0.375*0.0334*(c/h)*(cosd(rel_ang_out)/cosd(ang_in_b))*CLONSONC^2*((cosd(rel_ang_out)^2)/(cosd(ang_m)^3)); %Secondary pressure loss
%coefficient by Dunham.

#####
    † Clearance Loss      #####
####

if NorR == 1
    Xcl = 0;
else
    % Only in rotor

    if SorU == 0
        % In case of unshrouded turbines and CLONH = 0.01 as extracted from
        % Denton's work in 1993, figure 34.
        X3 = 0.5:75;
        Y3 = 60:-10:-60;

        Z3 = [[5      5      4.9     4.8     4.7     4.5     4      3.5     3      2.5     1.5     0.6     0.5     2      4      4.7];
               [3      2.9    2.7     2.5     2.35    2       1.75    1.4     0.75    0.4     0.4     1       1.75    3      4.1     4.75];
               [2.1    1.9     1.75   1.5     1.25    0.9     0.55    0.35    0.2     0.5     1       1.5     2.3     3.35   4.2     4.8];
               [1.4    1.1     0.9     0.7     0.4     0.25   0.1     0.1     0.65   1       1.4     1.8     2.5     3.5     4.24   4.35];
               [0.8    0.6     0.4     0.2     0.1     0.3     0.5     0.75   1       1.25    1.6     2.1     2.65   3.6     4.27   4.9];
               [0.4    0.1     0.05   0.1     0.3     0.6     0.75   1       1.25    1.5     1.75   2.25     2.75   3.8     4.29   4.95];
               [0     0.1     0.3     0.5     0.7     0.8     1.05   1.2     1.45   1.7     2       2.4     3       4     4.3     5];
               [0.75   0.9     1.1     1.25   1.4     1.5     1.75   1.8     2       2.25    2.45   2.8     3.4     4.07   4.35   5.1];
               [0.4    0.5     0.7     0.8     1       1.2     1.3     1.5     1.75   1.9     2.2     2.55   3.2     4.05   4.32   5.05];
               [0.75   0.9     1.1     1.25   1.4     1.5     1.75   1.8     2       2.25    2.45   2.8     3.4     4.07   4.35   5.1];
               [1.4    1.5     1.65   1.8     1.95   2.05   2.25   2.35   2.5     2.6     2.75   3.15   3.6     4.1     4.42   5.15];
               [2.1    2.25   2.4     2.6     2.75   2.9     3       3.1     3.3     3.4     3.45   3.6     4       4.2     4.5     5.2];
               [3      3.2     3.35   3.5     3.6     3.75   4       4.04   4.05     4.06   4.07   4.1     4.15   4.4     4.6     5.25];
               [5      5       4.9     4.9     4.9     4.9     4.9     4.85   4.8     4.7     4.5     4.7     4.75   4.8     4.85   5.3]];

        Xcl = interp2(X3,Y3,Z3,rel_ang_out,rel_ang_in,'linear')/100;

    else
        % In case of shrouded turbines as extracted from "The Effect Of Clearance
        % On Shrouded And Unshrouded Turbines At Two Levels Of Reaction" from Yoon
        % et al (2010) - Denton.
        %Cd = 0.6;% Contraction jet value suggested by Denton (1993)
        % The mass coefficient in cse of shrouded blades depends on the number of seals (aka SorU) as suggested on CTC 2008 by Denton in page 28
        mass_coeff = 0.6*CLONH*((pitch)/throat)*(1/sqrt(SorU));
        % The total loss coefficient is estimated from the next equation
        % given in Denton's work (1993)
        Xcl = 2*mass_coeff*(1 - (tand(rel_ang_in)/tand(rel_ang_out))*sind(rel_ang_out)^2);

    end
end

#####
    † Pressure Loss Coefficients      #####
####

% The losses are estimated as entropy loss coefficients. Brown in his work
% suggests that these last ones are similar to the enthalpy loss
% coefficients. To convert from entropy loss based coefficients to pressure
% ones he suggests next relation:
% (formulae extracted from Brown, 1972)
% Y = e^(1 + 0.5*(kappa - 1)*Ma^2)*(1/(kappa - 1))

convert = (1 + 0.5*(kappa - 1)*Ma^2)*(1/(kappa - 1));

Yp = Xp*convert;%Profile loss pressure coefficient
Yte = Xte*convert;%Trailing edge loss pressure coefficient
Ycl = Xcl*convert;%Clearance loss pressure coefficient
Ytot = Yp + Yte + Ycl + Ys;% Total loss based on pressure coefficients

```

**APPENDIX II**  
**VALIDATION STUDY**

**Table - Evaluated Data used for validation case n°2 as extracted from Svensdotter work (Svensdotter & Wei, 1995)**

Test Number	1449	1448	1445	1447	1446
v	0,33	0,43	0,52	0,60	0,68
m [kg/s]	1,93	1,85	1,85	1,83	1,82
P <sub>1</sub> [bar]	1,3660	1,3493	1,3588	1,3664	1,3732
T <sub>1</sub> [°C]	38,9	38,8	39,2	39,0	39,0
ρ <sub>1</sub> [kg/m <sup>3</sup> ]	1,522	1,505	1,521	1,523	1,529
Cx <sub>1</sub> [m/s]	44,2	43,2	42,7	42,0	41,6
α <sub>1</sub> [°]	0,00	0,00	0,00	0,00	0,00
P <sub>2</sub> [bar]	1,0257	1,0357	1,0536	1,0733	1,0873
T <sub>2</sub> [°C]	16,9	18,5	19,7	20,4	21,0
ρ <sub>2</sub> [m/s]	1,230	1,235	1,251	1,272	1,285
Cx <sub>2</sub> [m/s]	54,6	52,5	51,6	50,4	49,6
C <sub>2</sub> [m/s]	215,2	206,1	204,4	198,3	196,0
W <sub>2</sub> [m/s]	144,2	115,0	94,3	74,1	60,2
U <sub>2</sub> [m/s]	75,0	97,8	117,8	136,6	153,6
α <sub>2</sub> [°]	75,3	75,3	75,3	75,3	75,3
β <sub>2</sub> [°]	67,7	62,8	56,9	47,7	35,5
P <sub>3</sub> [bar]	1,0173	1,0072	1,0097	1,0165	1,0215
T <sub>3</sub> [°C]	19,0	18,0	17,1	16,5	16,2
ρ <sub>3</sub> [kg/m <sup>3</sup> ]	1,211	1,203	1,210	1,221	1,228
Cx <sub>3</sub> [m/s]	53,5	51,8	51,3	50,4	49,8
C <sub>3</sub> [m/s]	64,1	52,3	54,2	64,2	76,2
W <sub>3</sub> [m/s]	123,0	116,2	112,1	109,3	108,2
U <sub>3</sub> [m/s]	75,0	97,8	117,8	136,6	153,6
β <sub>3</sub>	64,2	63,5	62,8	62,6	62,7
Δh <sub>is</sub> [kJ/kg]	25,369	25,175	25,584	25,465	25,474
η	0,763	0,814	0,839	0,852	0,857

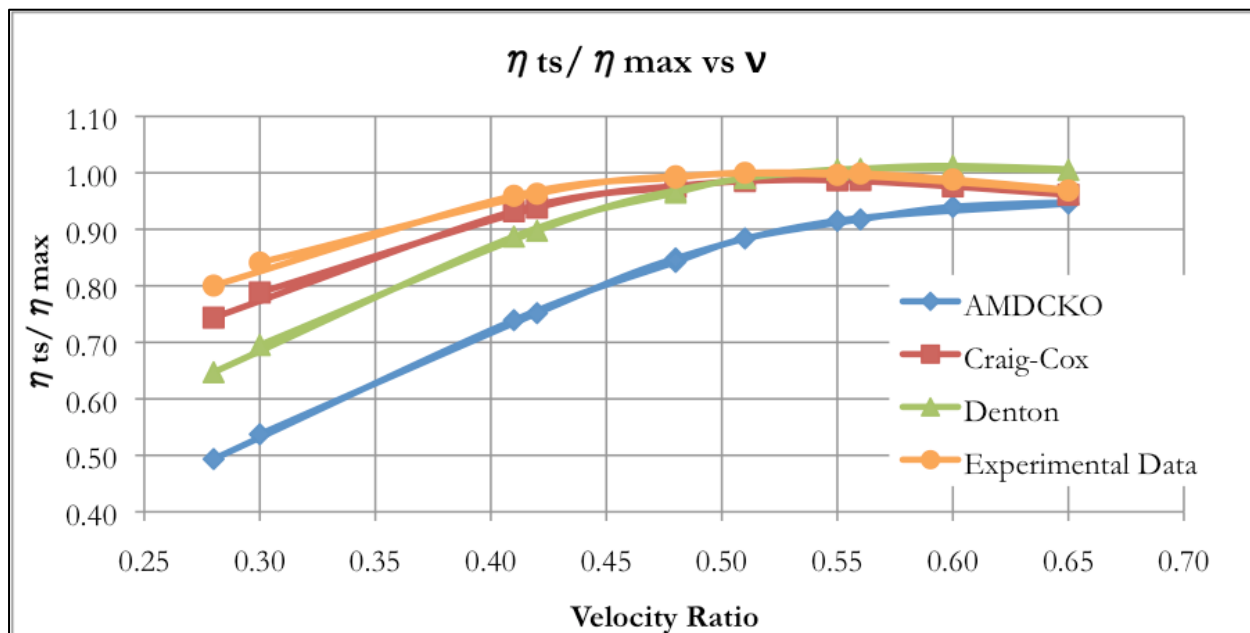


Figure - Validation Turbine 1 - Normalized Efficiency Vs Velocity Ratio

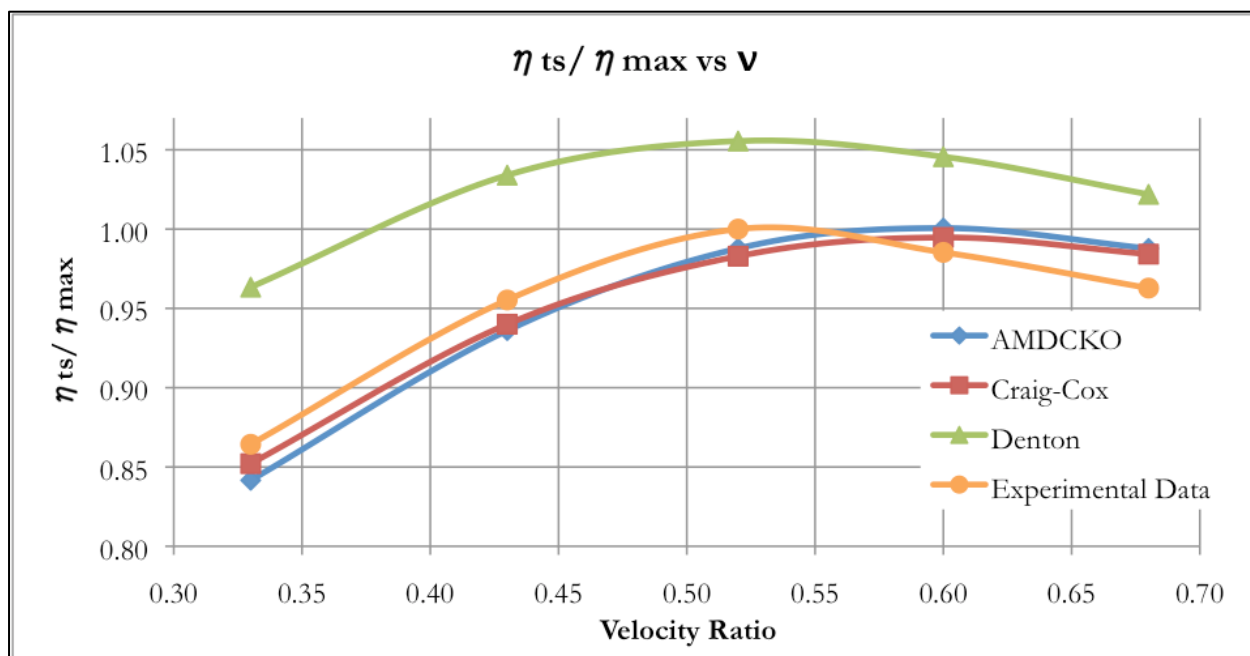


Figure - Validation Turbine 2 - Normalized Efficiency Vs. Velocity Ratio

## **APPENDIX III**

### **PARAMETRIC STUDY**

## Output Text Results from Parametric Study for AMDCKO

```

=====
# LUAX-T #
# Version 2.0 #
# David Olsson & Magnus Genrup #
# 2008 #
# Rafael Guedez #
# 2011 #
=====

Test_turbine_1
23-Mar-2011 14:49:02
PARAMETRIC STUDY
Ainley & Mathieson et al. RESULTS
=====

Stage 1
Outlet Angle      73.00
Load Coefficient   1.50
Optimum Point:    R =  0.25      TS Isentropic Efficiency =  72.02
=====
Reaction Degree == Flow Coeff == PR t-t == TT Iso Effic. == TS Iso Effic. == TT Pol Effic. == TS Pol Effic == T. Effic P&W == T. Effic. Kurzke ===
0.15   0.51   2.39   77.77   71.59   77.42   80.36   81.35   69.61
0.17   0.50   2.38   77.89   71.75   77.57   80.51   81.20   69.54
0.19   0.49   2.38   78.00   71.87   77.70   80.64   81.05   69.47
0.21   0.48   2.37   78.10   71.96   77.81   80.77   80.89   69.40
0.23   0.47   2.37   78.18   72.01   77.92   80.89   80.72   69.31
0.25   0.46   2.36   78.25   72.02   78.00   81.00   80.54   69.22
=====
Load Coefficient   1.60
Optimum Point:    R =  0.21      TS Isentropic Efficiency =  71.55
=====
Reaction Degree == Flow Coeff == PR t-t == TT Iso Effic. == TS Iso Effic. == TT Pol Effic. == TS Pol Effic == T. Effic P&W == T. Effic. Kurzke ===
0.15   0.53   2.55   77.67   71.39   77.07   80.16   81.20   70.33
0.17   0.52   2.55   77.81   71.49   77.23   80.35   81.07   70.28
0.19   0.51   2.54   77.92   71.54   77.37   80.52   80.92   70.21
0.21   0.50   2.53   78.02   71.55   77.48   80.67   80.76   70.13
0.23   0.49   2.52   78.11   71.54   77.59   80.82   80.61   70.05
0.25   0.48   2.52   78.18   71.49   77.67   80.96   80.44   69.96
=====
Load Coefficient   1.70
Optimum Point:    R =  0.17      TS Isentropic Efficiency =  71.03
=====
Reaction Degree == Flow Coeff == PR t-t == TT Iso Effic. == TS Iso Effic. == TT Pol Effic. == TS Pol Effic == T. Effic P&W == T. Effic. Kurzke ===
0.15   0.54   2.74   77.49   70.97   76.64   79.95   80.99   70.92
0.17   0.53   2.73   77.66   71.03   76.83   80.20   80.88   70.88
0.19   0.52   2.72   77.79   71.02   76.99   80.42   80.75   70.83
0.21   0.51   2.71   77.90   70.97   77.11   80.61   80.60   70.75
0.23   0.50   2.70   77.98   70.88   77.21   80.79   80.44   70.67
0.25   0.49   2.70   78.06   70.77   77.30   80.97   80.28   70.59
=====
Outlet Angle      74.00
Load Coefficient   1.50
Optimum Point:    R =  0.25      TS Isentropic Efficiency =  72.66
=====
Reaction Degree == Flow Coeff == PR t-t == TT Iso Effic. == TS Iso Effic. == TT Pol Effic. == TS Pol Effic == T. Effic P&W == T. Effic. Kurzke ===
0.15   0.48   2.40   77.86   72.24   77.51   80.17   81.31   69.59
0.17   0.47   2.39   77.98   72.40   77.66   80.31   81.16   69.53
0.19   0.46   2.38   78.07   72.52   77.77   80.43   81.00   69.45
0.21   0.45   2.38   78.16   72.60   77.88   80.54   80.84   69.37
0.23   0.44   2.37   78.24   72.65   77.97   80.65   80.66   69.29
0.25   0.44   2.37   78.29   72.66   78.04   80.75   80.47   69.19
=====
Load Coefficient   1.60
Optimum Point:    R =  0.21      TS Isentropic Efficiency =  72.23
=====
Reaction Degree == Flow Coeff == PR t-t == TT Iso Effic. == TS Iso Effic. == TT Pol Effic. == TS Pol Effic == T. Effic P&W == T. Effic. Kurzke ===
0.15   0.49   2.57   77.75   72.06   77.15   79.93   81.15   70.31
0.17   0.48   2.56   77.88   72.16   77.31   80.11   81.02   70.25
0.19   0.48   2.55   77.99   72.22   77.44   80.27   80.87   70.19
0.21   0.47   2.54   78.08   72.23   77.55   80.42   80.71   70.10
0.23   0.46   2.54   78.16   72.21   77.64   80.55   80.54   70.02
0.25   0.45   2.53   78.22   72.16   77.72   80.68   80.37   69.93
=====
Load Coefficient   1.70
Optimum Point:    R =  0.19      TS Isentropic Efficiency =  71.73
=====
Reaction Degree == Flow Coeff == PR t-t == TT Iso Effic. == TS Iso Effic. == TT Pol Effic. == TS Pol Effic == T. Effic P&W == T. Effic. Kurzke ===
0.15   0.51   2.75   77.56   71.67   76.71   79.69   80.94   70.90
0.17   0.50   2.74   77.72   71.73   76.90   79.92   80.82   70.85
0.19   0.49   2.73   77.85   71.73   77.05   80.13   80.68   70.79
0.21   0.48   2.72   77.96   71.69   77.17   80.32   80.53   70.72
0.23   0.47   2.71   78.03   71.59   77.26   80.49   80.37   70.64
0.25   0.46   2.71   78.10   71.48   77.35   80.65   80.21   70.55
=====
Outlet Angle      75.00
Load Coefficient   1.50
Optimum Point:    R =  0.23      TS Isentropic Efficiency =  73.24
=====
Reaction Degree == Flow Coeff == PR t-t == TT Iso Effic. == TS Iso Effic. == TT Pol Effic. == TS Pol Effic == T. Effic P&W == T. Effic. Kurzke ===
0.15   0.45   2.41   77.93   72.84   77.58   79.98   81.24   69.55
0.17   0.44   2.40   78.04   73.01   77.72   80.10   81.09   69.48
0.19   0.43   2.39   78.13   73.13   77.83   80.21   80.92   69.41
0.21   0.42   2.39   78.21   73.21   77.93   80.32   80.76   69.33
0.23   0.42   2.39   78.26   73.24   78.00   80.40   80.56   69.23
0.25   0.41   2.38   78.30   73.23   78.05   80.48   80.36   69.13
=====
Load Coefficient   1.60
Optimum Point:    R =  0.21      TS Isentropic Efficiency =  72.86
=====
```

```

=====
Reaction Degree == Flow Coeff == PR t-t == TT Iso Effic. == TS Iso Effic. == TT Pol Effic. == TS Pol Effic == T. Effic P&W == T. Effic. Kurzke ===
  0.15    0.46    2.58    77.81    72.68    77.21    79.71    81.08    70.26
  0.17    0.45    2.57    77.93    72.79    77.36    79.87    80.93    70.20
  0.19    0.45    2.56    78.03    72.84    77.48    80.02    80.78    70.13
  0.21    0.44    2.55    78.11    72.86    77.58    80.15    80.62    70.05
  0.23    0.43    2.55    78.18    72.84    77.66    80.28    80.45    69.97
  0.25    0.42    2.54    78.23    72.77    77.72    80.38    80.25    69.86
=====

Load Coefficient      1.70
Optimum Point:       R =  0.19          TS Isentropic Efficiency =  72.38
=====
Reaction Degree == Flow Coeff == PR t-t == TT Iso Effic. == TS Iso Effic. == TT Pol Effic. == TS Pol Effic == T. Effic P&W == T. Effic. Kurzke ===
  0.15    0.48    2.77    77.62    72.33    76.77    79.43    80.86    70.85
  0.17    0.47    2.76    77.77    72.38    76.94    79.65    80.73    70.79
  0.19    0.46    2.75    77.89    72.38    77.08    79.84    80.59    70.73
  0.21    0.45    2.74    77.98    72.34    77.19    80.01    80.43    70.65
  0.23    0.44    2.73    78.05    72.25    77.28    80.17    80.26    70.56
  0.25    0.44    2.72    78.10    72.12    77.34    80.31    80.09    70.48
=====

Outlet Angle        76.00
Load Coefficient     1.50
Optimum Point:       R =  0.23          TS Isentropic Efficiency =  73.77
=====
Reaction Degree == Flow Coeff == PR t-t == TT Iso Effic. == TS Iso Effic. == TT Pol Effic. == TS Pol Effic == T. Effic P&W == T. Effic. Kurzke ===
  0.15    0.42    2.42    77.98    73.41    77.63    79.78    81.14    69.48
  0.17    0.41    2.41    78.07    73.56    77.75    79.88    80.98    69.41
  0.19    0.40    2.41    78.14    73.67    77.84    79.97    80.79    69.32
  0.21    0.40    2.40    78.20    73.74    77.92    80.05    80.61    69.24
  0.23    0.39    2.40    78.25    73.77    77.98    80.13    80.42    69.14
  0.25    0.38    2.40    78.29    73.77    78.04    80.20    80.22    69.04
=====

Load Coefficient     1.60
Optimum Point:       R =  0.19          TS Isentropic Efficiency =  73.41
=====
Reaction Degree == Flow Coeff == PR t-t == TT Iso Effic. == TS Iso Effic. == TT Pol Effic. == TS Pol Effic == T. Effic P&W == T. Effic. Kurzke ===
  0.15    0.43    2.59    77.84    73.27    77.25    79.47    80.97    70.19
  0.17    0.42    2.59    77.96    73.37    77.38    79.62    80.82    70.12
  0.19    0.42    2.58    78.04    73.41    77.48    79.74    80.64    70.04
  0.21    0.41    2.57    78.10    73.41    77.56    79.85    80.46    69.95
  0.23    0.40    2.57    78.15    73.38    77.63    79.96    80.28    69.86
  0.25    0.39    2.56    78.19    73.31    77.68    80.06    80.09    69.76
=====

Load Coefficient     1.70
Optimum Point:       R =  0.17          TS Isentropic Efficiency =  72.98
=====
Reaction Degree == Flow Coeff == PR t-t == TT Iso Effic. == TS Iso Effic. == TT Pol Effic. == TS Pol Effic == T. Effic P&W == T. Effic. Kurzke ===
  0.15    0.44    2.79    77.64    72.93    76.79    79.16    80.75    70.77
  0.17    0.44    2.78    77.79    72.98    76.96    79.37    80.61    70.71
  0.19    0.43    2.77    77.89    72.97    77.08    79.54    80.45    70.64
  0.21    0.42    2.76    77.96    72.92    77.17    79.69    80.28    70.56
  0.23    0.41    2.75    78.01    72.82    77.24    79.82    80.09    70.46
  0.25    0.41    2.74    78.06    72.70    77.30    79.95    79.91    70.36
=====

===== OPTIMUM POINTS - PARAMETRIC STUDY RESULTS =====
=====

== Str. TE Angle == Load Coefficient == Optimum R == Optimum TS ISO Eff. == Flow Coeff == PR tt == Rtr TE Angle ==
== 73.00 == 1.50 == 0.25 == 72.02 == 0.46 == 2.36 == -5.64 ==
== 73.00 == 1.60 == 0.21 == 71.55 == 0.50 == 2.53 == -5.26 ==
== 73.00 == 1.70 == 0.17 == 71.03 == 0.53 == 2.73 == -4.49 ==
=====
== 74.00 == 1.50 == 0.25 == 72.66 == 0.44 == 2.37 == -5.63 ==
== 74.00 == 1.60 == 0.21 == 72.23 == 0.47 == 2.54 == -5.29 ==
== 74.00 == 1.70 == 0.19 == 71.73 == 0.49 == 2.73 == -7.51 ==
=====
== 75.00 == 1.50 == 0.23 == 73.24 == 0.42 == 2.39 == -2.38 ==
== 75.00 == 1.60 == 0.21 == 72.86 == 0.44 == 2.55 == -5.33 ==
== 75.00 == 1.70 == 0.19 == 72.38 == 0.46 == 2.75 == -7.72 ==
=====
== 76.00 == 1.50 == 0.23 == 73.77 == 0.39 == 2.40 == -2.18 ==
== 76.00 == 1.60 == 0.19 == 73.41 == 0.42 == 2.58 == -1.91 ==
== 76.00 == 1.70 == 0.17 == 72.98 == 0.44 == 2.78 == -4.62 ==
=====

===== I N L E T C O N D I T I O N S =====
=====

----- Inlet Properties -----
Inlet massflow      [kg/s]: 100.00
Inlet temperature   [°C]: 1423.00
Inlet pressure      [bar]: 18.52
Inlet enthalpy      [kJ/kg]: 1696.2
Inlet entropy       [J/kg K]: 1245.1
Inlet entropy change [J/kg K]: -0.00
Inlet fuel to air ratio [-]: 0.0200
Inlet gas constant  [J/kg K]: 292.68
Inlet specific heat [J/kg K]: 1316.3
Inlet Cp over Cv    [-]: 1.286
Inlet density        [kg/m³]: 3.710
----- Inlet Velocities & Angles -----
Inlet flow angle    [-]: 0.00
Inlet absolute velocity [m/s]: 85.00
Inlet meridional velocity [m/s]: 85.00
Inlet tangential velocity [m/s]: 0.00
Inlet speed of sound [m/s]: 798.3
Inlet mach number   [-]: 0.11

```

### Graphical Results from Parametric Study for AMDCKO

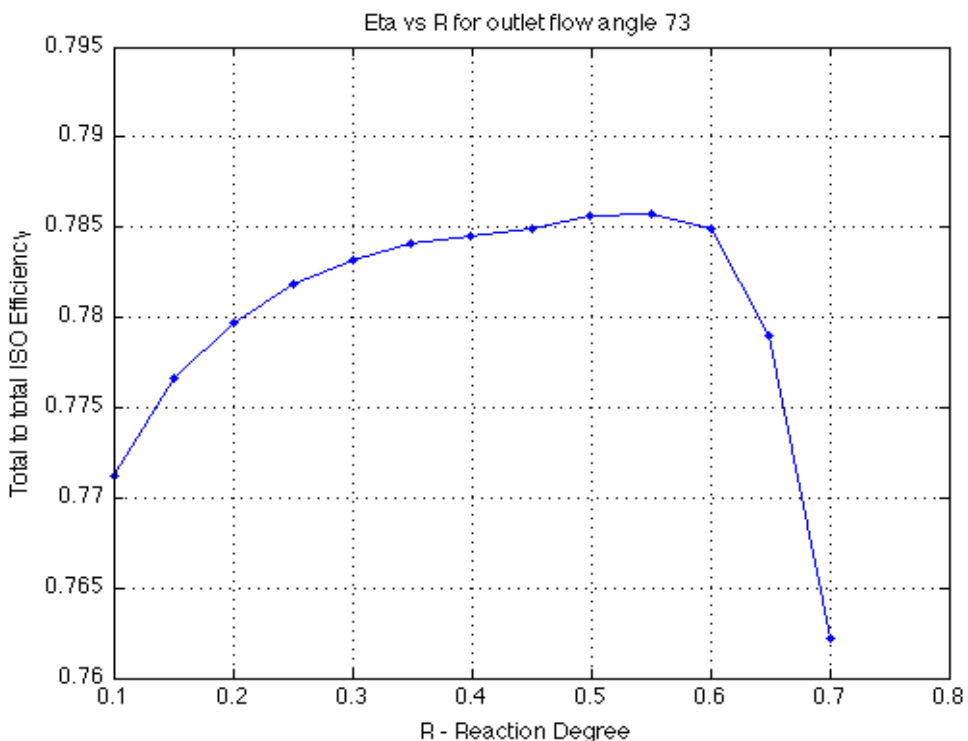


Figure - Total to Total Efficiency Prediction for reference case

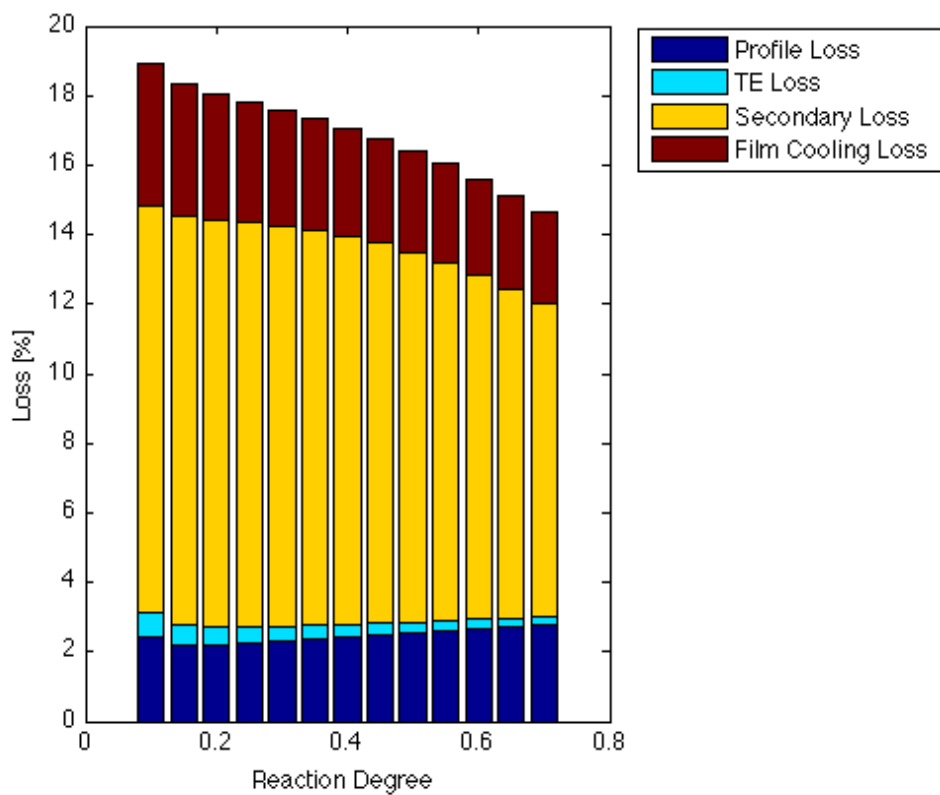


Figure - Breakdown of Losses in Stator for Reference Case

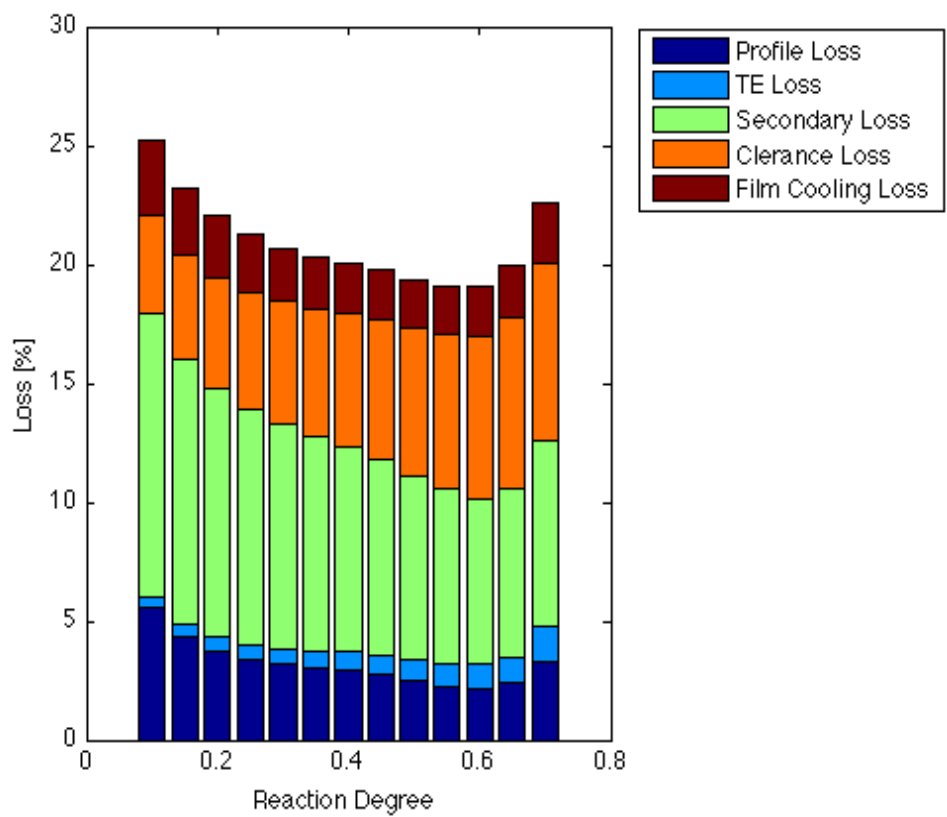


Figure - Breakdown of Losses in rotor for Reference Case

## Output Text Results from Parametric Study for Craig-Cox

```

=====
#          LUXX-T      #
#          Version 2.0   #
#          David Olsson & Magnus Genrup  #
#          2008           #
#          Rafael Guedez  #
#          2011           #
=====

Test_turbine_1
23-Mar-2011 21:32:06
PARAMETRIC STUDY
Craig & Cox RESULTS
-----

-
Stage 1
Outlet Angle      73.00
Load Coefficient   1.20
Optimum Point:    R =  0.38      TS Isentropic Efficiency = 74.51
=====
=
Reaction Degree == Flow Coeff == PR t-t == TT Iso Effic. == TS Iso Effic. == TT Pol Effic. == TS Pol Effic == T. Effic P&W == T. Effic. Kurzke ===
  0.30  0.40  1.93  79.74  73.94  80.44  82.90  79.84  65.30
  0.32  0.39  1.93  79.85  74.16  80.58  83.02  79.72  65.25
  0.34  0.39  1.93  79.94  74.31  80.69  83.11  79.57  65.18
  0.36  0.38  1.93  80.01  74.43  80.78  83.18  79.41  65.11
  0.38  0.37  1.92  80.05  74.51  80.85  83.25  79.23  65.03
  0.40  0.37  1.92  80.05  74.50  80.87  83.27  79.01  64.92
=====
=
Load Coefficient   1.40
Optimum Point:    R =  0.38      TS Isentropic Efficiency = 73.37
=====
=
Reaction Degree == Flow Coeff == PR t-t == TT Iso Effic. == TS Iso Effic. == TT Pol Effic. == TS Pol Effic == T. Effic P&W == T. Effic. Kurzke ===
  0.30  0.43  2.19  79.34  73.19  79.45  82.22  79.77  67.51
  0.32  0.43  2.19  79.48  73.28  79.61  82.40  79.68  67.46
  0.34  0.42  2.18  79.61  73.34  79.77  82.57  79.59  67.41
  0.36  0.41  2.18  79.74  73.36  79.91  82.74  79.49  67.36
  0.38  0.40  2.17  79.86  73.37  80.05  82.92  79.39  67.31
  0.40  0.39  2.17  79.96  73.33  80.17  83.08  79.27  67.25
=====
=
Load Coefficient   1.60
Optimum Point:    R =  0.32      TS Isentropic Efficiency = 71.59
=====
=
Reaction Degree == Flow Coeff == PR t-t == TT Iso Effic. == TS Iso Effic. == TT Pol Effic. == TS Pol Effic == T. Effic P&W == T. Effic. Kurzke ===
  0.30  0.46  2.51  78.64  71.49  78.17  81.57  79.26  68.97
  0.32  0.45  2.50  78.93  71.59  78.49  81.93  79.33  69.02
  0.34  0.45  2.49  79.09  71.55  78.66  82.16  79.27  68.98
  0.36  0.44  2.48  79.24  71.48  78.83  82.39  79.21  68.95
  0.38  0.43  2.48  79.39  71.38  79.00  82.63  79.14  68.90
  0.40  0.42  2.47  79.53  71.26  79.15  82.87  79.07  68.86
=====
=
Outlet Angle      74.00
Load Coefficient   1.20
Optimum Point:    R =  0.38      TS Isentropic Efficiency = 75.12
=====
=
Reaction Degree == Flow Coeff == PR t-t == TT Iso Effic. == TS Iso Effic. == TT Pol Effic. == TS Pol Effic == T. Effic P&W == T. Effic. Kurzke ===
  0.30  0.38  1.94  79.87  74.62  80.58  82.80  79.99  65.41
  0.32  0.37  1.93  79.98  74.82  80.72  82.91  79.86  65.34
  0.34  0.36  1.93  80.07  74.98  80.83  83.01  79.71  65.27
  0.36  0.36  1.93  80.13  75.08  80.91  83.08  79.54  65.19
  0.38  0.35  1.93  80.14  75.12  80.95  83.10  79.33  65.09
  0.40  0.34  1.93  80.11  75.09  80.93  83.10  79.08  64.97
=====
=
Load Coefficient   1.40
Optimum Point:    R =  0.36      TS Isentropic Efficiency = 74.10
=====
=
Reaction Degree == Flow Coeff == PR t-t == TT Iso Effic. == TS Iso Effic. == TT Pol Effic. == TS Pol Effic == T. Effic P&W == T. Effic. Kurzke ===
  0.30  0.41  2.20  79.51  73.95  79.64  82.12  79.95  67.63
  0.32  0.40  2.19  79.65  74.03  79.79  82.29  79.86  67.58
  0.34  0.39  2.19  79.77  74.08  79.94  82.46  79.75  67.53
  0.36  0.38  2.18  79.88  74.10  80.07  82.62  79.65  67.47
  0.38  0.38  2.18  80.00  74.09  80.21  82.79  79.53  67.41
  0.40  0.37  2.18  80.09  74.04  80.32  82.94  79.41  67.35
=====
=
Load Coefficient   1.60
Optimum Point:    R =  0.32      TS Isentropic Efficiency = 72.45
=====
=
Reaction Degree == Flow Coeff == PR t-t == TT Iso Effic. == TS Iso Effic. == TT Pol Effic. == TS Pol Effic == T. Effic P&W == T. Effic. Kurzke ===
  0.30  0.43  2.51  78.93  72.43  78.49  81.53  79.55  69.18
  0.32  0.43  2.50  79.14  72.45  78.73  81.81  79.55  69.18
  0.34  0.42  2.49  79.29  72.40  78.89  82.04  79.48  69.13
  0.36  0.41  2.49  79.43  72.32  79.05  82.26  79.40  69.08
  0.38  0.40  2.48  79.58  72.22  79.21  82.49  79.34  69.04
  0.40  0.39  2.48  79.71  72.08  79.35  82.72  79.25  69.00
=====
=
```

```

Outlet Angle      75.00
Load Coefficient   1.20
Optimum Point:    R =  0.36      TS Isentropic Efficiency =  75.67
=====
=
Reaction Degree == Flow Coeff == PR t-t == TT Iso Effic. == TS Iso Effic. == TT Pol Effic. == TS Pol Effic == T. Effic P&W == T. Effic. Kurzke ===
  0.30      0.35      1.94      79.97      75.24      80.69      82.68      80.11      65.47
  0.32      0.35      1.94      80.07      75.43      80.82      82.78      79.97      65.41
  0.34      0.34      1.94      80.15      75.58      80.92      82.87      79.81      65.34
  0.36      0.33      1.94      80.19      75.67      80.99      82.93      79.63      65.25
  0.38      0.33      1.94      80.16      75.66      80.98      82.92      79.38      65.12
  0.40      0.32      1.93      80.11      75.60      80.94      82.89      79.11      64.99
=====

=
Load Coefficient   1.40
Optimum Point:    R =  0.36      TS Isentropic Efficiency =  74.77
=====
=
Reaction Degree == Flow Coeff == PR t-t == TT Iso Effic. == TS Iso Effic. == TT Pol Effic. == TS Pol Effic == T. Effic P&W == T. Effic. Kurzke ===
  0.30      0.38      2.20      79.64      74.64      79.77      81.99      80.09      67.73
  0.32      0.37      2.20      79.77      74.72      79.93      82.16      80.00      67.67
  0.34      0.37      2.19      79.89      74.77      80.07      82.33      79.89      67.62
  0.36      0.36      2.19      80.00      74.77      80.20      82.48      79.77      67.55
  0.38      0.35      2.19      80.10      74.75      80.32      82.64      79.65      67.49
  0.40      0.35      2.18      80.18      74.68      80.42      82.78      79.51      67.41
=====

=
Load Coefficient   1.60
Optimum Point:    R =  0.32      TS Isentropic Efficiency =  73.22
=====
=
Reaction Degree == Flow Coeff == PR t-t == TT Iso Effic. == TS Iso Effic. == TT Pol Effic. == TS Pol Effic == T. Effic P&W == T. Effic. Kurzke ===
  0.30      0.41      2.52      79.10      73.21      78.67      81.39      79.74      69.31
  0.32      0.40      2.51      79.29      73.22      78.88      81.65      79.71      69.29
  0.34      0.39      2.50      79.43      73.16      79.04      81.87      79.63      69.24
  0.36      0.38      2.50      79.57      73.07      79.20      82.09      79.55      69.19
  0.38      0.38      2.49      79.71      72.97      79.36      82.32      79.48      69.15
  0.40      0.37      2.49      79.86      72.84      79.52      82.56      79.41      69.11
=====

=
Outlet Angle      76.00
Load Coefficient   1.20
Optimum Point:    R =  0.36      TS Isentropic Efficiency =  76.15
=====
=
Reaction Degree == Flow Coeff == PR t-t == TT Iso Effic. == TS Iso Effic. == TT Pol Effic. == TS Pol Effic == T. Effic P&W == T. Effic. Kurzke ===
  0.30      0.33      1.95      80.02      75.80      80.75      82.52      80.20      65.50
  0.32      0.32      1.95      80.11      75.98      80.87      82.62      80.05      65.43
  0.34      0.32      1.95      80.18      76.11      80.96      82.69      79.87      65.35
  0.36      0.31      1.94      80.17      76.15      80.98      82.70      79.63      65.23
  0.38      0.31      1.94      80.13      76.12      80.95      82.68      79.37      65.09
  0.40      0.30      1.94      80.06      76.05      80.90      82.64      79.08      64.95
=====

=
Load Coefficient   1.40
Optimum Point:    R =  0.34      TS Isentropic Efficiency =  75.37
=====
=
Reaction Degree == Flow Coeff == PR t-t == TT Iso Effic. == TS Iso Effic. == TT Pol Effic. == TS Pol Effic == T. Effic P&W == T. Effic. Kurzke ===
  0.30      0.35      2.21      79.70      75.25      79.84      81.82      80.19      67.79
  0.32      0.35      2.21      79.83      75.33      80.00      81.98      80.09      67.73
  0.34      0.34      2.20      79.96      75.37      80.14      82.15      79.99      67.67
  0.36      0.33      2.20      80.06      75.37      80.27      82.31      79.86      67.61
  0.38      0.33      2.20      80.14      75.32      80.37      82.45      79.71      67.53
  0.40      0.32      2.19      80.18      75.21      80.42      82.55      79.53      67.43
=====

=
Load Coefficient   1.60
Optimum Point:    R =  0.32      TS Isentropic Efficiency =  73.89
=====
=
Reaction Degree == Flow Coeff == PR t-t == TT Iso Effic. == TS Iso Effic. == TT Pol Effic. == TS Pol Effic == T. Effic P&W == T. Effic. Kurzke ===
  0.30      0.38      2.53      79.17      73.89      78.75      81.17      79.85      69.39
  0.32      0.37      2.52      79.36      73.89      78.96      81.43      79.81      69.37
  0.34      0.36      2.52      79.50      73.82      79.12      81.65      79.73      69.32
  0.36      0.36      2.51      79.65      73.74      79.29      81.89      79.65      69.27
  0.38      0.35      2.51      79.79      73.63      79.44      82.12      79.58      69.22
  0.40      0.34      2.50      79.92      73.49      79.59      82.35      79.49      69.17
=====

=====
=====
=====
=====
===== OPTIMUM POINTS - PARAMETRIC STUDY RESULTS =====
=====
=====
===== Str. TE Angle == Load Coefficient == Optimum R == Optimum TS ISO Eff. == Flow Coeff == PR t-t == Rtr TE Angle ==
=====
== 73.00 == 1.20 == 0.38 == 74.51 == 0.37 == 1.92 == -4.34 ==
== 73.00 == 1.40 == 0.38 == 73.37 == 0.40 == 2.17 == -16.88 ==
== 73.00 == 1.60 == 0.32 == 71.59 == 0.45 == 2.50 == -17.91 ==
=====
== 74.00 == 1.20 == 0.38 == 75.12 == 0.35 == 1.93 == -4.46 ==
== 74.00 == 1.40 == 0.36 == 74.10 == 0.38 == 2.18 == -14.80 ==
== 74.00 == 1.60 == 0.32 == 72.45 == 0.43 == 2.50 == -19.00 ==
=====
== 75.00 == 1.20 == 0.36 == 75.67 == 0.33 == 1.94 == -1.21 ==

```

```

== 75.00 == 1.40 == 0.36 == 74.77 == 0.36 == 2.19 == -15.69 ==
== 75.00 == 1.60 == 0.32 == 73.22 == 0.40 == 2.51 == -20.21 ==
=====
== 76.00 == 1.20 == 0.36 == 76.15 == 0.31 == 1.94 == -1.11 ==
== 76.00 == 1.40 == 0.34 == 75.37 == 0.34 == 2.20 == -13.34 ==
== 76.00 == 1.60 == 0.32 == 73.89 == 0.37 == 2.52 == -21.53 ==
=====

=====
= INLET CONDITIONS
=====
=----- Inlet Properties ----- -----
Inlet massflow [kg/s]: 100.00
Inlet temperature [°C]: 1423.00
Inlet pressure [bar]: 18.52
Inlet enthalpy [kJ/kg]: 1696.2
Inlet entropy [J/kg K]: 1245.1
Inlet entropy change [J/kg K]: -0.00
Inlet fuel to air ratio [-]: 0.0200
Inlet gas constant [J/kg K]: 292.68
Inlet specific heat [J/kg K]: 1316.3
Inlet Cp over Cv [-]: 1.286
Inlet density [kg/m³]: 3.710
----- Inlet Velocities & Angles -----
Inlet flow angle [°]: 0.00
Inlet absolute velocity [m/s]: 85.00
Inlet meridional velocity [m/s]: 85.00
Inlet tangential velocity [m/s]: 0.00
Inlet speed of sound [m/s]: 798.3
Inlet mach number [-]: 0.11

```

### Graphical Results from Parametric Study for Craig-Cox

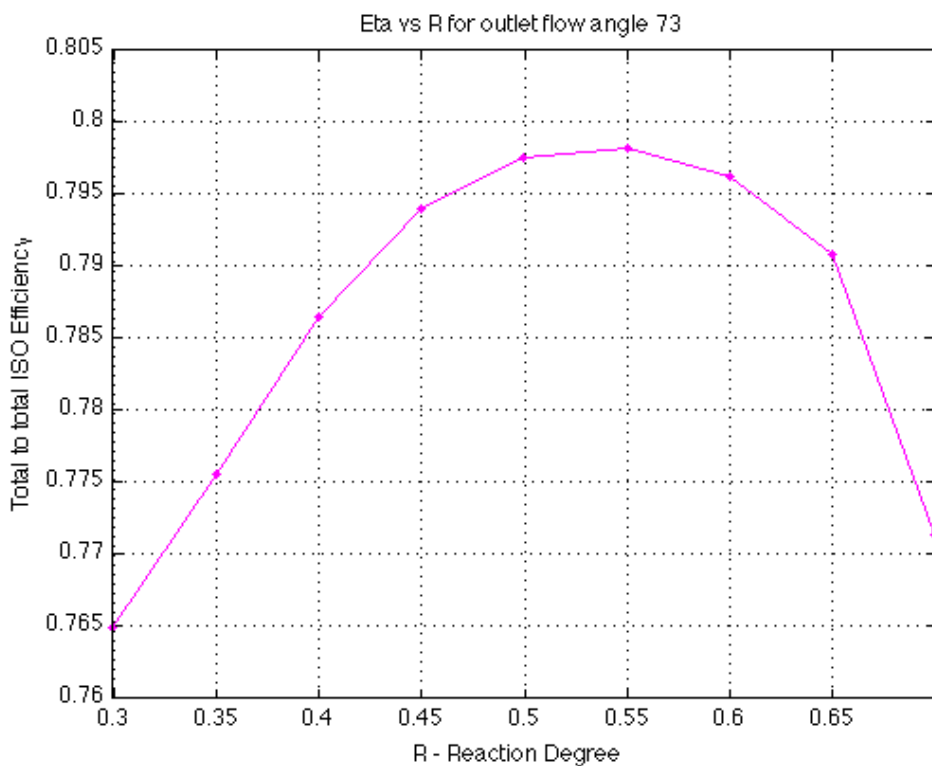


Figure - Total to Total Efficiency Prediction for reference case

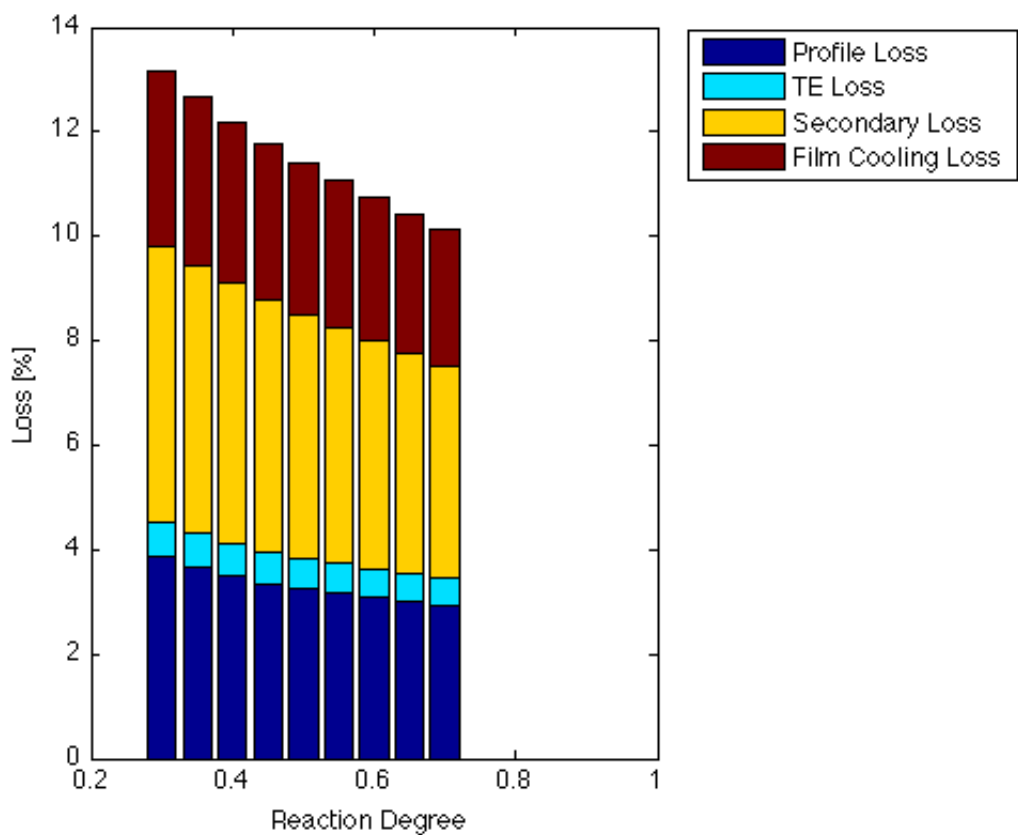


Figure - Breakdown of Losses in Stator for Reference Case

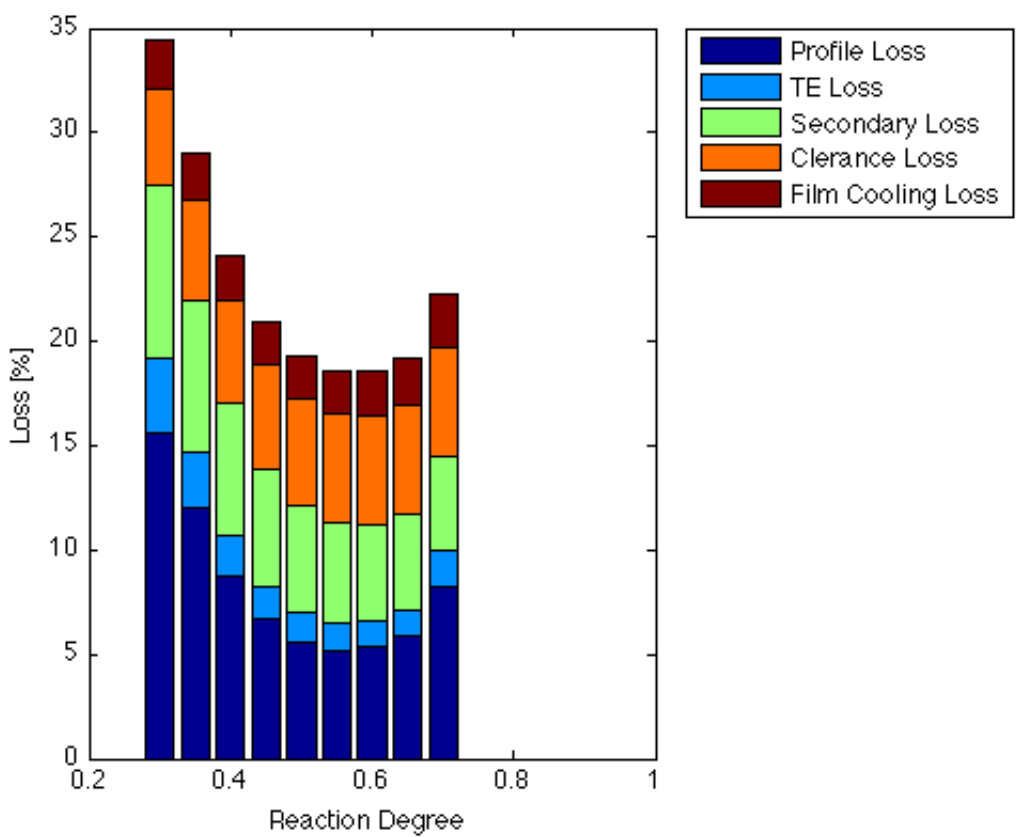


Figure - Breakdown of Losses in Rotor for Reference Case

## Output Text Results from Parametric Study for Denton

```

=====
# LUAX-T #
# Version 2.0 #
# David Olsson & Magnus Genrup #
# 2008 #
# Rafaell Guedez #
# 2011 #
=====

Test_turbine_1
23-Mar-2011 16:16:41
PARAMETRIC STUDY
Denton Loss Model RESULTS

Stage 1
Outlet Angle      73.00
Load Coefficient   1.50
Optimum Point:    R =  0.22    TS Isentropic Efficiency = 74.59
Reaction Degree == Flow Coeff == PR t-t == TT Iso Effic. == TS Iso Effic. == TT Pol Effic. == TS Pol Effic == T. Effic P&W == T. Effic. Kurzke ===
0.10   0.53   2.32   80.53   73.94   80.36   83.06   83.50   79.96
0.12   0.52   2.31   80.67   74.17   80.52   83.21   83.34   79.89
0.14   0.51   2.31   80.77   74.34   80.64   83.33   83.16   79.80
0.16   0.50   2.30   80.85   74.46   80.74   83.43   82.96   79.71
0.18   0.49   2.30   80.91   74.53   80.82   83.51   82.75   79.60
0.20   0.48   2.29   80.96   74.58   80.89   83.59   82.55   79.50
0.22   0.48   2.29   80.99   74.59   80.93   83.66   82.34   79.39
0.24   0.47   2.29   81.01   74.57   80.96   83.72   82.12   79.27
=====
Load Coefficient   1.60
Optimum Point:    R =  0.18    TS Isentropic Efficiency = 74.25
Reaction Degree == Flow Coeff == PR t-t == TT Iso Effic. == TS Iso Effic. == TT Pol Effic. == TS Pol Effic == T. Effic P&W == T. Effic. Kurzke ===
0.10   0.55   2.47   80.45   73.97   80.05   82.82   83.49   71.80
0.12   0.54   2.46   80.59   74.12   80.22   82.99   83.32   71.74
0.14   0.53   2.46   80.68   74.20   80.33   83.13   83.13   71.65
0.16   0.52   2.45   80.75   74.24   80.43   83.25   82.94   71.55
0.18   0.51   2.45   80.83   74.25   80.51   83.37   82.74   71.45
0.20   0.50   2.44   80.87   74.22   80.57   83.47   82.53   71.34
0.22   0.49   2.44   80.92   74.16   80.63   83.57   82.33   71.23
0.24   0.48   2.43   80.95   74.08   80.66   83.66   82.11   71.10
=====
Load Coefficient   1.70
Optimum Point:    R =  0.14    TS Isentropic Efficiency = 73.91
Reaction Degree == Flow Coeff == PR t-t == TT Iso Effic. == TS Iso Effic. == TT Pol Effic. == TS Pol Effic == T. Effic P&W == T. Effic. Kurzke ===
0.10   0.56   2.50   80.37   73.98   80.12   82.88   83.54   72.54
0.12   0.55   2.49   80.48   73.90   80.09   82.81   83.27   72.47
0.14   0.54   2.48   80.59   73.91   80.01   82.98   83.09   72.39
0.16   0.53   2.62   80.67   73.88   80.11   83.14   82.89   72.29
0.18   0.52   2.61   80.73   73.81   80.19   83.28   82.69   72.17
0.20   0.51   2.60   80.79   73.71   80.26   83.41   82.49   72.06
0.22   0.51   2.60   80.82   73.57   80.30   83.54   82.27   71.95
0.24   0.50   2.59   80.86   73.42   80.35   83.66   82.07   71.84
=====
Outlet Angle      74.00
Load Coefficient   1.50
Optimum Point:    R =  0.22    TS Isentropic Efficiency = 75.19
Reaction Degree == Flow Coeff == PR t-t == TT Iso Effic. == TS Iso Effic. == TT Pol Effic. == TS Pol Effic == T. Effic P&W == T. Effic. Kurzke ===
0.10   0.50   2.33   80.56   74.55   80.39   82.84   83.55   79.99
0.12   0.49   2.32   80.67   74.76   80.53   82.96   83.36   79.91
0.14   0.48   2.32   80.76   74.92   80.63   83.06   83.16   79.81
0.16   0.47   2.31   80.83   75.04   80.72   83.15   82.95   79.71
0.18   0.46   2.31   80.89   75.13   80.80   83.23   82.74   79.60
0.20   0.45   2.30   80.94   75.18   80.87   83.31   82.54   79.50
0.22   0.45   2.30   80.97   75.19   80.91   83.37   82.32   79.39
0.24   0.44   2.30   80.99   75.17   80.94   83.43   82.10   79.27
=====
Load Coefficient   1.60
Optimum Point:    R =  0.16    TS Isentropic Efficiency = 74.87
Reaction Degree == Flow Coeff == PR t-t == TT Iso Effic. == TS Iso Effic. == TT Pol Effic. == TS Pol Effic == T. Effic P&W == T. Effic. Kurzke ===
0.10   0.51   2.48   80.47   74.59   80.07   82.57   83.52   71.83
0.12   0.50   2.47   80.59   74.74   80.22   82.73   83.34   71.75
0.14   0.49   2.47   80.68   74.83   80.33   82.85   83.15   71.66
0.16   0.49   2.46   80.76   74.97   80.42   82.97   82.94   71.56
0.18   0.48   2.46   80.81   74.87   80.49   83.06   82.72   71.45
0.20   0.47   2.45   80.84   74.84   80.54   83.15   82.50   71.33
0.22   0.46   2.45   80.89   74.79   80.60   83.26   82.30   71.22
0.24   0.45   2.45   80.91   74.70   80.63   83.34   82.08   71.10
=====
Load Coefficient   1.70
Optimum Point:    R =  0.14    TS Isentropic Efficiency = 74.57
Reaction Degree == Flow Coeff == PR t-t == TT Iso Effic. == TS Iso Effic. == TT Pol Effic. == TS Pol Effic == T. Effic P&W == T. Effic. Kurzke ===
0.10   0.53   2.66   80.34   74.46   79.72   82.31   83.46   72.56
0.12   0.52   2.65   80.48   74.54   79.48   82.31   83.29   72.49
0.14   0.51   2.64   80.59   74.57   80.02   82.69   83.10   72.40
0.16   0.50   2.63   80.68   74.55   80.12   82.84   82.91   72.31
0.18   0.49   2.62   80.74   74.49   80.20   82.97   82.70   72.20
0.20   0.48   2.62   80.78   74.38   80.25   83.09   82.48   72.07
0.22   0.47   2.61   80.80   74.24   80.28   83.19   82.24   71.94
0.24   0.47   2.61   80.83   74.08   80.31   83.30   82.03   71.82
=====
Outlet Angle      75.00
Load Coefficient   1.50
Optimum Point:    R =  0.22    TS Isentropic Efficiency = 75.75
Reaction Degree == Flow Coeff == PR t-t == TT Iso Effic. == TS Iso Effic. == TT Pol Effic. == TS Pol Effic == T. Effic P&W == T. Effic. Kurzke ===
0.10   0.46   2.34   80.55   75.09   80.37   82.59   83.55   79.99
0.12   0.46   2.33   80.67   75.32   80.52   82.72   83.36   79.91
0.14   0.45   2.33   80.76   75.50   80.63   82.81   83.16   79.82
0.16   0.44   2.32   80.82   75.62   80.71   82.89   82.95   79.71
0.18   0.43   2.32   80.86   75.69   80.77   82.96   82.72   79.60
0.20   0.43   2.31   80.90   75.73   80.82   83.01   82.50   79.48
0.22   0.42   2.31   80.93   75.75   80.86   83.08   82.28   79.37
0.24   0.41   2.31   80.95   75.72   80.89   83.13   82.05   79.25
=====
```

Load Coefficient 1.60  
Optimum Point: R = 0.18 TS Isentropic Efficiency = 75.49

---

Reaction Degree == Flow Coeff == PR t-t == TT Iso Effic. == TS Iso Effic. == TT Pol Effic. == TS Pol Effic == T. Effic P&W == T. Effic. Kurzke ==

	0.10	0.12	0.14	0.16	0.18	0.20	0.22	0.24
0.48	2.50	2.49	2.48	2.48	2.47	2.47	2.46	2.46
0.58	75.16	75.32	75.42	75.48	75.49	75.45	75.38	75.28
80.05	80.20	80.42	80.49	80.53	80.57	80.56	80.58	80.58
82.30	82.45	82.70	82.80	82.87	82.94	82.99	82.27	82.01
83.52	83.34	83.15	83.15	82.73	82.73	82.21	82.27	82.03
71.83	71.76	71.67	71.57	71.46	71.34	71.21	71.21	71.07

---

Load Coefficient 1.70  
Optimum Point: R = 0.14 TS Isentropic Efficiency = 75.18

---

Reaction Degree == Flow Coeff == PR t-t == TT Iso Effic. == TS Iso Effic. == TT Pol Effic. == TS Pol Effic == T. Effic P&W == T. Effic. Kurzke ==

	0.10	0.12	0.14	0.16	0.18	0.20	0.22	0.24
0.49	2.68	2.66	2.65	2.65	2.64	2.64	2.63	2.62
80.31	75.04	75.13	75.18	75.17	75.12	80.19	82.68	82.70
79.69	82.02	82.22	80.80	80.11	82.54	82.91	82.70	82.01
82.34	83.25	83.28	83.10	82.54	82.91	82.31	82.20	81.82
83.52	83.34	83.14	82.91	82.68	82.70	82.47	82.25	81.95
72.55	72.49	72.41	72.31	72.20	72.08	71.82	71.95	71.05

---

Outlet Angle 76.00  
Load Coefficient 1.50  
Optimum Point: R = 0.20 TS Isentropic Efficiency = 76.21

---

Reaction Degree == Flow Coeff == PR t-t == TT Iso Effic. == TS Iso Effic. == TT Pol Effic. == TS Pol Effic == T. Effic P&W == T. Effic. Kurzke ==

	0.10	0.12	0.14	0.16	0.18	0.20	0.22	0.24
0.42	2.36	2.35	2.34	2.34	2.33	2.33	2.33	2.32
80.42	75.52	75.77	75.96	76.08	76.16	76.20	76.20	76.16
80.33	82.34	82.47	80.51	80.60	80.66	82.61	82.68	80.58
82.34	83.34	83.14	82.92	82.55	82.68	82.46	82.46	80.46
83.52	83.34	83.14	82.91	82.70	82.70	82.47	82.25	81.95
70.98	70.90	70.81	70.70	70.58	70.46	70.33	70.33	70.20

---

Load Coefficient 1.60  
Optimum Point: R = 0.18 TS Isentropic Efficiency = 75.96

---

Reaction Degree == Flow Coeff == PR t-t == TT Iso Effic. == TS Iso Effic. == TT Pol Effic. == TS Pol Effic == T. Effic P&W == T. Effic. Kurzke ==

	0.10	0.12	0.14	0.16	0.18	0.20	0.22	0.24
0.45	2.52	2.51	2.50	2.50	2.49	2.49	2.48	2.48
80.31	75.60	75.78	75.89	75.95	75.96	80.36	82.42	82.68
79.90	81.92	80.07	80.20	80.29	80.33	82.42	82.68	81.43
83.48	83.31	83.21	83.11	83.00	82.90	81.54	81.54	81.05
71.80	71.74	71.65	71.54	71.43	71.31	71.31	71.18	70.05

---

Load Coefficient 1.70  
Optimum Point: R = 0.14 TS Isentropic Efficiency = 75.66

---

Reaction Degree == Flow Coeff == PR t-t == TT Iso Effic. == TS Iso Effic. == TT Pol Effic. == TS Pol Effic == T. Effic P&W == T. Effic. Kurzke ==

	0.10	0.12	0.14	0.16	0.18	0.20	0.22	0.24
0.46	2.70	2.68	2.65	2.67	2.66	2.65	2.65	2.64
80.18	75.49	75.54	75.60	75.60	75.61	75.61	75.61	75.68
79.54	81.62	81.62	81.66	81.66	81.66	82.14	82.35	82.38
82.34	83.31	83.11	82.90	82.90	82.90	82.63	82.63	82.16
83.52	83.31	83.11	82.91	82.70	82.70	82.47	82.22	81.86
72.46	72.38	72.38	72.26	72.16	72.16	72.04	71.92	71.05

---

Load Coefficient 1.50  
Optimum Point: R = 0.20 TS Isentropic Efficiency = 75.66

---

Reaction Degree == Flow Coeff == PR t-t == TT Iso Effic. == TS Iso Effic. == TT Pol Effic. == TS Pol Effic == T. Effic P&W == T. Effic. Kurzke ==

	0.10	0.12	0.14	0.16	0.18	0.20	0.22	0.24
0.46	2.70	2.68	2.65	2.67	2.66	2.65	2.65	2.64
80.18	75.49	75.54	75.60	75.60	75.61	75.61	75.61	75.68
79.54	81.62	81.62	81.66	81.66	81.66	82.14	82.35	82.38
82.34	83.31	83.11	82.90	82.90	82.90	82.63	82.63	82.16
83.52	83.31	83.11	82.91	82.70	82.70	82.47	82.22	81.86
72.46	72.38	72.38	72.26	72.16	72.16	72.04	71.92	71.05

---

===== OPTIMUM POINTS - PARAMETRIC STUDY RESULTS =====

---

== Str. TE Angle == Load Coefficient == Optimum R == Optimum TS ISO Eff. == Flow Coeff == PR tt == Rtr TE Angle ==

	73.00	74.00	75.00	76.00
== 1.50	== 1.50	== 1.50	== 1.50	
== 0.22	== 0.22	== 0.22	== 0.20	
== 74.59	== 75.19	== 75.75	== 76.21	
== 0.48	== 0.45	== 0.42	== 0.40	
== 2.29	== 2.30	== 2.31	== 2.33	
== -1.79	== -1.68	== -1.59	== 1.82	
== 74.25	== 74.87	== 75.49	== 75.96	
== 0.51	== 0.49	== 0.45	== 0.42	
== 2.45	== 2.46	== 2.47	== 2.49	
== -1.88	== 1.23	== -1.83	== -1.89	
== 73.91	== 74.57	== 75.18	== 75.66	
== 0.54	== 0.51	== 0.48	== 0.44	
== 2.62	== 2.64	== 2.65	== 2.68	
== -1.54	== -1.52	== -1.53	== -1.61	

---

===== INLET CONDITIONS =====

---

----- Inlet Properties -----  
Inlet massflow [kg/s]: 100.00  
Inlet temperature [°C]: 1423.00  
Inlet pressure [bar]: 18.52  
Inlet enthalpy [J/kg]: 1696.2  
Inlet entropy [J/kg K]: 1245.1  
Inlet entropy change [J/kg K]: -0.00  
Inlet fuel to air ratio [-]: 0.0200  
Inlet gas constant [J/kg K]: 292.68  
Inlet specific heat [J/kg K]: 1316.3  
Inlet Cp over Cv [-]: 1.286  
Inlet density [kg/m³]: 3.710

----- Inlet Velocities & Angles -----  
Inlet flow angle [°]: 0.00  
Inlet absolute velocity [m/s]: 85.00  
Inlet meridional velocity [m/s]: 85.00  
Inlet tangential velocity [m/s]: 0.00  
Inlet speed of sound [m/s]: 798.3  
Inlet mach number [-]: 0.11

---

### Graphical Results from parametric study for Denton

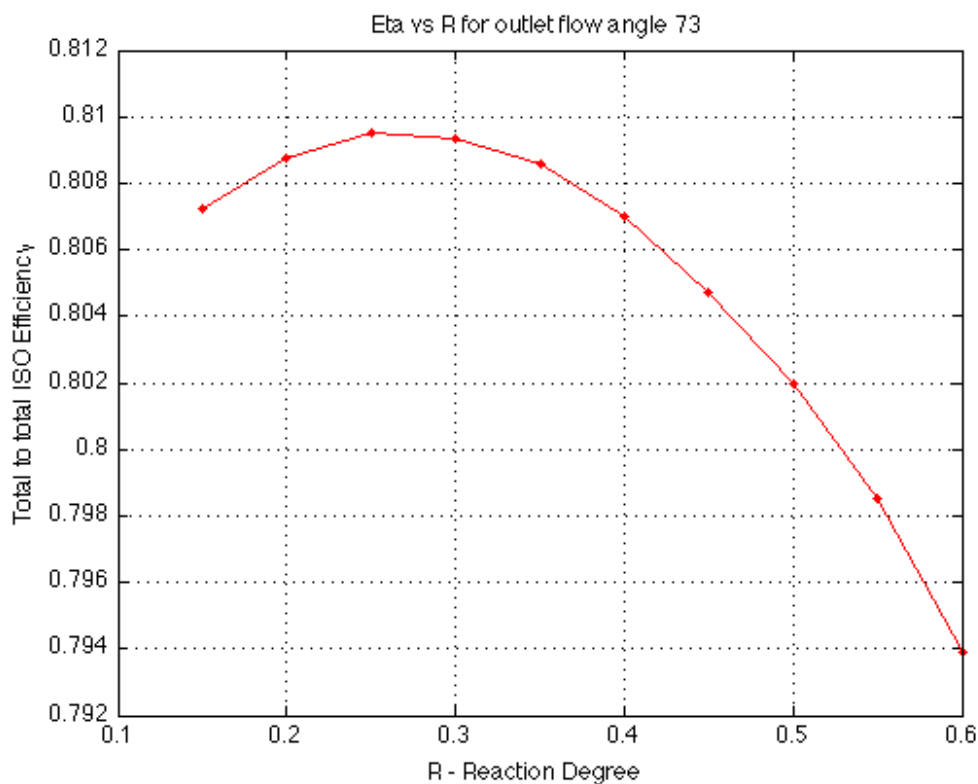


Figure - Total to Total Efficiency Prediction for reference case

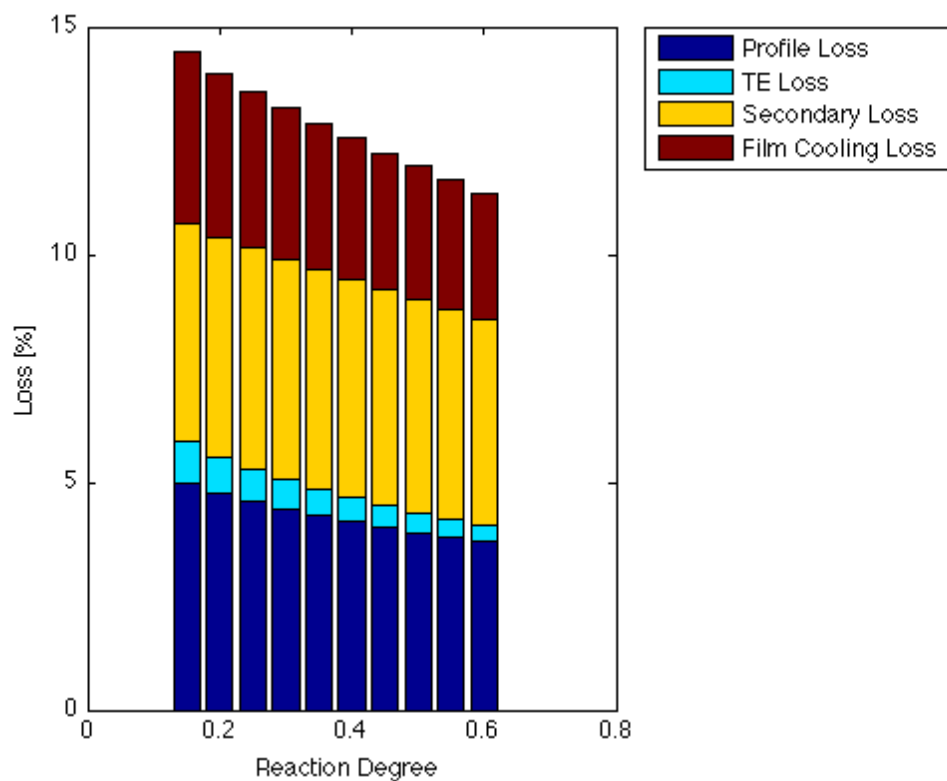


Figure - Breakdown of Losses in Stator for Reference Case

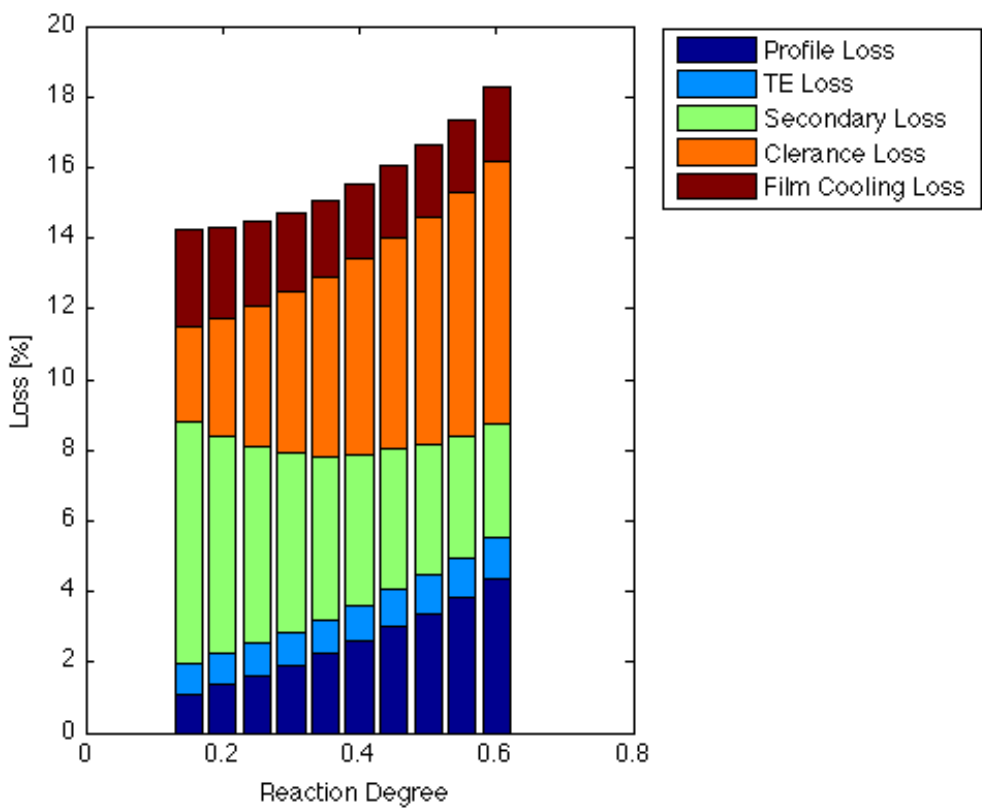


Figure - Breakdown of Losses in Rotor for Reference Case